Multisensory Interactions Concerning Human Self-motion

Thesis for the qualification of PhD

By Adrian Edward Ivan Thurrell

University College London

Under the supervision of

Professor Adolfo Bronstein

and

Dr Adar Pelah

The Experiments presented here were carried-out at The MRC Human Movement and Balance Unit (as was), Queen Square, London and in The Department of Physiology, Downing Street, Cambridge. These studies were supported by funding gratefully received from the MRC (studentship number G78/5763).

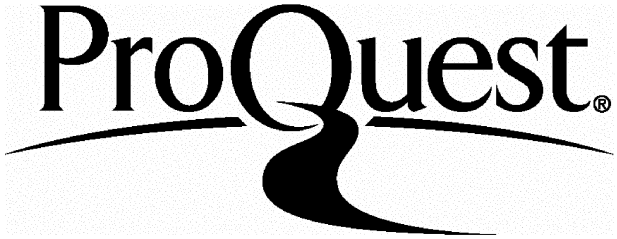

Abstract of Thesis

Humans move in their environment and have a number of different sources of information about their self-motion, e.g. visual, vestibular, proprioceptive and somatosensory signals. These signal sources must be combined to overcome their individual limitations.

As the eyes are mobile relative to the trunk, gaze direction must be taken into account if visual information is to be applied usefully to control posture. The orientation of the postural response to visual motion in various directions relative to the subject is investigated using two paradigms. In the first, using passive motion of the subject in a dark room, it is difficult for subjects to cognitively reconstruct the direction of gaze, and hence, the visual motion. The data show that the postural response may take account of the gaze direction independently of cognitively mediated knowledge of the geometry of the experimental conditions. In the second, comparisons are made between the accuracy of this reorientation during the visually induced perception of self-motion (vection) and object-motion perception and it is found that the accuracy of the reorientation is improved during conscious perception of self-motion (vection).

During locomotion, visual signals corresponding to object motion are distorted by motion components directly related to the speed and direction of movement by the observer. Thus, in order to allow a veridical interpretation of the visual signal by the observer, these self-motion components must be discounted, while at the same time retaining important information on their speed and progression. In experiments, the effects of proprioceptive, somatosensory and efference copy signals of self-motion are isolated by comparing the speed of a constant optic flow stimulus that is perceived while either standing or performing a motor activity. It is found, firstly, that the more locomotion-related a motor activity may be, the greater it reduces the perceived speed. And secondly, that the more locomotion-related a visual stimulus is, the greater its perceived speed is reduced while walking. It is therefore suggested that a tuning exists between locomotor activity and the types of visual signal (i.e. optic flow) that it normally introduces.

The above experiments suggest a network of self-motion signals that are combined dynamically to represent the movement of the body. This single representation is used both to control self-motion and to compensate for its effects on visual processes.

Table of Contents

Acknowledgements

During the course of my PhD many people have kindly offered their time as willing subjects, without whom this would be a small thesis indeed, many thanks therefore go to them. The support staff, both in London and Cambridge, have constructed and created various bits of equipment and software and their help is greatly appreciated. Both of my supervisors, Adolfo and Adar, my own student Miriam and a variety of other people have pretty much done the rest with suggestions and questions related to this work and must therefore receive the greatest portion of thanks.

Declaration

With the exception of the following sections, the contents of this thesis are entirely my own work.

In Chapter 2, the rationale behind this experiment belongs to Adolfo Bronstein, also Pierre Bertholon completed most of the equipment set-up and provided manual help with the execution of the experiment.

Chapter 4 continues and expands on the work I undertook as part of my undergraduate final year project at the University of Cambridge in 1998. That project may be considered to encompass pilot work demonstrating the basic 'Arthrovisual Effect' (see page 59) and the lack of an influence of walking on timing perception (see page 60). That pilot data itself is not, however, included in this thesis, more and better data having been collected since. Further pilot data was obtained during the following summer after my graduation and some of this was published in abstract form as Thurrell, Pelah and Distler (1998). Hartwig Distler provided advice on general programming matters when I wrote the original programs to run the experiments.

Also in Chapter 4, the data for the experiments controlling for the possible effect of attention (see page 59) and investigating the influence of various motor activities (see page 60) were collected by my own student Miriam Berry. This formed part of her undergraduate degree project at the University of Cambridge and was also published in abstract form as Pelah, Thurrell and Berry (2001). From the perspective of this thesis, her input was restricted to obtaining subjects and running experiments using bespoke computer programs designed and written by myself.

All bespoke computer programs and scripts used in the collection and analysis of data were written by myself and my be found on disk in Appendix B

Adrian Thurrell

Publications Incorporated into this Thesis

The following publications were incorporated into this thesis and may be found in their original form in Appendix A:

- Thurrell AEI, Pelah A, Distler HK (1998) The influence of non-visual signals of walking on the perceived speed of optic flow. *Perception* 27: 147 (meeting abstract)

- Thurrell AEI, Bertholon P, Bronstein AM (1999) Reorientation of a visually evoked postural response does not require cognitive knowledge of display relative angular position. Journal of Physiology (meeting abstract)

- Thurrell AEI, Bertholon P, Bronstein AM (2000) Reorientation of a visually evoked postural sway response during passive whole body rotation. *Experimental Brain Research* 133: 229-232

- Pelah A, Thurrell AEI, Berry M (2001) Reduction of perceived visual speed during locomotion: Evidence for quadrupedal pathways in human? *Journal of Vision* 1:307a (meeting abstract)

- Thurrell AEI, Bronstein AM (2001) Vection induced re-orientation in a visually evoked sway response (meeting abstract)

- Thurrell AEI, Bronstein AM (2002) Vection increases the magnitude and accuracy of visually evoked postural responses. *Experimental Brain Research* 147(4): 558-560

- Pelah A, Thurrell AEI, Berry M (2002) Reduction of perceived visual speed during walking: Evidence against the involvement of attentional or vestibular mechanisms. (meeting abstract)

- Thurrell AEI, Pelah A (2002) Reduction of perceived visual speed during walking: Effect dependent upon stimulus similarity to the visual consequences of locomotion. (meeting abstract)

Other published work was also carried-out in parallel with the work contained within this thesis, some of which may also be found at the end of Appendix A:

- Thurrell A, Jauregui-Renaud K, Gresty MA, Bronstein AM (2003) Vestibular influence on the cardiorespiratory responses to whole-body oscillation after standing. *Experimental Brain Research 150(3): 325-331*

List of Tables

List of Figures

Terms and Abbreviations

Term	Meaning
ANOVA	ANalysis Of VAriance
Arthrokinetic	A combination of Efference Copy, Proprioception and Somatic Sensation.
COM	Centre Of Mass
COP	Centre Of Pressure: the average position of the force upward from the support surface at any moment, if an object (such as a person) is not to fall over, this must, on average be directly below the COM.
Direction of disk motion	The average direction in which the top half of a rotating disk moves in space, i.e. horizontally and in the plane of the disk.
EOM	Extra-Ocular Muscle(s): any or all of the muscles responsible for rotating the eyeballs within their sockets.
Gaze	The direction in which the eyes are pointing in space.
Ground-plane	A visual stimulus intended to mimic a flat ground surface extending to a distant horizon, usually covered with a texture composed of many small dots thus providing a depth cue.
Lamellar flow	A pattern of optic flow where the motion is in the same direction at all points, i.e. as if the entire visual scene was drawn on a canvas that is being moved in front of the subject.
NOFS	Normalised Optic Flow Speed
NSF	Normalised Stride Frequency
NWV	Normalised Walking Velocity
Object motion	The motion in space of an object.
OMP	Object Motion Perception: the perception of visual motion as being caused by the motion of the visual scene in space, see Vection.
Optic flow	The pattern of visual motion resulting from an observer's self-motion.
Pitch	Rotation around an axis through the ears.
Retinal flow	The pattern of visual motion projected onto the retinae, similar to optic flow, but contains an additional component due to eye movements.
Roll	Rotation around an axis through the nose and the occiput.
s.d.	Standard Deviation
s.e.m.	Standard Error of the Mean
Self-motion	The motion in space of oneself.
The Arthrovisual Effect	The name given to the effect demonstrated in Chapter 4
Vection	The illusory perception of self-motion resulting from viewing large field visual motion.
VEPR	Visually Evoked Postural Response: the postural sway typically resulting from large-field visual motion.
Yaw	Rotation around an axis through the top and bottom of the head.

Chapter 1: General Introduction

Humans move around in the environment under self-control, and to accomplish this we require information about our position and self-motion. Even when we are not moving around, we do not just maintain our position passively, we must constantly adjust our posture, either of our whole body or of individual segments, again requiring information about position and self-motion. When at rest and during self-motion we must also be able to use the information that is collected by our exteroreceptive senses. This requires that the exteroreceptive senses account for our self-motion also using signals of our position and self-motion.

Humans do not have a single infallible source of this self-motion information; instead we have many senses that are each able to provide information on some aspects of self-motion. In order to accomplish the goals of controlled movement, controlled stationarity and sensory acquisition there must be a system to integrate these signals into a coherent whole.

Signals of Self-motion

Vision, the vestibular system, proprioception, somatic sensation and hearing can each provide relative motion information between two or more objects. However, in order to provide a complete signal of the motion of the body and objects in the environment, these senses must be combined. Some of the types of combination that may be used with the spatial senses are reviewed in Howard (1997). A framework for such a combination is presented in Figure 1. In this framework, the motion of any node may be determined relative to any other node using those signals forming links between them, either singly or in combination. For example, the motion of an illuminated object in an otherwise dark environment may be calculated from signals of the object-on-retinae position, the eye-in-head position and the head-on-trunk position (Wertheim, 1994). Mathematically, the combination of signals in series in this way amounts to a cascade of co-ordinate transformations to account for differences in the origin and alignment of nested frames-of-reference (Mittelstaedt, 1998). This network of signals provides a level of redundancy, allowing the position of each node to be determined even when some of the individual signals are unavailable or unreliable, either through disease (Edwards,

1946; Bles et al. 1983) or environmental factors (Edwards, 1946; Plooy et al. 1998; Maurer et al. 2000).

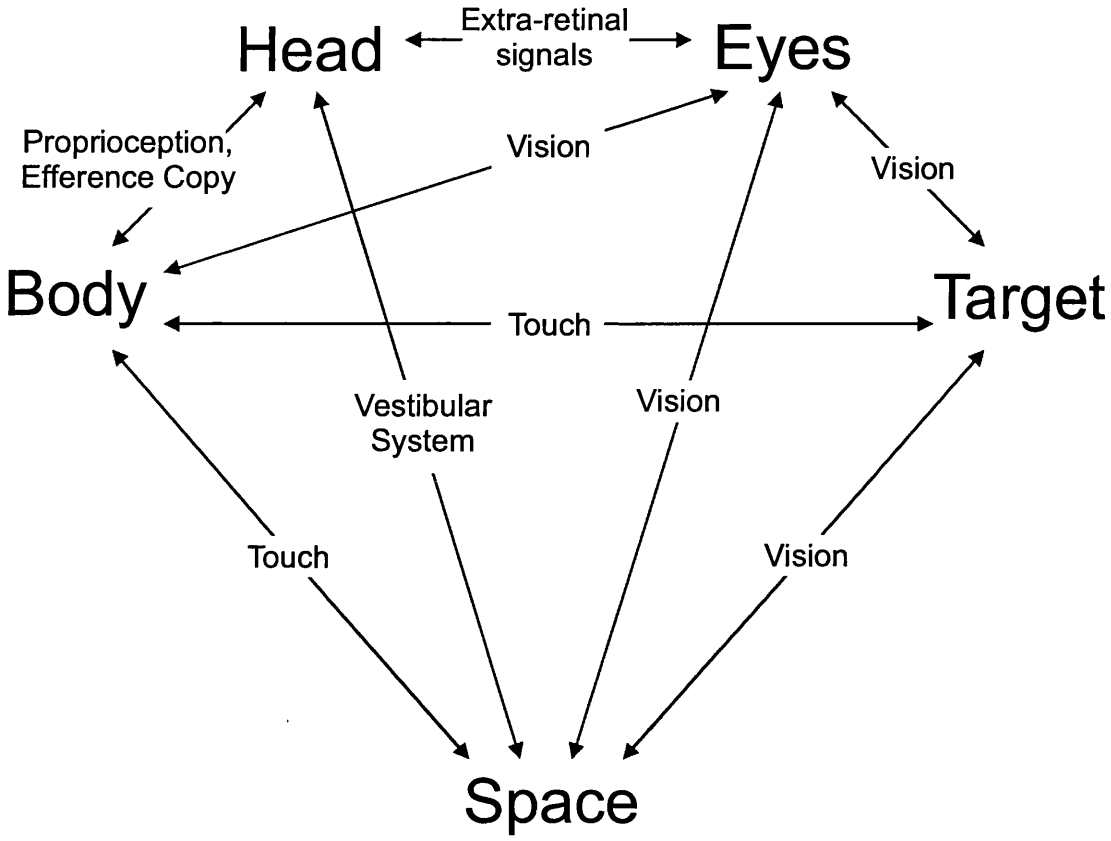

Figure 1: A simplified diagram of the inter-relation between body segments and the environment that may be involved in the determination of eye and target motion. Some connections in the diagram correspond to a physical link, e.g. Head-Body, with information signalling their relative motion. Whereas others, e.g. Eye-Space, do not represent a physical link, but signals providing information about their inter-relationship are available. For convenience, the Body is treated as an amalgamation of the limbs and the trunk; Touch refers to a combination of proprioception and other somatic senses and efference copy. Extra-retinal signals refer to just proprioception and efference copy for the eye muscles.

The Visual System

The usefulness of vision as an exteroceptive sense, i.e. for gathering information about the environment and objects within it, is self-evident. However, while there had for some time been evidence for the use of vision in self-motion perception (Tschermak, 1921) and in controlling movement (Edwards, 1946), it wasn't until Gibson (1950,

1954, 1966) that the concept of vision as a proprioceptive sense gained much attention. Gibson's suggestion was that there is a one-to-one relationship between the movements of the eyes in space and the resulting pattern of the optical array on the retinae, and therefore it should be possible to reconstruct the motion of the eyes from these retinal signals. This relationship holds under many conditions, but not all, most notably when the entire visual environment moves, which may give rise to a false perception of self-motion referred to as vection (Held et al. 1975; Dichgans and Brandt, 1978).

The Geometry of Optic flow

Gibson refers to the optic array on the retinae, which may be defined as the amount of light falling on each photoreceptor at each moment in time. Extracting motion signals from the optic array as it changes over time is not trivial and is referred to as the 'correspondence problem' (see Dawson, 1991) and amounts, roughly, to a two-dimensional cross-correlation of the optic array over time. Changes in the optic array on the retinae that are related to movement (as opposed to say, changes in colour) are referred to as optic flow and may take many forms. Assuming that the correspondence problem has been correctly solved, all the motion comprising the optic flow field must be a result either of self-motion or of object motion. Extracting self-motion signals from the form of the optic flow field is a difficult (sometimes impossible, see Warren and Hannon, 1988) task, as shown in Figure 5, that has attracted much research (see Visual Determination of Object Motion and Self-Motion in this chapter).

An optic flow field may be characterised by a number of fundamental components as shown for a fronto-parallel surface, in Figure 2. There are two zeroth order components, both consisting of lamellar flow: uniform vertical motion and uniform horizontal motion. At any instant these may, with equal validity, be considered to correspond to pitch and yaw rotations of the observer or vertical and horizontal translation of the observer. There are a number of interchangeable ways to categorise the four first order components, one example being expansion, rotation, deformation0 and deformation45. These roughly correspond to translation of the observer towards the scene or of the scene towards the observer; roll motion of the observer or the scene; and (in combination with expansion, see Figure 2) rotation of the scene or curvilinear motion of the observer about various axes perpendicular to the viewing direction. Higher orders also exist, but these can be considered to relate to non-rigid motion and the curvature of items in the scene and will not be considered further here. A more mathematical

treatment of this material may be found in Koenderink (1990), including the use of higher order components to establish orientation and curvature of visual surfaces.

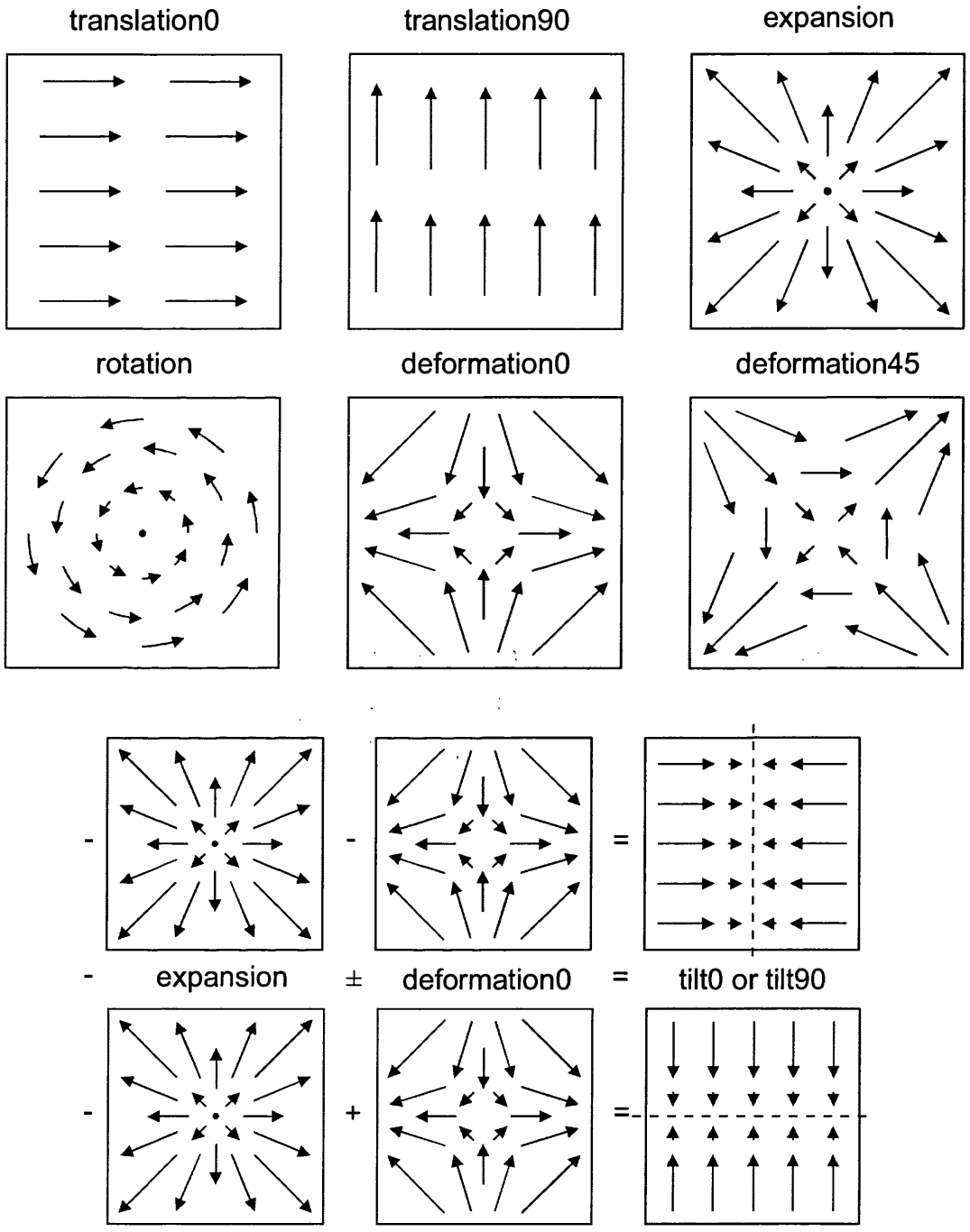

Figure 2: Zeroth and first order optic flow components of a moving scene (top). The lower panels show how expansion and deformation are combined to create tilt, which is of use to determine changes in the orientation of the scene (equivalent combinations of expansion and deformation45 result in tilt around axes at 45° to those shown here).

Gravito-Inertial Systems

A brief summary of their properties is included here, however for more information, a useful review of vestibular mechanisms may be found in Goldberg and Fernández (1975, 1984). Unlike the visual system, which detects self-motion indirectly via the relative position and motion between the eyes and the environment, gravito-inertial systems directly detect the accelerations acting on the head and body using the relative motion of internal components. There are two main consequences of this: the resulting signals are independent of the properties of the environment, and they are more sensitive to high frequency motion than low frequency motion. In humans, the main gravito-inertial receptors are the two vestibular organs in the head, consisting of the semi-circular canals and the otoliths, though there is also some evidence for other receptors in the trunk (Mittelstaedt, 1992; Mittelstaedt, 1996).

Semi-Circular Canals

There are three semi-circular canals in each vestibule: anterior, posterior and lateral, their axes being mutually orthogonal, thus allowing the detection of rotations around any axis. Each semi-circular canal is an otherwise continuous loop of fluid containing an enlargement called an ampulla, which is blocked by a flexible gelatinous mass called the cupula. When the rotational velocity of the head changes, the inertia of the fluid causes it to flow within the semi-circular canals. This deflects the cupula to the side and it is this deflection, picked-up by embedded sensory hair cells, that provides the signal of a change in rotation. During prolonged constant velocity rotation, fluid flow within the semi-circular canal gradually decreases and this restores the position of the cupula to its original position. The output of the hair cells also returns to resting baseline values. Consequently, the sensitivity of the semi-circular canals to low frequency and constant velocity rotations is poor, though this is improved by the neural circuitry of the 'velocity storage integrator' (Raphan et al. 1979).

Otoliths

There are two otolith organs per side, a Utricle and a Saccule, both of which detect linear accelerations. This is achieved by the maculae, which measure the shift in position of relatively dense statoconia suspended in fluid on a flexible gelatinous layer containing sensory hair cells. The orientation of the Utricle and Saccule are such that in combination they can signal linear acceleration in any direction. Unlike the semi-circular canals, the otoliths do have some sensitivity to constant and very low frequency

motions. One of these is a constant signal of the direction of gravity, or head tilt, as gravity is a constant acceleration (for a review, see Mittelstaedt, 1999). The other is measurement of constant speed yaw and roll rotation of the head using the difference in centripetal force acting on the otoliths on either side of the head (Mittelstaedt and Mittelstaedt, 1996).

Other Graviceptive Sources

As early as 1906, Trendelenburg hypothesised, from experiments on pigeons, the existence of additional graviceptors contained within the trunk. A number of studies have found evidence for graviceptive activity in the trunk in humans that have significant inputs into the postural system (Mittelstaedt, 1992; Mittelstaedt, 1996). These graviceptors are predominantly thought to be the kidneys due to the density difference between them and their capsules (Mittelstaedt, 1998) and the existence of afferent pathways terminating in the lateral reticular nucleus (Ammons, 1992). However, even in nephrectomized patients, there remains evidence for another graviceptor in the trunk (Mittelstaedt, 1998), possibly the large blood vessels (Erickson et al. 1976) or the entire abdominal viscera (von Giercke and Parker, 1994).

Proprioception, the Somatosensory System and Efference Copy

The proprioceptive and somatosensory systems are able to signal the relative position and motion between the body segments and objects that they are in direct contact with. The proprioceptive system is considered here to mean the combination of joint receptors, muscle spindles and Golgi tendon organs that are responsible solely for the elaboration of the relative position of the body segments. The somatosensory system is considered here to mean those sensory receptors contained within the skin that are responsible for the detection of the movement of objects across the skin. There is, however, overlap between these systems, with proprioceptive signals being incorporated into somatosensory signals in 'active touch' (Gibson, 1962), and with somatosensory signals from skin folding around the joints being incorporated into proprioceptive signals (Clark et al. 1979).

Efference copy is of a fundamentally different nature to proprioception and somatic sensation, being a copy of the outgoing muscle commands it is a signal of an intended action, not a signal in response to the outcome of an action. However, in the experiments in this thesis, all movements are active and so efference copy is never

dissociated from proprioceptive or somatosensory signals. As a consequence of this, these three signals are grouped together under the term 'Arthrokinetic' signals, and it is left for future experiments to elucidate their individual relations with respect to the effects described here.

These senses may signal self-motion by providing information about how the body is moving relative to objects in the environment. If an object is stationary, such as the ground, then a measure of the motion of the foot relative to it may be obtained from the somatosensory system and of the foot to the body using proprioceptive signals. Summing these signals using vector addition reveals the movement of the body relative to the ground, i.e. motion in space. This method relies on the stationarity of the contacted object, and that this contact is maintained, but under such circumstances is accurate and may override other signals of self-motion (Hlavacka et al. 1996).

Hearing

Hearing is primarily used to determine the presence, identity and position of noisy objects in the environment and the contribution of auditory cues as signals of self-motion is limited. However, this contribution is not zero, for example, their use in the control of posture has been demonstrated by Easton et al. (1998). However, in light of the limited use made of these signals, they will not be considered further here.

Multi-sensory Control of Posture

Posture refers to the neuromuscular control of the position and motion of the body and it's segments. For humans, the primary requirement of this control system is the ability to maintain an upright stance with respect to gravity. As an upright human is essentially a series of segments attached by flexible joints with a centre of gravity suspended above a small support base (Chow and Collins, 1995), there is no passive stability and postural control must be active both during locomotion and when standing still. This control system has as its inputs the various sensory systems mentioned above, and has as its outputs the force of muscle contraction in each of the skeletal muscles.

The information provided by each sensory modality may be unique or redundant with respect to other sensory modalities and have advantages and disadvantages for postural control. For example, the visual system provides a position signal relative to the environment, and so is not available in the dark or in environments lacking visual

contrast (e.g. a blizzard). The vestibular system is primarily effective at higher frequencies of sway, such as occur during sudden perturbation (Nashner, 1977; Diener et al. 1981; Nashner and Cordo 1981). The proprioceptive and somatosensory systems provide information about the position of body segments relative to each other and to a support surface (usually the ground), but may provide erroneous signals if the support surface moves, or is compliant. A consequence of the redundancies between signal sources is that the postural system can often still function in the absence of one or more signals. For example, in labyrinthine defective subjects (Fregly, 1974); in the dark or with the eyes closed (Bles et al. 1983); or when a subject's particular stance reduces cues from the support surface such as during the tandem Romberg test.

These redundancies are particularly important in resolving conflicting self-motion signals and during perceptual ambiguity. For example, during large-field visual motion, signals from the eyes may not be able to determine whether it is the environment that is moving or the subject. In this situation, the postural system must rely on signals arising from the vestibular and arthrokinetic systems. At other times, there may not just be a perceptual ambiguity in one sensory modality, as above, but in all modalities. For example, during constant velocity rotation around a vertical axis within a stationary visual environment, neither the visual nor the vestibular systems are able to determine the source of the resultant visual motion. This situation is in fact indistinguishable from being stationary but within a visual environment rotating around the same axis. In both these situations both perception of self-motion and perception of object-motion are equally valid. When environmental motion is erroneously perceived as self-motion it is termed Vection (Held et al. 1975; Dichgans and Brandt, 1978), and may result in postural adjustments (Dichgans et al. 1972; see Chapter 3: Accuracy of Reorientation of Visually Induced Sway during Vection).

The influence of visual (Edwards, 1946; Lee and Lishman, 1975; Lestienne et al. 1977; Stoffregen, 1986; Previc et al. 1993), vestibular (Nashner, 1971; Bisdorff et al. 1995), proprioceptive (Lund, 1980; Bronstein, 1996; Kavounoudias et al. 1999) and somatosensory (Jeka, 1994; Anastasopoulos et al. 1999) signals of self-motion have each received much attention and their individual properties well characterised. However, knowledge of their integration is less well understood, with some studies supporting a simple additive model (Roll et al. 1989) and others demonstrating effects of experience (Bronstein, 1986; Maki and Whitelaw, 1993). Whatever the details of the

integration of multiple sensory signals, there is wide agreement (Berthoz, 1981; Previc and Mullen, 1991) that manipulation of any of the above sources results in an altered central signal of self-motion and it is this which results in the postural responses observed.

Goals: Orientation and Equilibrium

Nashner and Cordo (1981), Amblard et al. (1985) and Roll et al. (1988) have all suggested that there are two primary goals for the human postural control system: orientation and equilibrium. Horak and Macpherson (1996) defined postural orientation as the positioning of the body segments relative to each other and to gravity. They defined postural equilibrium as that state in which all the forces acting on the body and its segments are balanced so as to maintain (static equilibrium) or achieve (dynamic equilibrium) the desired position and motion of the body and its segments. It should be evident that for each body segment, by staying as near as possible to such a balance point, less force needs to be exerted by the skeletal muscles to maintain posture. Similarly, an orientation may be chosen by the postural system (with the body in line with gravity) that serves to minimise the energy expenditure required to maintain upright posture. There is evidence using a statistical model of postural sway that the human postural system does indeed split the task of postural control in this way (Collins and De Luca, 1994). Interestingly, they proposed that it is more efficient (i.e. uses less energy) to allow a small quantity of spontaneous postural sway that it is for the postural control system to remove it altogether. Their explanation was that the input signals (from mechanoreceptors, etc.) are noisy, and so counteracting the noise in the signal with muscle activation uses more energy than is saved by being more accurately aligned against gravity. The amount of spontaneous postural sway can therefore be used as a simple measure of the noisiness of the afferent self-motion signals.

Signal Response Methodology

Treating the maintenance of posture like any other control system, there are two main ways to investigate its properties: an analysis of its spontaneous properties, and much more powerfully, changing the inputs to the system and measuring the resulting outputs.

Control of Spontaneous Sway

Rather than manipulating the sensory inputs to the postural system, for example by moving the visual scene, sway is investigated under natural conditions. In this way, the visual control of posture can be demonstrated quite easily by measuring the amount of sway when standing with the eyes open and with the eyes shut. Under these conditions, most people show a reduction in spontaneous body sway across all frequencies when the eyes are open (Dichgans et al. 1976; Lestienne et al. 1977).

This paradigm has been extended to investigate more detailed aspects of the visual control of posture (Lee and Lishman, 1975; Paulus et al. 1984; Kunkel et al. 1998), the use of the vestibular apparatus (Black and Nashner, 1985; Redfern and Furman, 1994; Peterka and Benolken, 1995), proprioception (Bles et al. 1980; Nougier et al. 1997), somatic sensation (Kotaka et al. 1986; Paulus et al. 1987) and the interactions between these signals (Day et al. 1993).

Experimentally Induced Sway

If the inputs to the postural system can be manipulated, and the outputs (sway) measured at the same time, then it is possible to relate one to the other and deduce how the postural system uses the input signal. For example, if a person is falling or leaning too far forward, their postural system will receive self-motion signals indicating that they are too far forward. The postural system will respond with corrective commands to the muscles to sway further backwards and this will cause them to decrease their inclination from the vertical until they are once-again standing upright. However, if during quiet upright stance, this person's signals of self-motion are manipulated, as in the classic moving-room paradigm (Lishman and Lee, 1973; Lee and Aronson, 1974; Lee and Lishman, 1975), then their 'corrective' response will in fact take them away from upright stance and cause them to lean backwards. We can then measure both the direction and the size of the inaccurate self-motion signal as of equal magnitude, but opposite direction to the resultant postural sway (Dichgans et al. 1975). In this way Lishman and Lee (1973), Lee and Aronson (1974), and Lee and Lishman (1975) demonstrated that vision is not purely an exteroceptive sense, but also a source of signals of self-motion as hypothesised by Gibson (1950, 1954, 1966). The moving room paradigm has since been used by many postural researchers, for example to investigate the effect of experience (Bronstein, 1986), flow structure (Stoffregen, 1985) and retinal location (Stoffregen, 1986).

Alternatives to the moving room for manipulating the visual input, include the real tilting room (Bles et al. 1980); artificial displays projected onto a surface (Lestienne et al. 1977; Fluckiger and Baumberger, 1988; Gielen and van Asten, 1990); and looking at a large textured disk, facing the subject and rotating around the axis of vision (Dichgans et al. 1972, 1975; Clément et al. 1985; Dijkstra et al. 1992). These have been used to investigate the influence of the speed of motion (Lestienne et al. 1977; Masson et al. 1995); temporal frequency of motion (van Asten et al. 1988a, b; Dijkstra et al. 1994; Giese et al. 1996); the spatial frequency of the display (Lestienne et al. 1977); visual conflict (Wolsley et al. 1996a) and the orientation of the visual motion (Stoffregen 1985; Gielen and van Asten, 1990; Wolsley et al. 1996a, b).

Orientation of the Signal Source

To be effective, the corrective responses of the postural system must reduce the disparity between the desired orientation of the body and the actual orientation of the body. A key requirement of this is that the corrective responses be in an appropriate direction. It is no use if the 'corrective' response to a detected backward sway is to sway more to the right: to reduce the disparity between actual and desired orientations the corrective response in this case must be forwards.

The task of matching the direction of the postural response to the direction of detected sway is made more complicated by the placement of the senses available for gathering the relevant self-motion information on different segments of the body. As is shown in Figure 3, the eyes may rotate relative to the head, which may rotate (and translate) relative to the trunk, which may rotate (and translate) relative to the feet. In turn this means that the visual, vestibular, proprioceptive and somatosensory signals that are integrated into the postural response must be reoriented (and possibly offset) into some common frame of reference. This common frame of reference is proposed to be that of the body part performing the action (Mittelstaedt, 1998). For example, during flexion of the ankles in the control of posture, the controlling sensory signals should all be converted into the frame of reference of the feet and support surface. For each component of a complex action this would require many frames-of-reference, as reviewed by Soechting and Flanders (1992).

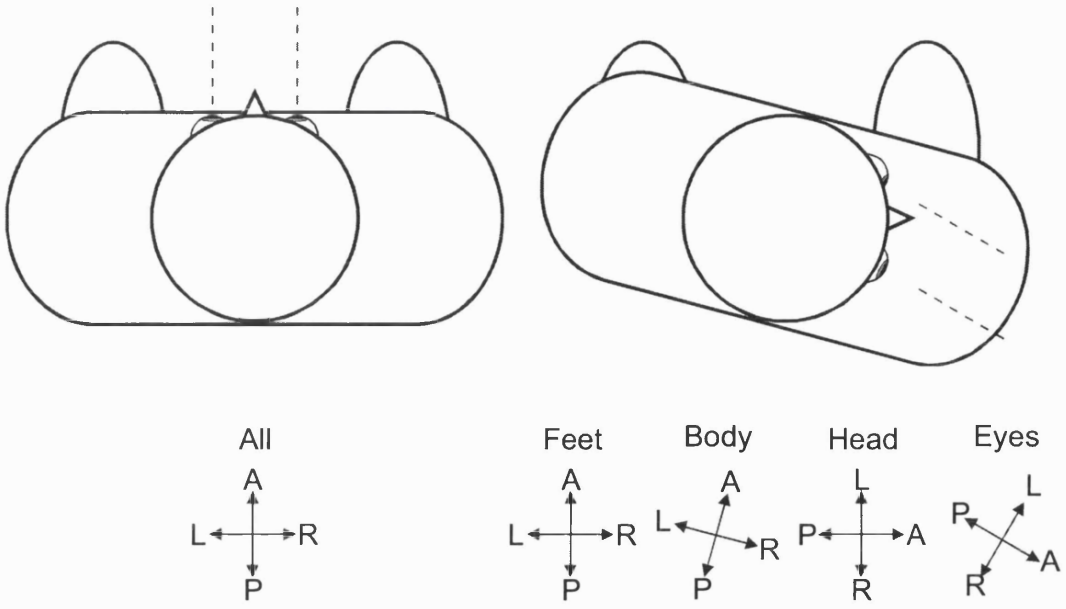

Figure 3: Self-motion signals during relative rotation of body segments. When the eyes, head, trunk and feet are all facing in the same direction (left), the relationship between both signals arising from, and actions mediated by, different levels is straight-forward. When the eyes, head, trunk and feet are rotated relative to each other (right) this relationship is less obvious. For example in the right diagram the head is rotated 90° relative to the feet: if the vestibular apparatus signals that the head is pitching forward, the correct righting response is not to press down with the toes, but to press down with the right foot. Labels are (A)nterior, (P)osterior, (R)ight and (L)eft.

Reorientation of Somatosensory Signals

Somatosensory signals arise from all over the body, with some requiring more or less reorientation than others. Signals of support pressure from the feet form a 'dynamometric map' that is used for human balance control (Kavounoudias, 1998). These signals are unique in postural control in that they do not *need* to be reoriented before they are used to control postural reflexes at the ankle. However, Hlavacka et al. (1992, 1996) found that use of information from the support surface in self-motion perception was gated by a comparison of such information with vestibular signals. If the support surface was deemed by this comparison to be moving then its contribution to self-motion perception was ignored. It is quite possible that such a gating may function in postural control.

On the other hand, signals of self-motion arising from the hands touching a stationary object must be tortuously reoriented to account for rotation of the many joints in the

arms before they can be used to control the activity of the ankle muscles. Nevertheless, reorientation of these signals and their use in postural control has been demonstrated by Rabin et al. (1999).

Reorientation of Vestibular Signals

The vestibular apparatus provide signals of head orientation and rotation with respect to gravity and linear acceleration. Using galvanic vestibular stimulation with rotations of the head to the right and left, Nashner and Wolfson (1974) demonstrated reversal of the postural response by signals of neck proprioceptive information. This was extended to composite rotations of the head and the trunk by Lund and Broberg (1983) who showed that this results in a galvanic sway response that is always in line with the inter-aural axis, i.e. complete reorientation of the vestibular signal into support surface co-ordinates occurs. These findings fit within a model of the transformation of vestibular information by neck position as part of an extended mechanism of co-ordinate transformations (Mergner et al. 1997).

Reorientation of Visual Signals

The eyes can extract self-motion signals from the optic array in line with Gibson's hypothesis (1950, 1954, 1966), but initially at least, these are in retino-centric co-ordinates and must be reoriented before they can be used by the postural system. Stoffregen (1985) inadvertently provided the first evidence that visual signals of self-motion are reoriented according to head rotations when investigating differences between the centre and periphery of the retinae with respect to postural control. These results were extended to include rotations of both the head and the eyes by Gielen and van Asten (1990), again using a projected corridor stimulus. Using the rotating disk type stimulus of Dichgans et al. (1972), Wolsley et al. (1996a, b) demonstrated this reorientation for a much larger range of eye and head rotations, both separately and in combination and proposed that it was mediated by proprioceptive signals from the neck. This was in line with a proposed proprioceptive chain from the feet to the eyes (Roll et al. 1989), the purpose of which is to tie together the other posturally relevant senses (Mittelstaedt, 1998).

Evidence of an additional, non-proprioceptive signal contributing to this reorientation of self-motion signals was produced by Gurfinkel et al. (1989). Using protracted head turning to adapt neck proprioceptors, they dissociated the subjects' imagined head position from the proprioceptive signal. By measuring the direction of the postural

response to galvanic stimulation in these subjects, they showed an influence of 'imagined' head position on the reorientation of the vestibular signal. Part of this thesis will investigate the role of such cognitive processes on the reorientation of visually induced sway (see Chapter 2: Reorientation of Visually Induced Sway During Whole Body Passive Rotation and Chapter 3: Accuracy of Reorientation of Visually Induced Sway during Vection).

Visual Determination of Object Motion and Self-Motion

Vision is used both as an exteroceptive sense, being used to estimate the properties, e.g. motion, of other objects in space, and also as a proprioceptive sense, providing a signal of self-motion (Gibson 1950, 1954, 1966). Both of these functions must be carried out both when the eyes are stationary and when they are moving (both relative to the environment and relative to other parts of the body), but the visual consequences of object and self-motion are far from independent.

Object Motion

The retinal signal from the eyes provides a signal of the position and movement of visible objects relative to the eyes themselves. When the eyes are stationary, this retinal signal also corresponds to the motion of the object in space. However, when the eyes are moving, the retinal signal would provide an erroneous measure of object motion in space (see Figure 4). Consequently, during eye motion, object-motion in space must be reconstructed as the vector sum of object-motion relative to the eyes (the retinal signal) and of eye motion in space (Mach, 1886; von Helmholtz, 1896). Mach and von Helmholtz both proposed the use of signals of the effort of 'will', in modern parlance, 'efference copy' as this signal of eye motion. However, since Gibson (1950, 1954, 1966), signals of the motion of the visual background across the retinae have also been considered to signal eye motion. When estimating eye motion, some studies have supported the need for an extra-retinal signal (Wertheim, 1981; Pola and Wyatt, 1989; Turano and Heidenreich, 1993; Freeman, 1999) and others have supported the sufficiency of the retinal signal (Andersen, 1990; Heeger and Jepson, 1990; Royden et al. 1994). However, in response to problems with both theories, an extension to the extra-retinal signal was proposed by Wertheim (1994) in which the eye position was in part determined by vestibular signals of the head position. This system corresponds to the Space - Head - Eyes - Target portion of Figure 1.

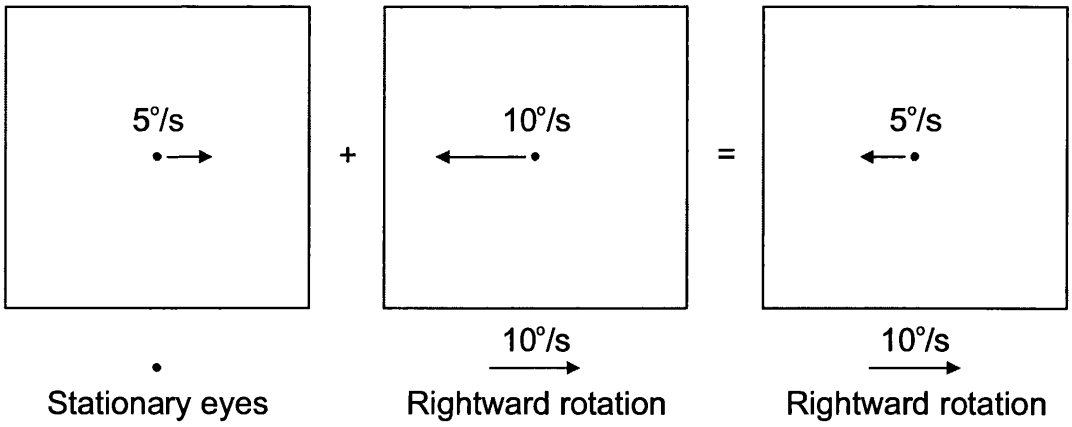

Figure 4: Object motion across the retina with and without eye rotation. When the eyes are stationary (left), the motion of an object across the retinae is directly related to the motion of the object in space. When the eyes are rotating, then the motion of an object across the retinae is only partly related to its motion in space. In this example, the eyes rotate to the right twice as fast as the object itself moves. The result is that the object moves on the retinae in the opposite direction to the direction in which it is moving in space. If the movements of the eyes are not somehow taken into account then this visual information coming from the eyes will be misleading.

If the signal(s) of eye motion are accurate, the perception of object motion should be the same during eye movements as with the eyes stationary. However, Fleischl (1882) and Aubert (1886) found that this is not the case, they observed that object motion in the absence of a background appears to be faster when the eyes are stationary than when the object is being pursued, now known as the Aubert-Fleischl phenomenon. A related phenomenon is found when pursuing a target against a background, in this case the background itself appears to move in the opposite direction to the eye movement (Filehne, 1922). Both of these phenomena indicate that the retinal signal is overestimated relative to the signal of eye motion, though which is more accurate is open to debate (see Howard, 1982).

Heading

The proprioceptive function of vision, as proposed by Gibson (1950, 1954, 1966), should ideally extract a set of self-motion signals corresponding to all of the six degrees of freedom of a body in space. The most studied aspect of this extraction is the direction of linear motion, or heading (see Lappe et al. 1999 for review), as distinct from rotation around an axis, such as occurs during head rotations or eye movements. Extraction of

heading provides a fundamentally useful signal for tasks such as navigation (Barinaga, 1996; Chance et al. 1998), walking to a target (Warren et al. 2000) and driving (Readinger et al. 2001).

All motion in three dimensions may be decomposed into six fundamental movements: translation along each axis; and rotation about each axis. Pure translational self-motion results in the characteristic optic flow pattern shown in the left panel of Figure 5 with expansion away from the heading direction, lamellar flow around the side, and then contracting flow behind the subject. If the whole optic flow field is visible then extracting the direction of travel (the heading) becomes a question of finding the line through both the centre of expansion and of contraction (Koenderink, 1990). Pure rotational self-motion results in the characteristic optic flow pattern shown in the right panel of Figure 5 where the visual motion rotates around the axis of rotation in the opposite direction to the self-motion. Again, if the whole optic flow field is visible then extracting the axis of rotation becomes a question of finding the line through both centres of rotation (Koenderink, 1990).

In practise humans can never see the whole optic flow field at once: we only have two eyes, each with a limited field-of-view (~160° × ~175°, horizontal × vertical), and they look in almost the same direction (total field-of-view: ~200° × ~175°). Additionally, the quality of this information is only high in the centre of vision, further reducing the usefulness of the retinal signal. When only a limited portion of the optic flow information is available, then the visual motion resulting from translation may resemble that from rotation. For example in Figure 5, looking to the side during forward motion results in a lamellar flow field (lower right face of the cube in the left panel) and looking to the side during rotation about a vertical axis results in a similar lamellar flow field (lower right face of the cube in the right panel). This forms a serious limitation to the use of visual information to determine self-motion in the manner Gibson suggested (1950, 1954,1966).

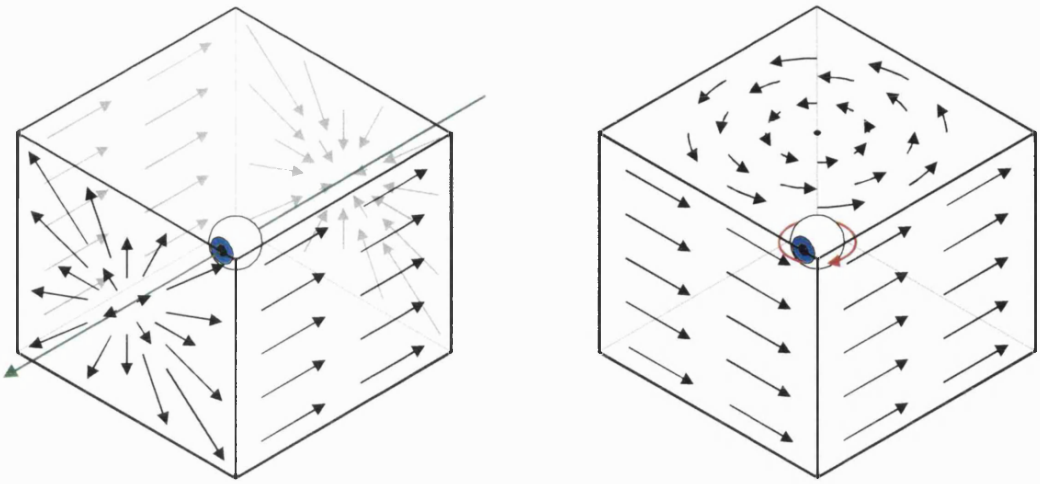

Figure 5: The geometry of optic flow during forward motion and yaw rotation. A person (represented by the eyeball) moving within the environment will see different patterns of optic flow depending on the type of movement they are making and the direction in which they are looking. For a person travelling in a straight line (green), if they are looking along the direction of travel, then they will see objects expanding outwards from the centre of view (front left face of the left cube). However, if they are looking to the side at 90° to the direction of travel, then they will see objects all moving past in the same direction (front right face of the left cube). For a person rotating (red) about a particular axis, then if they are looking along the axis of rotation they will see rotation of objects in the environment (top face of the right cube). However, if they are looking to the side at 90° to the axis of rotation, then they will see objects all moving past in the same direction (front faces of the right cube).

In fact, even when the limited field-of-view includes the point of expansion, concurrent eye rotations disguise its direction from the observer. In Figure 6, the effect of a concurrent rightward eye rotation on the perceived direction of the focus of expansion can be seen. The visual motion vectors at each point on the retinae resulting from the two types of motion are summed to produce the visual motion vectors when the movements are combined. The net effect is that the focus of expansion is shifted in the direction of the eye rotation and no longer corresponds to the direction of travel.

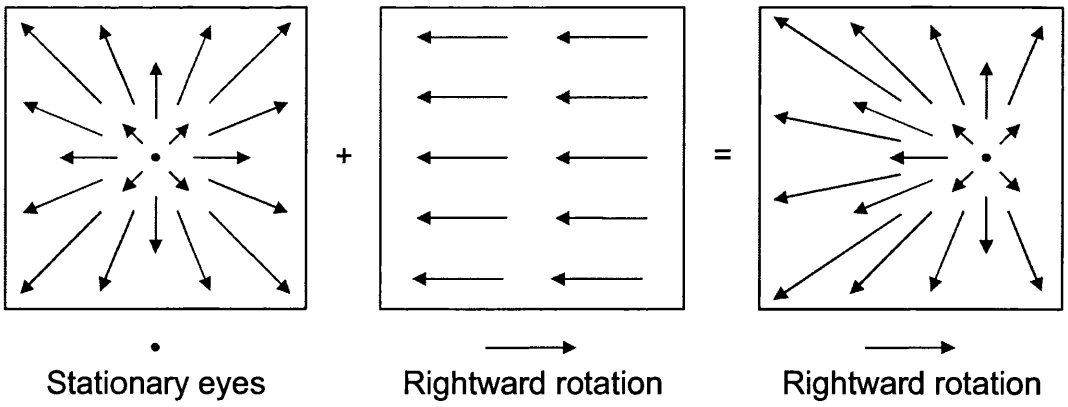

Figure 6: The optic flow pattern during forward motion with and without eye rotation. When the eyes are looking in the direction of travel and not rotating, objects will appear to expand away from the centre of vision (left panel, cf. Figure 5, left panel). When the eyes are rotating in a stationary environment, then objects will appear to move past in the opposite direction (centre panel, cf. Figure 5, right panel). During forward motion, when the eyes are also rotating, even at the moment when the eyes are looking along the direction of travel (i.e. they are looking in the same direction as in the lefthand panel), the motion of the environment on the retinae will be distorted such that the focus of expansion has moved on the retinae (righthand panel).

Three theoretical approaches to solve these problems are to use extra-retinal signals of eye movement; to use the differential motion of scene components at different depths; and to integrate visual trajectories over time. Changes in perception between conditions with and without eye motion, but with identical retinal flow have been taken as support for the use of extra-retinal signals (Banks et al. 1996; Crowell et al. 1998; Van den Berg, 1996; Warren, 1998). When presenting visual motion replicating the retinal flow field that would result from rectilinear self-motion combined with an eye rotation, a number of studies have demonstrated accurate self-motion perception (Cutting et al. 1997; Stone and Perrone, 1997; Van den Berg, 1992; Van den Berg, 1993; Van den Berg and Brenner, 1994; Warren and Hannon, 1988). These have been taken to support the sufficiency of the retinal signal for heading detection. However, the visual scenes used in these studies all contained depth information. When there is no depth information in the scene, the accuracy of heading perception drops (Royden et al. 1994; Warren and Hannon, 1990) suggesting that depth information normally helps heading perception. Another experiment (Royden et al. 1992) showed that heading perception without extra-retinal signals was only accurate during relatively slow eye movements,

and this was taken as evidence that the use of depth information depended on the speed of the eye movement. The authors did not, however, say whether when changing the eye movement speed, they maintained a constant movement size or a constant movement time. If the former were the case, then the improvement in results with slower eye movement speeds may actually be due to the longer observation times used, allowing the use of changes in retinal flow over time.

These experiments have resulted in a number of theoretical models of how heading is derived from the retinal flow signal, reviewed in Lappe et al. (1999). These models fall into two camps: template models (Perrone, 1992; Perrone and Stone, 1994; Zemel and Sejnowski, 1995; Perrone and Stone 1998) and models using a subspace algorithm (Heeger and Jepson, 1990; Lappe and Rauschecker, 1993). Essentially, in template models, each component of the optic-flow: rotation, expansion, etc. is extracted separately from the others; whereas in subspace algorithm models all components are extracted together by neurones forming a population encoding. Both types of model may be extended to integrate retinal and extra-retinal signals, e.g. van den Berg and Beintema (1997) for the template models.

The Requirement for Extra-Retinal Signals of Eye Motion

A primary requirement of the visual system is that we must be able to use the information that arrives at our retinae regardless of whether we are at rest or moving. This in turn requires a robust signal of eye motion in space, which could be derived from the retinal signal or from extra-retinal sources. Available evidence suggests that both retinal and extra-retinal signals of eye motion are used in the determination of both object motion and of heading, increasing the robustness of the resulting signal. What is less clear from the existing literature, is the nature of this extra-retinal signal. Mach (1886) and von Helmholtz (1996) both proposed the use of efference copy as this signal of eye motion. Roll et al. (1989) has supported the use of extra-ocular muscle proprioception. Wertheim (1994) has supported the use of vestibular signals to provide a more general 'reference signal' and Crowell et al. (1998) have provided evidence for the integration of neck proprioceptive signals. Additional components of this expanded extra-retinal signal, corresponding to portions of Figure 1, will be considered in detail later in this thesis.

Aims of this Thesis

A number of interactions between the spatial senses are investigated in the following chapters, that are proposed to add weight to the notion that the senses do not act in isolation, but as a coherent whole as described in Figure 1.

In the first experimental chapter (Chapter 2), the reorientation of a visually evoked sway response as demonstrated by Wolsley et al. (1996b) was investigated further. In the experiments of Wolsley et al. the postural response to a roll motion rotating disk was shown to be aligned to the direction of visual motion even when the eyes and/or head were rotated relative to the feet. Using a similar visual stimulus, but presented in dark surroundings and in such a manner as to reduce cognitive cues as to its orientation relative to the subject, the results are compared to those of Wolsley et al. to determine the influence of visual and cognitive cues on postural sway reorientation.

Chapter 3 uses the same roll motion visual stimulus as Wolsley et al. (1996b) and again investigates the accuracy of the alignment between the visual stimulus motion and the induced postural sway. The comparison in this chapter is between the accuracy of this sway response when the subject perceives veridical object motion or illusory self-motion (vection). This provides an alternative measure of the use of cognitive processes in the reorientation of sway responses compared to the experiment presented in Chapter 2.

Chapter 4 investigates the use of arthrokinetic information in the processing of vision, by measuring visual motion perception with varying amounts and types of arthrokinetic signals. The first experiment investigates the influence of arthrokinetic signals of walking on the perception of the speed of expansion of a virtual reality tunnel. The next four experiments are controls for attention, memory, head motion and changes in timing perception. The following experiments then investigate how this effect extends to other types of self-motion, the direction of self-motion, other optic flow patterns, the relative orientations of self-motion and visual motion and tries to quantify the effect by specifying the scale of the visual scene. Finally, a hemianopic blindsight patient is investigated in order to shed light on the neurological locus of the mechanism that is proposed to be responsible for these effects.

Additional introductory comments, specific to the rationale of each of these experiments will be presented at the beginning of each chapter.

Chapter 2: Reorientation of Visually Induced Sway During Whoie Body Passive Rotation

Abstract of Chapter

Visually evoked postural responses (VEPR) to a roll-motion rotating disk were recorded from normal subjects standing on a yaw axis motorised rotating platform. The disk was fluorescent so that subjects could be tested in an otherwise dark room. Movements of the head and centre of foot pressure were measured whilst subjects looked at the disk with eyes and head in the primary position and whilst the rotating platform moved the subjects randomly to 0, ±45 and ±90° angles from the visual stimulus. Subjects were instructed to maintain fixation on the centre of the rotating disk but the amount of horizontal eye and head movement used was not specified. Platform rotational velocity was set near threshold values for perception of self-rotation (~2°/s) so that subjects would find it difficult to reconstruct the angle travelled. The data showed that the VEPR occurred in the plane of disk rotation, regardless of body position with respect to the disk, and despite the subjective spatial disorientation induced by the experiment. Averages of the response revealed a good match (gain = 0.95) between disk orientation and sway direction. The horizontal gaze deviation required to fixate the centre of the disk was largely achieved by head motion (head 95%, eye 5%). The results confirm previous studies that VEPRs are reoriented according to horizontal gaze angle. In addition, we show that the postural reorientation is independent of cognitively or visually mediated knowledge of the geometry of the experimental conditions. In the current experiments, the main source of gaze position input that was required for VEPR reorientation was likely to be provided by neck afferents (Nakamura and Bronstein 1995). The results support the notion that vision controls posture effectively at any gaze angle and that this is achieved by combining visual input with proprioceptively mediated gaze-angle signals.

Introduction

Vision is used in conjunction with proprioceptive and vestibular signals for spatial orientation and balance control. If a subject, standing upright and looking straight ahead in a room, spontaneously starts to fall to the right, the optic flow will be to his/her left. The correct righting response for the subject in this case is to increase the pressure on

the right foot and decrease it on the left, such that the change in forces act to rotate the subject's body leftwards. The usual cause of large-field visual motion is the movement of the retina in space; therefore the subject treats large-field motion as if it was due to self-motion. If this retinal motion is simulated by a visual scene moving to the left when the subject is in fact upright, then the change in pressures at the feet will act to destabilise the subject to the left, i.e. in the same direction as the visual motion. The response to a large-field moving stimulus is therefore to sway in the same direction in space as the visual motion (Dichgans et al. 1975, Clément et al. 1985, Bronstein 1986).

A common feature of many previous experiments is the use of visual motion stimuli that are viewed by the subject looking straight ahead, i.e. with both the eyes centrally placed in the orbits and the head centrally placed on the shoulders (Dichgans et al. 1975, Clément et al. 1985, Bronstein 1986). However, Wolsley et al. (1996a, b) investigated the effect of supplying identical retinal inputs with the eyes and head at different positions in the yaw plane. It was found that subjects reoriented their main direction of sway, so as to match the direction of the visual stimulus, for a variety of combinations of head-on-trunk and eye-in-orbit positions. However, this experiment was run in a well-lit visual environment, with subjects instructed to position themselves actively. Thus subjects may have been able to determine their orientation, and that of the visual stimulus, both visually and cognitively. Herewith, we examine whether accurate reorientation of the VEPR still occurs during passive body rotation and with diminished visual/cognitive cues.

Methods

Eight normal subjects aged between 21 and 33 years of age were instructed to stand relaxed, with arms at their sides, binocularly fixating the centre of a visual display (see Figure 7). The visual display consisted of a large disk of diameter 0.9m positioned 40cm from each subject's nasion at eye level, such that it covered a large area of the subject's visual field (97°). This disk was viewed in the dark and was covered in randomly distributed fluorescent circles of 2cm diameter with a mean density of $320m^{-2}$ (16% of disk area) and could be rotated around the visual axis at an angular velocity of 40°/s either clockwise or anti-clockwise. Acceleration of the disk took less than 4s (less than 2s to 95% of final speed) and deceleration of the disk took less than 2s. The visual environment was otherwise completely dark.

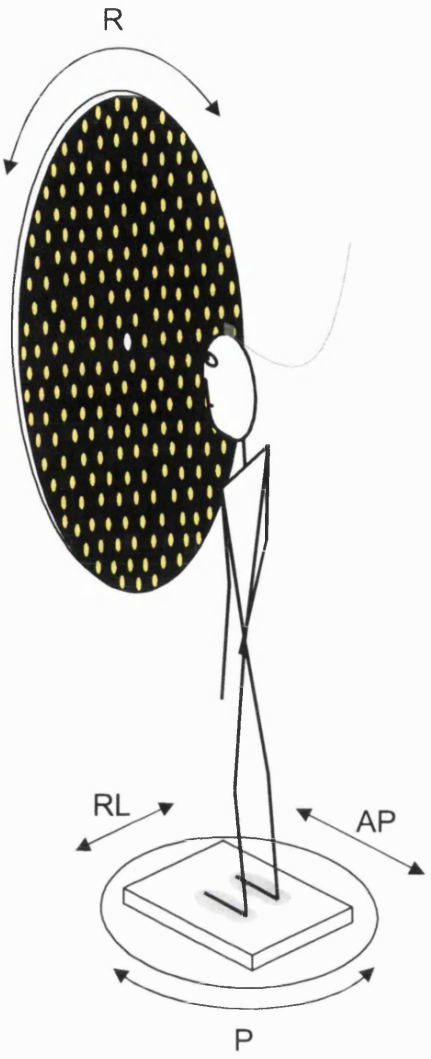

Figure 7: The Experimental Set-up. Subjects stood upon a posturography platform that measured the position of the COP along the anterior-posterior (AP) and right-left (RL) axes and which was itself supported upon a movable turn-table that could rotate along P. Subjects also wore the receiver of a 3D position sensing device on their heads (grey). The subjects viewed the centre of a large disk covered in luminous spots that could be rotated around R.

The subjects stood on a posturography platform (internal malleoli 3cm apart), which measured the position of the centre of foot pressure (COP) in the anterior-posterior and lateral directions. A 3-D magnetic search coil system (Polhemus 3space Fastrack) measured head position linearly in the anterior-posterior and right-left directions and yaw rotation. Horizontal DC electro-oculography was used to monitor that subjects fixated the centre of the disk and to reveal the relative extent of the head-on-trunk and eye-in-orbit rotations. The posturography platform was mounted on an externally

controlled rotating platform moving smoothly about a vertical axis at 2deg/s. This is near the reported values for perception of rotation (Hulk and Jongkees 1948, for review see Jongkees 1974). Pilot studies indicated that most subjects could not perceive being rotated with eyes closed at this speed. The visual stimulus could thus appear anywhere between -90° (left) and +90° (right) relative to the subjects' trunk mid-sagittal plane.

During a trial, each subject started facing the disk at one of five platform positions: -90°, -45°, 0°, +45°, or +90°. The stimulus sequence comprised the following contiguous periods (see Figure 9):

1) Stationary platform and stationary disk (15s)

2) Stationary platform with a rotating disk (30s)

3) Rotating platform and rotating disk (22.5-90s, depending on amplitude of platform rotation)

4) Stationary platform with a rotating disk (30s)

5) Stationary platform and stationary disk (15s)

The use of continuous rotational stimuli (which may result in adaptation and consequent alteration of the results) rather than transient stimuli (in which this is less likely) was chosen for three reasons:

- To reduce the influence of cognition, an 'unexpected' i.e. unpredictable trial sequence was required, and one of the means of achieving this was to rotate the subject relative to the disk during the disk rotation. A result of this is the long continuous stimuli during which adaptation may occur.

- The second reason is that transient stimuli (if they are truly transient rather than short continuous stimuli) induce smaller responses and therefore must be repeated and the mean calculated. Unfortunately, postural responses are very quickly suppressed when the invoking stimulus is repeated (Bronstein, 1986), therefore anything that reduces the number of repetitions also reduces this source of error.

- To maintain a greater degree of consistency with the experiments described in Wolsley et al. (1996a,b), thus allowing better comparison between those experiments and the current study.

There were 40 different possible trials: two disk rotation directions by five positions for the start-point by four positions for the end-point of platform rotation. Each subject experienced ten different trials in a Latin-square paradigm, the first trial starting and the last trial ending with the disk straight ahead. Trials were separated by one-minute intervals to ensure any residual sway from the previous trial had decayed, during which time subjects remained in the dark to prevent them from using visual cues to determine their orientation.

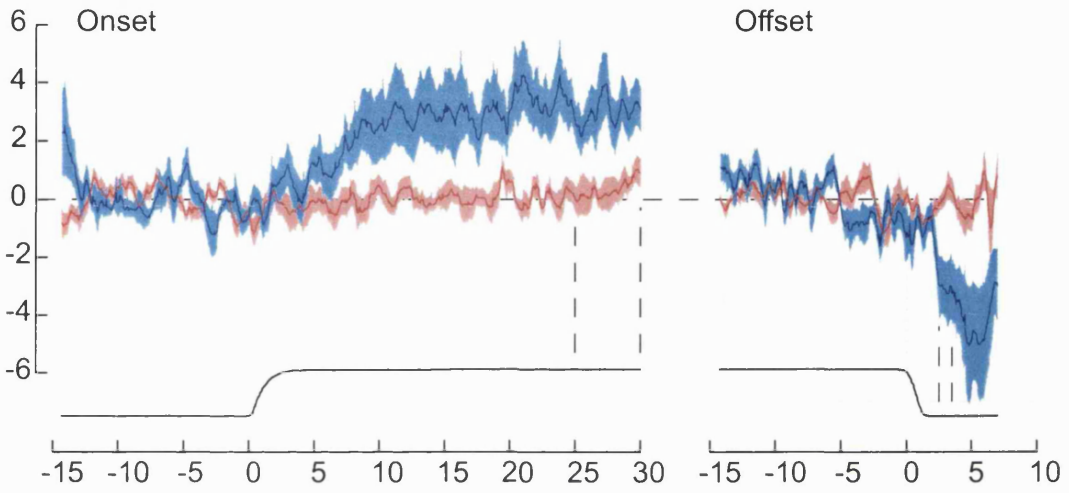

Figure 8: Mean ± s.e.m. COP data from all subjects aligned to show the onset and offset responses. Data is the intersubject average from all trials where the disk position and motion direction was -90° (left of the subject) and CCW during onset or offset. Blue traces are anterior-posterior, red traces are right-left (positive is anterior and rightwards). All traces are aligned such that the 15s base-line periods prior to disk rotation onset or offset (between the small dashed lines) are zero. The periods used to calculate the VEPR position are between the large dashed lines. Time is in seconds relative to the start of disk rotation or end of disk rotation (bottom trace).

All signals were sampled at 125 Hz and analysed off-line. COP was arithmetically normalised to represent the signal given by a 70kg mass. From Figure 8 it can be seen that the onset sway response is mush slower than the offset sway response, consequently the offset sway response was measured over a shorter time-span than that for the onset response. Five seconds of the onset response (mean position between 25 and 30s after the start of disk rotation) were measured, relative to the mean position during the 15s base-line period before disk rotation. For the offset response, one second was measured (mean position between 1 and 2s after cessation of disk rotation), relative to the mean

position during the 15s base-line period before cessation of disk rotation. Based on these position measurements, the average orientation of the VEPR was then calculated for all subjects at each onset or offset condition, e.g. for clockwise disk rotation at +45° platform position. In order to control for the effects of platform rotation in isolation, four of the original eight subjects were each rotated six times between -45° and +45° and vice-versa at 2°/s whilst fixating the stationary visual display. This control experiment showed that the subjects' COP shifted to the left or to the right by 1.05 ± 0.88cm (mean ± s.d.) for anti-clockwise and clockwise rotations (as viewed from above) respectively. Due to the randomisation process for disk and platform rotational direction this bias would be cancelled out in the main experiment.

Results

Signals of head yaw and horizontal eye positions showed that the steady state reorientation of gaze for all subjects was mainly due to rotation of the head on the trunk (95%, s.d. 5%) with the remaining 5% performed by the eyes. During subject rotation, the proportion of movement carried out by the eyes sometimes exceeded this until further rotation of the head occurred. Subjectively, subjects were unsure of the relative position between themselves and the visual stimulus; some reported disorientation.

Figure 9 shows raw sway platform traces from one subject (JB) during the condition where the disk started at a position of -45° (to the subject's left) before moving (relative to the subject) to +45° (to the subject's right). The traces show the onset of the VEPR, with forwards and rightwards sway, approximately 25 seconds after the start of the trial. As the platform rotates rightwards (between arrowheads, Figure 9) there is a reorientation of the COP from a right-anterior to a right-posterior position. On cessation of disk rotation (last arrow) the COP moves anteriorly and partly leftwards towards the original base-line position. Results for movements of the head are similar to those for movements of the COP and so are only summarised briefly where relevant.

VEPRs were normalised for each trial with respect to a 15s period preceding the onset or offset of disk rotation. The orientations of the VEPR (direction S, see Figure 10) at onset and offset of disk rotation were converted into degrees and compared to the direction of disk motion (direction D, see Figure 10) at onset and offset. The directions of the VEPR at both the onset and offset of disk rotation were measured for COP signals for all conditions. These are shown for a single subject in Figure 11 where a strong

reorientation of the VEPR by direction of disk motion can be seen (similar plots for each individual subject are in Appendix C). Each subject's sway reorientations were summarised by calculating the gain between the direction of sway S and the direction of disk motion D. Individual subjects showed gains of reorientation of VEPR at the onset of disk rotation of between 0.8 and 1.18 and gains at offset were between 0.45 and 0.95

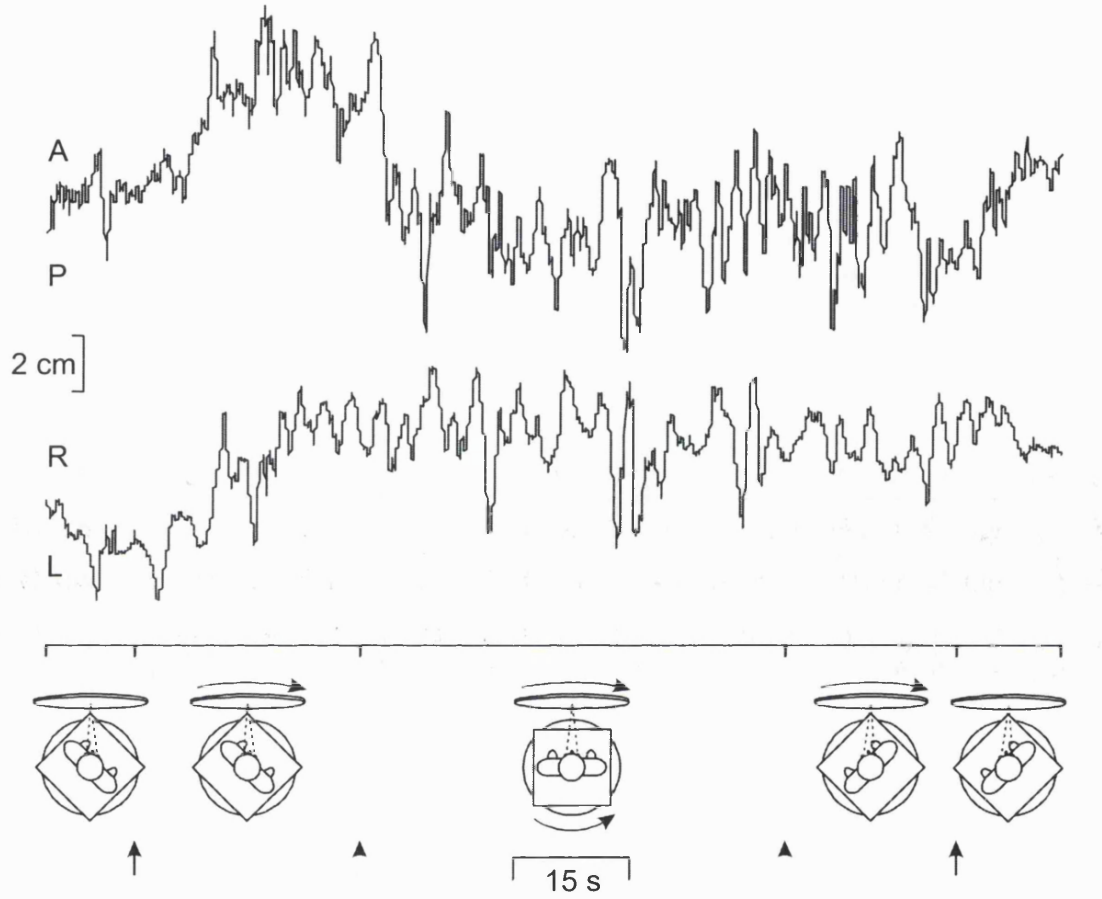

Figure 9: Raw COP data from a single trial for a single subject. Data is from subject JB for the condition with clockwise disk rotation, starting condition at -45° (left) and ending at +45° (right) relative to the subject, the two traces show the anterior-posterior (A-P) and right-left (R-L) movements of the COP. The period of disk rotation is shown between the arrows and platform rotation between the arrowheads. The sequence of events is also represented by the icons below.

The results for all subjects are shown in Figure 12, where the best-fit curves for all subjects reveal the gain of the VEPR reorientation at onset to be around unity ($y = 0.96x + 6.0$, $r^2 = 0.82$, as measured at the COP, and $y = 1.01x + 3.0$, $r^2 = 0.80$ measured at the level of the head; where x and y are visual motion and sway directions respectively).

The offset response had a gain of around 0.83 ($y = 0.68x + 8.0$, $r^2 = 0.58$ as measured by the COP, or $y = 0.98x + 1.8$, $r^2 = 0.82$ as measured at the level of the head). Variability of the computed gains of reorientation were computed using the following equation:

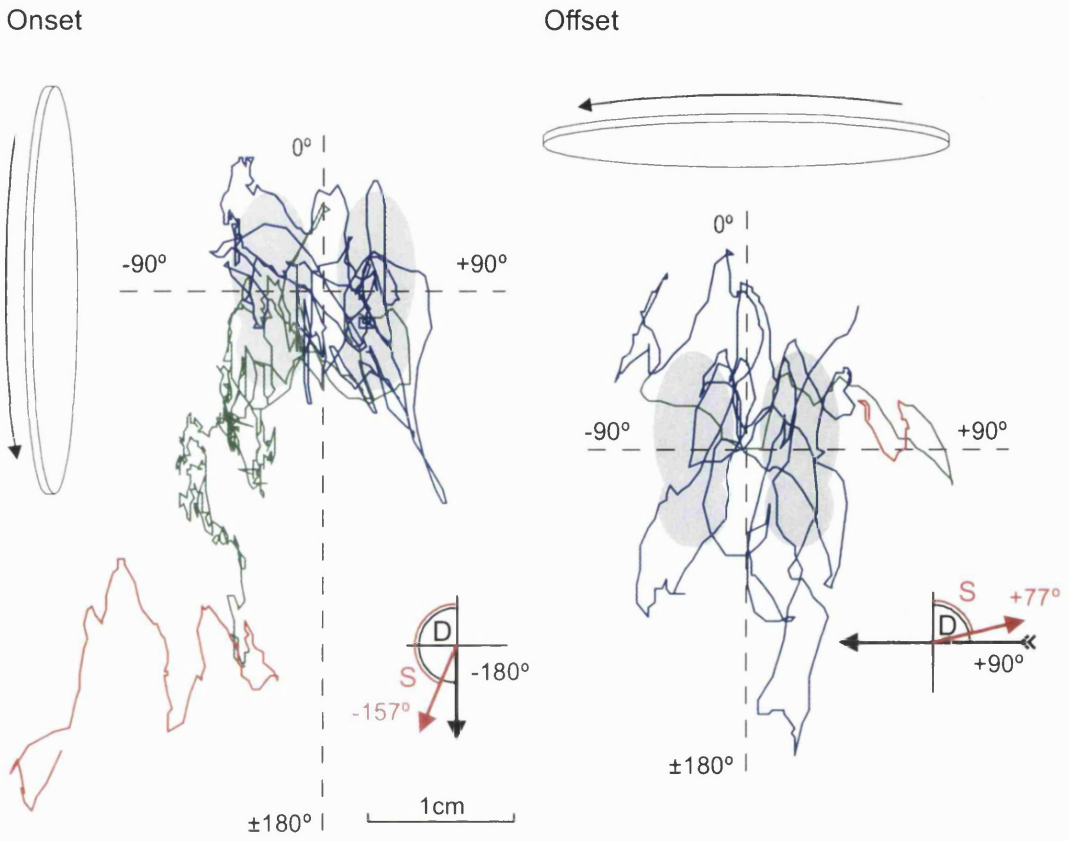

Figure 10: Spaghetti plot of a single trial for a single subject (JB). Coloured lines represent the position in the horizontal plane of the COP over time. The lines are coloured blue during the base-line periods, green during the transitional periods and red during the response periods. The directions were calculated between the mean base-line (blue) and mean response (red) periods and compared to the directions of disk motion (inset figures). The inset figures show the sway directions S (red) and the directions of disk motion D (black). These directions are compared directly for the onset, but the direction of disk motion D is reversed during the offset comparison (see Discussion).

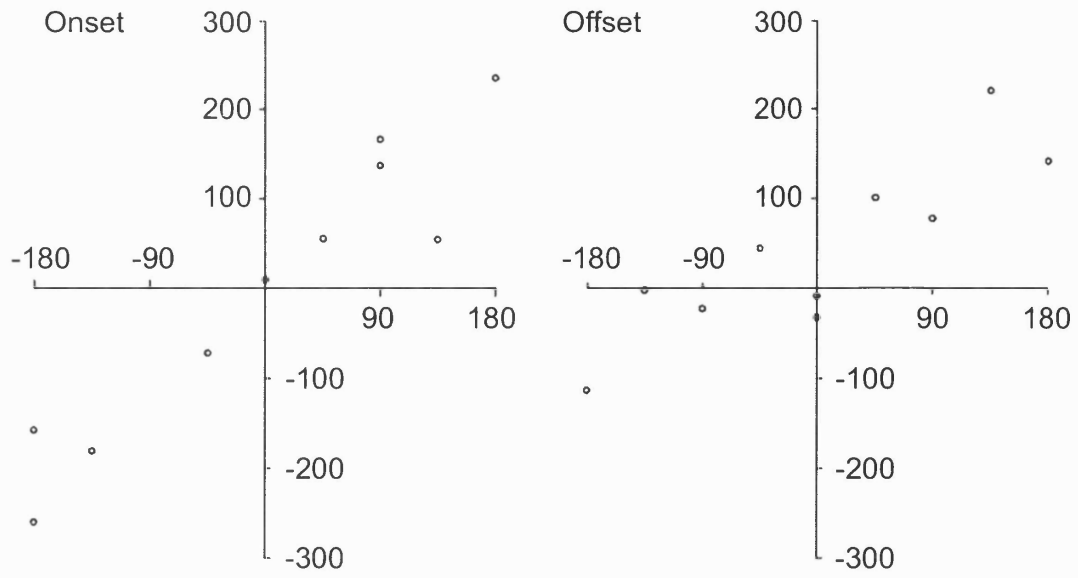

Figure 11: Scatter plot of all data for a single subject (JB). Direction of sway S (vertical axis) as measured by the position of the COP (see Figure 10) plotted against D, the predicted sway direction (horizontal axis). For the onset response (left) D is the direction of disk motion, for the offset (right) response D is the opposite direction. All values in degrees, with zero corresponding to the direction of the subject's toes, positive angles denoting sway to the right and negative angles sway to the left.

$$\sigma_a^2 = \frac{\sigma_e^2}{(N-1)\sigma_x^2}$$

Equation 1: Variance of the slope of a linear regression curve. Where a denotes the slope and the error variance was computed as:

$$\sigma_e^2 = (1-r^2)\sigma_y^2$$

Equation 2: Variance of the regression error.

Thus the onset VEPR reorientation gains were 0.96 ± 0.05 (mean ± s.e.m.) and 1.01 ± 0.06 for the COP and head respectively. The offset VEPR reorientation gains were 0.68 ± 0.07 and 0.98 ± 0.05 again for the COP and head respectively. These values (apart from for the offset condition measured by the COP, see Discussion) were not significantly different (two-tailed t-test; $p > 0.05$) from the figures of 1.02 ± 0.05

(calculated from published diagrams; mean ± s.e.m.) obtained from Wolsley et al. (1996b).

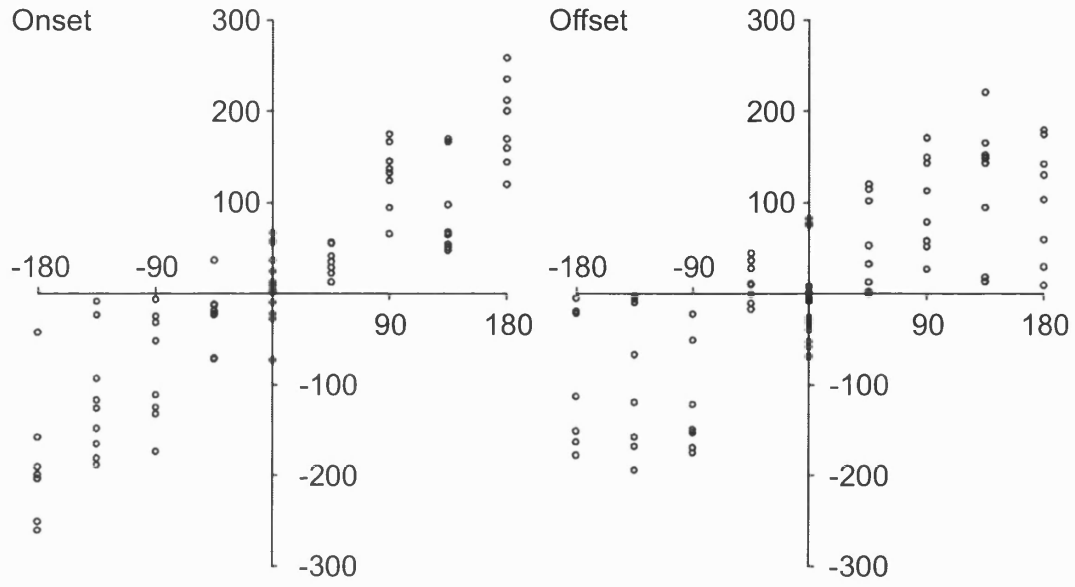

Figure 12: Scatter plot of all data from all subjects (amalgamation of plots in Appendix C). See Figure 11 for explanation. Data points for each of the onset and offset conditions are composed of 2 series: those with CW disk rotation and those with CCW disk rotation. These series overlap at 0° and at ±180°, i.e. D is 0° both for points collected with CW disk rotation when the disk was 90° to the left of the subject and *with CCW disk rotation when the disk was 90° to the right. There are, therefore, twice as many points at this position. In the opposite case, where D may be +180° or -180°, points with CW disk rotation are plotted as +180° and those with CCW disk rotation are plotted as -180°. This results in 2 overlapping series: that from -180° to 0° during CCW disk rotation and from 0° to +180° during CW disk rotation. During the offset condition these directions are reversed.*

Discussion

Many previous studies have shown that visual motion is capable of generating postural reactions (e.g. Edwards (1946); Dichgans et al. 1975; Lee and Lishman (1975); Bles et al. (1983); Allum and Pfaltz (1985); Clément et al. 1985; Bronstein 1986); Yardley et al. (1992); Timmann et al. (1994); Eggert et al. (1997); Severac et al. (1998). However, relatively few have investigated the influence of different positions of these stimuli relative to the subject (Stoffregen 1985; Gielen and Asten 1990; Wolsley et al. 1996b).

Wolsley et al. (1996b) reported an accurate reorientation of a VEPR during deviation of both the eyes in head and head on trunk. It was reasoned that, since the retinal motion stimulation was the same in the different positions, the postural reorientation must be due to eye-in-orbit and head-on-trunk position signals, possibly proprioceptive in origin. However, their experiment was conducted in a well-lit environment with Ss having prior cognitive knowledge of the position of the visual stimulus and of the relative rotations of the eyes and head. The present experiment was therefore conducted to test whether the reorientation of the VEPR is impaired by reduced cognitive and background visual information and by passive positioning of the Ss with a rotating platform.

In the present experiment the directions of VEPRs induced by both the onset and offset of disk rotation were measured. The gain of the reorientation of VEPR was ~0.99 at the onset but ~0.83 during the offset. This slight difference may be mostly explained by the reduced gain of offset VEPR reorientation at the level of the COP (0.68 ± 0.07 in this case versus 0.96 ± 0.05, 0.98 ± 0.05 and 1.01 ± 0.06 for the other conditions; all values mean ± s.e.m.). It is apparent from the right-hand panel of Figure 12 that this reduced gain is mostly due to the -180° and +180° positions, and if these positions are excluded from the analysis the gain is 0.87 ± 0.09, more closely comparable to the gains of VEPR reorientation in the other conditions. Why the apparent behaviour of the subjects was different between the COP and the head measurements for these conditions is unclear. One possible explanation would be that subjects are not comfortable swaying as far backwards as in other directions and this reduced component relative to any lateral sway results in an apparent rotation of the VEPR. It may be supposed also that the relative rapidity of the offset sway in comparison to the onset sway is more likely to activate such limiting mechanisms, explaining why the onset response does not show this behaviour. It may be possible to determine the direction of 'intended' sway more accurately by reducing the speed or area of the disk to reduce the amount and speed of sway induced so as not to overstep any such internal sway limits. However, this would unfortunately reduce the signal to noise ratio of each trial. Further work is required to test these hypotheses.

The main result of this experiment is the comparison with the data of Wolsley et al. (1996b). The lack of a significant difference between the gains of reorientation suggests that little or no role is played by cognition, background visual structure or active positioning in the reorientation of VEPRs.

The origin of the signals used to determine the direction of gaze for visual control of posture is not yet clear. For the neck, proprioception would seem more useful than efference copy due to the possibility of external forces acting on the head. Neck afferents have been shown to be the main source of information used to estimate head-trunk horizontal angular deviation (Nakamura and Bronstein 1995). In the current experiments, where 95% of gaze deviation was achieved by head-on-trunk deviation, neck proprioceptive information is therefore the most likely source. Neck proprioceptive afferents are also thought to be responsible for the reorientation of vestibularly (galvanic) elicited sway during head turns (Gregoric et al. 1978; Lund 1980; Lund and Broberg 1983). External forces do not normally act on the eyes and, therefore, efference copy or a mixture of efference copy and ocular proprioception has been favoured as the source of an eye-in-orbit position signal. In pointing and estimation tasks (Bridgeman and Stark 1991) physiological gains of oculomotor efference copy and proprioception were found to be 0.61 and 0.26 respectively. The finding that extra-ocular muscle vibration elicits directional postural responses (Roll et al. 1989) suggests that at least some ocular proprioceptive component influences postural control. The current experiments suggest that visual and proprioceptive signals combine in order to provide effective, gaze angle-independent, visual control of posture. This process appears to be largely independent of cognitive comprehension of the geometry involved.

Chapter 3: Accuracy of Reorientation of Visually Induced Sway during Vection

Abstract of Chapter

Movement of large visual scenes induces an illusion of self-motion (vection) and postural responses. We investigated if the conscious perception of self-motion is associated with changes in the magnitude and directional accuracy of visually evoked postural responses (VEPRs). Five normal subjects fixated the centre of a large disk rotating in the roll (coronal) plane. The disk was placed either in front of the subjects or obliquely 30° to their right or left; in these oblique positions disk fixation was achieved by horizontal ocular deviation alone (i.e. no neck deviation). Subjects indicated their subjective perceptual status, either vection or object motion, with a push button. The results confirmed that the direction of the visually evoked postural response was reoriented according to the different eye-disk positions. In addition, both the magnitude of the postural response, and the accuracy of its alignment with the rotational plane of the disk, were significantly increased during vection periods. The results show that conscious perception of self-motion correlates with enhanced visuo-postural performance. Since conscious perception is likely to arise at cortical levels, the findings suggest that the cortex may be one of the sites where gaze direction interacts with retinal motion signals to provide a self-motion signal in body-centric co-ordinates. Such interaction provides a substrate for spatial representation during motion in the environment.

Introduction

Locomotor or postural movements create relative motion between the subject and the visual environment (optic flow). Artificial full-field visual motion stimuli are often interpreted as due to self-motion and also induce subconscious visually evoked postural responses and sometimes a conscious illusion of sensation of self-motion termed vection (Dichgans et al. 1972). At other times, however, perception is correct and the viewer reports that they are stationary and the disk is moving (object-motion perception). These two percepts comprise a bi-stable pair such that, when viewing a large rotating disk, there will be alternating periods of vection (V) and of object-motion perception (OMP). However, illusory signals of self-motion that may result in vection

need not be consciously perceived to influence postural control under identical visual conditions (Previc and Mullen, 1991), and in fact, may have visuo-postural latencies many times shorter than vection (Clément et al.1983). However, a recent study found that postural sway during periods of vection was of a greater magnitude than during periods of object-motion perception (Kuno et al. 1999). It is possible that this effect is the result of improved visuo-postural control due to additional conscious processing of signals of self-motion during vection. If conscious perception of self-motion does improve visuo-postural control then the *accuracy* of the direction of VEPR should also be greater during periods of vection than during object motion perception. Conversely, if the accuracy of VEPR isn't greater during vection then this hypothesis can be discounted. These hypothesised changes in the accuracy of orientation of the induced postural sway, comparing vection versus object-motion perception, were investigated here.

Methods

Five normal subjects between the ages of 21 and 31 were instructed to stand, relaxed, with their arms at their sides and their feet slightly splayed and separated upon a force platform. Subjects wore a light helmet carrying the receiver of a magnetic search coil system (Polhemus 3space Fastrack) measuring head position in all six degrees of freedom. Subsequent data processing was performed identically upon the horizontal position of the centre of foot pressure (COP) and on horizontal head position. In their right hand subjects held a button to indicate their perceptual state (vection or object-motion). All signals were recorded at 125Hz. In half the trials subjects were to press this button when they perceived themselves to be moving (i.e. vection) and in the other half only when they perceived the visual display to be moving (object-motion perception). The visual display consisted of a large (1.8m diameter, visual angle 122°) white disk, with a central fixation point, covered in smaller (5-20cm diameter) circles of various colours. This disk was rotated either clockwise or anti-clockwise at $50^{\circ}s^{-1}$ and it was placed in one of three positions, all at 50cm from the subject's nasion: either directly ahead (P_C) of the subject or 30° to the left (P_L) or right (P_R), see Figure 13. The centre of the disk was fixated with eye deviation only, i.e. no neck deviation, and viewed against normal laboratory lighting. Each subject was tested at each orientation with the disk always rotating clockwise or always anti-clockwise.

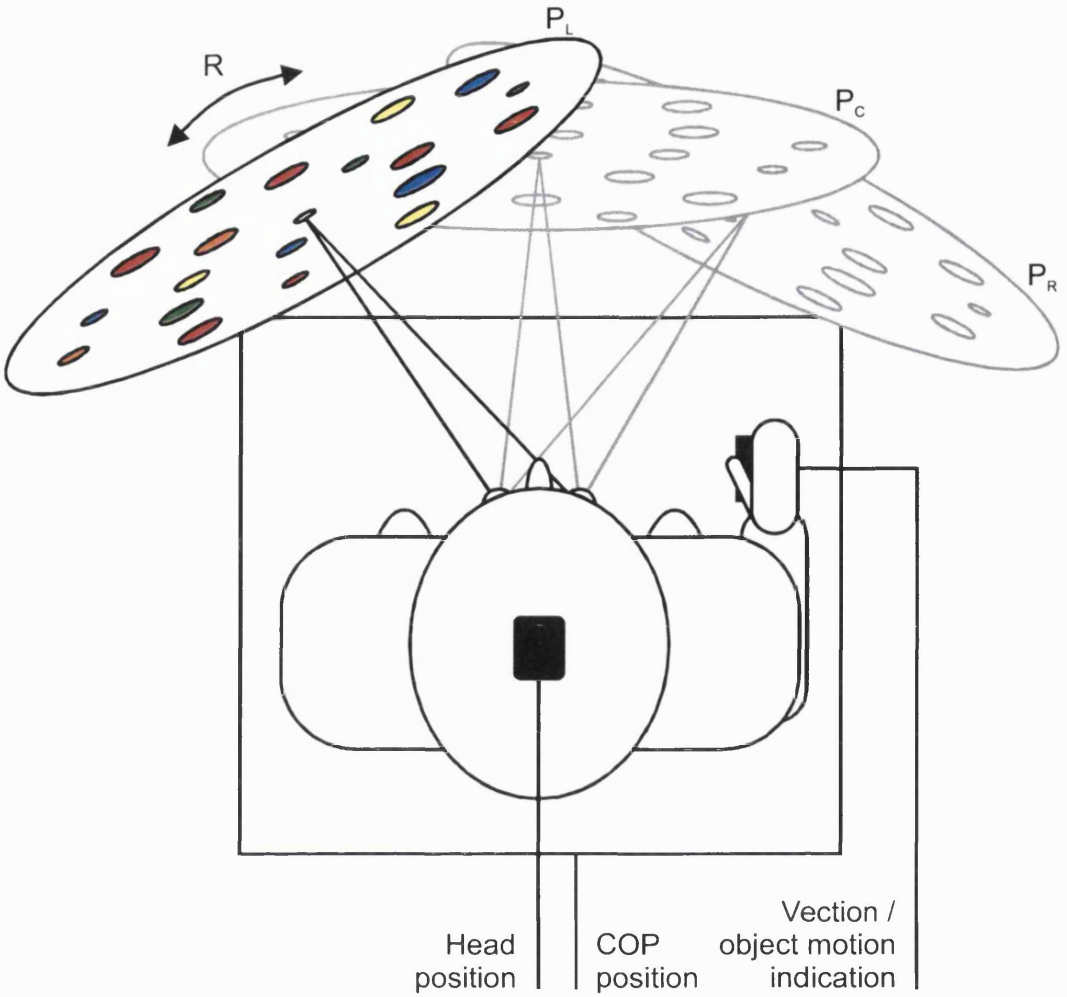

Figure 13: The experimental set-up from above. Subjects stood upon a posturography platform that measured the position of the COP in the horizontal plane. In their right hands subjects held a push button to indicate their perceptual state and also wore the receiver of a magnetic search coil on their heads. The subjects viewed the centre of a large disk covered in coloured spots that could be rotated either clockwise or anti-clockwise around R and placed, facing the subject, in one of three positions P_L, P_C, P_R.

Each trial lasted 300s with the disk being stationary for the first and last 10s, taking 7.5s to reach $50^{o}s^{-1}$ and 5s to stop. The remainder formed a central period of constant speed disk rotation that was divided into perceptual periods determined by each subject's indication of vection or object-motion (see Figure 14). Baseline positions were calculated as the means over the initial stationary period (0 - 10s) and the final 5s of the last stationary period. The second baseline period (final 5s) can be shorter than the first period as subjects return to this position much faster than they move away from it at the start of disk rotation, this can be seen in Figure 14 and is similar to the results of

Chapter 2 (Figure 8). Sway (both magnitude and the angular error relative to the direction of disk motion D) relative to both baseline positions was calculated during each perceptual period. Periods from the onset of disk rotation until the onset of the first vection percept and during the offset of disk rotation were discarded.

Results

The results for movements of the COP and of the head were similar and so the data for the head is only mentioned where statistical tests are used.

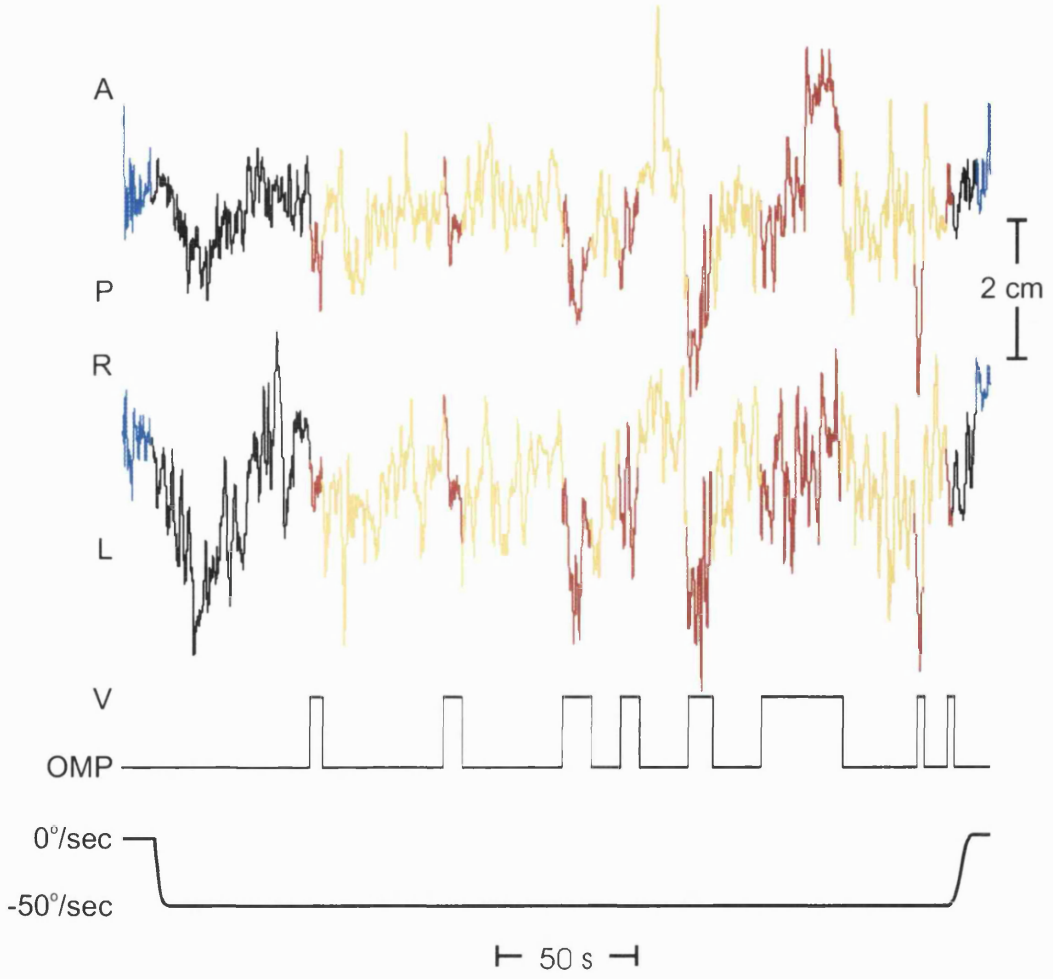

Figure 14: The time-course of a single trial with the disk at position P_L 30° to the left of centre, rotating anticlockwise for subject SP. Periods of vection (red) and object-motion perception (yellow) as indicated by the subject are compared to the baseline periods (blue). Intermediate periods during and immediately after the start or end of disk rotation (black) are not used for analysis.

The comparison of the sway magnitudes between vection and object motion perception was based on the mean positions of the COP during three conditions: mean of both baseline positions; mean of all positions during vection; mean of all positions during object motion perception (see Figure 15). For each trial, the lengths of the vectors from the mean baseline position to the mean vection and OMP positions were calculated. These values were then compared across all subjects and disk orientations. The data were found to be not normally distributed using a Lilliefors test, however they were paired: vection vs. OMP within each trial and so the populations were compared using the non-parametric, paired Wilcoxon signed rank test. Sway deviation from baseline was found to be significantly greater ($P < 0.05$, two tailed test) during vection than during object-motion perception at both the level of the head (5.8 ± 0.56mm vs. 4.3 ± 0.40mm, mean $\pm$ s.e.m.) and the COP (3.0 ± 0.39 mm vs. 1.7 ± 0.19mm).

Calculating the directions of the vector between the mean positions would be to lose most of the value of the data in the averaging process, therefore a different analysis was chosen. The direction of lines drawn between all combinations of baseline positions and positions during either vection or OMP were calculated (see Figure 15). The angle R between each of these 'sway' directions (S) and the direction of disk motion (D) was then calculated, it being a measure of the error of the sway direction. This error can be decomposed into bias (mean offset) and scatter (distribution width) components. Bias was low in comparison to scatter for most subjects as can be seen in Figure 16 for subject SP and Appendix C for the other subjects.

As bias was low, the angle R was rectified, such that it now represented the scatter in the sway direction. The mean values of these errors within each trial were computed for the vection and OMP conditions in each trial. The distribution of these mean scatters was not normal, and this was confirmed using a Lilliefors test. However, the values were paired within each trial, so the vection and OMP errors were compared using the non-parametric, Wilcoxon signed rank test. This revealed sway orientation (S) to be significantly more accurate (less scatter) with respect to disk motion direction (D) during periods of vection than during OMP ($32.6^\circ \pm 6.6^\circ$ vs. $51.4^\circ \pm 7.9^\circ$, mean $\pm$ s.e.m. direction error, at the level of the COP and $32.0^\circ \pm 6.7^\circ$ vs. $40.5^\circ \pm 7.1^\circ$ at the level of the head; $P < 0.05$). The results for the COP can be seen in Figure 17.

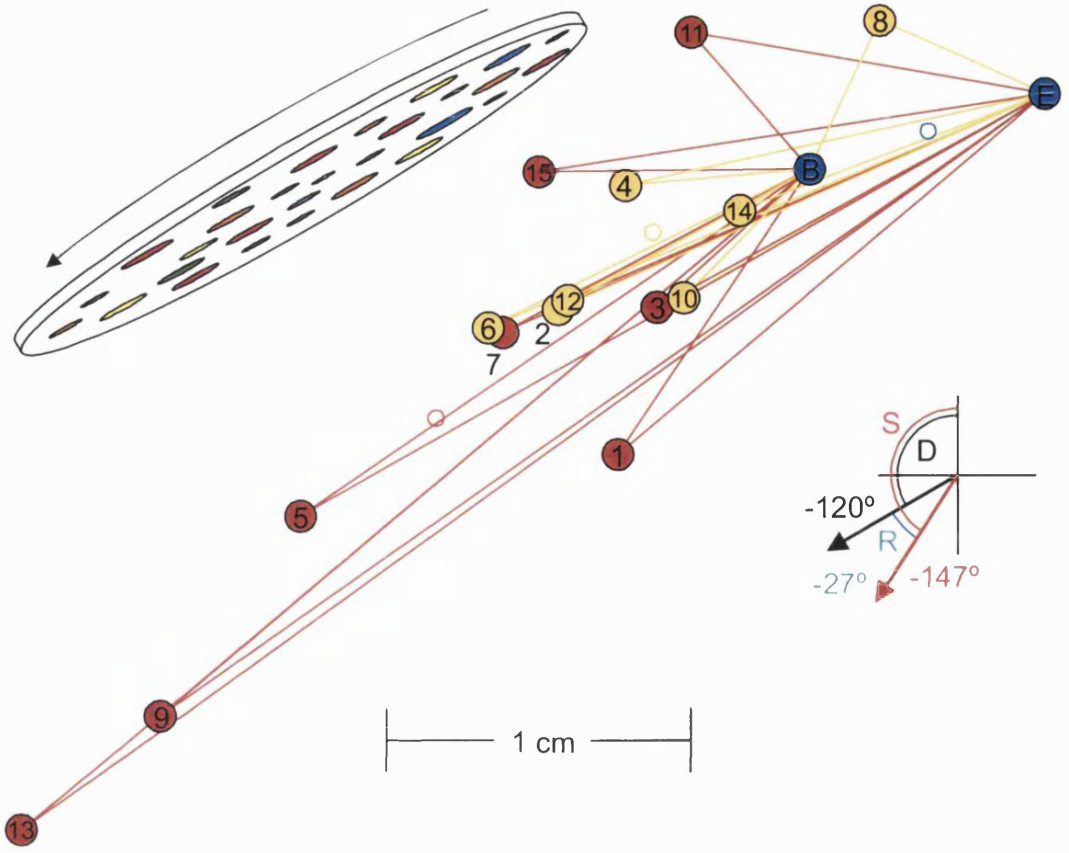

Figure 15: Epoch positions during a single trial (same trial as Figure 14). Data plotted showing the positions of sway during vection (red) and object motion perception (yellow) and the trajectories from each of these positions to both baseline positions (blue). Each epoch is labelled as the Beginning (B) or End (E) or with a number in time order. The sway magnitudes were calculated from the mean positions during the three conditions (red, yellow and blue rings). The sway directions during vection and object motion perception were calculated from lines draw between each baseline position and each epoch position of that type (red lines during vection, yellow lines during object motion perception). The direction of sway along each line was calculated (S) and compared to the direction of disk motion (D) to give a relative direction R as shown in the inset diagram (example is between B and 1).

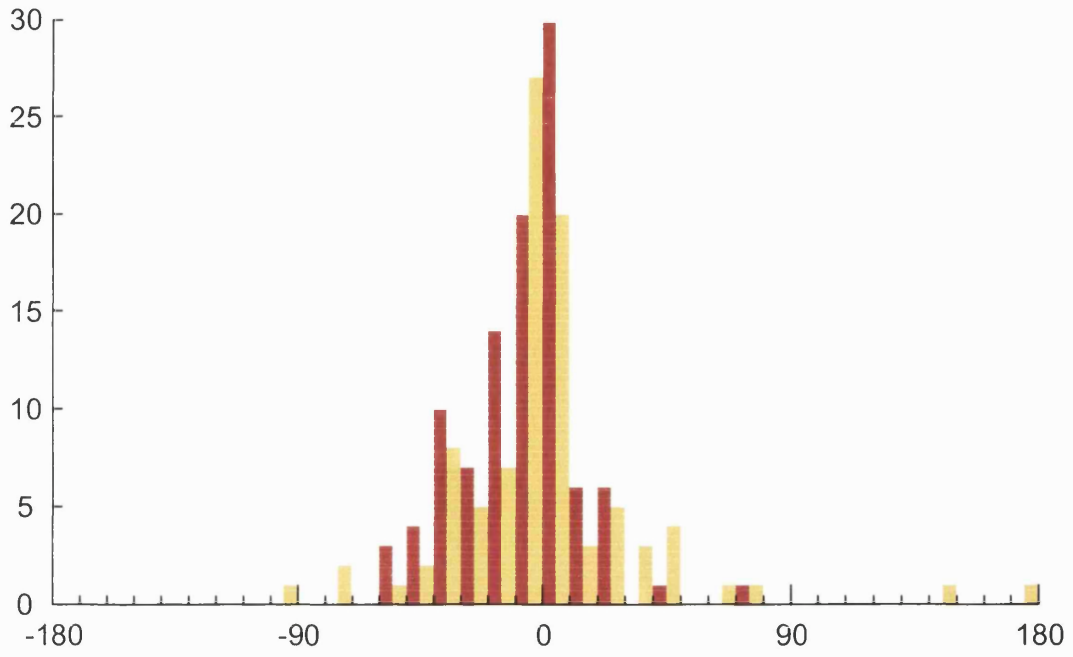

Figure 16: Histogram of R_V and R_{OMP} (sway direction relative to the direction of disk motion during vection (yellow) and OMP (red) respectively) for all epochs in all trials for a single subject (SP, same subject as in Figures 16, 17 and 18). Vertical axis denotes the number of trials per bin, horizontal axis denotes angle of error (°), bins are 10° wide. R_V = -6.3 ± 21.8 and R_{OMP} = -1.4 ± 32.0 (mean ± s.d.). This figure provides a summary of this single subject's performance, showing the bias and scatter in the sway direction, other subjects are shown in Appendix C.

Discussion

The results confirm data by Wolsley et al. (1996b) and Thurrell et al. (2000) showing that the direction of a visually evoked postural response tends to align with the plane of motion of the visual stimulus. Such re-alignment of retinal motion signals into body-centric co-ordinates by gaze direction, which may be mediated partly by proprioceptive input from the neck and the extra-ocular muscles (Roll et al.1989; Wolsley et al.1996b), is critical in making visuo-postural control functionally useful in different directions of gaze. Also in agreement with a previous study (Kuno et al. 1999), is the greater magnitude of visually evoked postural sway during vection than during object-motion perception. The new result emerging from the current study is the finding of a more accurate alignment of visually evoked postural sway during vection than during object-motion perception. This is consistent with the hypothesis that conscious perception of

self-motion improves visuo-postural control, though it does not necessarily indicate a causal relation between the two.

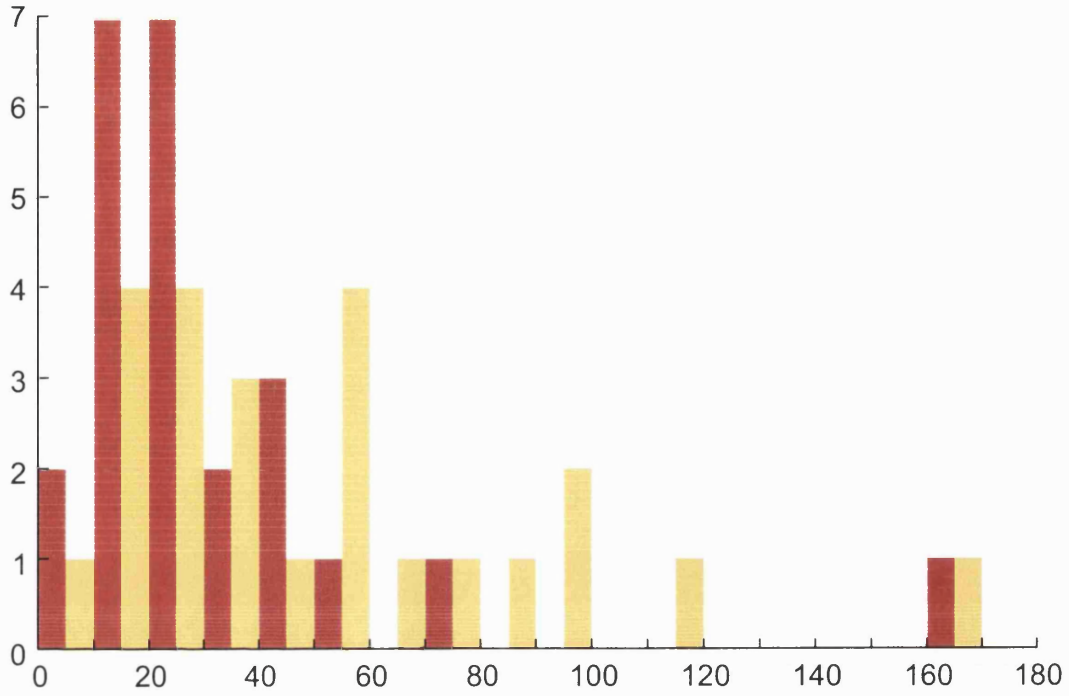

Figure 17: Histogram of sway direction errors, for all subjects. The error angles for each trial for sway during vection (red) and OMP (yellow) were compared. Vertical axis denotes the number of trials per bin, horizontal axis denotes angle of error (^{o}), bins are 10^o wide.

Chapter 4: A Mechanism to Counter the Influence of Locomotion on Visual Perception

Abstract of Chapter

To maximise the usefulness of information gathered about the environment, the visual system must be able to distinguish between retinal image motion that is due to object motion and that due to self-motion. During natural human locomotion optic flow speed is in part determined by walking speed, and consequently it is hypothesised that signals of walking speed may be used to discount the influence of self-motion on optic flow. We considered how non-visual signals of self-motion such as may accompany walking might influence the visual processing of optic flow.

In the initial experiment (1), subjects were required to match the perceived speeds of two artificially presented expanding optic flow patterns, one of which was viewed while walking on a treadmill. Walking speed was found to directly influence perceived optic flow speed with increased walking speed decreasing the perceived optic flow speed in a linear fashion. (2) Control experiments showed that the perceived optic flow speed was unaffected by attentional load or the head motion caused by walking. A comparison (3) was then made between the influence of proprioceptive signals on the visual processing of optic flow during four motor activities becoming progressively less similar to natural locomotion: Walking, Cycling, Arm Pedalling and Finger Tapping. As the motor activities became less similar to natural locomotion their influence upon optic flow speed perception steadily reduced, with Finger Tapping not influencing optic flow perception at all. (4) In a further study, the direction of walking, i.e. forwards or backwards, was not found to affect the above mechanism: both faster forward walking and faster backward walking reduced the perceived speed of expanding optic flow. Experiment (5) investigated how these signals influence the visual processing of five progressively less 'locomotor-like' patterns of optic flow: an expanding tunnel of concentric rectangles; a horizontal grating translating downward; a vertical grating translating rightward; a cartwheel rotating about the axis of vision; and a flashing stationary tunnel (control). In a complementary study (6), the angle between visual motion direction and walking direction was varied by rotating the treadmill. In a further study (7), the role of the primary visual cortex was also considered: a hemianopic 'blindsight' patient (GY) was tested to compare matching expanding optic flow speeds

with the intact and blind hemifields. Optic flow speed perception in both hemifields was strongly influenced by walking speed.

These results are mostly explained by the hypothesis that accurate visual perception is maintained during self-motion by using an estimate of the optic flow that should arise from that self-motion. In the absence of other cues, this estimate is based on non-visual signals of self-motion such as from the legs during walking. The weighting given to these signals is shown to be related to their correlation with locomotion.

Introduction

Accurate perception of the position of visual targets in space, and motion through it, has crucial survival advantages for many organisms, for instance for locating food, predators and for object recognition by means of perceptual grouping. However, for most organisms with vision, the eyes in space have six degrees of freedom: three of rotation (e.g. eyes within the head) and three of translation (e.g. eyes and head together), and movement of the eyes along or around any axis has a profound effect on the images projected on the retinae. Thus, any determination of the position or movement of an object in the environment using the visual system must take account of the movements of the eyes in space. A somewhat simplified diagram of the inter-relationship of possible sources of information with which to accomplish this is shown in Figure 1.

Retinal versus Extra-Retinal Signals of Eye Motion

Mach (1886) and von Helmholtz (1896) were two of the first to consider this problem, in the context of rotational eye movements within an implicitly stationary head (i.e. the Head-Eyes-Target link of Figure 1). Both concluded that the solution was to use signals of eye movement and position from sources external to the eyes, i.e. proprioception from the extraocular muscles and/or efference copy of their commands, collectively referred to as extra-retinal signals. This theory was refined over the next century, such that the main source of these extra-retinal signals of eye-in-head rotation is now considered to be efference copy, with proprioception relegated to the role of long-term parametric feedback (see Carpenter, 1988 for review). These extra-retinal signals would be used to remove changes in the retinal signal, (i.e. the signal travelling along the optic nerves) that are due to eye movements, and any remaining motion in the retinal signal could thus be treated as directly related to object position and movement in space. The

alternative view to this, in its strictest form, originated with Gibson (1950, 1954, 1966), who concluded that for certain environments all the necessary information about eye (as well as head and body) movements is contained in the visual image itself (the Eyes-Space connection of Figure 1). In this view, extra-retinal signals of eye position are, therefore, not needed to accurately determine object motion in space. This view has since been restricted, both in theory and after measurements of human psychophysics (Warren and Hannon, 1988) to just those visual environments containing information in depth.

The importance or otherwise of extra-retinal signals in self-motion perception has been investigated in psychophysical studies on the visual perception of heading: the determination of the direction of self-motion. The perception of heading has been found to be equally effective with real and simulated eye movements, given equivalent visual information and under some conditions (Warren and Hannon 1988), suggesting that extra-retinal signals are not always needed. For simulating eye movements, fixating subjects are shown the motion that would have been perceived had the eyes been moving (which assumes, incidentally, that static extra-retinal signals for fixation are ignored, see Lappe et al. 1999). On the other hand, heading performance with simulated eye movements drops to chance levels when depth information is removed (Warren and Hannon 1988) and heading errors increase markedly with faster, more typical simulated eye movement velocities (Royden et al.1992), both supporting the use of extra-retinal signals. Also, that human subjects are capable of using retinal instead of extra-retinal signals to determine visual motion does not necessarily mean that they normally will. This ability seems to vary between subjects, with only some human observers able to determine heading direction during simulated eye movements without static depth cues (though dynamic depth cues were still present) (Stone and Perrone, 1997). On balance, it seems that a composite of the two signals is used that may be dynamically altered depending on their exact values, such as the non-linear combinations shown by Brenner (1991), Brenner and van den Berg (1994), and Turano and Heidenreich (1996, 1999).

The Nature of the Extra-Retinal Signal

In order to account for percepts during visually induced sensations of self-motion (vection), a conceptual substitution is proposed for 'extra-retinal' (eye-in-head) signals by 'reference' (eye-in-space) signals (Wertheim 1994), made up of a combination of the former and also vestibular signals of head motion. This combined signal should

therefore resolve not only eye- but also head-movements in judging self-motion. In support of this framework, perception of visual direction is indeed influenced by whole-body rotation in the dark (e.g. Blouin et al. 1998), and visual motion perception and the motion after-effect (Harris et al.1981) are both influenced by passive, whole-body linear movement (Pavard and Berthoz 1977, Buizza et al. 1980). Its weakness, however, is that the vestibular apparatus has a poor response to low frequency motion (Goldberg and Fernández, 1975 and 1984) and is unable to detect constant velocity linear motion, leaving a gap in signalling self-motion during this type of movement when the environment is not visible. A more complete reference signal of motion of the eyes in space would include not only self-motion signals from the vestibular apparatus, but also those from the other sensory modalities shown in Figure 1.

Assuming a stationary torso, head-in-space signals could also be derived from a combination of efference copy and proprioception of the neck muscles. In avestibular patients, Mesland et al. (1996) showed the use of head-on-body signals in the perception of earth-relative object motion, while manipulation of neck proprioception was found to influence perception of visual targets in a manner indicative of their incorporation into signals of gaze direction (Biguer et al. 1988). Investigation of the interaction between efference copy, proprioception of the neck and vestibular signals showed perception was best explained by incorporating all three into the extra-retinal signal (Crowell et al. 1998), in a manner consistent with an extension to a reference signal of eye position in space (see Wertheim 1994).

The final link from eye to space from Figure 1 is between the body and space, as often the body is itself in motion and this must then also be taken into account. As it is rare (other than modern travelators and exercise treadmills) that we walk on moving surfaces, a natural alternative signal of self-motion would be that from locomotion. Arthrokinetic signals arising from locomotion, unlike vision, are available in the dark, and unlike vestibular signals, are available during constant velocity motion relative to the environment, though vestibular signals may provide a redundant measure of stride frequency, as this occurs within its optimal frequency range (Goldberg and Fernández, 1975, 1984). Some studies have demonstrated the influence of arthrokinetic signals from the legs on both self-motion perception and a visual motion after-effect (Pelah and Boddy, 1998). Jürgens et al. (1999) showed that subjects' perception of rotation on a platform was much more accurate when they stepped around the platform than during

purely passive rotation. The interaction between arthrokinetic signals of locomotion and visual motion signals was proposed to account for a visual motion after-effect resulting from a mismatch of visual motion and the locomotor signals from walking (Pelah and Barlow, 1996) that were suggested to result from the recalibration of sensory pathways by visuo-locomotor links. This interaction was also shown to influence the strength of a visual motion after-effect by Pelah and Boddy (1998). Evidence that purely passive proprioceptive signals from the legs may dominate over vestibular signals in self-motion perception under some circumstances (Hlavacka et al. 1996) supports the use of locomotor signals to determine self-motion. It may be hypothesised that these signals, in combination with trunk and neck proprioception, would accurately signal eye motion relative to the support surface and hence (unless on a moving walkway) the visual environment, and this would allow compensation for those optic flow components introduced by walking. The investigations presented here revolve around the use of these arthrokinetic signals during visual perception tasks.

The Current Study

The Arthrovisual Effect

The simplest and perhaps most ecologically relevant locomotor stimulus is walking in a straight line, resulting visually in an expanding pattern of optic flow for the observer. To test the hypothesis that arthrokinetic signals of self-motion are incorporated into an eye-in-space reference signal, and consequently used to process the retinal signal, changes in visual processing were assessed at a number of walking speeds on a treadmill. Treadmill walking dissociates locomotor signals from actual self-motion (as well as other possible signals of self-motion using gravito-inertial cues). A visual matching task, between the perceived velocity of the same constant optic flow stimulus during either walking or standing still isolated the effects of the locomotor signals.

Controls

Having established the influence of walking upon perceived optic flow velocity, various experiments were performed to determine its nature. These investigated the effect of differences in attentional load and head motion during walking, the influence the type of walking on the treadmill (i.e. self-powered vs. motorised), and the possibility that the influence is mediated as an after-effect.

Timing Perception Investigation

Visual motion perception may occur directly or indirectly via perception of distance and timing. This 'time-space construct' mechanism proposed for velocity representation relies on stable representation of both time and space to function accurately, and changes in motion perception of a constant stimulus must be attributable to one or the other. If motion perception is a function of a time-distance construct, then the arthrovisual effect will be a result of altered perceived size or timing perception during walking. A possible locus of such a mechanism could be within the cerebellum. The cerebellum has been shown to have neurones responsive to large field motion (Fushiki et al. 1994) and also neurones involved in visual speed perception (Ivry and Diener, 1991), that were proposed to be dependent on mechanisms of timing perception based in the cerebellum (Ivry and Keele, 1989).

Extension to other Motor Activities

Arthrokinetic signals are not limited to the legs and such signals arising from arm movements have been shown both to affect self-motion perception (Bles et al. 1995) and to enhance smooth pursuit tracking eye movements (de Graaf et al. 1994). The influence of arthrokinetic signals arising from the arms raises questions about the mechanism(s) involved in the use of such signals by the visual system. Might any movement of the limbs elicit changes in visual processing whether appropriate or not, or is there some specificity for the movement to be consistent with self-motion, i.e. is it only signals of limb movements that normally result in self-motion that alter visual processing? The proposed mechanism predicts that limb movements correlated with self-motion would alter visual processing appropriately to discount the effects of that self-motion. Also, the strength of this influence would be directly related to the degree of correlation between the limb movement and the self-motion. To determine whether this is the case, four activities sampling the range from natural locomotion to completely non-locomotor movements: Treadmill Walking, Stationary Cycling, Arm Pedalling and Finger Tapping, were performed by subjects whilst they performed the same optic flow matching task.

Walking Direction

During normal, forward walking, there results an expansion of objects around the direction of motion and it is this expansion component that must be removed for accurate vision. During backward walking the expansion of visual objects becomes a

contraction and should likewise be compensated for if visual perception is to remain accurate. This was investigated by getting subjects to perform the same visual-matching task during backward walking.

Extension to Other Optic flow Patterns

Some changes in the perception of motion of visual stimuli have been shown to be dependent on their global structure and proposed to be a consequence of their implied three dimensional motion (Bex and Makous, 1997). The perceptual constancy mechanism proposed here also suggests that the influence of walking speed would be specific to those optic flow patterns that are similar to those experienced during walking. A strong influence of walking is thus predicted during expanding flow when looking forwards towards one's destination, but not for flow rotating around the direction of travel. This prediction may be quantitatively tested as it would result in a cosine-tuning between the directions of locomotion and of apparent visual motion, i.e. the influence of walking speed would be proportional to the cosine of the angular difference between the walking and visual motion directions. This prediction was tested in the current study by comparing four optic flow patterns gradually becoming progressively less locomotor-like:

- Expanding optic flow is predicted to be strongly influenced by walking speed as the apparent motion of the components is in line with the subjects' motion. The angle between these two directions of motion is 0°, and the cosine is 1.0, predicting the maximum strength of the effect.

- The two gratings contain no global expanding optic flow components resulting in apparent motion in line with the subjects' walking direction, only apparent motion at 90° to the walking direction, the cosine of which is 0.0, predicting no effect. There are, however, regions where the local motion is parallel or anti-parallel to the walking direction, but these would be expected to cancel out, and therefore no influence of walking speed might be expected. However, if there are non-linearities in the system, those regions of the gratings moving in the same direction as the expanding tunnel may overpower those regions containing a contracting component. An example of a source of such a non-linearity would be found when walking outside or in a building with a high ceiling, the optic flow components present in the upper hemifield of vision are absent or very much reduced. Consequently, the

arthrovisual effect is predicted to be greater for the horizontal grating than for the vertical grating, which should show no effect.

- The Cartwheel also contains no expanding optic flow components overall, and local motion at all points is at 90° to the direction of walking. The cosine of the angle between walking and visual motion directions is 0.0, therefore the arthrovisual effect is predicted to be absent for the Cartwheel.

Investigation of Reorientation of the Arthrovisual Effect

Often when walking we turn our heads to look at an object to the side or are otherwise not looking in the direction of travel. We would expect from the hypothesis of Thurrell et al. (1998) that the processing of visual scenes viewed to either side of the subject's direction of travel would take account of this change, again with a cosine tuning between the direction of walking and that of visual motion:

- The arthrovisual effect is predicted to be strong during walking towards the visual display as the apparent motion of the visual components is normal to the display, i.e. in line with the subjects' motion. At this orientation, the angle between these two directions of motion is 0°, and the cosine is 1.0, predicting the maximum strength of the effect. At the intermediate position, there is an angle of 45° between the directions of apparent visual motion and walking, the cosine being 0.7, predicting a slightly smaller effect. When walking parallel to the display, there is an angle of 90° between the directions of apparent visual motion and walking, the cosine being 0.0, predicting no effect.

- The apparent visual motion for the horizontal grating is always at 90° to the direction of walking and so there should never be an arthrovisual effect. However, there may be some effect when walking towards the display (see Extension to Other Optic flow Patterns above).

- For the vertical grating, the apparent direction of visual motion is along the surface of the display and so is closest to the walking direction (with the strongest arthrovisual effect) when walking parallel to the display. This prediction is opposite to that for the Expanding Tunnel.

- For the Cartwheel, there is no direction of global motion, so the cosine tuning prediction method only works when walking towards the display, and no

arthrovisual effect is predicted. However, during outdoor walking the visual scene may often be approximated by a ground-plane. As forward motion occurs those parts of the ground near to the subject appear to move backwards faster than those further away, in essence at any moment the ground appears to be undergoing a shearing motion. This may be easily demonstrated by the reader looking sideways out of the window whilst they are a passenger in a train or car moving through a flat landscape. Rotation of the cartwheel may theoretically, for any instant in time, be decomposed into horizontal shear and vertical shear (Koenderink, 1990). When walking parallel to the display surface, this shear component may approximate a ground-plane moving backward past the subject (see Figure 18). As walking speed increases, with the visual axis off centre the above mechanism of perceptual constancy may reduce the shear component of the Cartwheel rotation, thus reducing the overall perceived speed of rotation. Therefore it may be expected that there will be an arthrovisual effect at this orientation.

Similar directional tuning has been found in studies of posture (Wolsley et al. 1996b, Chapter 2: Reorientation of Visually Induced Sway During Whole Body Passive Rotation) where processing of the visual input or motor output was modified by the direction of gaze (head and/or eye rotation) relative to that of the feet. This prediction was tested with the same set of optic flow patterns as above, but with the relative alignment between walking and the visual axis being 0° (mid-line position), 45° (mid-right) or 90° (full-right), see Figure 25.

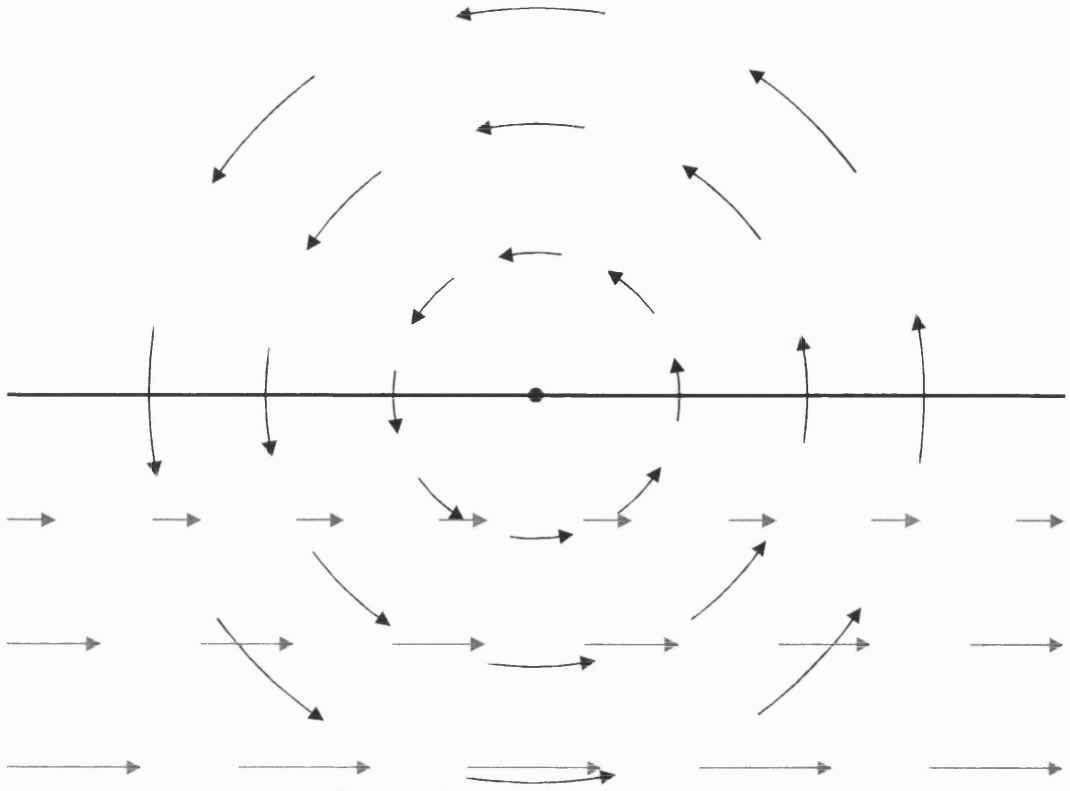

Figure 18: Relationship between the rotation of the Cartwheel and the shear of a ground plane when looking at the horizon (thick line) to the side of a subject walking through a flat landscape. It can be seen that the movement of the bottom half of the Cartwheel approximates the shearing motion of the ground-plane and may thus stimulate the same pathways.

Investigation of a Hemianopic Subject

At what stage of visual processing, and where in the brain the above mechanism of perceptual constancy may act, has not so far been investigated. Due to differences in locomotion between humans and other primates, single neurone recordings during walking are unlikely to be obtained and more indirect sources of information are required. Fortunately there is a large body of literature concerning the influence of eye movements on vision in primates to draw upon; though mostly concerned with eye-in-head motion some studies have investigated vestibular stimulation due to movements of the head. Most dorsal medial superior temporal (MSTd) neurones (in Rhesus monkeys) have large receptive fields and are tuned to a continuum of first-order optic flow motions (Graziano et al. 1994) making them ideal candidates for distinguishing self- and object-motion. Most MSTd neurones, unlike MT neurones, also respond selectively to externally induced visual motion and not to motion induced by eye movements

(Erickson and Thier 1991, in Macaque monkeys) or head rotations (Shenoy et al. 1999, in Rhesus monkeys). Indeed, MSTd neurones have been shown to alter their receptive fields to compensate for the effects of eye movements (Bradley et al.1996, in a Rhesus monkey). Vestibular stimulation by linear whole-body movements also influences the directional selectivity of MST neurones in a manner that may disambiguate self- and object-motion (Duffy 1998, in Rhesus monkeys). This use of vestibular signals of self-motion in visual processing in MST and the notion that self-motion signals should interact with vision in the same way regardless of their source suggests MST as a likely candidate area to incorporate proprioceptively derived signals of self-motion.

After lesion of the primary visual cortex (V1), conscious vision is abolished, however, there may still be considerable residual visual function (though the subjects report that they do not 'see'), and this condition is referred to as 'blindsight' (see Barbur et al. 1980 and Stoerig and Cowey, 1997 for review). In patient GY, a lesion of the left primary visual cortex occurred during childhood rendering him hemianopic, but has since demonstrated residual visual function in the affected area (Barbur et al. 1980 and Morland et al. 1999). Part of GY's residual vision is the ability to make comparisons between the velocity of pairs of moving stimuli when either or both are presented in the blind hemifield (Morland et al. 1999). This residual velocity sensitivity must result from signals that bypass V1, such as those arising from the pulvinar via the superior colliculus that have been shown to be required for continued activity in MT after V1 lesions (Rodman et al. 1990). These signals may then continue to higher visual areas, such as MSTd where we predict they should interact with other signals, such as those of self-motion. GY was therefore used to test the prediction that walking speed should influence optic flow speed perception in both the intact and blind hemifields.

Specification of Spatial Scale

If the hypothesised mechanism does indeed act to maintain perceptual constancy during walking then it will reduce the perceived optic flow speed by an amount equal to the walking speed. The optic flow stimulus used so far has been lacking any spatial scale preventing this prediction from being quantitatively tested: in the absence of any scaling information, any moving visual object may be small, close and moving slowly or it may be larger, further away and moving more quickly. A spatial scale may be provided using inherently scaled objects (i.e. those of a learnt constant size) or using stereoscopic, parallax, or accommodative signals. Stereopsis and parallax are able to accurately

specify spatial scale over the range required for this experiment and rely on fewer assumptions (knowledge of inter-ocular distance) by the visual system, compared to using the interpretation of objects with an inherent scale. They may also be provided either together or independently, allowing spatial scale to be strongly or weakly defined respectively. The prediction that the arthrovisual effect reduces perceived visual motion by an amount that compensates for the walking speed was tested by providing a spatial scale using stereopsis and/or parallax signals in the visual stimulus.

Methods

All the experiments and controls reported here involve variations on a basic method which will be presented first, followed by subsections denoting the changes made between this basic method for each variation.

The Main Method

Subjects stood or walked upon an exercise treadmill (Woodway Exo 43) placed directly in front of a large rear projection screen (see Figure 19) based on the locomotion simulator developed by Pelah et al. (1998). This treadmill is designed with a low friction belt such that when it is not electrically powered subjects may propel themselves by walking and pushing against the handrails with their arms, an action similar to pushing a trolley. The effort required to walk on the treadmill in this way was reduced to slightly more than natural walking by raising the front of the treadmill to give a gradient of 3%. This caused the subjects' own body weight to help move the belt, whilst subjects were unable to tell that it was not in fact horizontal. The walking speed of the subject was obtained from a sensor attached to the treadmill axis, which was electronically low pass filtered and digitally sampled at 35Hz and then digitally low pass filtered at 8Hz to remove noise.

The image projected on the screen was contained within a central area 1.9m wide by 1.43m high and approximately 0.9m from the subjects' eyes giving a viewing angle of 93° by 77°. Subjects wore ear defenders and welder's goggles restricting peripheral vision and reducing brightness by a factor of 100, thus ensuring that the border of the screen remained invisible at all times. The goggles allowed only monocular vision, always with the right eye, removing stereoscopic depth cues. Subjects were able to wear refracting spectacles inside the goggles if required, to correct their vision to normal. The

visual scene was produced by an LCD projector (InFocus LP740) at a resolution of 1024 by 768 pixels and a refresh rate of 70Hz updated on alternate frames. The visual scene was composed of a simulated tunnel in depth that consisted of 15 bright anti-aliased squares against a dark background (0.006 cdm^{-2}), as in Figure 19. The tunnel did not contain an inherent scale, but the following relative dimensions were specified: near-point relative to the observer = 0.4 x width; far-point relative to the observer = 5 x width; width = height. The squares of the tunnel obeyed the laws of perspective, increasing in thickness and size with decreasing simulated distance to the observer, and luminosity changing as a trapezoid function of simulated distance (maximum luminosity 1.51 cdm^{-2}). This allowed fading of the squares into the distance with perspective and a reduction in brightness near the border of the screen, applied in order to remove flicker. Subjects were required to fixate a fixation point 1 pixel square (0.12^{o} x 0.12^{o}, luminosity 1.51 cdm^{-2}) provided at the centre of the display approximately at each subject's eye level. Fixation was not checked independently of the subjects' own reports as it was judged to be an easy task.

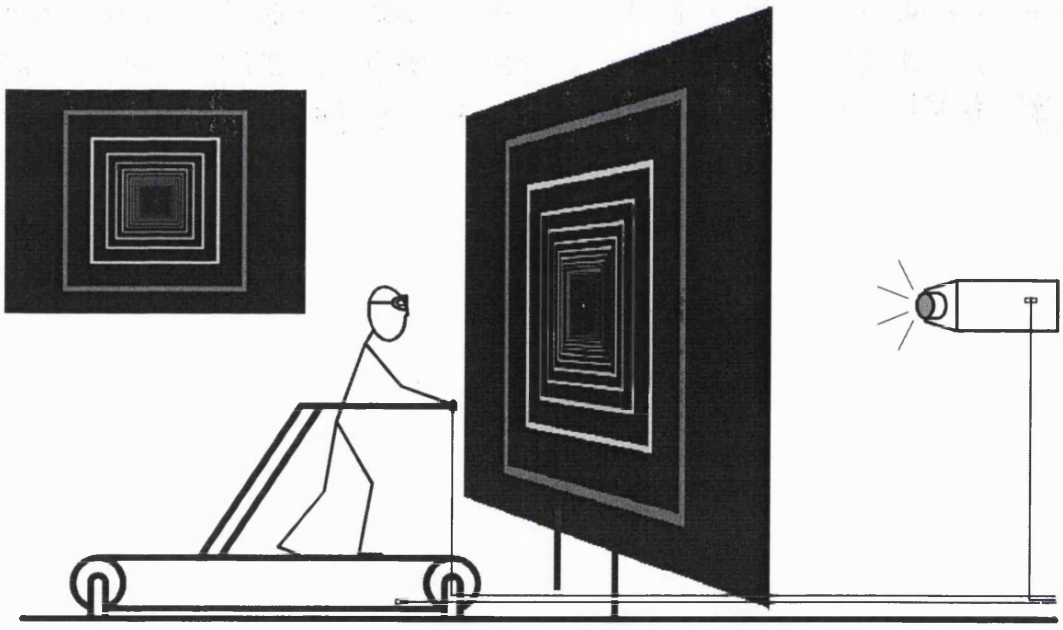

Figure 19: The basic set-up of the treadmill and the display screen and (inset) a screen-shot of the tunnel displayed to the subject. The experiments were all conducted in the dark (apart from the projected image), thus even if subjects turned their heads they could not see the border of the display screen. The only noise was from the treadmill rollers and was partially muffled both by a heavy curtain around the set-up and by the ear defenders worn by the subjects.

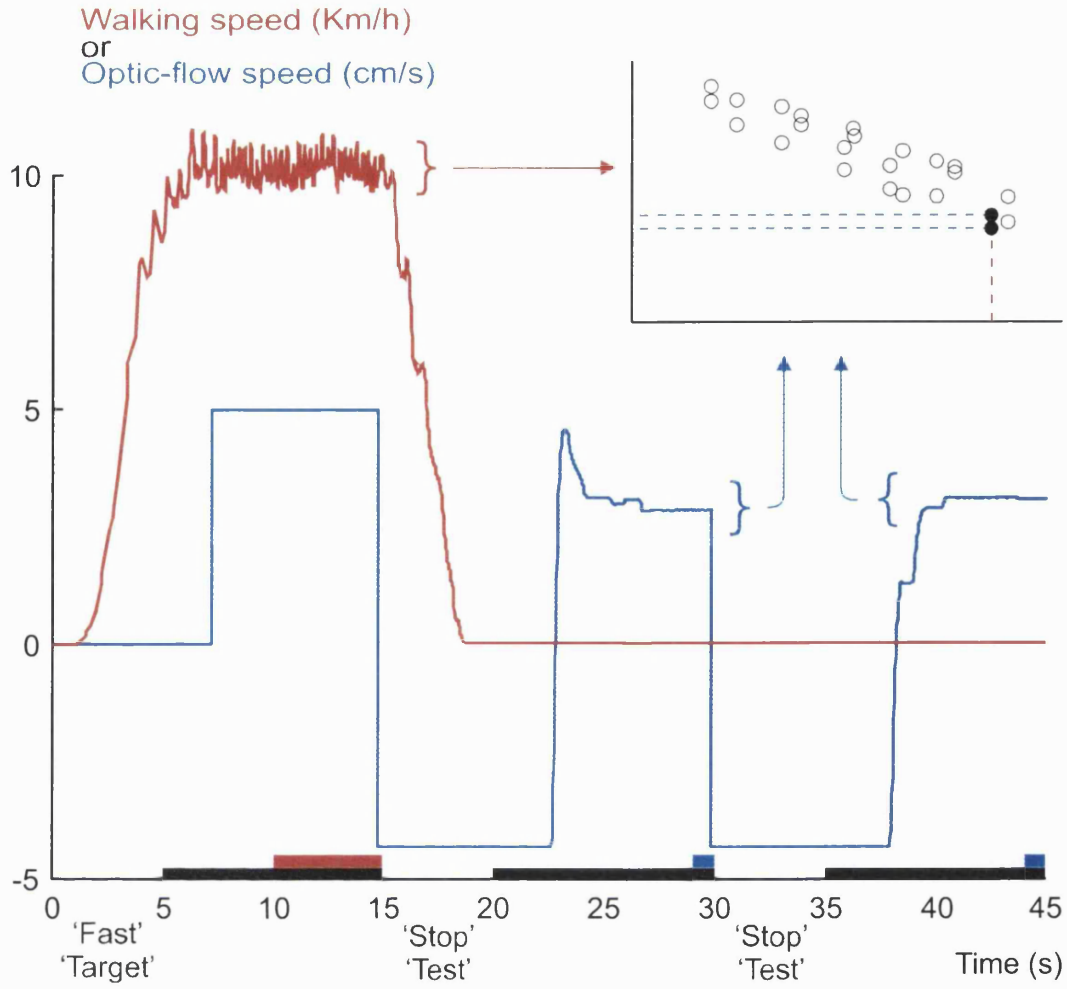

Figure 20: The time sequence of each type 1 trial. Instructions (printed below the time axis) were displayed for 5s each (thin portion of time-scale) alternating with the expanding tunnel (10s, thick portion). Mean settings during the last 1s (blue bars) of each test tunnel were plotted (inset) against the mean activity speed during the last 5s (red bar) of the target tunnel.

Subjects were required to perform a matching task between the perceived velocity of a 'target' visual motion scene and a number of 'test' scenes along the visual axis. These matches were made as a series of trials (see Figure 20): a 10s target presentation occurred during walking at one of six instructed speeds: 'stationary' (control), 'very slow', 'slow', 'normal', 'fast', or 'very fast,' and was followed by two stationary test presentations of 10s each. Instructions (presentation type and walking speed) were presented visually on the screen at the fixation point for 5s before each scene presentation. Subjects were instructed before each experiment to be walking at the instructed speed before the scene became visible and to adjust the test scene as quickly

and accurately as possible to match only the most recent target speed. Each experiment contained between five and twelve matches at each walking speed, resulting in a total session time of between 9 and 26 minutes.

The target velocity for the moving tunnel (expanding, simulating movement towards the subject) was always 5cm/s as measured by rectangle motion on the screen at the mid-hemifield position (27.8° from the fixation point, corresponding to $2.7°s^{-1}$ angular motion at the nodal point of each subject's eye). For the test presentations, the subjects used a rotating knob to control the velocity of the optic flow tunnel. The knob was attached to the right handrail of the treadmill such that subjects could rest their hand at all times while making an adjustment. At the beginning of each matching presentation the knob position was reset by the subject to a negative optic flow velocity. The output of the knob was digitally sampled and low pass filtered at 35Hz and 8Hz respectively, and a small amount of noise added to the signal to mask the pixel jitter at low tunnel speeds. A small random offset was added to the knob position before each presentation to prevent subjects learning to use the knob position as a cue.

Data analysis occurred off-line using the walking velocity and visual velocity recorded and averaged over the final 5s and 1s of scene presentation respectively (see Figure 20). The optic flow speeds of the test tunnel settings were all normalised as the relative proportion of the speed of the target tunnel. Likewise, the walking speeds were normalised as a proportion of the mean walking speed during the 'very fast' trials. The average optic flow speed was then plotted against the average walking speed for all the trials from a single subject (see Figure 20, inset). A measure of setting accuracy was calculated as the standard deviation of the optic flow velocity, and when this measure was over 0.5, suggesting the subject had not completed their adjustment, the trial was removed from further analysis. The order of presentation of conditions was randomised in all experiments. Prior to the beginning of an experiment, each subject was allowed practice walking on the treadmill at the various instructed speeds, and matching the visual scene by adjusting the knob.

Control Variations

Reversal of the Order of Walking and Standing

In the main, 'type 1' protocol subjects viewed the target while walking and matched it while standing still. However, in this variant, referred to as 'type 2' trials, the target

presentation occurred whilst subjects were stationary, with optic flow speed matching taking place in six subsequent presentations of the test scene while walking, once at each speed (see Figure 21). Matching during each of the six test scenes was to the target scene at the start of the block of presentations, i.e. that presented most recently. Type 2 trials control for the possibility that changes in matched optic flow speed during type 1 trials are due to the act of walking distracting the subject from remembering the target speed. On the other hand, type 1 trials control for the possibility that changes in matched optic flow speed during type 2 trials are due to the act of walking distracting the subject from setting the test speed.

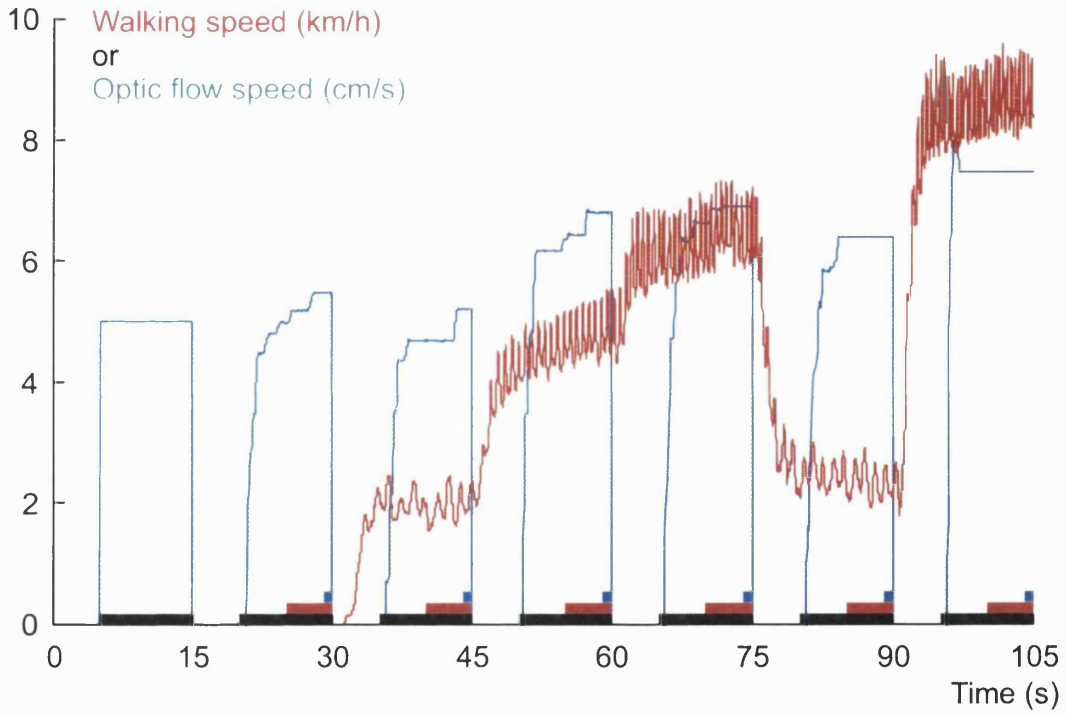

Figure 21: The time sequence of each type 2 trial. Instructions were displayed for 5s each (thin portion of time-scale) alternating with the expanding tunnel (10s, thick portion), as in the type 1 trials. Mean settings during the last 1s (blue bars) of each test tunnel were plotted against the mean activity speed during the last 5s (red bars) of the same test tunnel. These time periods were different as subjects were often still adjusting the optic flow speed until ~2s before the test tunnel disappeared, however, a minimum of 5s was required to average out the large variations in walking speed during each stride.

Attentional Control

The possibility that walking influences the matched optic flow speeds because it is a competing load (see Wickens, 1980 for review) was investigated by adding an additional attention task. For trials with this added condition, during the 10s target presentation while walking (i.e. type 1) subjects were instructed to listen through headphones to a pre-recorded series of five single digit numbers, and required to keep a running total which they were to call out immediately at the end of the presentation. Trials in which the subject miscalculated the total were discarded, as in such cases subjects may not have been sufficiently attentive.

Head Motion Control

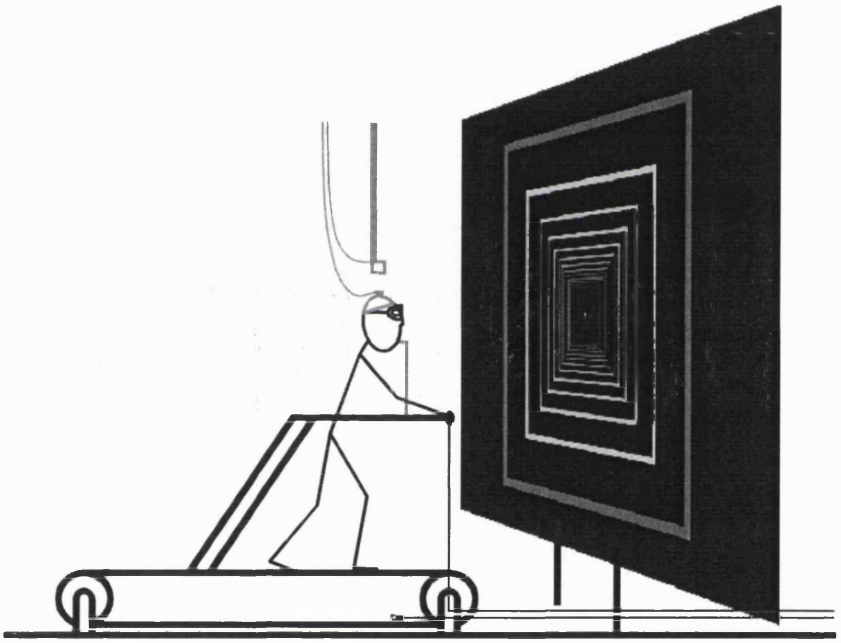

Figure 22: The set-up for the head motion control, showing the additional bite-bar mounted to the treadmill handrail and the Fastrack transmitter (ceiling mounted) and receiver (mounted on a lightweight helmet).

During treadmill walking, the head may oscillate in all six degrees of freedom, which may be argued as influencing the perceived optic flow. Thus, some trials were conducted with restricted head motion, using a rigid bite-bar attached to the treadmill at an adjustable level for each subject, while remaining out of view (see Figure 22). As an added test, head position was measured for one subject while walking using a Polhemus Fastrack magnetic position-sensing device, providing readings in all six degrees of freedom. The receiver of this device was attached to a light-weight helmet worn on the

top of the head, mechanically independent of the bite bar (other than via the subject's head), with position data being collected at 35Hz. Head position was linearly detrended over the 10s of each trial during which the scene was visible and its FFT power spectrum calculated. These power spectra were averaged across condition repeats and walking speeds and compared. Linear motion was reduced by a factor of up to 15 laterally and up to 5 otherwise, whilst rotational motion was reduced by a factor of approximately 10 for yaw and roll, though pitch motion amplitude was unchanged.

Motorised versus Self-Powered Walking

During the other experiments presented here, the subjects provide the motive force for the treadmill by walking on the unpowered belt and holding their bodies still by holding the handrails with their arms. Self-powered walking has experimental advantages: subjects naturally hold their head in an approximately constant place, simplifying the interpretation of results; and subjects can choose walking speeds to suit themselves. However, for all that, it has problems: it is not quite a 'natural' way to walk: subjects feel as if they are pushing a wheeled trolley; and subjects receive an explicit speed command that may bias their optic flow speed settings.

To ensure that this 'unnaturalness' was not influencing the results, a variation was performed with the treadmill belt powered electrically. This variation was conducted using the type 2 protocol (see Reversal of the Order of Walking and Standing). The on-screen instructions were altered to remove the walking speed commands, to show just 'target' or 'test', instead the treadmill was controlled externally to produce walking speeds of approximately 2, 3.5, 5, 6.5 and 8 km/h. The treadmill reached each new speed before the tunnel was displayed on screen, during which time the subject stood on the non-moving portion of the treadmill either side of the belt. The subject was required to walk with hands free, maintaining as well as possible a constant distance to the display screen. Due to the difficulties involved in this variation (e.g. stepping on and off a moving treadmill belt in the dark) only one subject (the author) was tested.

Other Variations

Timing Perception Investigation

Visual speed determination may, hypothetically, occur directly or as a construct of time and displacement, implying that walking may influence perceived optic flow speed directly or via changes in temporal processing. Experiments to determine the influence

of walking on temporal perception used a target consisting of an otherwise identical tunnel (see Figure 19, inset) that remained stationary but flashed in place at a frequency of 2Hz. The tunnel luminance varied with a raised cosine profile applied to all tunnel components (i.e. squares) individually, such that their relative brightness remained constant (except for the fixation point, which did not flash). Subjects were required to match the flashing frequency of the tunnel to that of the previously presented target.

Extension to other Motor Activities

To investigate whether arthrokinetic signals other than from walking influence visual motion perception, a number of naïve subjects performed the matching task with Treadmill Walking as before and also with Stationary Cycling, Arm Pedalling and Finger Tapping (see Figure 24: The experimental set-up for each activity.).

During walking trials the treadmill (Woodway Exo 43) was powered by the subjects themselves pushing against the handrails with their arms. Cycling trials were conducted using a stationary, recumbent exercise cycle (Tunturi Motivational Recumbent Cycle ECB F570), which was raised and altered to place the subjects' heads near to the position they maintained during walking trials. Arm Pedalling was conducted using the exercise cycle altered (see Figure 24: The experimental set-up for each activity.) to allow the arms to rotate the pedals, and again keeping the subjects' heads in the same position as that during cycling. In order to reduce fatigue and to allow the subjects to reach their desired speed sufficiently quickly, the resistance was set to minimum for this condition. Finger Tapping trials were conducted while standing on the treadmill (with the belt locked), such that subjects' heads were in the same position as during walking trials and their hands were resting on the handrails of the treadmill. Finger Tapping involved all four fingers on each hand being moved together, alternating hands, with a button positioned under the left hand to record the tapping frequency. Subjects were given practice beforehand in Treadmill Walking, Stationary Cycling, Arm Pedalling and Finger Tapping at the various instructed speeds. The Walking, Cycling and Arm Pedalling speeds of the subjects were obtained from sensors attached to the treadmill belt or to the spindle of the exercise cycle. These and the knob used to control the tunnel speed were electronically low pass filtered and digitally sampled at 30Hz and then digitally low pass filtered at 7Hz to remove noise. Subjects performed the same matching task as before, but the walking speed instructions: 'fast', etc. were to be

applied to each activity as appropriate and were required to be at this speed before the scene became visible.

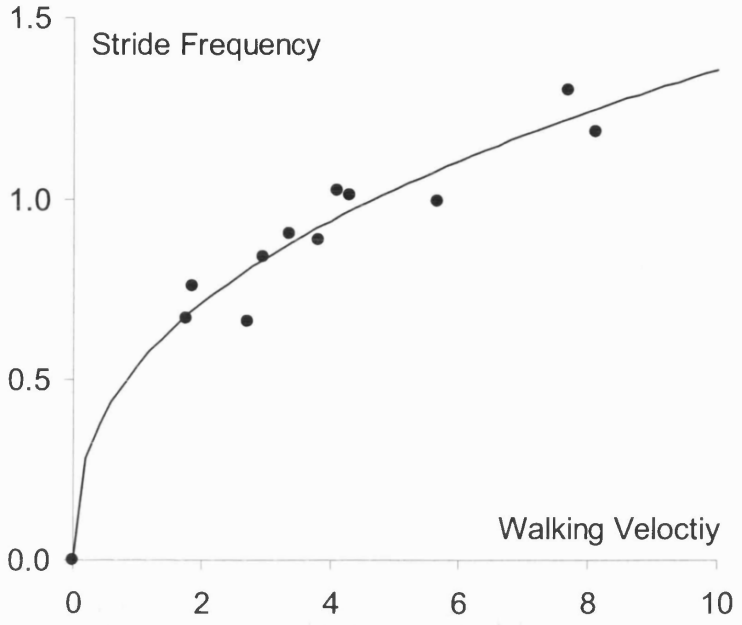

Figure 23: Plot of stride frequency versus walking speed for a single subject (BKW). Each point represents the walking speed and stride frequency for a single trial, calculated as described in the methods. Stride frequency increases approximately with the square-root of walking speed, in this subject the line of best fit is: $SF = 0.54 \times WV^{0.40}$

The visual scene was increased in resolution to 1280 by 1024 pixels (single pixel visual angle was 0.09° or 0.07° at the central fixation point), using a different LCD projector (InFocus LP740) and a screen refresh rate of 60Hz, again updated on alternate frames. The aspect ratio of the image projected on the screen was altered and now was contained within a central area 1.9m wide by 1.52m high. During experimental trials this image was approximately 0.9m (Walking, Finger Tapping) or 1.2m (Cycling, Arm Pedalling) from the subjects' eyes, subtending visual angles of 93° by 80° and 77° by 65° respectively. The fixation point was increased in size to three pixels square (0.28° × 0.28°, luminosity 1.51 cdm^{-2}) at the centre of the display. The visual scene was otherwise unchanged. The target velocity for the tunnel was 5cm/s as before, however as the subjects' heads were further from the screen during the Cycling and Arm

Pedalling trials, this corresponded to 2.1°/s angular motion at the mid-hemifield position 21.6° from the fixation point.

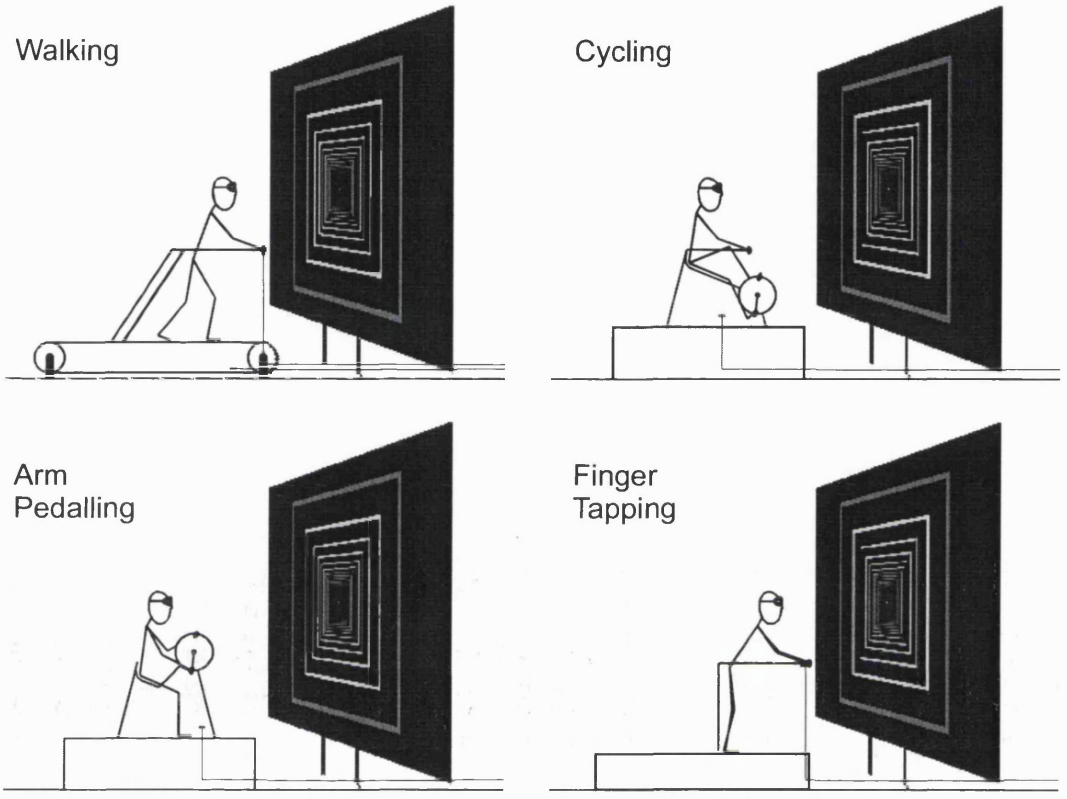

Figure 24: The experimental set-up for each activity. Subjects' heads were level with the centre of the display at all times, but further from the screen (1.2m vs. 0.9m) during the Cycling and Arm Pedalling trials. Subjects adjusted the speed of the test scenes using a knob positioned near the right hand at all times.

Activity speeds were normalised as a proportion of the mean speed during the 'very fast' trials of that type. Walking may be considered as a translational process, with speed measured by distance covered per unit time, or it can also be considered as a cyclical activity with speed measured by stride frequency. Therefore, for walking trials, both the stride frequency as well as walking speed were calculated as follows:

- The walking speed over the 10s of scene presentation was 4^{th} order bandpass filtered between 0.75 - 9.0Hz

- The power spectrum was then calculated using the Yule-Walker autoregressive algorithm (Marple, 1987). The use of a parametric spectral model, as produced by the Yule-Walker method, allows the main frequency component in the sample to be found with arbitrary accuracy, unlike using the FFT.

- The modal frequency was then found and divided by two to convert step frequency into stride frequency and these values checked by eye in plots of walking speed against stride frequency to remove erroneous values.

The stride frequency varies non-linearly with walking speed, as shown in Figure 23, but is highly correlated for each subject.

Walking Direction

To allow investigation into the influence of the direction of walking, some subjects were required to walk backwards as well as forwards. Backwards walking conditions were conducted by adding two new walking speed instructions: 'slow back' and 'fast back', intermixed as part of a longer trial involving walking both forwards and backwards. Walking backwards on the treadmill required subjects to pull on the handrail of the treadmill, as if dragging a trolley, they were given practice performing this beforehand. In this variation, the type 2 protocol was used, such that target presentations occurred whilst subjects were stationary, with target matching taking place in eight subsequent presentations of the test scene, each while walking at one of the instructed speeds (see Figure 21). Matching during each of the eight test scenes was to the target scene at the start of the presentation block, i.e. to the target that was presented most recently.

Extension to Other Optic flow Patterns

Five visual scenes were tested, containing optic flow progressively less like that found during forward motion: (1) Moving Tunnel, (2) Horizontal Grating, (3) Vertical Grating, (4) Cartwheel and (5) a Flashing Tunnel. These scenes were presented at a resolution of 1280 by 1024 pixels and updated at 30Hz. A fixation point 3 pixels square (0.28° x 0.28°, luminosity 1.51 cd/m^2) was provided at the centre of the display approximately at each subject's eye level for all optic flow patterns, the structure of the remainder of each scene being as follows:

(1, 5) The two tunnels were identical to those used previously, but reiterated here for convenience. They were composed of a simulated square tunnel in depth (simulated relative dimensions, near-point relative to the observer = 0.4 x width, far-point relative

to the observer = 5 x width) that consisted of 15 bright, anti-aliased squares against a dark (0.006 cd/m^2) background (see Figure 25, top left). The squares obeyed laws of perspective: increasing in thickness and size with decreasing simulated distance from the observer and luminosity changing as a trapezoid function of simulated distance (maximum luminosity 1.51 cdm^{-2}). This allowed fading of the rectangles into the distance with perspective and a reduction in brightness near the border of the screen to remove edge flicker. (1) The Moving Tunnel simulated translation in depth with speed measured in the plane of the screen of tunnel components at the mid-hemifield position (~27.8° away from fixation) thus at this point the 5cm/s (expanding) target speed used corresponded to angular motion of 2.7°/s at each subject's eye. (5) The Flashing Tunnel exhibited sinusoidal variations in brightness of all tunnel components together with a target speed of 2.0Hz.

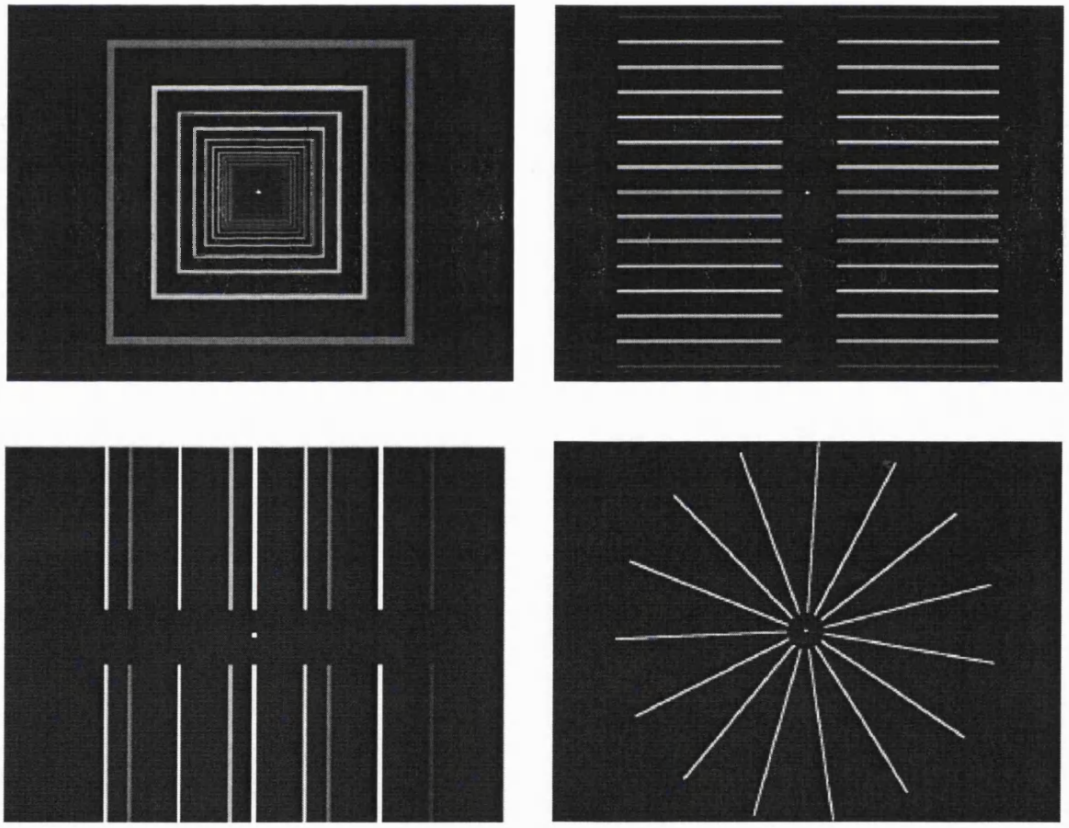

Figure 25: The different optic flow patterns. The tunnel (top left) either expanded or flashed; the horizontal grating (top right) moved downwards; the vertical grating (bottom left) moved rightwards; and the cartwheel (bottom right) rotated anti-clockwise.

(2, 3) The two gratings were composed of 15 bright (luminosity 1.51 cd/m^2), equally spaced, anti-aliased lines against a dark (0.006 cd/m^2) background (see Figure 25, top right, bottom left). Lines extended across the full height (or a width equal to the height) of the screen except for a gap (10% of screen height) in the centre to prevent overlap with the fixation point. As lines neared the edges of the screen they faded into and out of existence with a trapezoid brightness profile (maximum luminosity 1.51 cd/m^2) to prevent edge flicker. Grating speed was measured as the distance traversed across the screen in centimetres, again the target speed being 5cm/s. Other than orientation, horizontal and vertical gratings were identical, the Horizontal Grating always moving downward and the Vertical Grating always moving rightward.

(4) The Cartwheel was composed of 15 bright (luminosity 1.51 cd/m^2) spokes, against a dark (0.006 cd/m^2) background (see Figure 25, bottom right). The spokes rotated anti-clockwise around the axis of vision, their overall diameter was equal to the screen height, with a blank gap with a diameter of 10% of the screen height around the fixation point. Cartwheel speed was measured in the same manner as the Moving Tunnel: that of the components in the plane of the screen at the mid-hemifield position, the target speed was also 5cm/s.

Investigation of Reorientation of the Arthrovisual Effect

During walking we do not always look in the direction of travel, to test whether the hypothesised mechanism can account for this, a reduced number of subjects were tested with the treadmill rotated relative to the screen (see Figure 26). This rotation could be 0° (mid-line position, i.e. face-on), 45° (mid-right) or 90° (full-right), the experiment was repeated using all five optic flow patterns (see Extension to Other Optic flow Patterns above) at each orientation. These subjects were instructed to view the scenes presented at the mid-right and full-right positions by rotating the head on the neck rather than the eyes in the head and to otherwise maintain the orientation of their bodies to that of the treadmill. The position and orientation of the head was monitored during the experiment using a Polhemus Fastrack magnetic position-sensing device providing six degrees of freedom. The receiver of this device was attached to a light helmet worn on the top of the head with position data being collected at 30 Hz. For each visual pattern there were six matches at each walking speed, with five visual patterns giving a total session time per orientation of approximately 70 minutes. Subjects were rested between optic flow

patterns and testing of different orientations for each subject occurred on separate days to reduce fatigue.

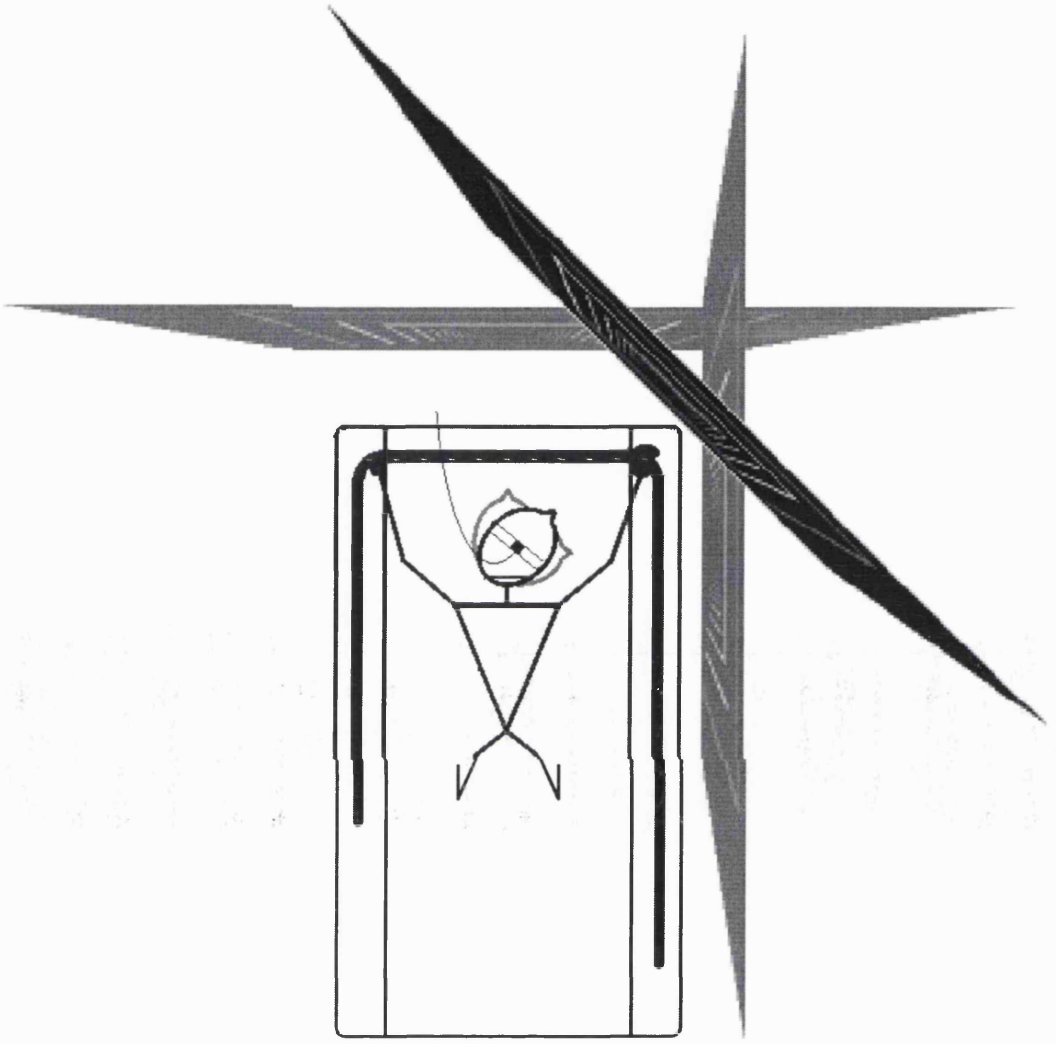

Figure 26: The set-up to investigate head-on-trunk rotations from above. The screen was rotated relative to the treadmill between sessions, and the subject's head was tracked using a magnetic position-sensing device.

Investigation of a Hemianopic Subject

To enable independent testing of each hemifield of 'blindsight' patient GY, the Moving Tunnel was modified to enable presenting of only the left or right half at a time. The fixation point was also moved slightly away from the centre of expansion of the tunnel, as GY has some macular sparing in the blind hemifield and this ensured that the tunnel was only visible to the designated side (see Figure 27). GY has been shown to be able to accurately compare the velocities of stimuli when either or both are presented in the

blind hemifield (Morland et al. 1999). In this modified experiment, the target optic flow speed was displayed either to the blind hemifield or to the intact hemifield (control), but the test optic flow presentation was always displayed only to the intact hemifield. This allowed a conscious matching of the target speed irrespective of the side of target display.

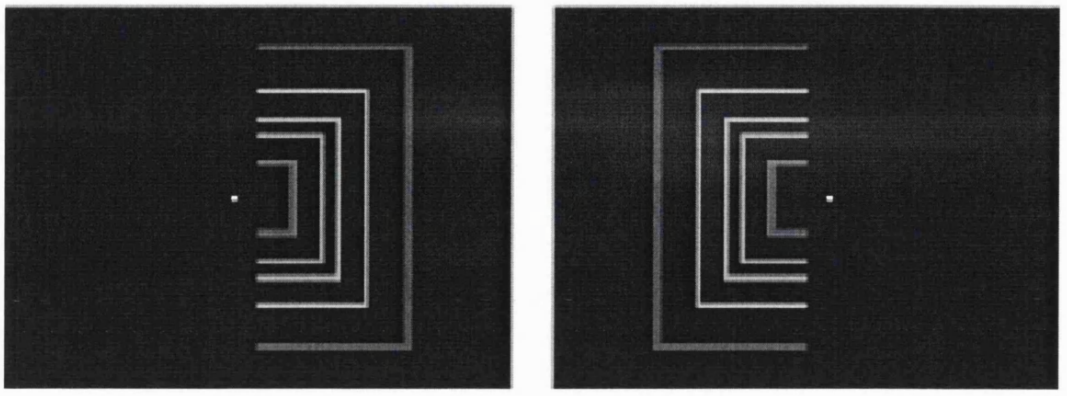

Figure 27: The new visual stimuli for testing a hemianopic patient.

Specification of Spatial Scale

If the arthrovisual effect is the result of a mechanism to maintain perceptual constancy during self-motion, the reduction in perceived visual speed should equal the walking speed. This can only be tested if the visual scene contains a spatial scale providing an unequivocal value for the reduction of perceived speed. This spatial scale was provided using stereopsis and/or parallax in a new visual display while subjects performed the same matching task as before.

Subjects stood or walked upon an exercise treadmill placed directly in front of a CRT monitor (see Figure 28). The positions of the eyes in space were monitored during the experiment using a Polhemus Fastrack magnetic position-sensing device. The receiver of this device was attached to a light helmet worn on the top of the head with eye positions calculated as rigid displacements from this position. Position data for each eye was collected at 30 Hz. The CRT display was 32cm wide by 24cm high and during experimental trials it was approximately 25cm from the subjects' eyes giving a field of view of ~65° by 51°. Subjects wore stereoscopic shutter goggles, restricting peripheral vision, though the entirety of the screen remained visible at all times, and with transmission ratios of ~50% (open) and ~0.05% (closed). The goggles allowed vision with only one eye at a time, synchronised with the CRT display to present alternate

frames to the left and right eyes. The display had a resolution of 1280 by 1024 pixels, fully anti-aliased, and a refresh rate of 60Hz allowing presentation to each eye at 30Hz. The visual scene comprised a tunnel in depth composed of two or three bright squares on a dark background. The tunnel had simulated dimensions of width 2m, height 2m, near point 2m behind the display screen, length 6m and component line width of 10cm. Perspective projection with these parameters gave the tunnel an approximately similar appearance to that during previous experiments except for the reduced number of tunnel components. A fixation point 1.2cm in diameter was simulated, floating in space 6m behind the display screen and at the same height above the floor of the tunnel as the subject's eyes. The luminosity of the tunnel components again changed as a trapezoid function of simulated distance. This allowed fading of the rectangles into the distance with perspective and a reduction in brightness near the limits of the display to remove edge flicker and prevent apparent vignetting of the tunnel by the display edges. The tunnel simulated translation in depth with the target speed used being equal to 3.1 kmph, this gave a mid-hemifield angular speed at the subjects' eyes of 4.0°/s, marginally faster than in the previous experiments.

Tunnel stimuli could be presented with and without stereoscopic depth and with and without motion parallax information, therefore, there were four types of tunnel: (1) Control, with both parallax information and stereopsis indicating a flat scene at the distance of the display screen. (2) With only stereopsis indicating a three dimensional tunnel. (3) With only motion parallax indicating a three dimensional tunnel. (4) Full 3D with both motion parallax and stereoscopic depth. Subjects were each tested using three out of the four types of tunnel corresponding to absent (1), weak (2 or 3) or strong (4) specifications of tunnel scale. For each tunnel there were 6 matches at each walking speed, with five visual patterns giving a total session time of approximately 45 minutes, subjects were rested between tests to reduce fatigue, which was higher during these than during previous experiments. Subjects were given practice with treadmill walking at the various instructed speeds and matching the tunnel speeds, particularly with immersing themselves within the 3D tunnel, their stereopsis was also tested beforehand.

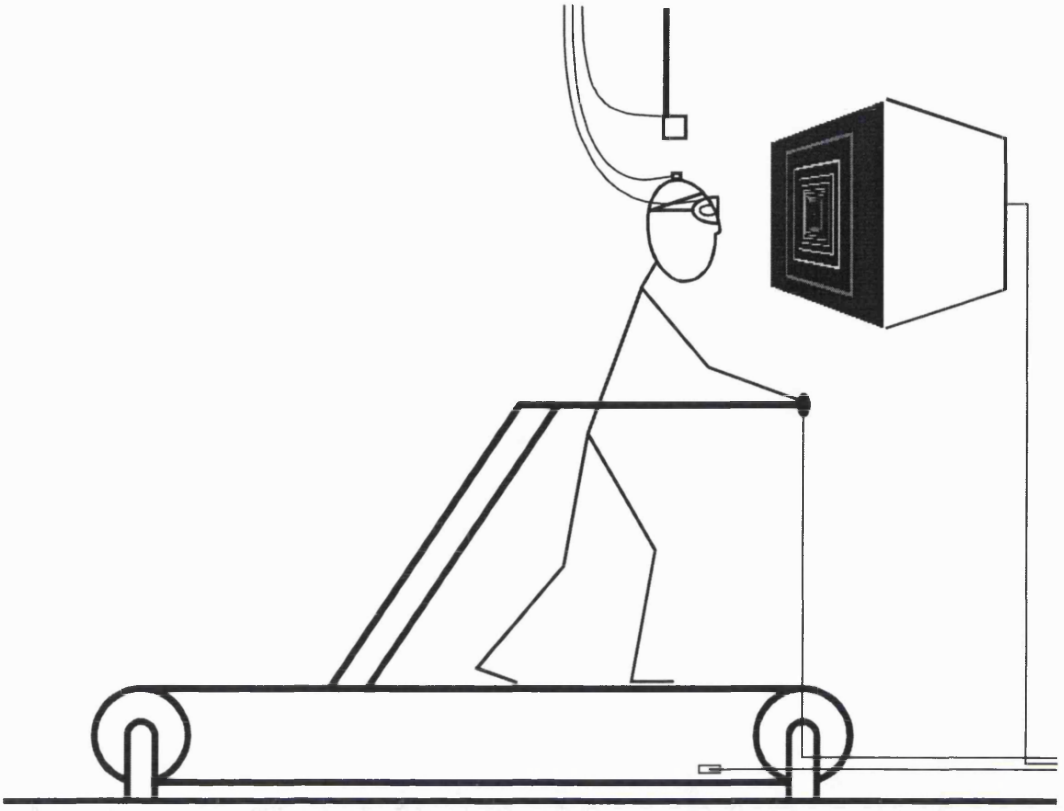

Figure 28: The set-up and the stimulus for specifying the spatial scale. Stereoscopic information was provided using by alternating the image presented to the two eyes, whilst parallax information was provided by calculating the displayed scene using information about the position of the head from a magnetic position sensing device.

Results

A number of control trials were conducted where no walking was involved, interspersed within the other experimental trials, these occurred both with a screen resolution of 1024 x 768 and at 1280 x 1024. These trials form a measure of each subject's accuracy in matching a previously seen target velocity under the simplest viewing conditions. The conditions involved standing for both target (constant speed 5cm/s) and matching presentations, while viewing the basic expanding tunnel stimulus. Each subject made a minimum of six matches in this condition with the mean and s.d. for each subject being calculated (see Figure 29). Subjects individually had slight biases towards higher or lower matched velocities than the target value, but were generally self-consistent in their matches, apart from subjects AC and EJ. These two subjects were unable to match between the target and the test flow speeds and so were removed from further analysis. The Lilliefors test showed that the matches made at each of the two resolutions for the

remaining subjects were normally distributed ($P > 0.05$). These populations were then compared using the t-test and F-test (both two tailed, $P > 0.05$), revealing no difference between the intersubject means or the variances, suggesting that display resolution does not affect subjects' matching ability.

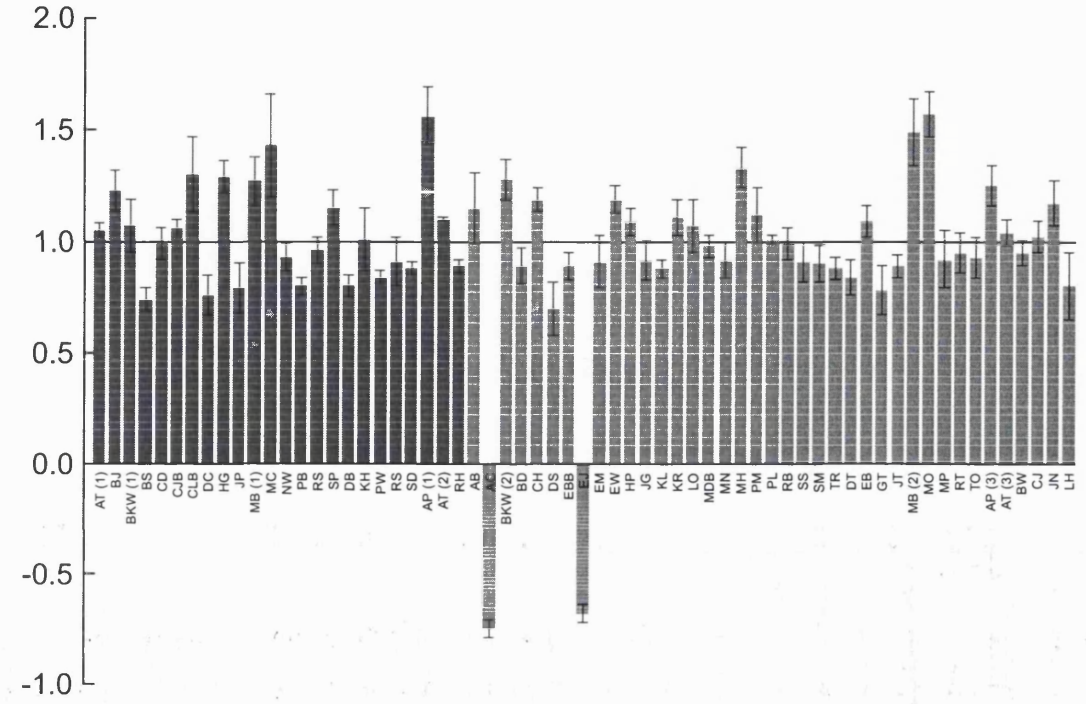

Figure 29: Mean (± s.e.m.) matched normalised optic flow speed without walking for all subjects. The dark bars represent matches from trials with a display resolution of 1024 x 768 at 35Hz, the light bars represent matches from trials with a display resolution of 1280 x 1024 at 30Hz. There was no significant difference between the matches made at these two resolutions. Some individual subject averages were significantly different from the target velocity (1.0), but the mean of all subjects was not significantly different (mean = 0.97, s.d. = 0.37), indicating that subjects were generally able to make good matches. Subjects AC and EJ were grossly inaccurate, and were removed from further analysis.

The Arthrovisual Effect

The influence of walking speed on the matched optic flow speeds was investigated in the same trials as were used above, interspersed within the other experimental trials. A mixture of naïve (91%) and non-naïve (9%) subjects were used for this condition. Walking speed had a profound effect on the values matched by subjects to the constant

target velocity. An example of the influence of walking speed on the perceived speed of tunnel expansion is shown in Figure 30. The line of best fit intercepts the optical speed axis near the target speed of 5cm/s showing unbiased optic flow perception during standing (cf. Figure 29). Matched speed settings indicate the speeds that the subjects consider perceptually equivalent to the constant optic flow target stimulus, i.e. the target tunnel is perceived to be moving slower with increasing walking speed. The slope of the line of best fit can be used to measure the strength of this effect, which for the subject in Figure 30 (CJB) was -0.37 and significantly different from zero ($P < 10^{-14}$).

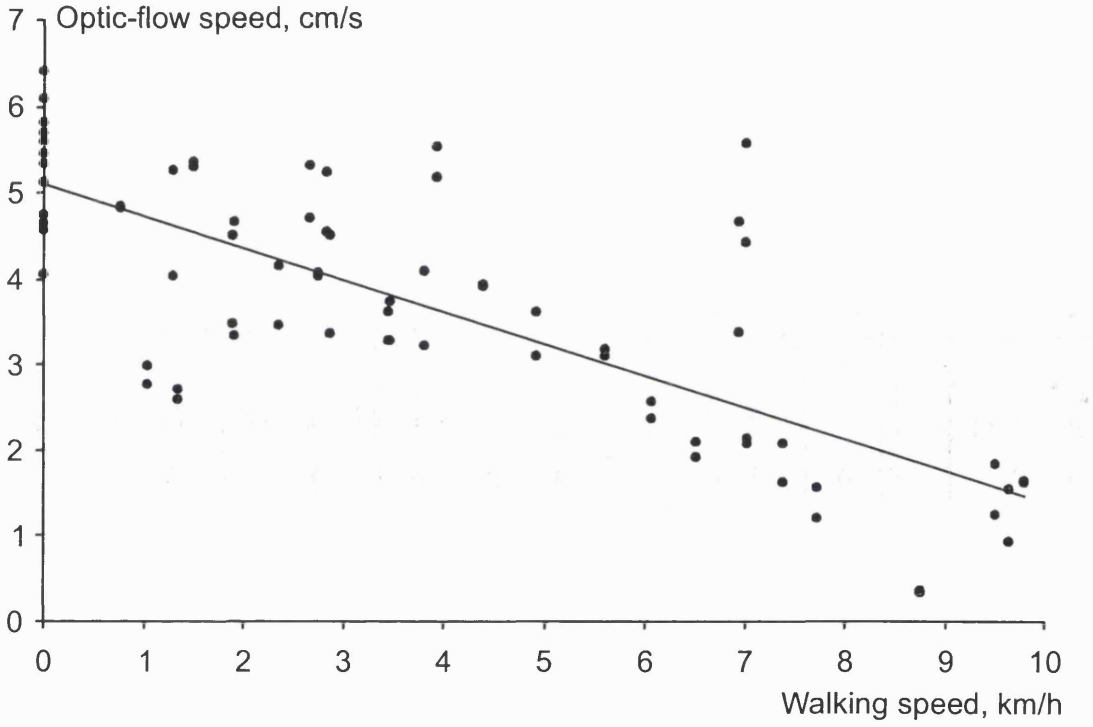

Figure 30: Unnormalised data showing the basic reduction in perceived optic flow speed during faster walking for a single subject (CJB) referred to as the arthrovisual effect. The similarity of the matched values to the target values when standing during both target and test can also be seen. The linear line of best fit had a y-intercept of 5.09, and a slope of -0.37 that was significantly different from zero ($R^2 = 0.59$, $P < 10^{-14}$). For the purpose of comparison with later graphs, plotting normalised optic flow speed against normalised walking speed gave a best-fit y-intercept of 1.02 and a slope of -0.65

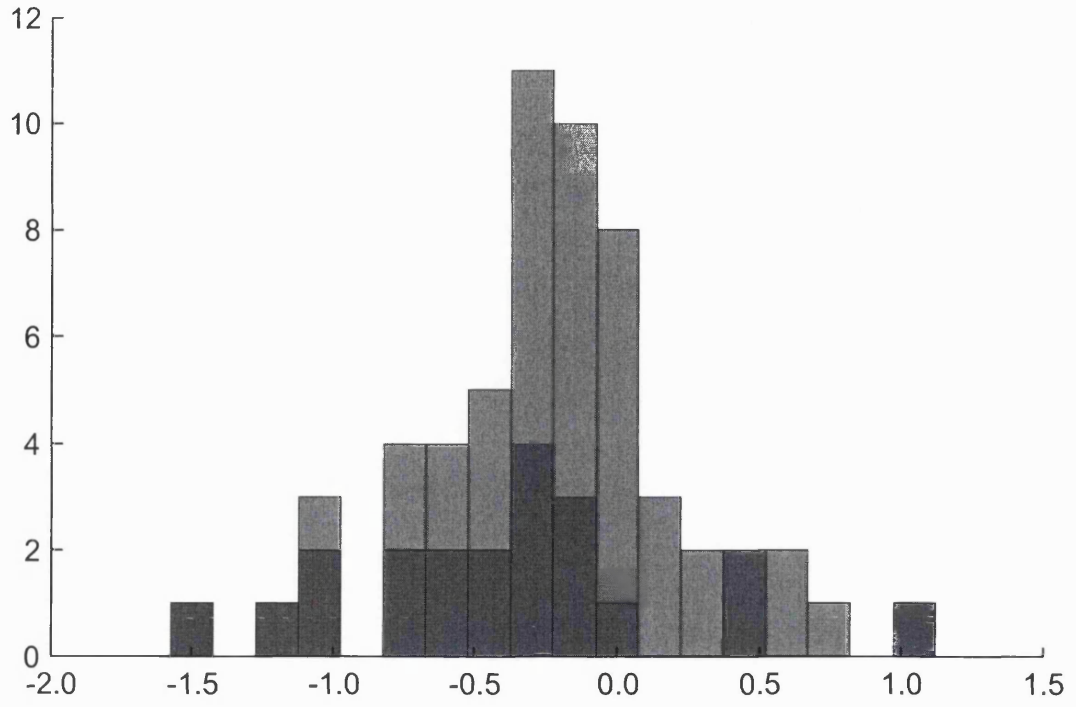

Figure 31: Histogram of the best-fit slopes of perceived normalised optic flow speed versus normalised walking speed. Bin width = 0.15, centred on 0.0. The distribution of slopes was normal, shown using the Lilliefors test and the mean (-0.19) significantly less than zero (T-test, $P < 0.05$). The trials included here are taken from all experiments where the subject matched the expanding tunnel during walking using the type 1 protocol, some subjects are therefore included more than once as they were used for more than one experiment. The dark portion of bars represent matches from trials with a display resolution of 1024 x 768 at 35Hz and the light portion of bars represent matches from trials with a display resolution of 1280 x 1024 at 30Hz. There was no significant difference between the best-fit slopes at these two resolutions (unpaired two-tailed t-test, $P > 0.05$).

Again, there are two populations of trials: those at a resolution of 1024 x 768 and those at 1280 x 1024. These populations were both determined to be normally distributed using the Lilliefors test ($P > 0.05$) and so were compared using parametric methods. The means were -0.39 and -0.15 for the low and high-resolution populations respectively and these were not significantly different using a two-tailed t-test ($P > 0.05$). The variances were 0.22 and 0.14 for the low and high-resolution populations respectively and these also were not significantly different using an F-test ($P > 0.05$). Therefore the data from the two populations was combined for further analysis. This new combined population was shown to be normally distributed using the Lilliefors test. The mean of

this combined population (-0.23) is significantly different from zero using a two-tailed t-test ($P < 0.05$). Therefore, walking speed does have a significant influence on visual speed perception in the population tested. Many subjects, including naïve subjects who were unaware that the target speed was always the same, confirmed the observation verbally that the optic flow speed looks progressively slower when walking faster.

Control Variations

Reversal of the Order of Walking and Standing

It is possible that walking causes in some way a disruption of the subject's ability to remember the target optic flow velocity, so to test for this, complementary (type 2) experiments were conducted in which the order of events was altered. Target presentation occurred during standing while matching occurred during walking, preventing any supposed disruption by walking of establishing a memory of the target velocity (see Methods). In the type 2 protocol, the slopes of the lines of best fit plotting optic flow settings against walking speed were of opposite sign (as expected) and not significantly different (two-tailed, unpaired t-test) in magnitude from the equivalent slopes for type 1 trials (Figure 32, Table 1).

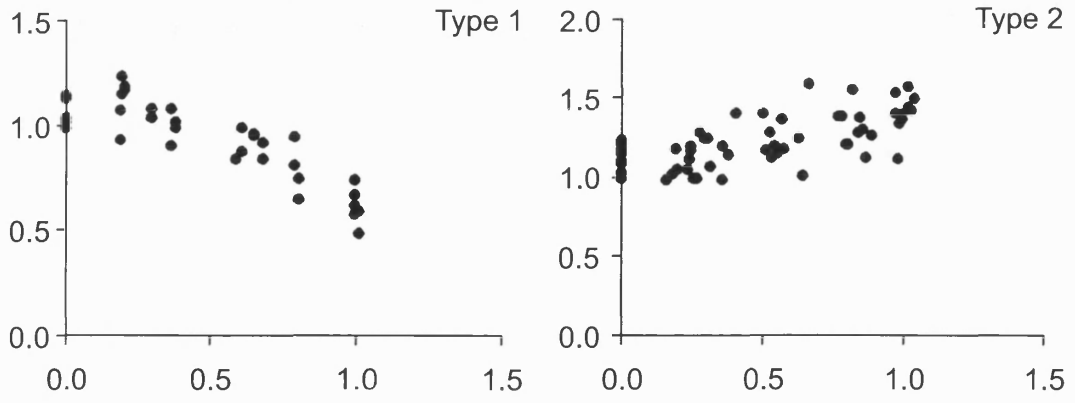

Figure 32: Comparison of the arthrovisual effect during type 1 and type 2 trials for a single subject (AT) showing the similarity of the magnitude of the slopes of the lines of best fit (-0.47 and +0.32 for types 1 and 2 respectively). This difference reflects the influence of walking speed on the remembered target and on the concurrently matched optic flow speed respectively.

Type 1 Trials				Type 2 Trials			
Subject	Intercept	Slope	R^2	Subject	Intercept	Slope	R^2
AT	1.15	-0.47	0.72	AP	1.49	0.55	0.12
BJ	1.17	-0.37	0.13	AT	1.06	0.32	0.46
BW	1.18	-1.00	0.49	FP	0.88	0.81	0.69
BS	0.68	1.02	0.59	RH	0.81	1.06	0.68
CD	0.94	-0.11	0.07				
CJB	1.02	-0.65	0.59				
CLB	1.21	0.00	0.00				
DC	0.97	-0.10	0.01				
HG	1.36	-0.81	0.64				
JP	0.82	-0.59	0.36				
MB	1.46	-1.02	0.57				
MC	1.65	-1.49	0.65				
NW	0.82	-0.34	0.36				
PB	0.80	0.47	0.34				
RS	0.90	0.51	0.22				
SP	1.03	-0.71	0.60				
DB	0.80	-0.46	0.45				
KH	1.13	-1.19	0.75				
PW	0.94	-0.19	0.10				
RS	0.98	-0.34	0.25				
SD	0.91	-0.29	0.26				
Mean	**1.04**	**-0.39**		**Mean**	**1.06**	**0.68**	
s.e.m	**0.05**	**0.13**		**s.e.m**	**0.18**	**0.18**	

Table 1: Slopes measuring the arthrovisual effect during type 1 and type 2 trials. The data from subject AT are shown in more detail in Figure 32. A Lilliefors test showed that the data was normally distributed ($P > 0.05$) so the means were compared using an unpaired T-test (two-tailed). The magnitudes of the slopes were not significantly different ($P > 0.05$).

Attentional Control

Changes in motion perception due to attentional load have been reported for first-order motion (Sahraie et al. 2001) and for motion after-effects (Chaudhuri 1990). To investigate the possibility that the influence of walking velocity on perceived optic flow speed may be due to changes in attentional load, a comparison was made between performance with and without a concurrent numerical aural-verbal task. The strength of the effect (as measured by the slope of the best-fit line) during the attentional task was slightly lower than during control trials, though this difference was not significant (two-tailed, paired t-test; see Table 2), suggesting that cognitive overload was not responsible for the reported effect.

Subject	Without Attentional Task			With Attentional Task		
	Intercept	Slope	R^2	Intercept	Slope	R^2
AT	1.15	-0.47	0.72	1.16	-0.50	0.58
BJ	1.17	-0.37	0.13	0.93	0.77	0.38
BW	1.18	-1.00	0.49	0.75	-0.73	0.59
BS	0.68	1.02	0.59	0.91	0.63	0.26
CD	0.94	-0.11	0.07	0.85	-0.06	0.02
CJB	1.02	-0.65	0.59	1.24	-0.78	0.67
CLB	1.21	0.00	0.00	0.95	0.28	0.29
DC	0.97	-0.10	0.01	1.54	-0.23	0.27
HG	1.36	-0.81	0.64	0.91	0.52	0.14
JP	0.82	-0.59	0.36	1.01	-0.62	0.36
MB	1.46	-1.02	0.57	1.38	-0.12	0.02
MC	1.65	-1.49	0.65	1.26	-1.10	0.55
NW	0.82	-0.34	0.36	0.59	-0.10	0.07
PB	0.80	0.47	0.34	0.82	0.56	0.19
RS	0.90	0.51	0.22	1.11	0.39	0.28
SP	1.03	-0.71	0.60	0.88	-0.58	0.51
Mean	**1.07**	**-0.35**		**1.02**	**-0.10**	
s.e.m	**0.07**	**0.17**		**0.06**	**0.15**	

Table 2: Comparison of the arthrovisual effect with and without a concurrent attentional task. A Lilliefors test showed that the data was normally distributed ($P > 0.05$) so the means were compared using a paired T-test (two-tailed). The magnitudes of the slopes were not significantly different ($P > 0.05$).

Head Motion Control

Movement of the head that results in vestibular stimulation causes an increase in visual motion detection thresholds and latencies (Probst et al. 1986) and there is, therefore, the possibility that the vestibular effect may extend as well to a reduction of supra-threshold perceived object motion speeds. When walking the head oscillates in all six degrees of freedom (see Figure 33) which, if this vestibular hypothesis is correct, may provide a mechanism for the described effect if the magnitude of the stimulation increased with walking speed. To determine whether head motion during walking indeed causes the observed changes in perceived optic flow speed, some trials were conducted with restricted head motion. Using a bite bar rigidly attached to the treadmill, a comparison was made between treadmill walking with unrestricted or restricted head motion.

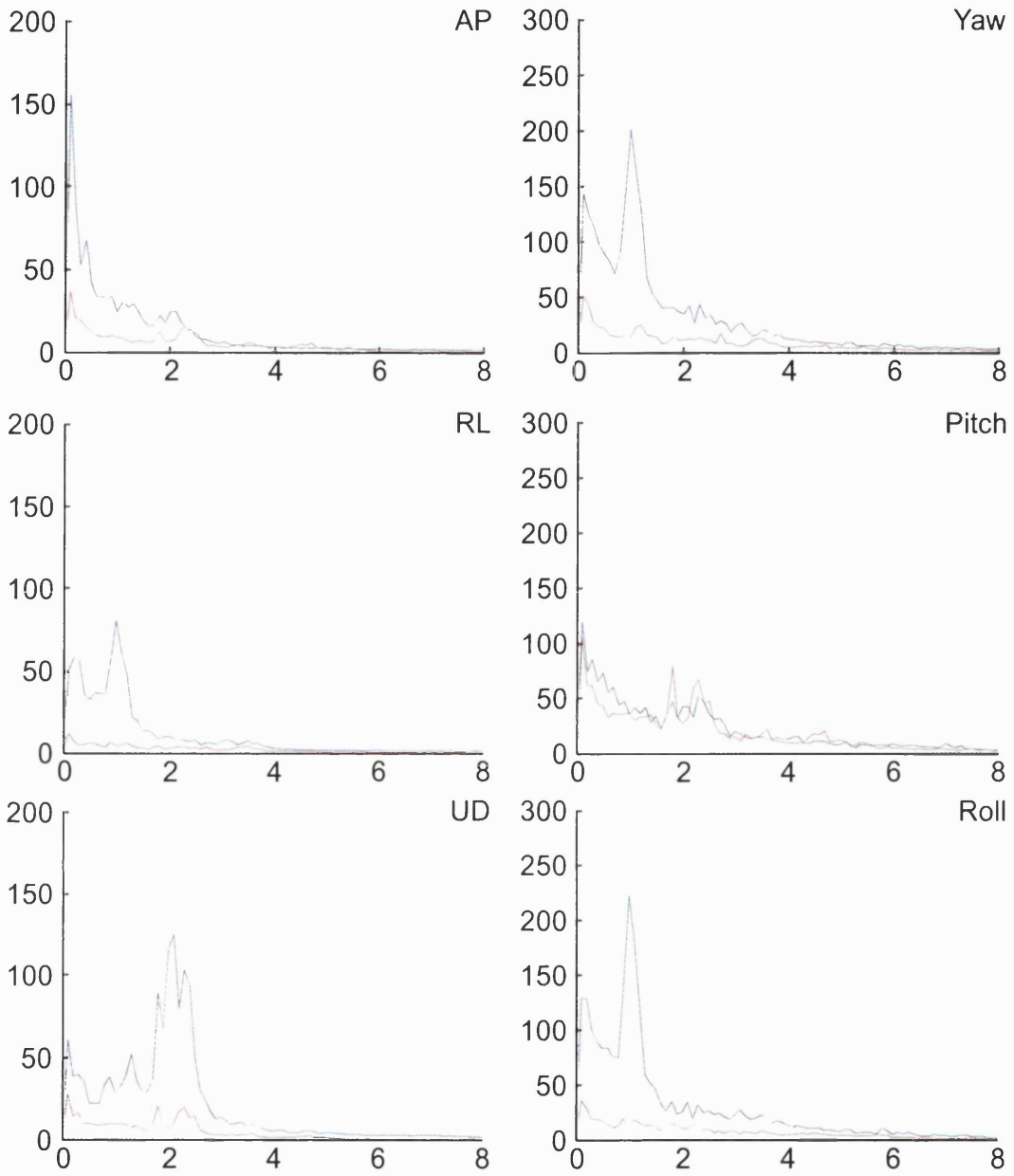

Figure 33: Spectra of head motion in each degree of freedom with and without restriction of head motion using a bite-bar for a single subject (MB). The spectra are averaged over all trials. AP, RL and UD motion were reduced approximately by factors of 5, 15 and 5 respectively, while Yaw, Pitch and Roll motion were reduced approximately by factors of 10, 0 and 10.

Though the influence of walking speed on perceived optic flow speed was on average lower during the reduced head motion condition (Table 3), this difference was not significant ($P > 0.05$). When comparing the amount of head motion between the conditions, the head was not held completely rigid, but motion in all axes of freedom except for pitch was reduced by a factor of between 5 and 15 (see Figure 33). If the

postulated mechanism were to predominantly work via pitch motion then little or no difference would be expected. However, this seems unlikely given that Probst et al. (1986) found significant effects on visual motion detection thresholds using yaw motion. Also, rotations of the head in pitch and yaw have a similar influence on the retinal image, and so they would be expected to have a similar influence on visual motion perception. The mechanism leading to reduced visual speed perception while walking cannot therefore be attributed principally to the vestibular system.

	Unrestricted Head Motion			**Restricted Head Motion**		
Subject	Intercept	Slope	R^2	Intercept	Slope	R^2
AT	1.15	-0.47	0.72	1.02	-0.50	0.67
DC	0.97	-0.10	0.01	0.85	-0.01	0.00
HG	1.36	-0.81	0.64	0.85	-0.02	0.00
MB	1.46	-1.02	0.57	1.79	-0.60	0.34
MC	1.65	-1.49	0.65	1.35	-0.32	0.09
NW	0.82	-0.34	0.36	0.92	-0.35	0.18
PB	0.80	0.47	0.34	0.82	-0.07	0.02
Mean	**1.17**	**-0.54**		**1.09**	**-0.27**	
s.e.m.	**0.13**	**0.26**		**0.15**	**0.10**	

Table 3: Comparison of the arthrovisual effect with restricted and unrestricted head motion. A Lilliefors test showed that the data was normally distributed so the means were compared using a paired T-test (2-tailed). The magnitudes of the slopes were not significantly different ($P > 0.05$).

Motorised versus Self-Powered Walking

To determine the influence of the slightly 'unnatural' walking during the previous experiments, the strength of the arthrovisual effect was compared during this 'unnatural' walking and the more 'natural' walking occurring during powered treadmill walking. Due to the difficulties involved in this experiment, only a single subject (AT) was tested, and not when standing still during the comparison phase (no points along the y-axis), and the results of this comparison are shown in Figure 34. The slopes of best fit for the two conditions are 0.38 ± 0.06 (mean ± s.e.m.) for Self-powered Walking and 0.51 ± 0.07 for the Motorised Walking, these values are significantly different (two-tailed t-test; $P < 0.05$), indicating a stronger effect during 'natural' walking. This would be plausible, as there are fewer contra-indicators to movement in this condition as the hands are not in contact with a stationary object.

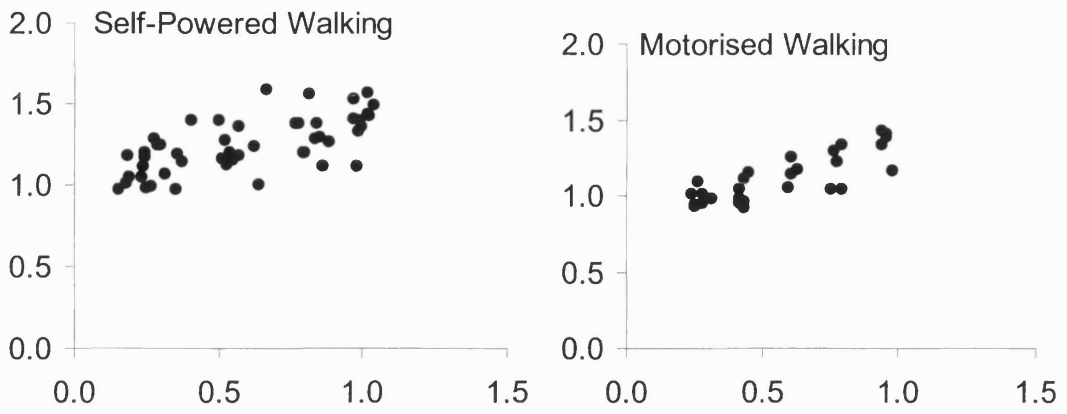

Figure 34: Comparison of the arthrovisual effect during motorised and self-powered walking. As data from the same subject (AT) was used for both plots, walking speed in both *is normalised by the mean 'Very Fast' speed during the self-powered condition. The slopes of best fit are 0.38 ± 0.05 (mean ± s.e.m.) for Self-powered Walking and 0.51 ± 0.07 for the Motorised Walking, while the intercepts are 1.02 and 0.82 respectively. As these conditions were conducted as type 2 trials, the slopes are positive, which indicates a reduced perceived visual speed at higher walking speeds.*

Other Variations

Timing Perception Investigation

As discussed in the Introduction, there exists the possibility that walking affects not visual speed *per se* but rather timing, which could theoretically influence speed as one of its constructs. The strength of the influence of walking speed on visual speed perception compared to its influence on temporal frequency perception (see Table 4). The strengths of the influence of walking speed on temporal frequency perception were not normally distributed (Lilliefors test, $P < 0.05$) thus comparisons involving these two conditions are made using non-parametric tests. An initial comparison of the slopes for the two conditions suggests no difference using a Wilcoxon signed rank test ($P > 0.05$). This test is, in effect, telling us that the changes in the slope from one condition to the other are not always in the same direction. However, we can test the slightly less stringent condition that in moving from the expanding to the flashing tunnel, the influence of walking speed is reduced (i.e. the slopes becomes closer to zero). Thus, comparing the absolute slopes (again using a Wilcoxon signed rank test) reveals a significant difference ($P < 0.05$), i.e. the effect of walking speed is greater on the perception of visual motion than on timing perception. This suggests that changes in the

perception of visual motion could not occur solely as a consequence of changes in timing perception.

	Expanding Tunnel			Flashing Tunnel		
Subject	Intercept	Slope	R^2	Intercept	Slope	R^2
DB	0.80	-0.46	0.45	1.04	-0.14	0.19
KH	1.13	-1.19	0.75	1.01	-0.20	0.25
PW	0.94	-0.19	0.10	0.91	-0.12	0.14
RS	0.98	-0.34	0.25	0.91	-0.02	0.01
SD	0.91	-0.29	0.26	0.84	-0.01	0.00
DT	0.83	0.08	0.02	1.01	-0.21	0.06
EB	0.98	0.04	0.01	0.91	0.03	0.01
GT	0.63	0.36	0.24	0.36	0.13	0.15
JT	0.89	0.08	0.02	0.92	0.03	0.02
MB	1.78	-0.66	0.24	1.42	-0.74	0.48
MO	1.54	-0.71	0.34	1.08	0.13	0.02
MP	0.84	-0.09	0.02	0.82	0.00	0.00
RT	0.91	-0.01	0.00	0.89	0.06	0.01
TO	0.82	0.32	0.28	0.97	-0.04	0.01
AP	1.21	-0.36	0.44	0.97	0.03	0.06
AT	1.10	-0.43	0.64	0.95	-0.14	0.29
BW	0.99	-0.25	0.30	1.00	-0.03	0.01
CJ	0.98	-0.07	0.02	0.96	-0.06	0.11
JN	1.03	-0.24	0.18	0.98	0.00	0.00
LH	0.58	0.60	0.30	0.97	-0.06	0.00
Median	**0.96**	**-0.21**		**0.96**	**-0.03**	
s.e.m	**0.06**	**0.09**		**0.04**	**0.04**	

Table 4: Comparison of the influence of walking on the perception of optic flow speed and flashing frequency. The five subjects initialled in bold were tested with the visual display at a resolution of 1024 x 768 and refresh frequency of 35Hz, the remainder being tested at 1280 x 1024 and 30Hz, the results from both resolutions were combined for analysis. The absolute slopes of the lines of best fit for the expanding and flashing tunnels were 0.34 ± 0.07 (mean ± s.e.m.) and 0.11 ± 0.04 respectively, these values were significantly different (paired two-tailed t-test, $P < 0.05$).

Extension to other Motor Activities

To determine the types of motor activity than can affect the perception of optic flow speed, subjects' visual motion perception was tested using the following four different motor activities under otherwise identical conditions, and the results are shown in Table 5:

Subject	Walking			Cycling			Arm Pedalling			Finger Tapping		
	Intercept	Slope	R^2	Intercept	Slope	R^2	Intercept	Slope	R^2	Intercept	Slope	R^2
AB	1.05	-0.02	0.00	0.94	0.05	0.02	0.79	0.31	0.31	0.96	0.13	0.05
AC	-0.76	0.04	0.03	-0.75	0.22	0.52	-0.71	0.21	0.60	-0.84	0.14	0.71
BD	0.76	-0.16	0.09	0.77	-0.09	0.03	0.84	-0.17	0.08	1.10	-0.02	0.00
BKW	1.16	-0.81	0.63	1.07	-0.71	0.49	0.94	-0.20	0.06	0.72	-0.03	0.00
CH	1.03	-0.03	0.00	0.91	0.32	0.21	0.97	0.02	0.00	0.94	0.01	0.00
DS	0.89	-0.02	0.00	1.07	0.09	0.01	0.89	0.07	0.02	1.50	-0.29	0.12
EB	0.95	-0.11	0.02	1.08	-0.22	0.18	0.57	0.26	0.09	0.92	0.16	0.07
EJ	-0.64	-0.05	0.03	-0.64	-0.07	0.06	-0.45	-0.31	0.28	-0.68	0.01	0.00
EM	0.91	-0.47	0.42	0.84	-0.24	0.30	0.86	-0.09	0.07	1.02	-0.14	0.07
EW	1.11	-0.37	0.35	1.04	-0.27	0.47	0.93	-0.26	0.28	0.87	-0.01	0.00
HP	1.05	-0.23	0.25	1.08	-0.37	0.46	1.08	-0.15	0.13	1.11	0.13	0.12
JG	0.93	-0.48	0.29	0.88	-0.20	0.24	0.77	-0.19	0.17	0.82	0.06	0.02
KL	1.08	-0.12	0.04	0.98	-0.12	0.13	1.45	-0.57	0.35	0.90	-0.12	0.07
KR	1.12	-0.08	0.03	0.97	0.16	0.10	1.15	-0.03	0.01	0.95	0.11	0.05
LO	1.41	-0.56	0.22	0.93	-0.26	0.09	0.92	-0.05	0.01	1.25	-0.49	0.25
MDB	1.00	-0.10	0.08	0.91	-0.02	0.00	1.13	-0.06	0.01	0.96	0.02	0.00
MN	0.86	-0.34	0.35	0.91	-0.21	0.27	1.03	-0.51	0.49	0.85	0.11	0.05
MH	1.52	-1.04	0.67	1.08	-0.57	0.78	0.95	-0.29	0.14	1.11	-0.20	0.18
PM	0.82	0.69	0.41	0.80	0.34	0.20	0.57	0.39	0.17	0.79	0.27	0.15
PL	0.95	-0.01	0.00	0.95	-0.03	0.02	0.78	0.03	0.01	0.96	0.12	0.10
RB	1.25	0.15	0.03	0.94	0.15	0.13	0.92	0.10	0.09	1.06	0.16	0.07
SM	0.96	-0.19	0.20	1.02	-0.14	0.18	0.91	-0.01	0.00	1.02	0.04	0.02
SS	0.91	0.54	0.32	0.96	0.21	0.17	1.53	0.17	0.01	0.99	0.08	0.03
TR	0.94	-0.27	0.45	0.91	-0.12	0.12	1.10	0.21	0.08	0.92	-0.05	0.02
Mean	**1.03**	**-0.18**		**0.96**	**-0.10**		**0.96**	**-0.05**		**0.99**	**0.00**	
s.e.m	**0.04**	**0.08**		**0.02**	**0.06**		**0.05**	**0.05**		**0.04**	**0.04**	

Table 5: Slopes of perceived optic flow speed plotted against motor activity speed. Two subjects (AC and EJ) are greyed above as they were removed from analysis due to being unable to match optic flow speeds when standing still (see Figure 29).

- Walking is the most natural of the activities considered here and as such is predicted to have the greatest influence on visual speed perception.
- Cycling is a more 'indirect' activity than walking, in that there is not a one to one relationship between the speed achieved and either cadence or effort; cadence was used for comparability with other activities.
- Arm pedalling was conducted in the same manner as cycling and therefore the same considerations apply.
- Finger tapping has no inherent speed, as it is completely non-locomotor, so must be measured as a frequency of action.

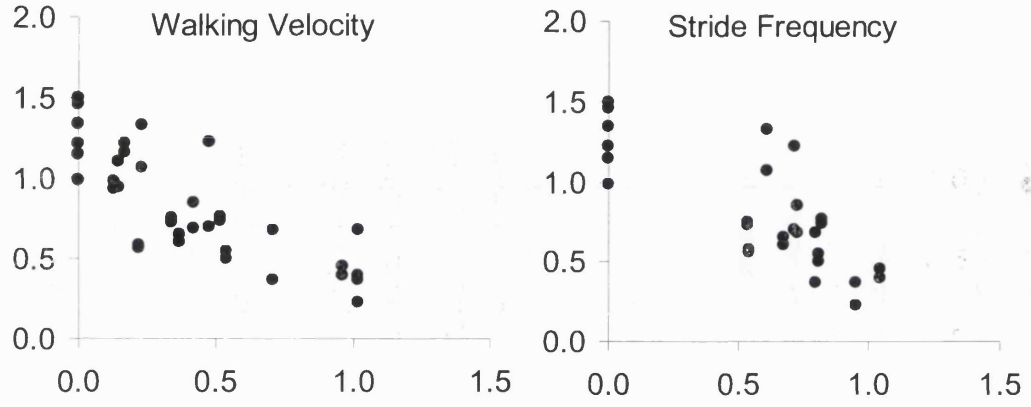

Figure 35: Comparison of plotting the perceived speed of optic flow versus walking speed or versus stride frequency for a single subject (BKW). Line of best fit measured using walking speed: NOFS = 1.16 - 0.81 × NWV, R^2 = 0.63 Line of best fit measured using stride frequency: NOFS = 1.09 - 0.58 × NSF, R^2 = 0.44

As walking may be measured as a translational or a cyclical process (see Figure 23), either walking velocity or stride frequency may be used to measure the activity speed a comparison was made to determine the best measure to use. Both walking velocity and stride frequency were distributed normally (Lilliefors test, $P > 0.05$), and no significant differences (paired two-tailed t-test, $P > 0.05$) were found between these measures in terms of their influence on optic flow speed perception (see Figure 35 for data from a single subject). Therefore, for the purposes of comparison with the other experiments, walking velocity was used as a measure of activity speed.

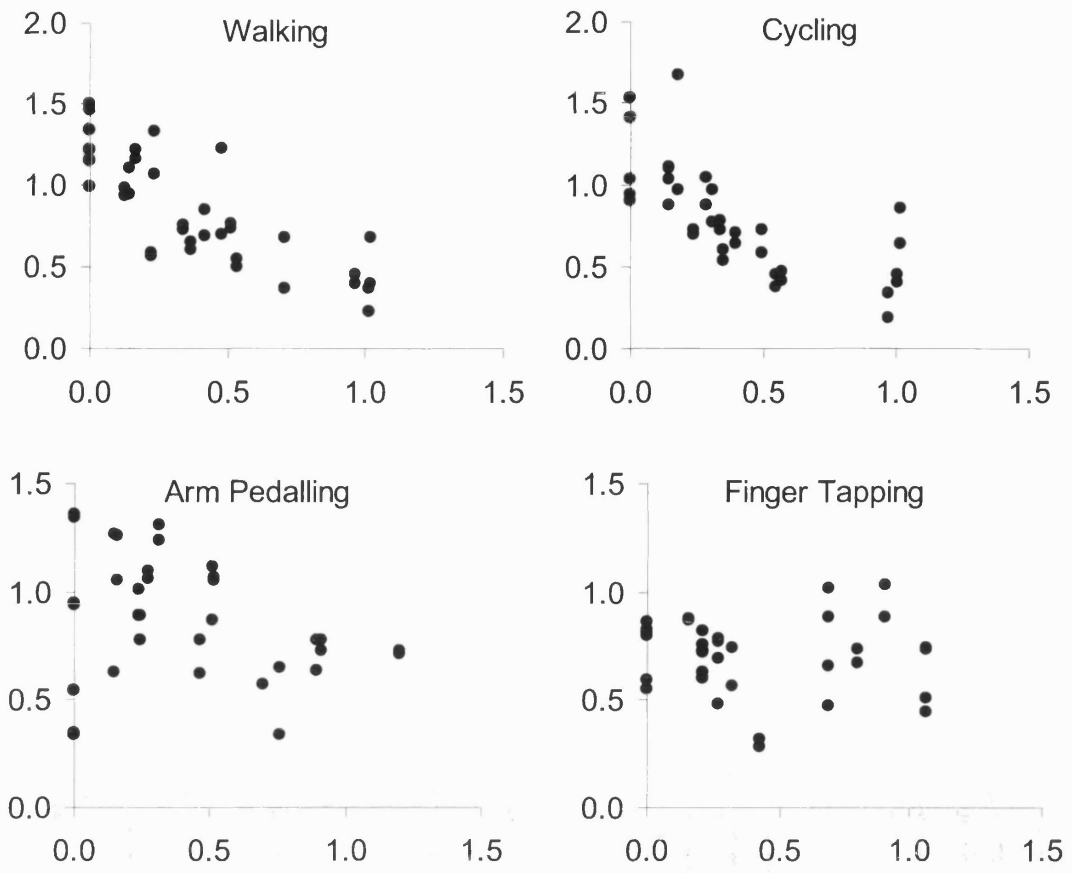

Figure 36: Comparison of matched optic flow speed during different motor activities for a single subject (BKW), for all subjects, see Appendix C. Line of best fit during Walking: NOFS = 1.16 - 0.81 × NWV, R^2 = 0.63 and P < 0.05 Line of best fit during Cycling: NOFS = 1.07 - 0.71 × NWV, R^2 = 0.49 and P < 0.05 Line of best fit during Arm Pedalling: NOFS = 0.94 - 0.20 × NWV, R^2 = 0.06 and P > 0.05 Line of best fit during Finger Tapping: NOFS = 0.72 - 0.03 × NWV, R^2 0.00 and P > 0.05

Differences in the natural rates of each type of action were removed by normalising to the mean of the fastest rates at which each subject performed. The comparison between the motor activities showed a trend from Walking through Cycling and Arm Pedalling to Finger Tapping in the strength of the influence of the motor activity on optic flow speed perception (see Figure 36 for a single subject and Figure 37 for the group summary). The effect strengths for each activity were shown to be normally distributed using the Lilliefors test ($P > 0.05$) therefore parametric statistics are used for comparisons. A 2-way anova with subject and activity as the factors shows that the effect strengths for the activities are significantly different ($P < 0.05$). As the relative influences of the activities on visual motion perception is relatively well defined, one-tailed tests are used to compare the activities. The effect strength

for Walking was significantly different from zero (t-test, $P < 0.05$), and was also significantly greater than for Cycling, Arm Pedalling or Finger Tapping (paired t-test, $P < 0.05$). The effect strength for Cycling was significantly different from zero (t-test, $P < 0.05$), and was also significantly greater than for Finger Tapping (paired t-test, $P < 0.05$). These results confirm that the effect strengths are in the following order: Walking > Cycling > Arm Pedalling > Finger Tapping = 0.

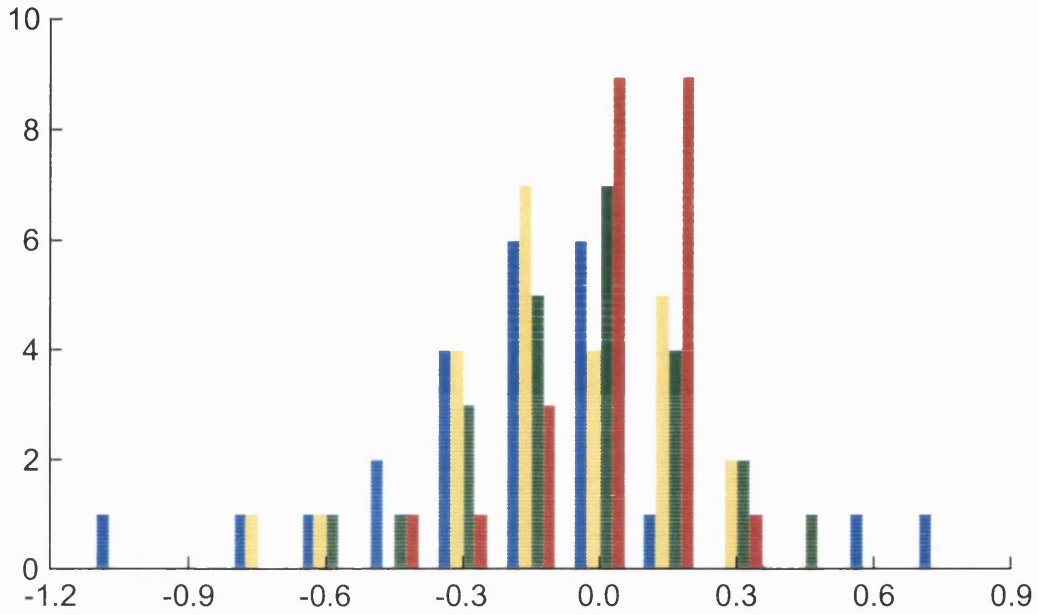

Figure 37: Intersubject histograms of the strength of the arthrovisual effect (measured using slope) across motor activities. Blue = Walking, yellow = Cycling, green = Arm Pedalling, red = Finger Tapping. Histogram bins are 0.15 units wide, eother side of the bin centred at 0.0 Although there is considerable overlap, it can be seen that the spread of slopes during walking is more negative (i.e. stronger effect) than that for Finger Tapping, with the other two conditions in between.

Walking Direction

Three subjects were used to compare walking forwards and backwards on perceived optic flow speed. This investigation was conducted with the modified order of events referred to as type 2 trials, in which subjects were stationary during the target presentation and walking during the matching presentations (see Methods). As walking speed increased it reduced the perceived optic flow speed of the concurrently viewed scene (now the matching scene) therefore the matched optic flow speeds are now higher than the target speed (see Figure 38). Best-fit slopes were of opposite sign, but otherwise similar to those found previously (see

Table 6). During backward walking the more negative the walking speed, the greater the matched optic flow speed, producing a line of best fit similar to that for forward walking but mirrored in the Y axis. This suggests that walking speed but not direction influences the processing of optic flow speed.

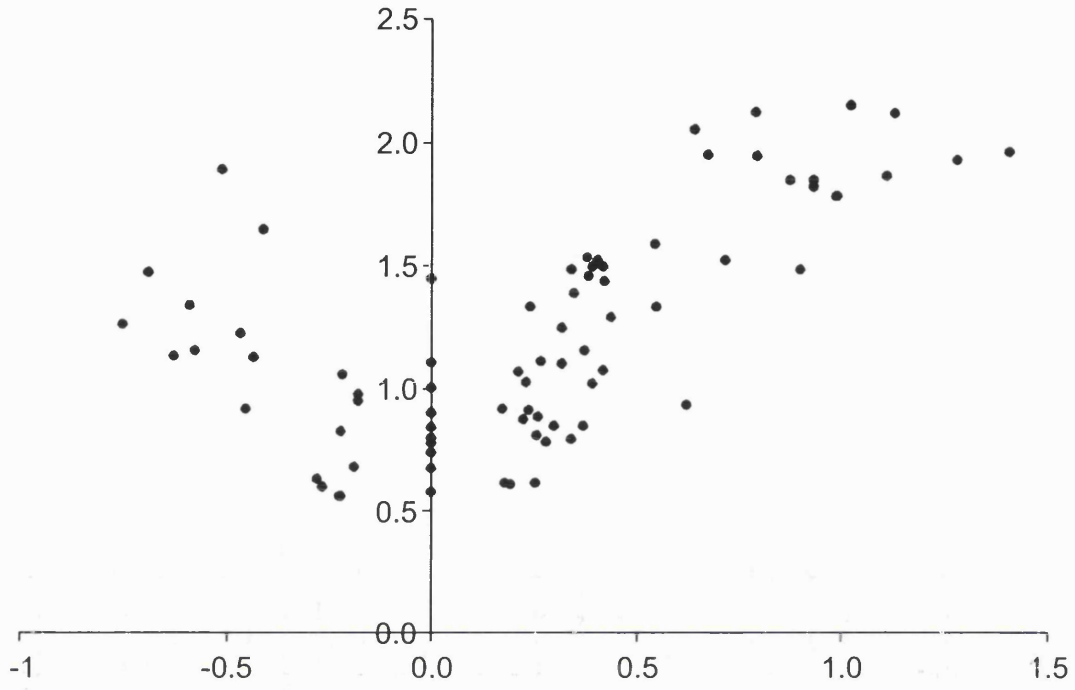

Figure 38: Normalised optic flow speed (NOFS) plotted against normalised walking velocity (NWV) showing the influence of walking direction on the arthrovisual effect in a single subject (RH). Line of best fit during backwards walking: NOFS = 0.80 - 0.76 × NWV, R^2 = 0.30 and P < 0.05 Line of best fit during forwards walking: NOFS = 0.81 + 1.06 × NWV, R^2 = 0.68 and P < 0.05

Subject	**Backwards**		**Forwards**	
	Slope	P	Slope	P
AP	-0.70	0.163	0.55	0.055
AT	-0.18	0.018	0.32	1.69×10^{-9}
RH	-0.76	0.002	1.06	9.11×10^{-16}

Table 6: Summary of the influence of walking direction on the arthrovisual effect across all three subjects.

Extension to Other Optic flow Patterns

To determine the types of optic flow pattern influenced by walking speed, subjects' visual motion perception was tested for each of four different optic flow patterns under otherwise identical conditions (see Table 7). The effect strengths for each pattern were shown to be

normally distributed using the Lilliefors test ($P > 0.05$), therefore parametric statistics are used for comparisons. A two-way anova with subject and pattern as the factors shows that the effect strengths for the patterns are not significantly different ($P > 0.05$). However, this test is for the relatively stringent condition that the changes in the slope from one pattern to the other are always in the same direction. Testing was performed on the slightly less stringent condition that the influence of walking speed is reduced (i.e. the magnitude of the slopes reduce, regardless of sign) for some patterns (e.g. the Cartwheel) relative to others (e.g. the Expanding Tunnel). Thus, comparing the slope magnitude (using a Friedman non-parametric two-way ANOVA test as the data is not now normally distributed) also does not reveal a significant difference ($P > 0.05$), i.e. the arthrovisual effect is no different between the optic flow patterns tested.

Investigation of the Reorientation of the Arthrovisual Effect

Six subjects were used to investigate the tuning of the direction of walking relative to the direction of the axis of vision. The results are summarised in Table 8 and Figure 39. The effect strengths for each combination of pattern and orientation were shown to be not normally distributed using the Lilliefors test ($P < 0.05$), therefore non-parametric statistics are used for comparisons. As the current hypothesis predicts that the influence of orientation on the arthrovisual effect will depend heavily on the optic flow pattern used orientation and pattern were compared separately rather than using a three-way test. The effect strengths across patterns and orientations were compared separately using Friedman non-parametric ANOVAs (two-way ANOVAs with either subject and pattern as factors or with subject and orientation as factors). These analyses did not reveal any significant differences ($P > 0.05$) between either the optic flow patterns (confirming the results above) or the orientations. Again, this test is for the relatively stringent condition that the changes in the slope from one pattern to the another and one orientation to another are always in the same direction. Testing was repeated for the slightly less stringent condition that the influence of walking speed is reduced (i.e. the magnitudes of the slopes reduce, regardless of sign) for some conditions relative to others. Thus, comparing the absolute slopes (again using Friedman non-parametric two-way ANOVAs) again does not reveal a significant difference ($P > 0.05$), i.e. the arthrovisual effect is no different between the optic flow patterns or the orientations tested.

Subject	Expanding Tunnel			Horizontal Grating			Vertical Grating			Cartwheel		
	Intercept	Slope	R^2	Intercept	Slope	R^2	Intercept	Slope	R^2	Intercept	Slope	R^2
DT	0.83	0.08	0.02	0.88	-0.04	0.00	0.90	0.00	0.00	0.76	0.07	0.03
EB	0.98	0.04	0.01	0.84	-0.01	0.00	0.95	-0.09	0.02	0.80	0.06	0.01
GT	0.63	0.36	0.24	2.40	-0.58	0.16	0.81	0.08	0.01	0.91	-0.11	0.06
MB	1.78	-0.66	0.24	1.52	-0.87	0.35	1.76	-0.96	0.36	1.19	-0.15	0.05
MO	1.54	-0.71	0.34	1.28	-0.66	0.49	1.06	-0.50	0.37	1.18	-0.53	0.46
MP	0.84	-0.09	0.02	0.69	0.10	0.03	0.87	-0.15	0.04	0.82	0.04	0.01
RT	0.91	-0.01	0.00	0.94	0.02	0.00	0.68	0.17	0.07	0.86	-0.17	0.08
TO	0.82	0.32	0.28	1.17	-0.12	0.06	0.94	-0.12	0.10	1.00	-0.01	0.00
AP	1.21	-0.36	0.44	1.38	-0.37	0.49	1.36	0.06	0.02	1.09	0.02	0.01
AT	1.10	-0.43	0.64	0.99	-0.28	0.50	1.06	-0.43	0.68	0.91	-0.07	0.11
BW	0.99	-0.25	0.30	0.85	0.05	0.04	0.98	0.11	0.08	0.99	-0.06	0.05
CJ	0.98	-0.07	0.02	0.93	0.02	0.00	1.04	0.01	0.00	0.89	-0.14	0.19
JN	1.03	-0.24	0.18	1.00	-0.27	0.32	1.04	-0.23	0.16	0.96	0.02	0.00
LH	0.58	0.60	0.30	0.57	0.72	0.28	0.66	0.28	0.04	0.55	0.35	0.15
Mean	**1.02**	**-0.10**		**1.10**	**-0.16**		**1.01**	**-0.13**		**0.92**	**-0.05**	
s.e.m	**0.09**	**0.10**		**0.13**	**0.11**		**0.08**	**0.09**		**0.05**	**0.05**	

Table 7: Slopes of perceived optic flow speeds for each pattern plotted against walking speed. There is neither a trend of effect strength from Expanding Tunnel > Horizontal Grating > Vertical Grating > Cartwheel as measured by slope nor as measured by absolute slope.

		Expanding Tunnel			Horizontal Grating			Vertical Grating			Cartwheel		
Mid-Line	Subject	Intercept	Slope	R^2	Intercept	Slope	R^2	Intercept	Slope	R^2	Intercept	Slope	R^2
	AP	1.21	-0.36	0.44	1.38	-0.37	0.49	1.36	0.06	0.02	1.09	0.02	0.01
	AT	1.10	-0.43	0.64	0.99	-0.28	0.50	1.06	-0.43	0.68	0.91	-0.07	0.11
	BX	0.99	-0.25	0.30	0.85	0.05	0.04	0.98	0.11	0.08	0.99	-0.06	0.05
	CJ	0.98	-0.07	0.02	0.93	0.02	0.00	1.04	0.01	0.00	0.89	-0.14	0.19
	JN	1.03	-0.24	0.18	1.00	-0.27	0.32	1.04	-0.23	0.16	0.96	0.02	0.00
	LH	0.58	0.60	0.30	0.57	0.72	0.28	0.66	0.28	0.04	0.55	0.35	0.15
	Mean	**0.98**	**-0.13**		**0.95**	**-0.02**		**1.02**	**-0.03**		**0.90**	**0.02**	
	s.e.m	**0.10**	**0.17**		**0.12**	**0.18**		**0.10**	**0.11**		**0.08**	**0.08**	
Mid-Right	Subject	Intercept	Slope	R^2	Intercept	Slope	R^2	Intercept	Slope	R^2	Intercept	Slope	R^2
	AP	1.09	-0.23	0.22	1.45	-0.33	0.31	1.36	-0.13	0.04	0.97	0.02	0.01
	AT	1.10	-0.36	0.60	1.18	-0.47	0.63	1.02	-0.25	0.42	0.98	-0.07	0.08
	BX	0.94	-0.33	0.29	0.59	0.30	0.21	0.86	-0.19	0.11	0.80	-0.05	0.02
	CJ	0.94	-0.04	0.01	1.01	-0.13	0.17	0.89	0.02	0.00	0.99	-0.28	0.47
	JN	1.06	-0.32	0.31	0.97	0.02	0.00	1.01	-0.14	0.03	1.01	-0.11	0.05
	LH	0.84	0.19	0.06	0.98	0.04	0.00	0.80	0.19	0.06	1.01	-0.27	0.17
	Mean	**0.99**	**-0.18**		**1.03**	**-0.10**		**0.99**	**-0.08**		**0.96**	**-0.13**	
	s.e.m	**0.05**	**0.10**		**0.13**	**0.12**		**0.09**	**0.07**		**0.04**	**0.05**	
Full-Right	Subject	Intercept	Slope	R^2	Intercept	Slope	R^2	Intercept	Slope	R^2	Intercept	Slope	R^2
	AP	0.96	-0.38	0.64	1.39	-0.25	0.24	1.36	-0.19	0.06	0.95	-0.07	0.06
	AT	1.11	-0.03	0.01	0.95	-0.02	0.00	1.14	-0.42	0.62	1.04	-0.15	0.33
	BX	0.97	0.15	0.14	0.85	0.04	0.01	0.95	0.04	0.01	0.98	-0.03	0.02
	CJ	1.03	-0.13	0.04	1.05	-0.01	0.00	0.94	-0.11	0.09	0.86	-0.03	0.01
	JN	1.22	-0.35	0.36	1.37	-0.64	0.56	1.12	-0.26	0.23	0.97	-0.21	0.23
	LH	0.67	0.40	0.22	1.00	0.06	0.00	0.75	0.25	0.13	0.90	-0.03	0.00
	Mean	**0.99**	**-0.06**		**1.10**	**-0.14**		**1.04**	**-0.11**		**0.95**	**-0.09**	
	s.e.m	**0.08**	**0.13**		**0.10**	**0.12**		**0.09**	**0.10**		**0.03**	**0.03**	

Table 8: Slopes of perceived optic flow speed plotted against walking speed during rotations of the visual display. This data is summarised graphically in Figure 39.

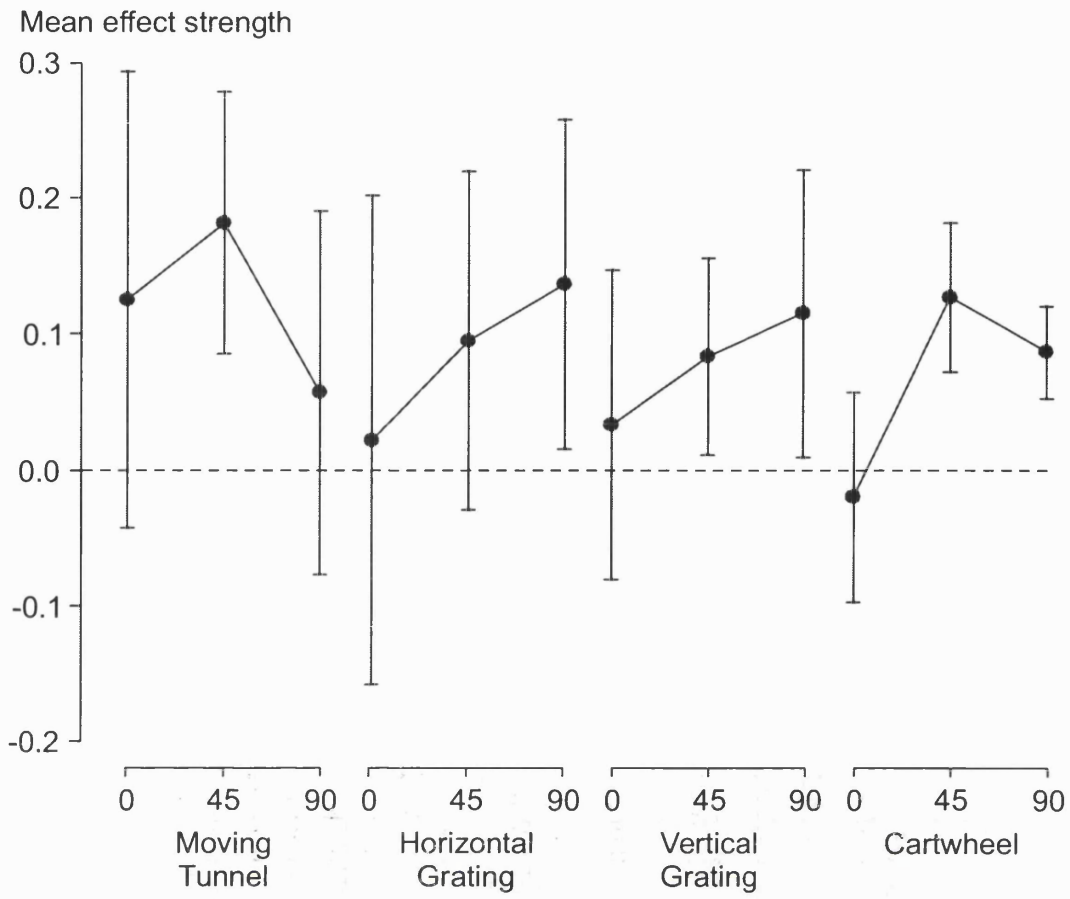

Figure 39: Intersubject means (± s.e.m.) of the strength of the arthrovisual effect during reorientation of the visual display. As the direction of walking and the direction of visual motion become more aligned (0° for the Moving Tunnel, 90° for the Vertical Grating) the influence of walking on the perceived speed of the optic flow pattern becomes more pronounced. See main text for other conditions.

Investigation of a Hemianopic Subject

In order to narrow down the neural location of the arthrovisual effect, a hemianopic subject GY was tested with the visual stimulus confined to either the sighted or blindsighted hemifields. GY reported a sensation of movement when the Moving Tunnel was presented in his blind hemifield, though he maintained that there was no conscious sensation of vision, in accordance with descriptions of his residual vision (Barbur et al. 1980). He showed a strong arthrovisual effect (see Figure 40) when viewing both the target and test scenes with his intact visual hemifield giving a linear best-fit intercept of 1.02 and a slope of -0.77 ± 0.08 (mean ± s.e.m.). GY was then tested viewing the target scene with his blind hemifield but viewing of the test scene with his intact hemifield, the linear line of best fit having intercepts of 0.89 and a slope of –0.70

± 0.10. The magnitude of the slope is slightly higher when viewing with the intact hemifield, however, there was no significant difference between the linear best-fit slopes ($P > 0.05$).

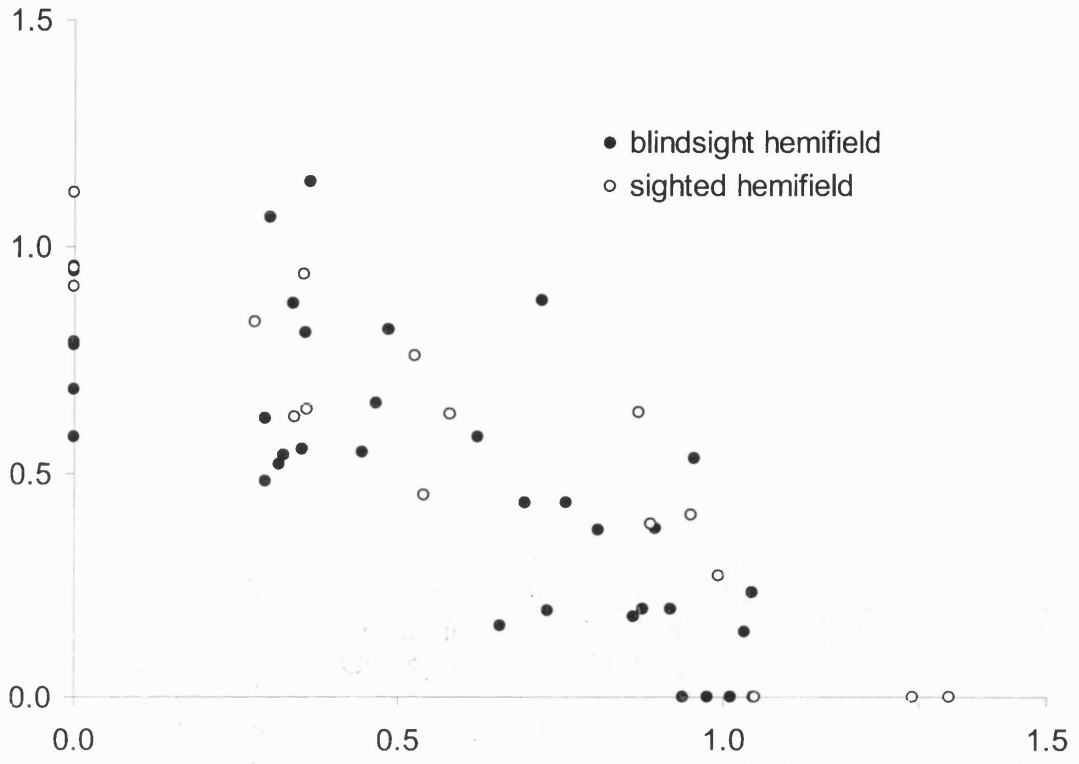

Figure 40: Comparison of the strength of the arthrovisual effect in the sighted and blindsighted hemifields of the hemianopic subject GY. Normalised optic flow speed (NOFS) is plotted against normalised walking velocity (NWV). Line of best fit with the target shown to the sighted hemifield: NOFS = 1.02 - 0.77 × NWV, R^2 0.85 Line of best fit with the target shown to the blindsight hemifield: NOFS = 0.89 - 0.70 × NWV, R^2 0.58 The slopes of these lines of best fit are not significantly different at the P = 0.05 level.

Specification of Spatial Scale

The arthrovisual effect is predicted to remove exactly that quantity of visual motion that would, in overground walking, be due to each particular walking speed. By specifying the visual scale more accurately this hypothesis becomes testable. All five subjects tested in this experiment were shown to have a strong, reliable reduction in perceived tunnel expansion speed during walking (see Extension to Other Optic flow Patterns). However, whilst one subject (AP) maintained a strong influence of walking speed on

perceived tunnel speed across the new conditions, for the remainder there seemed to be no consistent effect and a large variability between conditions (see Table 9). As there was neither a robust arthrovisual effect, nor an apparent trend in the differences between the conditions, no further statistical analysis was performed on this data.

No Scale				**Stereo**		
Subject	Intercept	Slope	R^2	Intercept	Slope	R^2
AP	0.95	-0.34	0.57	1.01	-0.30	0.57
AT	1.15	-0.20	0.21	1.14	-0.29	0.25
BW	0.87	-0.05	0.02	0.91	0.14	0.08
CJ	0.89	0.00	0.00			
JN	1.15	0.08	0.06	1.03	-0.02	0.00
Mean	**1.00**	**-0.10**		**1.02**	**-0.12**	
s.e.m	**0.07**	**0.08**		**0.05**	**0.13**	
Parallax				**Both**		
Subject	Intercept	Slope	R^2	Intercept	Slope	R^2
AP				0.96	-0.26	0.13
AT				1.21	-0.06	0.01
BW				0.93	0.11	0.06
CJ	0.98	-0.06	0.02	0.93	-0.10	0.05
JN				1.07	0.05	0.01
Mean	**0.98**	**-0.06**		**1.02**	**-0.05**	
s.e.m				**0.06**	**0.07**	

Table 9: Comparison of the strength of the arthrovisual effect across different methods of specification of the spatial scale. Each subject participated in three conditions: with no supplied scale, with a single scale cue and with both scale cues. When tested, subject CJ did not have stereoscopic vision and so was supplied with parallax rather than stereo images for the single cue condition.

Discussion

The results from subjects standing still during both the target and matching parts of each trial show that subjects were well able to make comparisons between two optic flow speeds. This is not new, but it forms the foundation upon which this chapter rests.

The Arthrovisual Effect

Subjects matched a constant optic flow velocity lower during faster walking than slower walking, indicating that walking faster made the optic flow look slower, and did so consistently across subjects (Figure 31). The display was monocular, and contained no familiar objects with an inherent scale, however a possible cue for scale is the symmetrical vertical structure of the tunnel: as the fixation-point at mid-height is level

with the subjects' eyes, the tunnel must be twice this height. However, this cue was subjectively weak, allowing subjects to interpret the scene alternatively as large, far away and moving quickly or small, close and moving more slowly (or perhaps something in between). Without robust depth cues, it cannot be determined whether the reduction in perceived optic flow velocity is by an amount that would accurately compensate for the speed of walking. At the same time, however, the results are consistent with an hypothesis of perceptual constancy: that the visual system uses arthrokinetic signals from the legs during walking to modulate the perceived velocity of optic flow so as to establish the absolute velocity of objects in space.

From Figure 31 it can be seen that there is a good deal of inter-subject variation in the strength and indeed the presence of this effect. Some of this variation is undoubtedly due to the experimental methods used, but at the same time it is unlikely, given the spread of results, that all subjects are using arthrokinetic signals in visual processing at all. A parallel may be draw here with stereoscopic vision, where despite its obvious benefits, there remain many people who do not use the information from both eyes to the fullest extent (e.g. subject CJ). In a similar vein, there are likely to be factors in childhood that promote or inhibit the development of the underlying mechanisms that result in the arthrovisual effect. It would certainly be interesting to investigate this possibility further, probably by means of a questionnaire.

Neurones in primate dorsal medial superior temporal (MSTd) area have a number of suitable properties for implementing the proposed visual constancy mechanism for self-motion. Most MSTd neurones have large receptive fields and are tuned to a continuum of first-order optic flow motions (Graziano et al. 1994), making them ideal candidates for selecting self-motion from a complex motion stimulus. Many MSTd neurones, unlike MT neurones, also respond selectively to externally induced visual motion but not to motion induced by eye movements (Erickson and Their, 1991 and Bradley et al. 1996) or head rotations (Shenoy et al. 1999). Vestibular stimulation by linear whole-body movements also influences the direction selectivity of MST neurones in a manner that may disambiguate self- and object-motion (Duffy, 1998; Bremmer et al. 1999). Signals of self-motion for MST neurones may arrive from the vestibular nucleus, a multi-sensory area whose neurones appear to encode self-motion whether derived from the vestibular apparatus (e.g. Daunton and Thomsen, 1979) or visually from large field motion causing vection (Dichgans and Brandt, 1972). Proprioceptive signals of neck

motion also play an important part in shaping the output of vestibular neurones (Gdowski and McCrea, 2000), whilst electrical stimulation of nerves in the limbs has been shown to affect the activity of vestibular nucleus neurones (Jian et al. 2002). The latter findings suggest that limb proprioceptive signals may be incorporated into signals of self-motion encoded by the vestibular nuclei, though this has not yet been confirmed electrophysiologically.

The current study provides a possible mechanism for findings that the strength of the MAe is greatly reduced when the adapting stimulus is viewed concurrently with stimuli indicating self-motion. If the MAe results from activity in the same neurones as are responsible for perception of the adapting motion, as shown by Tootell et al. (1995), then a mechanism that influences the perception of visual motion will also influence the MAe. In the motion after-effect study of Pelah and Boddy (1998), it is possible that a reduction in perceived speed while walking resulted in less adaptation and therefore a weaker after-effect, compared to that perceived during standing. This would parallel the reduced motion after-effect reported when adaptation took place during passive vestibular stimulation (Harris et al. 1981), which may be explained similarly by a reduction in the perceived speed of visual motion during passive linear acceleration (Pavard and Berthoz, 1977).

Control Variations

Trial Order Reversal

Comparison between subjects' matching during type 1 and type 2 trials revealed no difference in the size of the effect, but a reversal of its direction. This shows that walking does not 'distract' subjects from remembering the visual speed or making a proper match to the remembered speed. It is consistent with signals of walking speed reducing perceived optic flow speed only during walking, as part of a mechanism of perceptual constancy, but not as an after-effect (since in type 2 trials matching occurs during walking not after).

Attentional Control

A concurrent attentional task did not alter effect strength. Indeed, if attentional limitations were causing the effect then narrowing the cognitive bottleneck would be expected to heighten its influence not reduce it. The attentional task used in the current study has limitations in that a numerical task may be expected to interfere with spatial

processing relatively little (Wickens, 1980). A possible improvement for future studies would be to use a more spatial task such as navigating around an imaginary grid.

Head Motion Control

Examining the head-stabilised data suggested that vestibular signals are not primarily responsible for the described effect, however the lack of head stabilisation in pitch renders this statement relatively uncertain. The slight reduction, however, could also be explained within the proposed context, as head oscillations are a normal component of walking and may combine with the complex of proprioceptive signals in judging walking speed.

Motorised versus Self-Powered Walking

The comparison of motorised versus self-powered walking showed that the style of walking was not responsible for the arthrovisual effect, indeed the effect was stronger during the more 'natural' electrically powered condition than in the self-powered condition.

Other Variations

Timing Perception Investigation

In the current study, no subject reported any change in apparent dimensions of the tunnel with walking speed; therefore the 'time-space construct' mechanism would require changes in time perception alone. There was no significant effect of walking velocity on timing perception (see Table 4), suggesting that the influence of walking speed on optic flow perception does not occur via changes to a time-distance construct. Indeed, perception of velocity at higher walking speeds is such that the tunnel actually appears stationary to some subjects, suggesting that velocity and position are quite separable, a finding which is difficult to reconcile with a 'time-distance construct' mechanism.

Extension to other Motor Activities

Comparison of the intersubject mean arthrovisual effect strengths revealed a steady reduction in effect strength as the activity became less similar to natural locomotion, with Finger Tapping having no significant influence on visual perception. Cycling utilises much of the same musculature as walking, but with a different co-ordination pattern, and even for experienced cyclists there would be no direct relationship between cadence and translational speed. Arm Pedalling utilises different muscles to those used

in cycling, though with a broadly similar cyclical action. The most important similarity here is likely to be that between Arm Pedalling and the swinging of the arms that naturally accompanies walking. The reader can demonstrate for themselves the importance of arm movements during walking by attempting to lock his arms to his body while walking, this is both awkward and feels unnatural. Another similarity could be between Arm Pedalling and our time as infants during which we crawl around on all fours, even though crawling infants are not renowned for their high rates of optic flow! Finger Tapping utilises none of the same muscles as natural locomotion and it is hard to envisage that it has any correlation with self-motion, and still less with providing locomotive force. This steady decline in effect strength, from locomotor-similar to locomotor-dissimilar movements, supports the hypothesis (Thurrell et al. 1998) that signals of limb movement are influencing visual motion perception via a mechanism, the normal purpose of which is to remove those optic flow components that occur during, and as a consequence of, natural locomotion.

Walking Direction

The hypothesis of Thurrell et al. (1998) would also predict that during backward walking this same mechanism would again act to remove those components of optic flow resulting from translation of the eyes, resulting in an overestimation of optic flow speed during faster backward walking. A more precise prediction would be that data points collected during backward walking would lie along an extension to the line of best fit through data points obtained during standing still and forward walking. The results, however, indicate that backward walking has the same effect as forward walking, i.e. faster backward walking also reduces the perceived speed of optic flow, and this does not directly fit the hypothesis. Two modifications to the hypothesised mechanism can, however, explain all the results. 1) The simplest is that the direction of locomotion is ignored, perhaps as a consequence of the rarity of backward walking. 2) Backward walking is normally accompanied by contracting, not expanding, optic flow. If the hypothesised mechanism was the result of learning, backward walking may influence only contracting optic flow in the manner predicted. If at the same time, backward walking activated the mechanism due to its similarities to forward walking (much as the cycling action does), it would decrease the perceived optic flow speed. This finding does, however, suggest that it is not the subject's intention or expectation of the outcome of the action that alters perception, but rather the signals of limb movement, e.g. proprioceptive signals, themselves.

Extension to Other Optic flow Patterns

Comparison of the intersubject mean arthrovisual effect strengths did not reveal any significant differences, such as the hypothesised reduction in effect strength as the optic flow pattern became less similar to that experienced during natural locomotion. It may well be that this is the case, however, it would be inconsistent with other studies investigating the processing of different optic flow patterns (Stoffregen, 1985). A more detailed study with more subjects is required to provide a concrete answer to this question. It would also be interesting to determine the influence of walking speed on some of the complementary flow types to those investigated here, namely a Contracting Tunnel and upward drifting Horizontal Grating.

Investigation of Reorientation of the Arthrovisual Effect

The hypothesis of Thurrell et al. (1998) predicted that as the direction of self-motion, as indicated by signals of walking, became less closely aligned with the direction of visual motion, then the strength of the arthrovisual effect would decrease. Comparison of the intersubject mean arthrovisual effect strengths did not reveal any significant differences between orientations for any optic flow pattern. Again, this may well be the case, however, given the small number of subjects and that it would be inconsistent with other studies investigating the processing of optic flow patterns and signals of self-motion in different directions (Wolsley et al. 1996b; Duffy, 1998), this conclusion should be treated with caution. A more detailed study containing more subjects is required to confirm or refute these findings. If a significant influence of orientation can be found using more subjects, then investigating the interaction between orientation and optic flow pattern for some of the complementary flow types to those investigated here, namely a Contracting Tunnel, an upward drifting Horizontal Grating and a clockwise Cartwheel would further test predications of the proposed arthrovisual mechanism.

Investigation of a Hemianopic Subject

In GY's blind hemifield, those visual signals that would normally travel via area V1 are unavailable, GY's remaining abilities in this hemifield, i.e. his residual vision, must therefore depend on alternative pathways. The residual vision demonstrated here, the ability to sense and compare the velocity of moving stimuli, is thought to occur in area MT, using visual signals from the superior colliculus via the inferior pulvinar nucleus (see Rodman et al. 1990). GY's ability to make repeatable velocity comparisons between the blind and intact hemifields is consistent with use of these remaining

pathways. V1 must not be required for the arthrovisual effect occurs in GY's blind hemifield as it occurs with a strength comparable to that in the intact hemifield, i.e. signals travelling via the pulvinar and superior colliculus are sufficient. MSTd is directly above area MT in the visual processing hierarchy and has a number of other demonstrable properties that would make it suitable for combining walking and optic flow signals: many MSTd neurones, unlike MT neurones, respond selectively to externally induced visual motion but not to motion induced by eye movements (Erickson and Thier, 1991) or head rotations (Shenoy et al. 1999). Vestibular stimulation by linear whole-body movements also influences the direction selectivity of MST neurones in a manner that may disambiguate self- and object-motion (Duffy, 1998; Bremmer et al. 1999).

Signals of eye motion (whether this is eye-in-head motion or locomotion of the whole body) must interact with retinal signals to compensate for those eye movements either early or late in visual processing (van den Berg and Beintema 1997). In the former, compensation for eye movements occurs before local velocity signals are combined into signals of global flow, whereas in the latter, signals of global flow are created first and these are then matched to altered templates to result in compensated global signals of optic flow. In the first possibility, the same compensation must occur (in the intact hemifield) in two pathways: in the geniculo-striate pathway and in the tecto-fugal pathway. In the second possibility, the compensation need only occur in one place (probably in MSTd), and this must be considered the more likely scenario.

Specification of Spatial Scale

Contrary to their previous performances (see Table 7) four of the five subjects showed no significant reduction in perceived tunnel speed during walking in any condition, and for the remaining subject the effect was weaker than during previous experiments (see Table 7). Subject CJ displayed poor stereoscopic vision, and though he commented that he did not perceive the tunnel as three-dimensional, his results were comparable to those of the other subjects. Certainly none of the subjects displayed an effect resulting in a slope of -1 between the perceived tunnel speed and walking speed, i.e. true perceptual constancy, as was predicted. This disappearance of the effect does not seem to be due to the presence or absence of either stereopsis or parallax as there is no apparent difference between the conditions, though the small number of subjects would make such a difference difficult to see. Possible reasons for the lack of an effect could be the strain

on the subjects of maintaining a three-dimensional percept of the stimulus in the virtual reality environment. Factors such as accommodative mismatch from the close screen distance, time lag between subject motion and screen updating, and the simplified nature of the stimulus itself (its reduced visual angle and it only being two or three squares instead of 12 or 13). With technical refinements, most of these problems may be overcome and the prediction of a reduction in perceived tunnel speed equal to the walking speed may be tested. However, the last possibility, that the altered 'tunnel' structure, consisting of only two or three concentric squares at any one time, should be investigated further. With the reduced number of tunnel components, signals of the displacement of individual components become stronger relative to signals of velocity. If walking does not influence these displacement signals as it does signals of motion, this could explain the lack of an effect here. With a more advanced three-dimensional stimulus and/or alternative stimuli that produce strong displacement signals, it should be possible to test these two possibilities.

Conclusions

We present experimental results, based on a new 'arthrovisual' effect, that reveal an important mechanism used by the visual system to maintain perceptual constancy during self-motion. This is achieved by the modulation of visual motion signals, at a level no lower than area MT though probably in MSTd, by arthrokinetic signals from the limbs that correlate with self-motion through the environment. This mechanism forms the end of a chain of signals expressing motion and position of the eyes relative to the head, to the body and to the ground (see Figure 1), and as such helps to provide a reference signal of eye motion in space (cf. Wertheim 1994). Within this framework no single signal is accurate in all situations, so to enable robust determination of eye movements and hence visual perception, many signals must work in combination such that when conditions prevent one from providing useful information another may replace it. The mechanism responsible for the arthrovisual effect therefore works in parallel with mechanisms incorporating other signals, e.g. from the vestibular apparatus (Harris et al. 1981; Duffy, 1998). As a consequence of this, there should also be a general caution when studying vision in isolation, as signals may be interpreted in vastly different ways depending upon the co-incident information from other modalities.

Chapter 5: General Conclusions

In this thesis a number of interactions between signals of self-motion were investigated. Each of these signals is only one of many signals of self-motion used by the human brain and therefore would normally act in concert with the other signals as shown in Figure 1. Chapters 2 and 3 described experiments using postural sway as a measure of the combined self-motion signal after manipulation of its visual or proprioceptive components. Chapter 4 described investigations on how efference copy and proprioceptive signals influence visual motion processing, presumably by providing signals of self-motion.

Relationship Between Cognition and the Reorientation of Signals of Self-Motion Between the Eyes and Feet

Visual signals of self-motion arise in retino-centric co-ordinates, whereas postural control presumably acts in body-centric co-ordinates, such that during the visual control of posture, unless the two are aligned physically, an internal reorientation must occur. Previous experiments (Wolsley et al. 1996a + b) had shown an accurate reorientation of this self-motion signal during head and/or eye rotations in a visible, well-structured environment. A similar reorientation of vestibular signals had been demonstrated by Nashner and Wolfson (1974) and appeared to be mediated at least partially by cognitive processes (Gurfinkel et al. 1989). Whether the reorientation as demonstrated by Wolsley et al. (1996a + b) could still occur without the cognitive cues afforded by a visible background was unknown, i.e. whether proprioceptive and efference copy signals of neck position were sufficient for this reorientation. In Chapter 2 this was tested by replicating the experimental paradigm of Wolsley et al. but altered to remove visual and cognitive cues. The reorientation of visual cues in postural control was found to be as good in the current experiment without cognitive knowledge as in the experiment of Wolsley et al. with cognitive cues. The comparison of the results in Chapter 2 with the findings of Wolsley et al. may be open to question, as there were a number of differences between these experiments, such as the size and speed of the rotating disk used. Due to this, and the minimal data presented in the study of Wolsley et al. it was not possible to meaningfully compare the resulting sway accuracy's statistically. Also, the lack of a difference between the two sets of results does not indicate that cognitive

mechanisms are not used, but rather that non-cognitive mechanisms are sufficient. For these reasons an alternative test of the use of cognitive cues was used in Chapter 3.

In Chapter 3 all aspects of the stimulus were kept constant at all times and the presence or absence of vection used as a measure of the presence or absence of self-motion related cognitive cues. Measurement of the accuracy of the alignment of the sway direction with the direction of disk motion showed that during periods of vection, i.e. when cognitive cues are available, sway is more accurately aligned. This suggests that cognitive cues are useful to the reorientation mechanism(s) involved, even if they need not always be used. That postural responses may occur before vection is perceived (Previc and Mullen, 1991; Clément et al. 1983) suggest the presence or absence of vection may not be a suitable measure of the availability of cognitive mechanisms of reorientation. Further experiments that should be carried-out to circumvent these criticisms could involve some of the following: Prolonged head-on-neck and/or eye-in-head turning prior to the measurement of sway, directly analogous to the experiment of Gurfinkel et al. (1989), and/or use of a visual stimulus that is less obvious in the direction of motion induced, such as a virtual cloud of dots where movement en masse is disguised by additional random motion.

Signals of Self-Motion Influence Visual Perception During Walking

Self-motion, or more specifically motion of the eyes, alters image motion across the retinae, thus the retinal signal is different from what it would have been without such concurrent eye motion. The structure of the environment and the motion of the eyes through the environment directly relate to the changes in the retinal signal. Thus, this modification of the retinal signal may be used in the Gibsonian sense (1950, 1954, 1966) to reconstruct a signal of eye- and consequently self-motion, such as that used in the visual control of posture (see Chapters 2 and 3). Alternatively, signals of self-motion may be used to remove these modifications of the retinal signal; this would be required for tasks requiring a signal of an object's position or motion in space. A number of non-visual signals may be used to determine eye- and/or self-motion (e.g. Wertheim, 1994; Crowell et al. 1998). These may be combined with knowledge of the environmental structure to discount the visual modifications resulting from the eye-motion. In Chapter 4: A Mechanism to Counter the Influence of Locomotion on Visual Perception, the use of arthrokinetic signals of self-motion from the limbs to remove these visual alterations

is investigated. The results suggest, despite much intersubject variation, that arthrokinetic signals do influence visual processing in a manner consistent with their forming an extension to the 'reference signal' of Wertheim (1994).

The experimental paradigm involved comparing the perception of visual motion velocity during walking and standing still using a matching to target task. In order to complete each experiment in a reasonable time and to reduce the effort required from each subject the matching was conducted during short bursts of walking. During overground walking such a brief change in speed would result in concomitant vestibular stimulation. However, during treadmill walking this linear vestibular acceleration does not occur (disregarding the cyclical oscillations at the stride frequency), generating an inconsistency between the vestibular and arthrokinetic signals. Hlavacka et al. (1996) showed that arthrokinetic information from the legs is only used if the support surface is perceptually stationary in comparison to vestibular signals. It may be, in the current experiments, that arthrokinetic signals from the legs are moderated by vestibular signals in a similar manner. Differences in this comparison, with some subjects using arthrokinetic signals and some ignoring them, could explain the inter-subject variability in arthrovisual effect strength. If this is the case, further studies using longer periods of walking at constant speed on the treadmill before the matching task should result in a more consistent effect between subjects. Care should be taken in such experiments as longer periods of walking may result in recalibration of the links between walking and visual motion, as found by Pelah and Barlow (1996).

Within their limitations, as discussed in Chapter 4, the control variations and the investigation of different motor activities are consistent with arthrokinetic signals from the legs forming an extension to the 'reference signal' model of Wertheim (1994). The investigations of different optic-flow patterns and of the relative orientations of the walking direction and visual motion probably do not fit the model due to a lack of subjects, and this lack should be rectified with future studies. The investigation into the specification of spatial scale did not provide useful values of the effect strength due to technical reasons. To allow comparison with the walking speed directly, this experiment should be repeated with a more advanced stimulus. The results from backward walking do not fit so easily into this framework, as the effect appears to change sign, increasing the perceived optic-flow speed as walking speed becomes faster. Whether this is because walking direction information is simply ignored, or because backward walking

only affects contracting flow remains to be seen. However, either way incorporating this forms the largest problem for any model which uses arthrokinetic signals as signals of self-motion. Further work is required to differentiate between all the various possibilities (which are not necessarily included in this thesis), one possibility would be to investigate the motion after-effect during backward walking, as it is thought to be a product of the same mechanism.

Summary

In conclusion, in this thesis results are presented that demonstrate two main mechanisms: The usefulness of cognitive processing, when available, for the interpretation of signals of self-motion. The usefulness of arthrokinetic signals from the limbs (particularly the legs) in modulating visual signals of motion. Both these mechanisms form parts of the network of signals of self-motion as presented in Figure 1 that are proposed to form a single model of motion of the body and its parts.

References

Allum JHJ, Pfaltz CR (1985) Visual and vestibular contributions to pitch sway stabilization in the ankle muscles of normals and patients with bilateral peripheral vestibular deficits. Experimental Brain Research 58: 82-94.

Amblard B, Cremieux J, Marchand AR, Carblanc A (1985) Lateral orientation and stabilisation of human stance: static versus dynamic visual cues. Experimental Brain Research 61: 21-37.

Ammons WS (1992) Bowditch Lecture. Renal afferent inputs to ascending spinal pathways. American Journal of Physiology 262: R165-R176.

Anastasopoulos D, Bronstein AM, Haslwanter T, Fetter M, Dichgans J (1999) The role of somatosensory input for the perception of verticality. Annals of the New York Academy of Sciences 871: 379-383.

Andersen GJ (1990) Segregation of optic flow into object and self-motion components: Foundations for a general model. In: Perception and control of self-motion (Warren R, Wertheim AH, eds), pp 127-141. London: Erlbaum.

Aubert H (1886) Die Bewegungsemptindung. Pflugers Archiv 39: 347-370.

Banks MS, Ehrlich SM, Backus BT, Crowell JA (1996) Estimating heading during real and simulated eye movements. Vision Research 36: 431-443.

Barbur JL, Ruddock KH, Waterfield VA (1980) Human visual responses in the absence of the geniculo-calcarine projection. Brain 103: 905-928.

Barinaga M (1996) Researchers find neurons that may help us navigate. Science 273: 1489-1490.

Berthoz A (1981) Intersensory interaction in motion perception. In: Attention and performance, Vol. IX (Long J, Baddeley A, eds), pp 27-45.

Bex PJ, Makous W (1997) Radial motion looks faster. Vision Research 37: 3399-3405.

Biguer B, Donaldson IML, Hein A, Jeannerod M (1988) Neck muscle vibration modifies the representation of visual motion and direction in man. Brain 111: 1405-1424.

Bisdorff AR, Anastasopoulos D, Bronstein AM, Gresty MA (1995) Subjective postural vertical in peripheral and central vestibular disorders. Acta Oto-laryngologica Supplement 520: 68-71.

Black FO, Nashner L (1985) Postural control in four classes of vestibular abnormalities. In: Vestibular and visual control on posture and locomotor equilibrium (Igarashi M, Black O, eds), pp 271-281. Basel: Kargel.

Bles W, Kapteyn TS, Brandt T, Arnold F (1980) The mechanism of physiological height vertigo. II. Posturography. Acta Oto-laryngologica 89: 534-540.

Bles W, Vianney de Long JMB, deWit G (1983) Compensation for labyrinthine defects examined by use of a tilting room. Acta Oto-laryngologica 95: 576-579.

Bles W, Jelmorini M, Bekkering H, de Graaf B (1995) Arthrokinetic information affects linear self-motion perception. Journal of Vestibular Research 5: 109-116.

Blouin J, Okada T, Wolsley CJ, Bronstein AM (1998) Encoding target-trunk relative position: cervical versus vestibular contribution. Experimental Brain Research 122: 101-107.

Bradley DC, Maxwell M, Andersen RA, Banks MS, Shenoy KV (1996) Mechanisms of heading perception in primate visual cortex. Science 273: 1544-1547.

Brandt T, Buchele W, Arnold F (1977) Arthrokinetic nystagmus and ego-motion sensation. Experimental Brain Research 30: 331-338.

Bremmer F, Ilg UJ, Thiele A, Distler C, Hoffmann KP (1997) Eye position effects in monkey cortex. I. Visual and pursuit-related activity in extrastriate areas MT and MST. Journal of Neurophysiology 77: 944-961.

Bremmer F, Kubischik M, Pekel M, Lappe M, Hoffmann K-P (1999) Linear vestibular self-motion signals in monkey medial superior temporal area. Annals of the New York Academy of Sciences 871: 272-281.

Brenner E (1991) Judging Object Motion During Smooth Pursuit Eye-Movements: the Role of Optic Flow. Vision Research 31: 1893-1902.

Brenner E, van den Berg AV (1994) Judging Object Velocity During Smooth-Pursuit Eye-Movements. Experimental Brain Research 99: 316-324.

Bridgeman B, Stark L (1991) Ocular Proprioception and Efference Copy in Registering Visual Direction. Vision Research 31: 1903-1913.

Britton TC, Day BL, Brown P, Rothwell JC, Thompson PD, Marsden CD (1993) Postural Electromyographic Responses in the Arm and Leg Following Galvanic Vestibular Stimulation in Man. Experimental Brain Research 94: 143-151.

Bronstein AM (1986) Suppression Of Visually Evoked Postural Responses. Experimental Brain Research 63: 655-658.

Bronstein AM (1996) 'Audiometry of the ankles'. A quick check on the single most important sensory input for balance control. British Journal of Audiology 30: 63.

Buizza A, Léger A, Droulez J, Berthoz A, Schmid R (1980) Influence of otolithic stimulation by horizontal linear acceleration on optokinetic nystagmus and visual motion perception. Experimental Brain Research 39: 165-176.

Carpenter RHS (1988) The proprioceptive input. In: Movements of the eyes pp 225-246.

Chance SS, Gaunet F, Beall AC, Loomis JM (1998) Locomotion mode affects the updating of objects encountered during travel: The contribution of vestibular and proprioceptive inputs to path integration. Presence - Teleoperators and Virtual Environments 7: 168-178.

Chaudhuri A (1990) Modulation of the motion aftereffect by selective attention. Nature 344: 60-62.

Chow CC, Collins JJ (1995) Pinned polymer model of posture control. Physical Review E - Statistical Physics, Plasmas, Fluids and Related Interdisciplinary Topics 52: 907-912.

Clark FJ, Horch KW, Bach SM, Larson GF (1979) Contributions of cutaneous and joint receptors to static knee-position sense in man. Journal of Neurophysiology 42: 877-888.

Clément G, Jacquin T, Berthoz A (1983) Habituation of postural readjustments induced by motion of visual scenes. In: Vestibular and visual control on posture and locomotor equilibrium (Igarashi, Black, eds), pp 99-104. Basel: Karger.

Clément G, Jacquin T, Berthoz A (1985) Habituation of postural readjustments induced by motion of visual scenes. In: Vestibular and visual control on posture and locomotor equilibrium (Igarashi M, Black O, eds), pp 99-104. Basel: Karger.

Collins JJ, De Luca CJ (1994) Random walking during quiet standing. Physical Review Letters 73: 764-767.

Crowell JA, Banks MS, Shenoy KV, Adersen RA (1998) Visual self-motion perception during head turns. Nature Neuroscience 1: 732-737.

Cutting JE, Vishton PM, Fluckiger M, Baumberger B, Gernt JD (1997) Heading and path information from retinal flow in naturalistic environments. Perception and Psychophysics 59: 426-441.

Daunton N, Thomsen D (1979) Visual modulation of otolith-dependent units in cat vestibular nuclei. Experimental Brain Research 37: 173-176.

Dawson MR (1991) The how and why of what went where in apparent motion: modeling solutions to the motion correspondence problem. Psychological Review 98: 569-603.

Day BL, Steiger MJ, Thompson PD, Marsden CD (1993) Effect of vision and stance width on human body motion when standing: implications for afferent control of lateral sway. Journal of Physiology 469: 479-499.

de Graaf B, Bos JE, Wich S, Bles W (1994) Arthrokinetic and Vestibular Information Enhance Smooth Ocular Tracking During Linear (Self-)Motion. Experimental Brain Research 101: 147-152.

Dichgans J, Mauritz KH, Allum JHJ, Brandt T (1976) postural sway in normals and atactic patients. Agressologie 17: 15-24.

Dichgans JM, Held R, Young LR, Brandt T (1972) Moving visual scenes influence the apparent direction of gravity. Science 178: 1217-1219.

Dichgans JM, Brandt T, Held R (1975) The role of vision in gravitational orientation. Fortschritte der Zoologie 23: 255-263.

Dichgans JM, Brandt T (1978) Visual-vestibular interaction: Effects on self-motion perception and postural control. In: Volume 8 (Held R, Leibowitz H, Teuber H, eds), New York: Springer-Verlag.

Diener HC, Horak F, Stelmach G, Guschlbauer B, Dichgans JM (1981) Direction and amplitude precuing has no effect on automatic posture responses. Experimental Brain Research 84: 219-223.

Dijkstra TM, Gielen CCAM, Melis BJ (1992) Postural responses to stationary and moving scenes as a function of distance to the scene. Human and Movement Science 11: 195-203.

Dijkstra TM, Schoner G, Gielen CCAM (1994) Temporal stability of the action-perception cycle for postural control in a moving visual environment. Experimental Brain Research 97: 477-486.

Duffy CJ (1998) MST neurons respond to optic flow and translational movement. Journal of Neurophysiology 80: 1816-1827.

Easton RD, Greene AJ, Dizio P, Lackner JR (1998) Auditory cues for orientation and postural control in sighted and congenitally blind people. Experimental Brain Research 118: 541-550.

Edwards AS (1946) Body sway and vision. Journal of Experimental Psychology 36: 526-535.

Eggert T, Straube A, Schroeder K (1997) Visually induced motion perception and visual control of postural sway in congenital nystagmus. Behavioural Brain Research 88: 161-168.

Erickson HH, Sandler H, Stone HL (1976) Cardiovascular function during sustained +G stress. Aviation, Space, and Environmental Medicine 47: 250-258.

Erickson RG, Thier P (1991) A neuronal correlate of spatial stability during periods of self-induced visual motion. Experimental Brain Research 86: 608-616.

Fleischl EV (1882) Physiologisch-optische Notizen, 2 Mitteilung. Sitzung Wiener Bereich der Akademie der Wissenschaften 3: 7-25.

Fluckiger M, Baumberger B (1988) The perception of an optical flow projected on the ground surface. Perception 17: 633-645.

Freeman TCA (1999) Path perception and Filehne illusion compared: model and data. Vision Research 39: 2659-2667.

Fregly AR (1974) Vestibular ataxia and its measurement in man. In: Handbook of sensory Physiology Vol. VI/2 (Kornhuber HH, ed).

Fushiki H, Sato Y, Miura A, Kawasaki T (1994) Climbing fiber responses of Purkinje cells to retinal image movement in cat cerebellar flocculus. Journal of Neurophysiology 71: 1336-1350.

Gdowski GT, Mccrea RA (2000) Neck proprioceptive inputs to primate vestibular nucleus neurons. Experimental Brain Research 135: 511-526.

Gibson JJ (1950) The problem of the stable and boundless visual world. In: The perception of the visual world pp 145-162. Boston: Houghton Mifflin.

Gibson JJ (1954) The visual perception of objective motion and subjective movement. Psychological Review 61: 304-314.

Gibson JJ (1962) Observations on active touch. Psychological Review 69: 477-491.

Gibson JJ (1966) The pickup of ambient information: scanning. In: The senses considered as perceptual systems pp 250-265. Boston: Houghton Mifflin.

Gielen CCAM, van Asten WNJC (1990) Postural Responses To Simulated Moving Environments Are Not Invariant For The Direction Of Gaze. Experimental Brain Research 79: 167-174.

Giese MA, Dijkstra TM, Shoner G, Gielen CCAM (1996) Identification of the nonlinear state-space dynamics of the action-perception cycle for visually induced postural sway. Biological Cybernetics 74: 427-437.

Goldberg JM, Fernandez C (1975) Vestibular mechanisms. Annual Review of Physiology 37: 129-162.

Goldberg JM, Fernandez C (1984) The vestibular system. In: Volume 3 (Darian-Smith, ed), pp 977. Bethesda: American Physiological Society.

Goodwin GM, Mccloskey DI, Matthews PB (1972) Proprioceptive illusions induced by muscle vibration: contribution by muscle spindles to perception? Science 175: 1382-1384.

Graziano MSA, Andersen RA, Snowden R (1994) Tuning of MST neurons to spiral motions. Journal of Neuroscience 14: 54-67.

Gross CG (1991) Contribution of striate cortex and the superior colliculus to visual function in area MT, the superior temporal polysensory area and inferior temporal cortex. Neuropsychologia 29: 497-515.

Gurfinkel VS, Popov KE, Smetanin BN, Shlykov VY (1989) Changes in the direction of vestibulomotor responses in the process of adaptation to prolonged static head turning in man. Neurophysiology 21: 159-164.

Harris LR, Morgan MJ, Still AW (1981) Moving and the motion aftereffect. Nature 293: 139-141.

Heeger DJ, Jepson A (1990) Visual Perception of Three-Dimensional Motion. Neural Computation 2: 129-137.

Held R, Dichgans JM, Bauer J (1975) Characteristics of moving visual areas influencing spatial orientation. Vision Research 15: 357-365.

Hlavacka F, Mergner T, Schweigart G (1992) Interaction of vestibular and proprioceptive inputs for human self-motion perception. Neuroscience Letters 138: 161-164.

Hlavacka F, Mergner T, Bolha B (1996) Human self-motion perception during translatory vestibular and proprioceptive stimulation. Neuroscience Letters 210: 83-86.

Horak FB, Macpherson JM (1996) Postural orientation and equilibrium. In: Handbook of Physiology: Regulation and integration of multiple systems (Rowell LB, Shepherd JT, eds), pp 255-292. New York: American Physiological Society.

Howard IP (1982) Human visual orientation. In: Human visual orientation pp 309-334. Chichester: Wiley.

Howard IP (1997) Interactions within and between the spatial senses. Journal of Vestibular Research 7: 311-345.

Hulk J, Jongkees LBW (1948) The normal cupulogram. Journal of Laryngology 62: 70-75.

Ivry RB, Keele SW (1989) Timing functions of the cerebellum. Journal of Cognitive Neuroscience 1: 136-152.

Jeka JJ, Lackner JR (1994) Fingertip contact influences human postural control. Experimental Brain Research 495-502.

Jian BJ, Shintani T, Emanuel BA, Yates BJ (2002) Convergence of limb, visceral, and vertical semicircular canal or otolith inputs onto vestibular nucleus neurons. Experimental Brain Research 144: 247-257.

Jongkees LBW (1974) Pathology of vestibular sensation. In: Vestibular system: Psychophysics, applied aspects and general interpretations (Kornhuber HH, ed), pp 413-450. New York: Springer-Verlag.

Jürgens R, Boss T, Becker W (1999) Estimation of self-turning in the dark: comparison between active and passive rotation. Experimental Brain Research 128: 491-504.

Kavounoudias A, Roll R, Roll JP (1998) The plantar sole is a 'dynamometric map' for human balance control. Neuroreport 9: 3247-5232.

Kavounoudias A, Gilhodes JC, Roll R, Roll JP (1999) From balance regulation to body orientation: two goals for muscle proprioceptive information processing? Experimental Brain Research 124: 80-88.

Koenderink JJ (1990) Some theoretical aspects of optic flow. In: Perception and control of self-motion (Warren R, Wertheim AH, eds), pp 53-68. London: Erlbaum.

Kotaka S, Croll GA, Bles W (1986) Somatosensory ataxia. In: Disorders of posture and gait (Bles W, Brandt T, eds), pp 178-183. New York: Elseiver.

Kunkel M, Freudenthaler N, Steinhoff BJ, Baudewig J, Paulus W (1998) Spatial-frequency-related efficacy of visual stabilisation of posture. Experimental Brain Research 121: 471-477.

Kuno S, Kawakita T, Kawakami O, Miyake Y, Watanabe S (1999) Postural adjustment response to depth direction moving patterns produced by virtual reality graphics. Japanese Journal of Physiology 49: 417-424.

Lappe M, Rauschecker JP (1993) A neural network for the processing of optic flow from ego-motion in man and higher mammals. Neural Computation 5: 374-391.

Lappe M, Bremmer F, van den Berg AV (1999) Perception of self-motion from visual flow. Trends in Cognitive Science 3: 329-336.

Lee C, Lishman JR (1975) Visual proprioceptive control of stance. Journal of Human Movement Studies 1: 87-95.

Lee DN, Aronson E (1974) Visual proprioceptivve control of standing in human infants. Perception and Psychophysics 15: 529-532.

Lestienne F, Soechting JF, Berthoz A (1977) Postural readjustments induced by linear motion of visual scenes. Experimental Brain Research 28: 363-384.

Lishman JR, Lee DN (1973) The autonomy of visual kinaesthesis. Perception 2: 287-294.

Lund S (1980) Postural effects of neck muscle vibration in man. Experientia 36: 1398.

Lund S, Broberg C (1983) Effects Of Different Head Positions On Postural Sway In Man Induced By A Reproducible Vestibular Error Signal. Acta Physiologica Scandinavica 117: 307-309.

Mach E (1886) Further investigation of space-sensations. In: The analysis of sensations pp 122-170. NY, Dover, London: Constable.

Maki BE, Whitelaw RS (1993) Influence of expectation and arousal on center of foot pressure responses to transient postural perturbations. Journal of Vestibular Research 3: 25-39.

Marple SL (1987) In: Digital Spectral Analysis Prentice-Hall.

Masson G, Mestre DR, Pailhous J (1995) Effects of the spatio-temporal structure of optical flow on postural readjustments in man. Experimental Brain Research 103: 137-150.

Maurer C, Mergner T, Bolha B, Hlavacka F (2000) Vestibular, visual, and somatosensory contributions to human control of upright stance. Neuroscience Letters 281: 99-102.

Mesland BS, Finlay AL, Wertheim AH, Barnes GR, Morland AB, Bronstein AM, Gresty MA (1996) Object motion perception during ego-motion: patients with a complete loss of vestibular function vs. normals. Brain Research Bulletin 40: 459-465.

Mittelstaedt H (1992) Somatic versus vestibular gravity reception in man. Annals of the New York Academy of Sciences 656: 124-139.

Mittelstaedt H (1996) Somatic graviception. Biological Psychology 42: 53-74.

Mittelstaedt H (1998) Origin and processing of postural information. Neuroscience and Biobehavioral Reviews 22: 473-478.

Mittelstaedt H (1999) The role of the otoliths in perception of the vertical and in path integration. Annals of the New York Academy of Sciences 871: 334-344.

Mittelstaedt ML, Mittelstaedt H (1996) The influence of otoliths and somatic graviceptors on angular velocity estimation. Journal of Vestibular Research 6: 355-366.

Morland AB, Jones SR, Finlay AL, Deyzac E, Le S, Kemp S (1999) Visual perception of motion, luminance and colour in a human hemianope. Brain 122: 1183-1198.

Nakamura T, Bronstein AM (1995) The Perception of Head and Neck Angular Displacement in Normal and Labyrinthine-Defective Subjects - A Quantitative Study Using A Remembered Saccade Technique. Brain 118: 1157-1168.

Nashner L, Wolfson P (1974) Influence of head position and proprioceptive cues on short latency postural reflexes evoked by galvanic stimulation of the human labyrinth. Brain Research 67: 255-268.

Nashner L (1977) Fixed patterns of rapid postural responses among leg muscles during stance. Experimental Brain Research 30: 13-24.

Nashner L, Cordo PJ (1981) Relation of automatic postural responses and reaction-time voluntary movements of human leg muscles. Experimental Brain Research 43: 395-405.

Nashner LMA (1971) A model describing vestibular detection of body sway motion. Acta Oto-laryngologica 72: 429-436.

Nougier V, Bard C, Fleury M, Teasdale N (1997) Contribution of central and peripheral vision to the regulation of stance. Gait and Posture 5: 34-41.

Paulus W, Straube A, Brandt T (1984) Visual stabilization of posture: physiological stimulus characteristics and clinical aspects. Brain 107: 1143-1163.

Paulus W, Straube A, Brandt T (1987) Visual postural performance after loss of somatosensory and vestibular function. Journal of Neurosurgery and Psychiatry 50: 1542-1545.

Pavard B, Berthoz A (1977) Linear acceleration modifies the perceived velocity of a moving visual scene. Perception 6: 529-540.

Pelah A, Barlow HB (1996) Visual illusion from running. Nature 381: 283.

Pelah A, Secker B, Bishop A, Askham C (1998) A wide-field simulator for studying visuo-motor interactions in locomotion. Journal of Physiology 506: 12P.

Pelah A, Boddy A (1998) Adaptive modulation of the motion after-effect by walking. Journal of Physiology 506: 111P.

Pelah A, Thurrell AEI, Berry M (2001) Reduction of perceived visual speed during locomotion: Evidence for quadrupedal perceptual pathways in human? Journal of Vision 1: 307a-307a.

Perrone JA (1992) Model for the computation of self-motion in biological systems. Journal of the Optical Society of America Part A, Optics and Image Science 9: 177-194.

Perrone JA, Stone LS (1994) A model for the self-motion estimation within primate extrastriate visual cortex. Vision Research 34: 2917-2938.

Perrone JA, Stone LS (1998) Emulating the visual receptive field properties of MST neurons with a template model of heading estimation. Journal of Neuroscience 18: 5958-5975.

Peterka RJ, Benolken MS (1995) Role of somatosensory and vestibular cues in attenuating visually induced postural sway. Experimental Brain Research 105: 101-110.

Plooy A, Tresilian JR, Mon-Williams M, Wann JP (1998) The contribution of vision and proprioception to judgements of finger proximity. Experimental Brain Research 118: 415-420.

Pola J, Wyatt H (1989) The perception of target motion during smooth pursuit eye movements in the open-loop condition: characteristics of retinal and extraretinal signals. Vision Research 29: 471-483.

Previc FH, Mullen TJ (1991) A comparison of the latencies of visually induced postural change and self-motion perception. Vestibular Research 1: 317-323.

Previc FH, Kenyon RV, Boer ER, Johnson BH (1993) The effects of background visual roll stimulation on postural and manual control and self-motion perception. Perception and Psychophysics 54: 93-107.

Probst T, Brandt T, Degner D (1986) Object-motion detection affected by concurrent self-motion perception: Psychophysics of a new phenomenon. Behavioural Brain Research 22: 1-11.

Rabin E, Bortolami SB, Dizio P, Lackner JR (1999) Haptic stabilization of posture: changes in arm proprioception and cutaneous feedback for different arm orientations. Journal of Neurophysiology 82: 3541-3549.

Raphan T, Matsuo V, Cohen B (1979) Velocity storage in the vestibulo-ocular reflex arc (VOR). Experimental Brain Research 35: 229-248.

Read HL, Siegel RM (1997) Modulation of responses to optic flow in area 7a by retinotopic and oculomotor cues in monkey. Cerebral Cortex 7: 647-661.

Redfern MS, Furman JM (1994) Postural sway of patients with vestibular disorders during optic flow. Journal of Vestibular Research 4: 221-230.

Rodman HR, Gross CG, Albright TD (1990) Afferent basis of visual response properties in area MT of the Macaque. II. Effects of superior colliculus removal. Journal of Neuroscience 10: 1154-1164.

Roll JP, Roll R (1988) From eye to foot: a proprioceptive chain involved in postural control. In: Posture and gait:development, adaptation and modulation. (Amblard B, Berthoz A, Clarac F, eds), pp 155-164. Amsterdam, Oxford: Elseiver.

Roll JP, Vedel JP, Roll R (1989) Eye, head and skeletal muscle spindle feedback in the elaboration of body references. Progress in Brain Research 80: 113-123.

Royden CS, Banks MS, Crowell JA (1992) The perception of heading during eye movements. Nature 360: 583-585.

Royden CS, Crowell JA, Banks MS (1994) Estimating heading during eye movements. Vision Research 34: 3197-3214.

Sahraie A, Milders M, Niedeggen M (2001) Attention induced motion blindness. Vision Research 41: 1613-1617.

Severac CA, Bessou M, Bessou P (1998) Anteroposterior dynamic balance reactions to circular movement of the visual field without ocular pursuit. Experimental Brain Research 123: 382-386.

Shenoy KV, Bradley DC, Andersen RA (1999) Influence of gaze rotation on the visual response of primate MSTd neurons. Journal of Neurophysiology 81: 2764-2786.

Soechting JF, Flanders M (1992) Moving in three-dimensional space: frames of reference, vectors, and coordinate systems. Annual Review of Neuroscience 15: 167-191.

Stoerig P, Cowey A (1997) Blindsight in man and monkey. Brain 120: 535-559.

Stoffregen TA (1985) Flow structure versus retinal location in the optical control of stance. Journal of Experimental Psychology 11: 554-565.

Stoffregen TA (1986) The role of optical velocity in the control of stance. Perception and Psychophysics 39: 355-360.

Stone LS, Perrone JA (1997) Human heading estimation during visually simulated curvilinear motion. Vision Research 37: 573-590.

Thurrell, A. E. I, Pelah, A, and Distler, H. K. The influence of non-visual signals of walking on the perceived speed of optic flow. Perception 27, 147. 1998.

Thurrell AEI, Bertholon P, Bronstein AM (2000) Reorientation of a visually evoked postural sway response during passive whole body rotation. Experimental Brain Research 133: 229-232.

Thurrell AEI, Pelah A (2002) Reduction of perceived visual speed during walking: Effect dependent upon stimulus similarity to the visual consequences of locomotion.

Timmann D, Belting C, Schwarz M, Diener HC (1994) Influence of visual and somatosensory input on leg EMG responses in dynamic posturography in normals. Electroencephalography and Clinical Neurophysiology 93: 7-14.

Tootell RB, Reppas JB, Dale AM, Look RB, Sereno MI, Malach R, Brady TJ, Rosen BR (1995) Visual motion aftereffect in human cortical area MT revealed by functional magnetic resonance imaging. Nature 375: 139-141.

Trendelenburg W (1906) Uber die Bewegung der Vogel nach Durchschneidung hinterer Ruckenmarkswurzeln. Ein Beitrag zur Physiologie des Zentralnervensystems der Vogel (nach Untersuchungen an Columbia domestica). Archiv der Anatomie und Physiologie 1-126.

Tschermak A (1921) Der exakte subjectivismus in der neuren sinnesphysiologie. Pflugers Archiv fur Gesamte Physiologie des Menschen und der Thiere 188: 1-20.

Turano KA, Heidenreich SM (1993) Speed discrimination in stabilised viewing. Investigative Ophthalmology and Visual Science 34: 976.

Turano KA, Heidenreich SM (1996) Speed discrimination of distal stimuli during smooth pursuit eye motion. Vision Research 36: 3507-3517.

Turano KA, Heidenreich SM (1999) Eye movements affect the perceived speed of visual motion. Vision Research 39: 1177-1187.

van Asten WN, Gielen CC, van der Gon JJ (1988a) Postural movements induced by simulated motion of differently structured environments. Experimental Brain Research 73: 371-383.

van Asten WN, Gielen CC, van der Gon JJ (1988b) Postural movements induced by rotations of visual scenes. Journal of the Optical Society of America Part A, Optics and Image Science 5: 1781-1789.

van den Berg AV (1992) Robustness of perception of heading from optic flow. Vision Research 32: 1285-1296.

van den Berg AV (1993) Perception of heading. Nature 365: 497-498.

van den Berg AV, Brenner E (1994) Why two eyes are better than one for judgements of heading. Nature 371: 700-702.

van den Berg AV (1996) Judgements of heading. Vision Research 36: 2337-2350.

van den Berg AV, Beintema JA (1997) Motion templates with eye velocity gain fields for transformation of retinal to head centric flow. Neuroreport 8: 835-840.

von Giercke HE, Parker DE (1994) Differences in otolith and abdominal viscera graviceptor dynamics: implications for motion sickness and perceived body position. Aviation, Space, and Environmental Medicine 65: 747-751.

von Helmholtz H (1896) The direction of vision. In: Handbuch der Physiologischen Optik Vol. 3 (Southall JPC, ed), pp 242-281. Optical Society of America.

Warren WH, Hannon DJ (1988) Direction of self-motion is perceived from optical flow. Nature 336: 162-163.

Warren WH, Hannon DJ (1990) Eye movements and optical flow. Journal of the Optical Society of America Part A, Optics and Image Science 7: 160-169.

Warren WH (1998) Perception of heading is a brain in the neck. Nature Neuroscience 1: 647-649.

Warren WH, Zosh W, Sahuc S, Duchon A, Kay B (2000) Optic flow vs. egocentric direction in the visual control of walking. Investigative Ophthalmology and Visual Science 41.

Wertheim AH (1981) On the relativity of perceived motion. Acta Psychologica 48: 97-110.

Wertheim AH (1994) Motion perception during self-motion: the direct versus inferential controversy revisited. Behavioral and Brain Sciences 17: 293-355.

Wickens CD (1980) The Structure of Attentional Resources. Attention and Performance 8: 239-257.

Wolsley CJ, Buckwell D, Sakellari V, Bronstein AM (1996a) The effect of eye/head deviation and visual conflict on visually evoked postural responses. Brain Research Bulletin 40: 437-442.

Wolsley CJ, Sakellari V, Bronstein AM (1996b) Reorientation of visually evoked postural responses by different eye-in-orbit and head-on-trunk angular positions. Experimental Brain Research 111: 283-288.

Yardley L, Lerwill H, Hall M, Gresty MA (1992) Visual destabilisation of posture in normal subjects. Acta Oto-laryngologica 112: 14-21.

Zemel RS, Sejnowski TJ (1995) Grouping components of three-dimensional moving objects in area MST of visual cortex. In: Advances in neural information processing systems 7 (Tesauro G, Touretzky DS, Leen TK, eds), pp 165-172. Cambridge: MIT.

Appendix A: Publications

The influence of non-visual signals of walking on the perceived speed of optic flow

A. E. I. Thurrell, A. Pelah, H. K. Distler*

(Department of Physiology, University of Cambridge, Downing Street, Cambridge, CB2 3EG;
* Max-Planck-Institut fur biologische Kybernetik, Spemannstrasse 38, D 72076 Tubingen,

The main observation

We noted during the course of a different study that the speed of a motion stimulus appeared slower if one was engaged in the activity of walking. We set out to test this observation and confirmed it, as reported here.

Methods

EXPERIMENTAL PROCEDURE - Experiments consisted of ten blocks, each consisting of nine 10 s trials, with a 5 s blank interval between trials. At the beginning of each block subjects were shown the stimulus (one of four possible types, see Fig. 2) at a given target speed, and in the subsequent test trials they were required to match the speed to the target by adjusting a hand-held knob. The subject remained standing while viewing the target stimulus. But while making the settings the subject either stood (control) or walked (forward or backward) according to written instructions displayed on the screen at the beginning of each trial: 'very slow,' 'slow,' 'normal,' 'fast,' 'very fast,' 'fast back,' 'slow back' or 'stand.' Walking speed and visual test speed settings were averaged over the last 5 s of each trial.

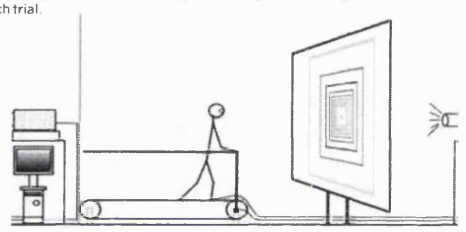

Figure 1

EXPERIMENTAL SET-UP - The experimental set-up consisted of a large rear-projected image (90 deg x 75 deg) in front of a non-motorised treadmill upon which the subject could walk at their chosen pace and direction.

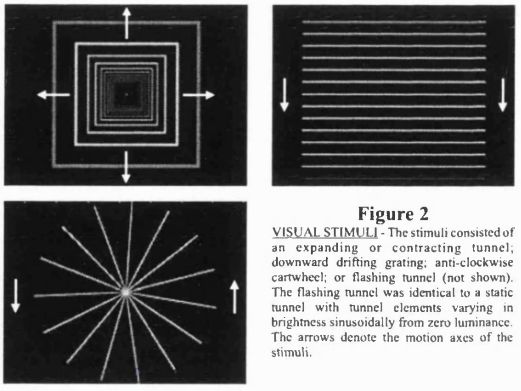

Figure 2

VISUAL STIMULI - The stimuli consisted of an expanding or contracting tunnel; downward drifting grating; anti-clockwise cartwheel; or flashing tunnel (not shown). The flashing tunnel was identical to a static tunnel with tunnel elements varying in brightness sinusoidally from zero luminance. The arrows denote the motion axes of the stimuli.

Results

The results showed an increase in matched visual speed settings with increased walking speed. This effect did not depend on either the direction of walking or on the direction of the visual stimulus (see Fig. 3). The strength of the effect was, however, affected by the type of stimulus used (see Fig. 4); the apparent speed of the flashing tunnel (having no motion components) remaining unaffected by walking.

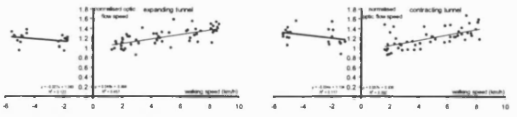

Figure 3

Results for subject AT showing the effect of walking speed on matched optical flow speed settings for the expanding or contracting tunnel, with either forward or backward walking.

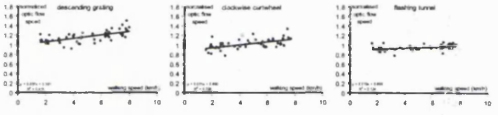

Figure 4

Results for subject AT showing the effect of walking speed on matched optical flow settings for different stimuli. Target speeds were: tunnel: 3.2 deg/sec at mid hemifield; grating: 3.2 deg/sec at fixation point; cartwheel: 1/5 revolutions/sec; flashing tunnel: 2Hz.

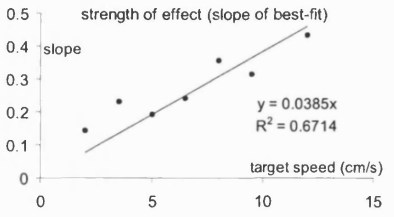

Figure 5

The strength of the effect for subject AT the expanding tunnel stimulus, as measured by the slope of the linear best-fit curve of matched optic flow speed plotted against forward walking velocity for seven target speeds: 2, 3.5, 5, 6.5, 8, 9.5, and 12 cm/s.

Conclusions

Walking speed affects visual speed perception, such that motion is underestimated progressively as walking speed increases. The mechanism(s) responsible respond equally to walking in either direction, and likewise make no distinction between opposite stimulus directions. The response is to motion *per se* rather than a space-time construct, as shown by the absence of an effect of walking on the flashing tunnel matches. The strength of the effect appears to be related to the similarity of the stimulus to true optic flow, i.e. tunnel>grating>cartwheel. The strength of the effect is also proportional to the target velocity, suggesting a ratiometric alteration of visual perception by activity.

These observations suggest that visual perception is altered by general motor activity, perhaps due to alterations in a central pattern generator. A mechanism acting in series with a visual filter for optical flow would account for the result.

[*See also* Poster B16: Distler, Pelah, Bell & Thurrell "The perception of absolute speed during self-motion"]

Reorientation of a visually evoked postural response does not require cognitive knowledge of display relative angular position

A E I Thurrell, P Bertholon, A M Bronstein
MRC Human Movement and Balance Unit, 8-11 Queen Square, London, WC1N 3BG

Introduction

Vision is used as an accompaniment to proprioception and vestibular signals in the control of posture. These control mechanisms have been investigated using visual stimuli experimentally moved to simulate the visual conditions that occur when a subject spontaneously sways. A previous experiment investigated the reorientation of a visually evoked postural sway response during fixation an off centre visual stimulus (Wolsley et al. 1996). It was discovered that subjects reorient their visually evoked postural sway response to match the direction of the visual stimulus for a variety of combinations of head-on-neck and eye-in-orbit rotations. However, this experiment was run in a well-lit, structured visual environment, where subjects were able to determine the orientation of the stimulus relative to themselves. As a consequence of the instructions received, subjects also had full cognitive knowledge of their orientation relative to the visual stimulus. The present experiment was run with a dark visual environment to remove external visual cues and a reduced instruction set. It is proposed that this approach can reveal the importance of cognitive knowledge and/or background visual texture for the reorientation of the visually evoked postural sway response.

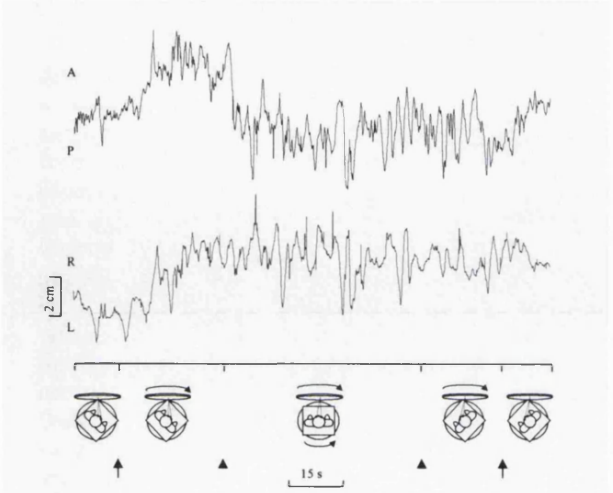

Fig.1 Raw posturography platform traces from subject JB, conditions as icons, the traces show the anterior-posterior and right-left movements of the centre of pressure of the feet. Visual stimulus rotation occurs between the arrows, subject rotation between the arrowheads.

Methods

Eight normal subjects were instructed to stand, fixating the centre of the visual stimulus - this consisted of a large luminous disk facing the subject and could be rotated (40°/sec) around the visual axis in either direction with the visual environment otherwise dark. Subjects stood on an externally controlled platform that could be rotated (2°/sec) to change the position of the subject relative to the visual stimulus. Sway was measured at the level of the centre of pressure (COP) and of the head. The sequence of events during each trial were: an initial period to measure base-line position; a period of visual stimulus rotation at one of five positions relative to the subject; a period of rotation of the subject to a different position relative to the visual stimulus; a further period of visual stimulus rotation; and a final period with no rotation (Fig.1, bottom panel).

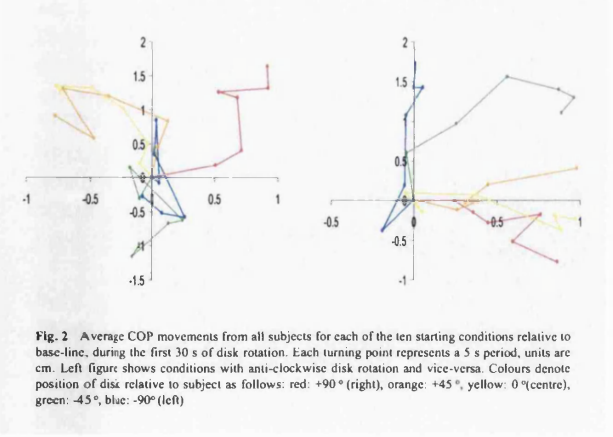

Fig. 2 Average COP movements from all subjects for each of the ten starting conditions relative to base-line, during the first 30 s of disk rotation. Each turning point represents a 5 s period, units are cm. Left figure shows conditions with anti-clockwise disk rotation and vice-versa. Colours denote position of disc relative to subject as follows: red: +90 ° (right), orange: +45 °, yellow: 0 °(centre), green: -45 °, blue: -90° (left)

Results

Data from individual subjects (Fig. 1) were combined into groups of matching start or end positions and normalised to show the change in sway position induced by visual stimulus rotation onset or offset respectively (Fig. 2). The directions of the visually evoked postural sway response at the start and the relaxation back to centre are compared graphically with the orientation of the visual stimulus (Fig. 3). These direction vectors converted to degrees can then be compared statistically (Fig. 4) revealing an average gain of reorientation from straight ahead of 0.9.

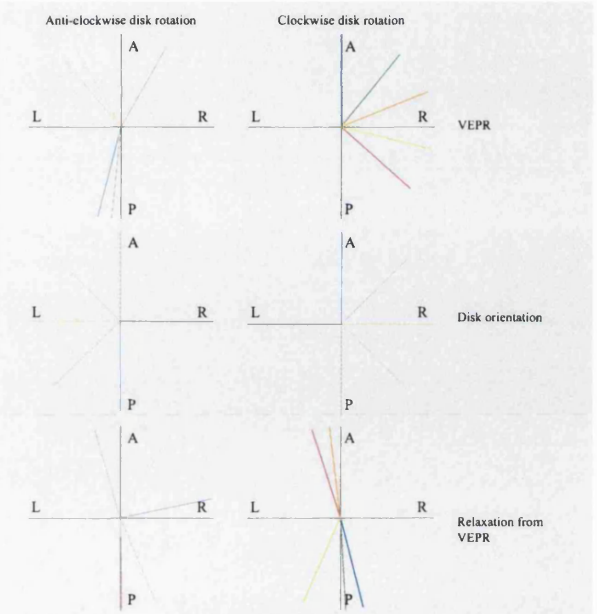

Fig.3 Direction of the visually evoked postural response (VEPR) and relaxation back to centre when the visual stimulus stopped for each condition compared with the orientation of motion of the visual stimulus. Left figure shows conditions with anti-clockwise disk rotation and vice-versa. Colours as Fig. 2

Discussion

The ability to use visual cues for posture is important physiologically, and this should be present in any direction of gaze. These experiments confirm that postural responses do reorient according to gaze angle. The mechanism for reorientation requires signal(s) of the misalignment between the visual and locomotor systems; these signals may originate from efference copy, proprioception, vision or cognitive knowledge of the environment. By reducing the cognitive and background visual signals compared with previous experiments their importance can be determined. The present experiment revealed a gain of reorientation of 0.9 which is not significantly different from that of Wolsley et al. (1996) where they found a gain of reorientation of 1.08 ± 0.2. Thus, we propose that cognition and background visual structure do not play a role in this reorientation.

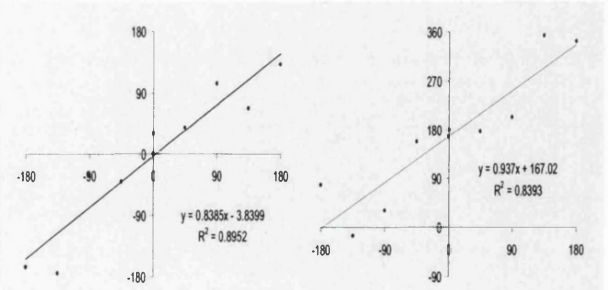

Fig. 4 Direction of sway in degrees from centre plotted against visual stimulus motion for onset (left) and offset (right) conditions.

References

Wolsley C J, Sakellari V, Bronstein A M (1996) *Reorientation of visually evoked postural responses by different eye-in-orbit and head-on-trunk angular positions* Exp. Brain Res.111: 283-288

Exp Brain Res (2000) 133:229–232
Digital Object Identifier (DOI) 10.1007/s002210000373

RESEARCH ARTICLE

A. Thurrell · P. Bertholon · A.M. Bronstein

Reorientation of a visually evoked postural response during passive whole body rotation

Received: 8 July 1999 / Accepted: 25 January 2000 / Published online: 14 April 2000

Abstract Visually evoked postural responses (VEPR) to a roll-motion rotating disk were recorded from normal subjects standing on a yaw axis motorised rotating platform. The disk was fluorescent so that subjects could be tested in an otherwise dark room. Movements of the head and centre of foot pressure were measured while subjects looked at the disk with their eyes and head in the primary position and while the rotating platform moved the subjects randomly to 0, +/–45° and +/–90° angles from the visual stimulus. Subjects were instructed to maintain fixation on the centre of the rotating disk but the amount of horizontal eye and head movement used was not specified. Platform rotational velocity was set near threshold values for perception of self-rotation (~2°/s) so that subjects would find it difficult to reconstruct the angle travelled. The data showed that the VEPR occurred in the plane of disk rotation, regardless of body position with respect to the disk, and despite the subjective spatial disorientation induced by the experiment. Averages of the response revealed a good match (gain=0.95) between disk orientation and sway direction. The horizontal gaze deviation required to fixate the centre of the disk was largely achieved by head motion (head 95%, eye 5%). The results confirm previous results that VEPRs are reoriented according to horizontal gaze angle. In addition, we show that the postural reorientation is independent of cognitively or visually mediated knowledge of the geometry of the experimental conditions. In the current experiments, the main source of gaze position input required for VEPR reorientation was likely to be provided by neck afferents. The results support the notion that vision controls posture effectively at any gaze angle and that this is achieved by combining visual input with proprioceptively mediated gaze-angle signals.

Key words Vestibular · Posture · Visual motion · Proprioception · Human

A. Thurrell · P. Bertholon · A.M. Bronstein (✉)
MRC Human Movement and Balance Unit,
8–11 Queen Square, London, WC1 N 3BG, UK

Introduction

Vision is used in conjunction with proprioceptive and vestibular signals for spatial orientation and balance control. If a subject, standing upright and looking straight ahead in a room, spontaneously starts to fall to the right, the optic flow will be to his/her left. The correct righting response for the subject in this case is to increase the pressure on the right foot and decrease it on the left, such that the change in forces acts to rotate the subject's body leftwards. The usual cause of large-field visual motion is the movement of the retina in space; therefore large-field motion is treated as if it was due to self-motion by the subject. If this retinal motion is simulated by a visual scene moving to the left when the subject is in fact upright, then the change in pressures at the feet will act to destabilise the subject to the left, i.e. in the same direction as the visual motion. The response to a large-field moving stimulus is therefore to sway in the same direction in space as the visual motion (Dichgans et al. 1975; Clément et al. 1985; Bronstein 1986).

A common feature of many previous experiments is the use of visual motion stimuli that are viewed by the subject looking straight ahead, i.e. with both the eyes centrally placed in the orbits and the head centrally placed on the shoulders (Dichgans et al. 1975; Clément et al. 1985; Bronstein 1986). However, Wolsley et al. (1996) investigated the effect of supplying identical retinal inputs with the eyes and head at different positions in the yaw plane. It was found that subjects reoriented the main direction of sway, so as to match the direction of the visual stimulus, for a variety of combinations of head-on-trunk and eye-in-orbit positions. However, this experiment was run in a well-lit visual environment, with subjects instructed to position themselves actively. Thus subjects may have been able to determine their orientation, and that of the visual stimulus, visually and cognitively. Here we examine whether accurate reorientation of visually evoked postural responses (VEPR) still occurs during passive body rotation and with diminished visual and cognitive cues.

Methods

Eight normal subjects aged between 21 and 33 years of age were instructed to stand relaxed, with arms at their sides, fixating the centre of a visual display. The visual display consisted of a large disk of diameter 0.9 m positioned 40 cm from the subject's nasion at eye level, such that it covered a large area of the subject's visual field (97°). This disk was covered in randomly distributed fluorescent circles of 2 cm diameter with an average density of 320 m^{-2} and could be rotated around the visual axis at an angular velocity of 40 /s either clockwise or anti-clockwise. Acceleration and deceleration of the disk took less than 2 s. The visual environment was otherwise dark.

The subjects stood on a posturography platform (internal malleoli 3 cm apart), which measured the position of the centre of foot pressure (COP) in the anterior–posterior and lateral directions. A 3-D magnetic search coil system (Polhemus 3space fastrack) measured head position in anterior–posterior, right–left directions and yaw. Horizontal DC electro-oculography was used to check that subjects fixated the centre of the disk and to reveal the relative extent of the head-on-trunk and eye-in-orbit rotations. The posturography platform was mounted on an externally controlled rotating platform moving smoothly about a vertical axis at 2°/s. This is near the reported values for perception of rotation (Hulk and Jongkees 1948; for review see Jongkees 1974); pilot studies indicated that most subjects could not perceive being rotated when their eyes were closed. Thus the visual stimulus could appear between –90° (left) and +90° (right) relative to the subjects' trunk mid-sagittal plane.

During a trial, each subject started facing the disk at one of five platform positions: –90, –45, 0, +45, +90. The stimulus sequence was as follows (see Fig. 1, bottom panel): 1) stationary platform, stationary disk (15 s), 2) stationary platform, rotating disk (30 s), 3) rotating platform, rotating disk (22.5–90 s, depending on amplitude of platform rotation), 4) stationary platform, rotating disk (30 s) and 5)stationary platform and disk (15 s). These periods were contiguous. There were 40 different possible trials: two disk rotation directions vs five positions for the start-point and four positions for the end-point of platform rotation. Each subject experienced ten different trials in a Latin-square paradigm, the first trial starting and the last trial ending with the disk straight ahead. Subjects remained in the dark between trials to prevent use of visual cues to determine their orientation.

All signals were sampled at 125 Hz and analysed offline. COP was arithmetically normalised to represent the signal given by a 70 kg mass. Five seconds of the onset response (average position between 25 and 30 s of disk rotation) were measured, relative to the average position during the 15 s before disk rotation. For the offset response, 1 s was measured (between 1 and 2 s after cessation of disk rotation), relative to the average position during the last 15 s of disk rotation. Based on these position measurements, the average orientation of the VEPR was then calculated for all subjects at each onset or offset condition, e.g. clockwise disk rotation at +45° platform position. In order to control for the effects of platform rotation in isolation, four subjects were rotated six times each between –45° and +45° and vice versa at 2°/s while fixating the stationary visual display. This control experiment showed that subjects' COP shifted by a mean of 1.05 cm, SD 0.88 cm, in the direction of body rotation; due to the randomisation process for disk and platform rotational direction this bias would be cancelled out.

Results

Signals of head yaw and horizontal eye positions showed that the steady-state reorientation of gaze for all subjects was mainly due to rotation of the head on the trunk (95%, SD 5%), with the remaining 5% performed by the eyes. During subject rotation, the proportion of movement carried out by the eyes sometimes exceeded this until further rotation of the head occurred. Subjectively, subjects were unsure of the relative position between themselves and the visual stimulus; some reported disorientation.

Figure 1shows raw sway platform traces from one subject (JB) during the condition where the disk started

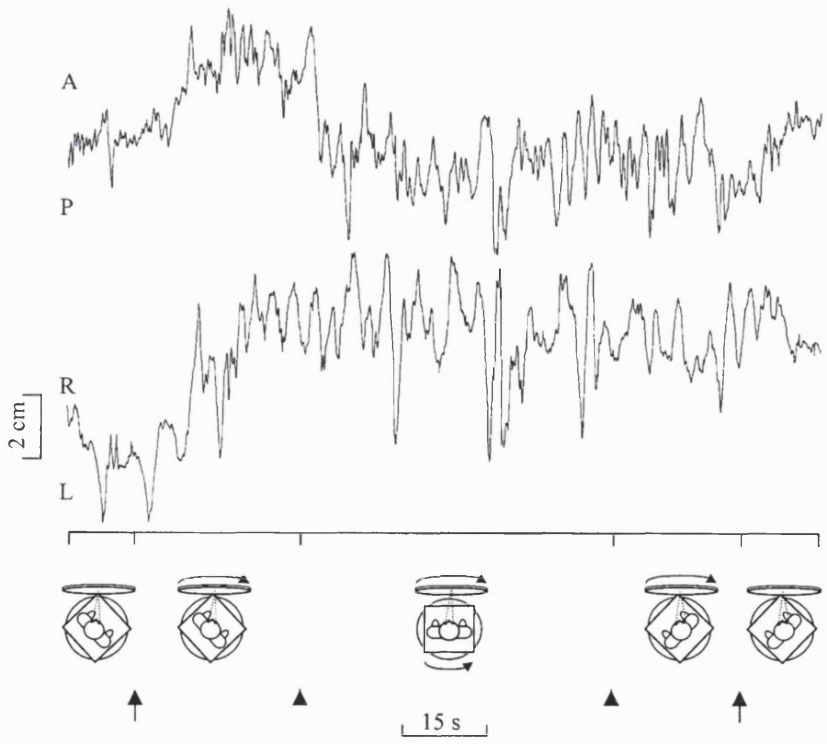

Fig. 1 Raw platform traces from subject JB for the condition with clockwise disk rotation: starting condition at –45° (left), ending at +45° (right) relative to the subject. The two traces show the anterior (*A*)–posterior (*P*) and right (*R*)–left (*L*) movements of the centre of foot pressure. The period of disk rotation is shown between the *arrows* and platform rotation between the *arrowheads*. The sequence of events is also represented by the *icons* below

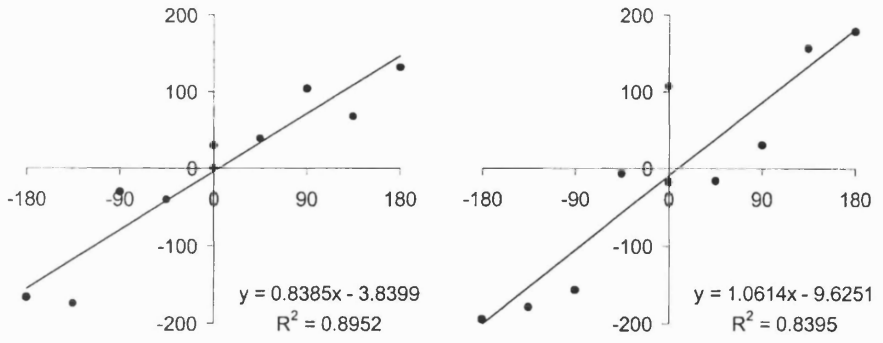

Fig. 2 Direction of sway (*abscissa*), as measured by the position of the centre of foot pressure, plotted against direction of disk upper half motion, i.e. predicted sway direction (*ordinate*). Conditions were onset (left) and offset (right) of disk rotation. All values in degrees, with zero corresponding to the direction of the subject's toes

at a position of –45° before moving (relative to the subject) to +45°. The traces show the onset of the VEPR, with forwards and rightwards sway, at circa 25 s. As the platform rotates rightwards (between arrowheads, Fig. 1) there is a reorientation of the COP from a right anterior to a right posterior position. On cessation of disk rotation (last arrow) the COP moves anteriorly and partly leftwards towards the original baseline position.

Visually evoked postural reponses were normalized with respect to a 15 s period preceding the onset or offset of disk rotation. The orientation of the VEPR after 30 s (onset) or 1 s (offset) was converted into degrees relative to the subjects' trunk mid-sagittal plane for direct comparison with the orientation of the visual display. The reorientation of the VEPR at both the onset and offset of disk rotation, measured for COP signals for all conditions, is summarised graphically in Fig. 2; a strong reorientation of VEPR by relative disk position can be seen. The best-fit curve reveals that the gain of the reorientation response at onset is ~0.82 (y=0.84x–3.8, r^2=0.90, as measured at the COP, and y=0.80x+4.61, r^2=0.95 measured at the level of the head, where x and y are visual motion and sway directions respectively). The offset response (at 1 s after the end of disk rotation) had a gain around unity (y=1.06x–9.63, r^2=0.84 as measured by the COP, or y=1.05x–7.3, r^2=0.96 as measured at the level of the head).

Discussion

Many previous studies have shown that visual motion is capable of generating postural reactions (e.g. Dichgans et al. 1975; Clément et al. 1985; Bronstein 1986); however, relatively few have investigated the influence of different positions of these stimuli relative to the subject (Stoffregen 1985; Gielen and Asten 1990; Wolsley et al 1996). Wolsley et al. (1996) reported an accurate reorientation of a VEPR during deviation of both the eyes in head and head on trunk. It was reasoned that, since the retinal motion stimulation was the same in the different positions, the postural reorientation must be due to eye-in-orbit and head-on-trunk position signals, possibly proprioceptive in origin. However, their experiment was conducted in a well-lit environment with subjects having prior cognitive knowledge of the position of the visual stimulus and of the relative rotations of the eyes and head. The present experiment was therefore conducted to test whether the reorientation of the VEPR is affected by reduced cognitive and background visual information and by passive positioning of the subjects on a rotating platform.

In the present experiment the directions of VEPRs induced by both the onset and offset of disk rotation were measured. The gain of the reorientation of VEPR was ~0.8 at the onset but ~1.0 during the offset. This slight difference may be explained by the fact that the posturally-relevant sensory cues for vertical realignment of the body during disk rotation are conflicting, but those for realignment after disk rotation has ended are not. A comparison with the data of Wolsley et al. (1996), who found a gain of reorientation of 1.08±0.2 (calculated from published diagrams), suggests that little or no role is played by cognition, background visual structure or active positioning in the reorientation of VEPRs.

The origin of the signals used to determine the direction of gaze for visual control of posture is not yet clear. For the neck, proprioception would seem useful due to the possibility of external forces acting on the head. Neck afferents have been shown to be the main source of information used to estimate head–trunk horizontal angular deviation (Nakamura and Bronstein 1995). In the current experiments, where 95% of gaze deviation was achieved by head-on-trunk deviation, neck proprioceptive information is therefore the most likely source. Neck proprioceptive afferents are also thought to be responsible for the reorientation of vestibularly (galvanic) elicited sway during head turns (Lund and Broberg 1983; Britton et al 1993). External forces do not normally act on the eyes and, therefore, efference copy or a mixture of efference copy and ocular proprioception has been favoured as source of an eye-in-orbit position signal. In pointing and estimation tasks (Bridgeman and Stark 1991) physiological gains of oculomotor efference copy and proprioception were found to be 0.61 and 0.26 respectively. The finding that extra-ocular muscle vibration elicits directional postural responses (Roll et al. 1989) suggests that at least some ocular proprioceptive component influences postural control. The current experiments suggest that visual and proprioceptive signals

combine in order to provide effective, gaze angle-independent, visual control of posture. This process appears to be largely independent of cognitive comprehension of the geometry involved.

Acknowledgement Support from the CEC grant "Access to large scale facilities" is gratefully acknowledged.

References

Bridgeman B, Stark L (1991) Ocular proprioception and efference copy in registering visual direction. Vision Res 31:1903–1913

Britton TC, Day BL, Brown P, Rothwell JC, Thompson PD, Marsden CD (1993) Postural electromyographic responses in the arm and leg following galvanic vestibular stimulation in man. Exp Brain Res 94:143–151

Bronstein AM (1986) Suppression of visually evoked postural responses. Exp Brain Res 63:655–658

Clément G, Jacquin T, Berthoz A (1985) Habituation of postural readjustments induced by motion of visual scenes. In: Igarashi M, Black O (eds) Vestibular and visual control on posture and locomotor equilibrium. Seventh Int. Symp. Int. Soc. Posturography, Houston, Texas. Karger, Basel, pp 99–104

Dichgans J, Brandt T, Held R (1975) The role of vision in gravitational orientation. Fortschr Zool 23:255–263

Gielen CCAM, van Asten WNJC (1990) Postural responses to simulated moving environments are not invariant for the direction of gaze. Exp Brain Res 79:167–174

Hulk J, Jongkees LBW (1948) The normal cupulogram. J Laryngol 62:70–75

Jongkees LBW (1974) Pathology of vestibular sensation. In: Kornhuber HH (ed) Vestibular system: Psychophysics, applied aspects and general interpretations. Handbook of sensory physiology. Springer, Berlin Heidelberg New York, pp 413–450

Lund S, Broberg C (1983) Effects of different head positions on postural sway in man induced by a reproducible vestibular error signal. Acta Physiol Scand 117:307–309

Nakamura T, Bronstein AM (1995) The perception of head and neck angular displacement in normal and labyrinthine-defective subjects. Brain 118:1157–1168

Roll JP, Vedel JP, Roll R (1989) Eye head and skeletal muscle spindle feedback in the elaboration of body references. Prog Brain Res 80:113–123

Stoffregen TA (1985) Flow structure versus retinal location in the optical control of stance. J Exp Psychol Hum Percept Perform 11:554–565

Wolsley C J, Sakellari V, Bronstein A M (1996) Reorientation of visually evoked postural responses by different eye-in-orbit and head-on-trunk angular positions. Exp Brain Res 111: 283–288

Reduction of perceived visual speed during locomotion: Evidence for quadrupedal perceptual pathways in humans?

Adar Pelah [1], Adrian E. I. Thurrell [1,2] and Miriam Berry [1]

ap114@cam.ac.uk, a.thurrell@ion.ucl.ac.uk and mb305@cam.ac.uk

1) Department of Physiology, University of Cambridge, Downing Street, Cambridge, CB2 3EG

2) MRC Human Movement and Balance Unit, Institute of Neurology, National Hospital for Neurology and Neurosurgery, Queen Square, London, WC1N 3BG

Introduction

Movement of the eyes has a profound effect on the images projected on the retinae. Thus in any visual determination of the position or movement of an object, account must be made of the movements of the eyes in space. Von Helmholtz (1896) concluded that the solution was to use extra-retinal signals to reveal object position and movement in space. Wertheim (1994) suggested the replacement of the concept of extra-retinal signals by that of reference signals which encode the motion of the eyes in space rather than rotation of the eyes in their sockets relative to the head in order to account for percepts during sensations of ego-motion (vection). This concept allows easy extension of the reference signal to include not just ego-motion from vestibular or vection-inducing optic flow, but signals from other sensory modalities as well, providing a common reference frame for interaction. A number of studies have found influences of limb proprioceptive and somatosensory signals on self-motion perception (Bles et al. 1995), ocular tracking (de Graaf et al. 1994) and visual motion perception (Brandt et al. 1977, Pelah et al. 1996). We reported previously (Thurrell et al. 1998) that perceived optic flow speed is reduced linearly with walking speed on an exercise treadmill. As it is rare to walk on a moving surface, we postulated this mechanism would preserve world constancy during normal self-motion. The hypothesis that this effect is due to mechanisms of perceptual constancy would be bolstered if the effect were strongest for motor activities similar to natural locomotion (walking). We tested the effect under four motor activities progressively less similar to natural locomotion: walking; cycling; 'arm pedalling' and finger tapping.

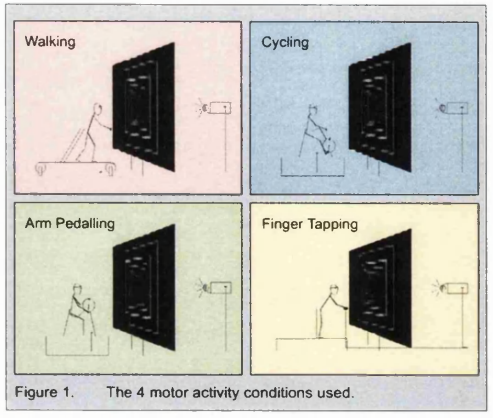

Figure 1. The 4 motor activity conditions used.

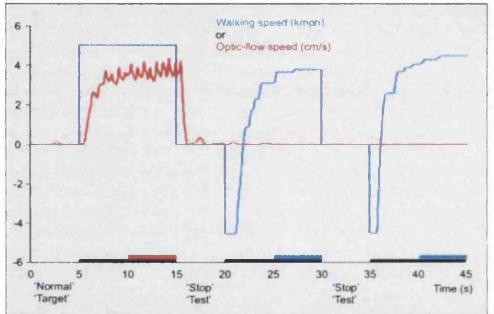

Figure 2. The time sequence of each trial. Instructions were displayed for 5s each (thin black line) alternating with the tunnel (10s, thick black lines). Mean settings during the last 5s of each test tunnel (blue bars) were plotted against the mean walking speed during the last 5s of the target tunnel (red bar), see Figure 3. Activity speed (red) in km/h, visual velocity (blue) in cm/s at mid-hemifield position, data from subject BRD (walking).

Methods

24 experimentally naïve subjects between the ages of 19 and 25 were tested. Goggles were worn allowing vision only from the right eye and restricting peripheral vision to within the confines of the visual display. The visual stimulus consisted of a large screen (1.9m x 1.2m) on which was rear-projected a moveable tunnel composed of 15 bright squares on a dark background. A bright fixation point was also present on the centre of the tunnel and maintained at eye level. The image resolution was 1280 x 1024 refreshed at 30Hz, fully anti-aliased and tunnel components faded in and out of the background luminosity to reduce motion artefacts.

The conditions:

- The walking condition was performed on an exercise treadmill powered by the locomotion of the subject whilst holding the hand-rails, allowing direct control of their walking velocity.
- Cycling conditions were performed on an exercise bicycle placed to minimise changes in eye position from walking.
- For the 'arm pedalling' condition, the exercise bicycle was raised and the resistance reduced for comfort.
- Finger tapping conditions were performed while standing on the treadmill, tapping all 4 fingers on each hand together, alternating hands. See Figure 1.

The order of the experiments was counterbalanced across the subjects, with 18 trials for each motor activity and subject. Subjects adjusted the test tunnel velocity using a potentiometer placed near their right hand.

Each trial was 45s long (see Figure 2):

An instruction denoting a target presentation and for the motor activity speed, either 'stop', 'very slow', 'slow', 'normal', 'fast' or 'very fast' was displayed for 5s giving the subject time to reach this speed from rest before…

- A target tunnel velocity (always expanding at +5cm/s at the mid-hemifield position) was presented for 10s.
- The tunnel was removed for 5s and replaced with instructions to stop the motor activity and adjust the tunnel velocity. The tunnel velocity was to be adjusted to that perceived during the motor activity.
- A test tunnel whose velocity was controlled by the subject was presented for 10s.
- A second test tunnel followed in an identical manner.

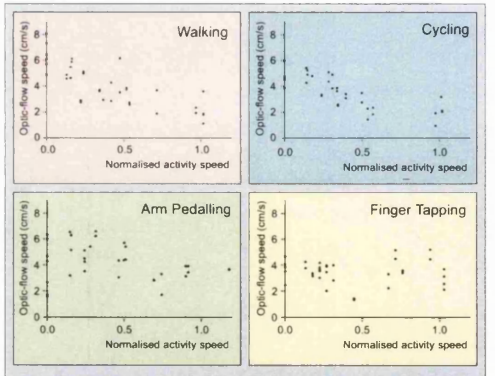

Figure 3. Perceived visual velocity plotted against normalised motor activity for each of the 4 activities. Data show accurate perception without motor activity and reduced perceived velocity at higher activity speeds for walking, cycling and arm pedalling. Slopes of linear best fits were -3.9 (walking), -3.2 (cycling), -0.8 (arm pedalling) and 0.0 (finger tapping). Target tunnel velocity was always +5cm/s (expanding). Data from subject BKW.

Results

- 15 out of 20 subjects showed the previously reported effect of reduced perceived visual velocity due to walking. Remaining subjects produced anomalous results possibly due misinterpretation of instructions or lack of immersion in the environment.
- The effect of walking speed on the perceived visual velocity was significantly greater than the other activity conditions.
- The effects of cycling and arm pedalling were both significantly different from zero, but not from each other.
- The effect of finger tapping on the perceived visual velocity was not significantly different from zero.

Discussion

Confirming our previous findings, visual motion perception is influenced by walking. Cycling and arm pedalling, as activities less similar to locomotion, were also found to influence visual motion perception. Finger tapping, however, was not found to have any effect upon visual motion perception, see Figure 4. This trend may be explained by the similarity of the activity to natural locomotion: Walking as the 'gold standard', would be the quintessential activity for which this effect would be expected; cycling uses many of the same muscles, but with a different coordination pattern and is less natural; arm pedalling may replicate some aspects of arm swing during walking whereas finger tapping is completely unrelated to locomotion. An intriguing alternative to the similarity of arm pedalling to arm swing would be that this activity activates vestigial quadrupedal pathways present as a result of our evolutionary heritage or our days as infants crawling on all fours.

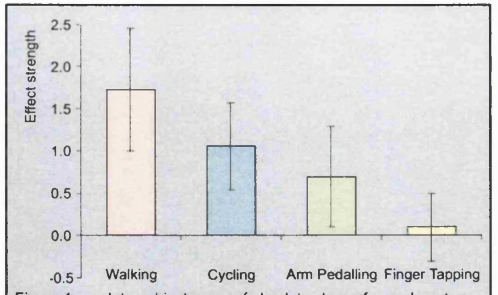

Figure 4. Intersubject mean of absolute slopes for each motor activity showing the trend in effect magnitude from walking to finger tapping. Error bars denote ±1.96 standard errors.

References

Bles W, Jelmorini M, Bekkering H, de Graaf B (1995) Arthrokinetic information affects linear self-motion perception. J.Vestib.Res. 5: 109-116

Brandt T, Buchele W, Arnold F (1977) Arthrokinetic nystagmus and ego-motion sensation. Exp.Brain Res. 30: 331-338

de Graaf B, Bos JE, Wich S, Bles W (1994) Arthrokinetic and Vestibular Information Enhance Smooth Ocular Tracking During Linear (Self-)Motion. Exp.Brain Res. 101: 147-152

Pelah A, Barlow HB (1996) Visual illusion from running. Nature 381: 283

Thurrell, A. E. I, Pelah, A, and Distler, H. K. (1998) The influence of non-visual signals of walking on the perceived speed of optic flow. Perception 27, 147

von Helmholtz H (1896) The direction of vision. In: Southall JPC (ed) Handbuch der Physiologischen Optik Vol. 3. Optical Society of America, pp 242-281

Wertheim AH (1994) Motion perception during self-motion: the direct versus inferential controversy revisited. Behavioral and Brain Sciences 17: 293-355

Vection induced re-orientation in a visually evoked sway response

Adrian E. I. Thurrell and Adolfo Bronstein

a.thurrell@ion.ucl.ac.uk and a.bronstein@ion.ucl.ac.uk

Academic Department of Neuro-otology, Division of Neuroscience, Imperial College, Charing Cross Hospital, London, W6 8RP

Introduction

'or visual control of posture to be successful there must a compensation for any change in position of the eyes ıtive to the feet. A previous study (Wolsley et al. 1996) ›wed that a visually evoked postural response (VEPR) to l-plane visual-motion was reoriented both by head-on-nk and eye-in-head rotation. Thurrell et al. (2000) ended these results to show that this reorientation was dependent on cognitive knowledge of environment ›metry. During viewing of large moving scenes subjects y perceive themselves to be moving (vection) or the ne to be moving, perception alternating spontaneously ween these two states. It has been shown (e.g. Kuno et al. 99) that the degree of vection correlates with the **gnitude** of visually induced postural sway. We pected that the **accuracy** of the orientation of this ually induced postural response to the direction of the ving visual stimulus would be increased during periods vection relative to those periods during object motion ception.

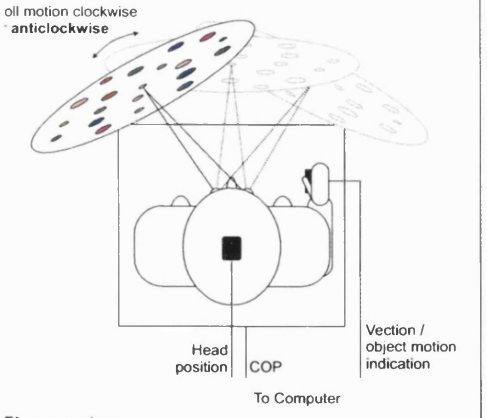

Figure 1 The experimental set-up showing the hree disk positions. Data from the **left disk** ›osition **rotating anticlockwise** used in Figures ! and 3.

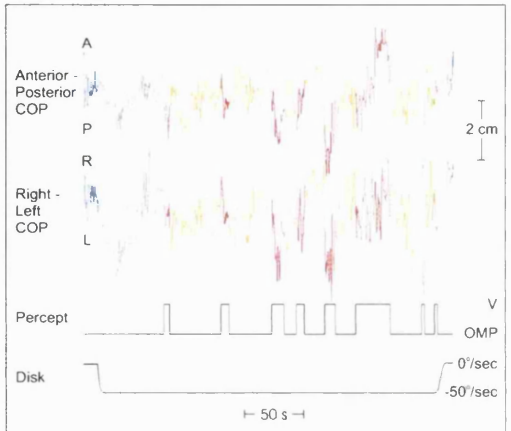

Figure 2 Raw signals from a single trial (with the disk 30° left, rotating anticlockwise) showing periods of vection and object motion perception signalled by the subject to be compared to the stationary periods.

Methods

- Subjects were required to stand, looking either straight ahead or ~30° to the right or left using only horizontal eye rotation at the centre of a large rotating (±50°/sec about the visual axis) disk (see Fig. 1).
- Trials were conducted either monocularly or binocularly.
- Posture was measured via the **head position** (Polhemus Fastrack) and the **centre of foot pressure (COP)**.
- Alternations between **vection** and **object-motion perception** were indicated using a hand-held **push button**.
- The position of the head and the COP was averaged during periods of: disk stationarity (baseline); vection and object motion (see Figs. 2 and 3).
- The errors between the direction of disk motion and the directions of sway from baseline to vection and object motion positions were calculated (see Fig. 3b).

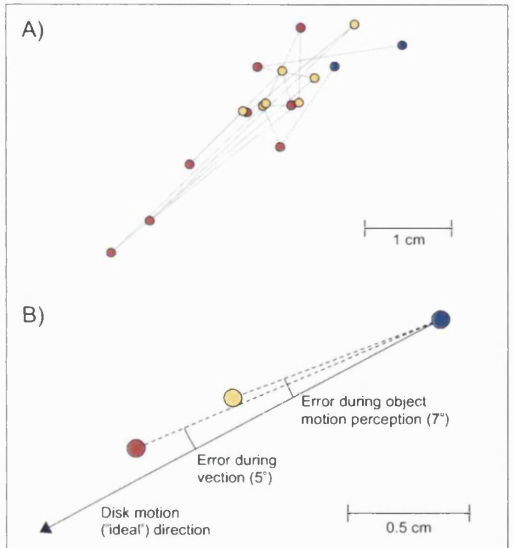

Figure 3 Data (same trial as figure 2) plotted showing the direction and increased magnitude of sway during vection compared to object motion perception. a) Average positions during **each** periods of stationarity, vection or object motion perception. b) Positions averaged over **all** periods of stationarity, vection or object motion perception, showing directions of sway and errors with respect to disk motion direction.

Results

- ANOVA indicated that sway orientation was **more accurate** with respect to disk orientation **during vection** than during object motion perception (13° vs. 19° mean direction error; $P < 0.05$).
- There was no statistically significant difference between monocular and binocular viewing.
- Visually induced sway amplitude was larger during vection than object motion perception ($P < 0.05$; see Fig. 3b).

Discussion

These results show a significantly more accur reorientation of visually evoked postural sway dur vection than object motion perception. The increa accuracy observed during vection suggests that consci perception of self-motion, presumably at a cortical le may interact more effectively with gaze position sign This indicates that visual control of body sway is **impro when vision signals self-motion!**

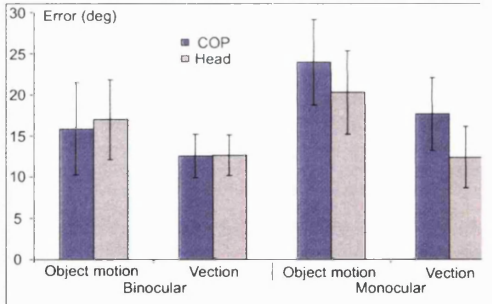

Figure 4 Mean (± standard error) of directiona errors showing greater accuracy of sway durin vection vs. object motion perception and durin binocular vs. monocular viewing (expected due t additional depth cues from stereopsis, but nc statistically significant).

References

Wolsley CJ, Sakellari V, Bronstein AM. Reorientation of visu evoked postural responses by different eye-in-orbit and head-on-tr angular positions. Exp. Brain Res. 1996; 111; 283-288

Kuno S, Kawakita T, Kawakami O, Miyake Y, Watanabe S Post adjustment response to depth direction moving patterns produce virtual reality graphics. Japanese Journal of Physiology 1999; 49: 4 424

Thurrell AEI, Bertholon P, Bronstein AM. Reorientation of a visu evoked postural response during passive whole body rotation. E Brain Res. 2000; 133; 229-232

Experimental Brain Research
DOI 10.1007/s00221-002-1296-1

Research Note

Vection increases the magnitude and accuracy of visually evoked postural responses

A. E. I. Thurrell · A. M. Bronstein(✉)

A.E.I. Thurrell · A.M. Bronstein
Academic Department of Neuro-otology, Division of Neuroscience and Psychological Medicine, Imperial College Faculty of Medicine, Charing Cross Hospital, London W6 8RP, UK

✉ E-mail: a.bronstein@ic.ac.uk
Phone: +44-20-88467523
Fax: +44-20-88467577

Received: 29 May 2002 / **Accepted:** 23 September 2002 / **Published online:**

Abstract. Movement of large visual scenes induces an illusion of self-motion (vection) and postural responses. We investigated if the conscious perception of self-motion influences the magnitude and directional accuracy of visually evoked postural responses. Five normal subjects fixated the centre of a large disk rotating in the roll (coronal) plane. The disk was placed either in front of the subjects or obliquely 30 deg to their right or left; in these oblique positions disk fixation was achieved by horizontal ocular deviation alone (i.e. no neck deviation). Subjects indicated their subjective perceptual status, either vection or object motion, with a push button. The results confirmed that the direction of the visually evoked postural response was reoriented according to the different eye-disk positions. In addition, both the magnitude of the postural response and the accuracy of its alignment with the disk rotational plane were significantly increased during vection periods. The results show that conscious perception of self-motion enhances visuopostural performance. Since conscious perception is likely to arise at cortical levels, the findings indicate that the cortex is one of the sites where gaze direction interacts with retinal motion signals to provide a self-motion signal in body-centric co-ordinates. Such interaction provides a substrate for spatial representation during motion in the environment.

Keywords. Human - Posture - Vision - Vection - Visuomotor

Introduction

Locomotor or postural movements create relative motion between the subject and the visual environment (optic-flow). Artificial full-field visual motion stimuli are often interpreted as due to self-motion and induce subconscious visually evoked postural responses and sometimes a conscious

illusion of sensation of self-motion termed vection (Dichgans et al. *1972*). At other times, however, perception is correct and the viewer reports that they are stationary and the disk is moving (object-motion perception). These two percepts comprise a bi-stable pair such that, when viewing a large rotating disk, there will be alternating periods of vection and of object-motion perception. However, illusory signals of self-motion that may result in vection need not be consciously perceived to influence postural control under identical visual conditions (Previc and Mullen *1991*), and in fact may have visuopostural latencies many times shorter than vection (Clément et al. *1983*). However, a recent study found that postural sway during periods of vection was of a greater magnitude than during periods of object-motion perception (Kuno et al. *1999*). Therefore, it could be expected that the induced postural sway during vection would become more accurately aligned with the moving visual stimulus. This would suggest, in turn, that conscious perception of self-motion improves visuopostural control. These expected changes in the accuracy of orientation of the induced postural sway, comparing vection versus object-motion perception, were investigated here.

Materials and methods

Five normal subjects between the ages of 21 and 31 years were instructed to stand, relaxed, with their arms at their sides and their feet slightly splayed and separated upon a force platform. Subjects wore a light helmet carrying the receiver of a magnetic search coil system (Polhemus 3space Fastrack) measuring head position in all six degrees of freedom. Subsequent data processing was performed identically upon the horizontal position of the centre of foot pressure (COP) and on horizontal head position. In their right hand subjects held a button to indicate their perceptual state (vection or object-motion). All signals were recorded at 125 Hz. In half the trials subjects were to press this button when they perceived themselves to be moving (i.e. vection) and in the other half only when they perceived the visual display to be moving (object-motion perception). The visual display consisted of a large (1.8 m diameter, visual angle 122°) white disk, with a central fixation point, covered in smaller (5-20 cm diameter) circles of various colours. This disk was rotated either clockwise or anticlockwise at 50°/s and it was placed in one of three positions, either directly ahead of the subject or 30° to the left or right (see Fig. 1a), all at 50 cm from the subject's nasion. The centre of the disk was fixated with eye deviation only, i.e. no neck deviation, and viewed against normal laboratory lighting. Each subject was tested at each orientation with the disk always rotating clockwise or always anticlockwise. Each trial lasted 300 s with the disk being stationary for the first and last 10 s, taking 7.5 s to reach 50°/s and 5 s to stop. The remainder formed a central period of constant speed disk rotation that was divided into perceptual periods determined by each subject's indication of vection or object-motion (see Fig. 1b). Baseline positions were calculated as the means over the initial stationary period (0-10 s) and the final 5 s of the last stationary period. Sway (magnitude and the angular error relative to the orientation of disk motion) relative to both baseline positions was calculated during each perceptual period. Periods from the onset of disk rotation until the onset of the first vection percept and during the offset of disk rotation were discarded. The means of the sway magnitudes and direction errors across all periods for each perceptual state were calculated for each trial (see Fig. 1c).

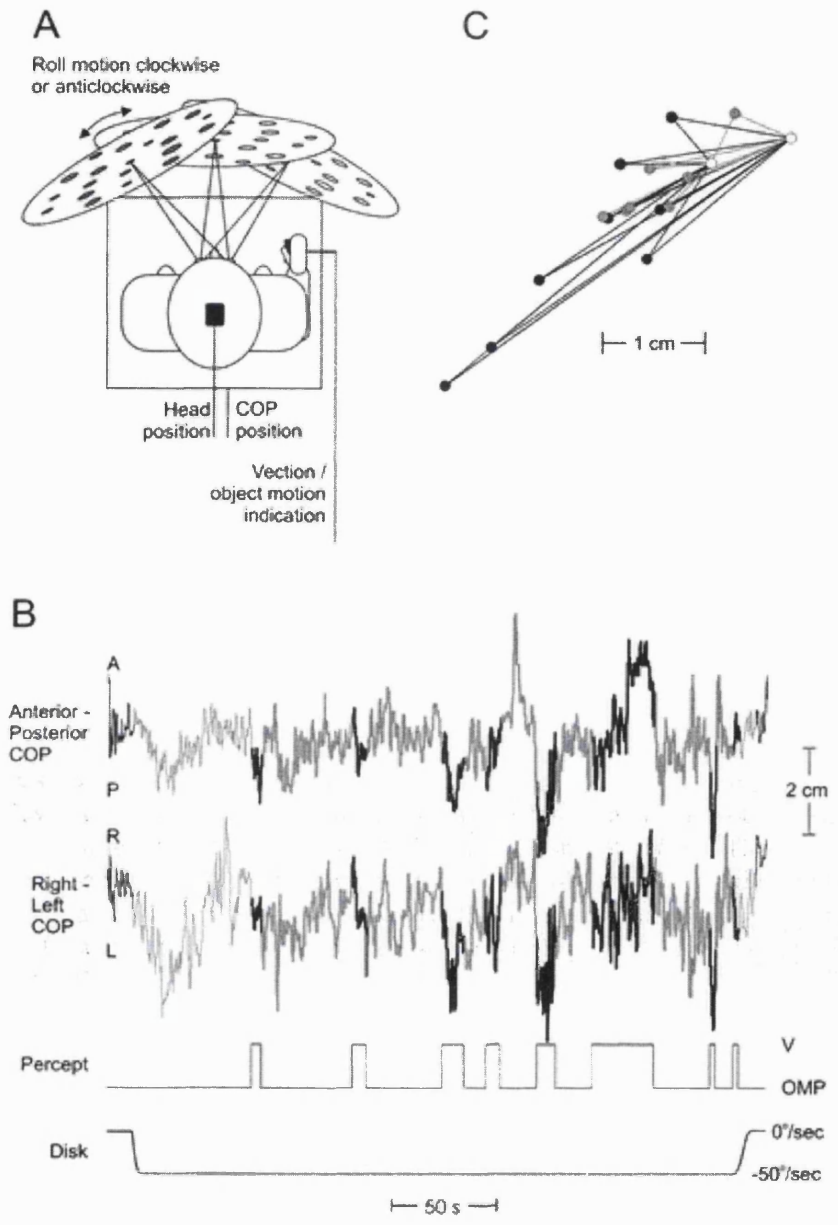

Fig. 1. A The experimental set-up from above, showing the three disk positions relative to the subject. **B** Raw time signals from a typical trial (with the disk 30° left, rotating anticlockwise) showing periods of vection (*thick black lines*) and object-motion perception (*thick grey lines*) signalled by the subject to be compared to the baseline periods (*thin black lines*). Intermediate periods during and immediately after start or cessation of disk rotation (*thin grey lines*) are not used for analysis. **C** Data plotted showing the positions of sway during vection (*black*) and object motion perception (*grey*) and the trajectories from each of these positions to both baseline positions (*white*) from which the mean error direction for that trial was calculated

Results

The grand averages across all subjects and disk orientations of sway magnitude were calculated for each perceptual state (vection or object-motion perception). Sway deviation from baseline was found to be significantly greater ($P<0.05$, paired t-test) during vection than during object-motion perception at both the level of the head (5.8±0.56 mm vs 4.3±0.40 mm, mean ± SEM) and the COP (3.0±0.39 mm vs 1.7±0.19 mm).

Angular errors were also collapsed across subjects and disk orientations to reveal angular errors for each perceptual state (vection and object-motion perception). Comparison of the grand average of these errors revealed sway orientation to be significantly more accurate with respect to disk motion direction during periods of vection than during object-motion perception (32.6±6.6° vs 51.4±7.9°, intersubject mean ± SEM direction error, at the level of the COP and 32.0±6.7° vs 40.5±7.1° at the level of the head; $P<0.05$, paired t-test).

Discussion

The results confirm data by Wolsley et al. (*1996a*) and Thurrell et al. (*2000*) showing that the direction of a visually evoked postural response tends to align with the plane of motion of the visual stimulus. Such realignment of retinal motion signals into body-centric co-ordinates by gaze direction, which may be mediated partly by proprioceptive input from the neck and the extraocular muscles (Roll et al. *1989*; Wolsley et al. *1996b*), is critical in making visuopostural control functionally useful in different directions of gaze. Also in agreement with a previous study (Kuno et al. *1999*) is the greater magnitude of visually evoked postural sway during vection than during object-motion perception. The new result emerging from the current study is the finding of a more accurate alignment of visually evoked postural sway during vection than during object-motion perception. Since the perception of self-motion presumably arises at a cortical level, the implication is that the cerebral cortex is one of the sites where retinal motion signals are reoriented by gaze direction to allow for the visual control of self-motion. Indeed, neurons responsive to both retinal-flow and eye position have been found in areas MSTd (Bremmer et al. *1997*) and 7a (Read and Siegel *1997*), and our findings concur with the authors' claim that such cortical neurons could provide a substrate for spatial representation during motion in the environment.

Acknowledgement. Support from the MRC, studentship number G78/5763, is gratefully acknowledged.

References

Bremmer F, Ilg UJ, Thiele A, Distler C, Hoffmann KP (1997) Eye position effects in monkey cortex. I. Visual and pursuit-related activity in extrastriate areas MT and MST. J Neurophysiol 77:944-961

Clément G, Jacquin T, Berthoz A (1983) Habituation of postural readjustments induced by motion of visual scenes. In: Igarashi, Black (eds) Vestibular and visual control on posture and locomotor equilibrium. Karger, Basel, pp 99-104

Dichgans JM, Held R, Young LR, Brandt T (1972) Moving visual scenes influence the apparent direction of gravity. Science 178:1217-1219

Kuno S, Kawakita T, Kawakami O, Miyake Y, Watanabe S (1999) Postural adjustment response to depth direction moving patterns produced by virtual reality graphics. Jpn J Physiol 49:417-424

Previc FH, Mullen TJ (1991) A comparison of the latencies of visually induced postural change and self-motion perception. Vestib Res 1:317-323

Read HL, Siegel RM (1997) Modulation of responses to optic flow in area 7a by retinotopic and oculomotor cues in monkey. Cereb Cortex 7:647-661

Roll JP, Vedel JP, Roll R (1989) Eye, head and skeletal muscle spindle feedback in the elaboration of body references. Prog Brain Res 80:113-123

Thurrell AEI, Bertholon P, Bronstein AM (2000) Reorientation of a visually evoked postural sway response during passive whole body rotation. Exp Brain Res 133:229-232

Wolsley CJ, Buckwell D, Sakellari V, Bronstein AM (1996a) The effect of eye/head deviation and visual conflict on visually evoked postural responses. Brain Res Bull 40:437-442

Wolsley CJ, Sakellari V, Bronstein AM (1996b) Reorientation of visually evoked postural responses by different eye-in-orbit and head-on-trunk angular positions. Exp Brain Res 111:283-288

Reduction of perceived visual speed during walking: Effect dependent upon stimulus similarity to the visual consequences of locomotion

Adrian E. I. Thurrell [1, 3] and Adar Pelah [2, 3]

a.thurrell@ion.ucl.ac.uk and ap114@cam.ac.uk

1) MRC Human Movement and Balance Unit, Institute of Neurology, National Hospital for Neurology and Neurosurgery, Queen Square, London, WC1N 3BG

2) Department of Electronics, University of York, Heslington, York, YO10 5DD United Kingdom

3) Department of Physiology, University of Cambridge, Downing Street, Cambridge, CB2 3EG

Introduction

Movement of the eyes has a profound effect on the images projected on the retinae. Thus in any visual determination of the position or movement of an object, account must be made of the movements of the eyes in space. We reported previously (Thurrell et al. 1998) that perceived optic-flow speed is reduced linearly with walking speed. As it is rare to walk on a moving surface, we postulated this mechanism would preserve world constancy during normal self-motion. Previous findings that this effect is tuned to motor activities similar to natural locomotion (walking) support this hypothesis (Pelah et al. 2001). The hypothesis that this effect is due to mechanisms of perceptual constancy would be bolstered if the effect were also strongest for optic-flow patterns similar to those experienced during natural locomotion (walking). We therefore tested the effect on five optic-flow patterns progressively less similar to natural locomotion: an Expanding Tunnel, a Horizontal Grating, a Vertical Grating, a rotating Cartwheel and a Flashing Tunnel.

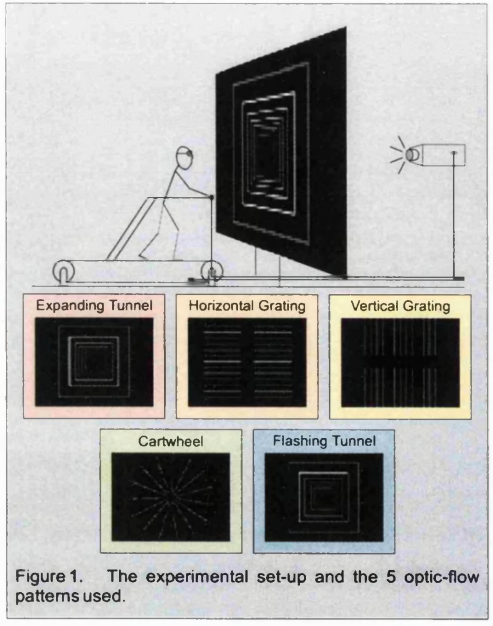

Figure 1. The experimental set-up and the 5 optic-flow patterns used.

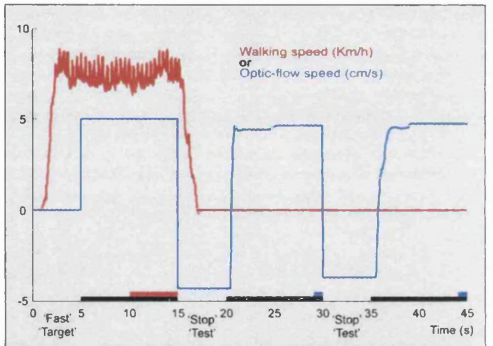

Figure 2. The time sequence of each trial. Instructions were displayed for 5s each (thin portion of time-scale) alternating with the tunnel (10s, thick portion). Mean settings during the last 1s of each test tunnel (blue bars) were plotted against the mean walking speed during the last 5s of the target tunnel (red bar), see Figure 3.

Methods

15 naïve subjects between the ages of 21 and 57 were tested. Walking was performed on an exercise treadmill powered by the locomotion of the subject whilst holding the hand-rails, allowing direct control of their walking velocity. Monocular goggles were worn also restricting peripheral vision. The visual stimulus consisted of a large screen directly in front of the treadmill on which optic-flow patterns were rear-projected. A fixation point was always present at eye level in the centre of the screen. The image resolution was 1280 x 1024 refreshed at 30Hz and fully anti-aliased to reduce motion artefacts.

The five conditions:

- The Expanding Tunnel consisted of 15 bright rectangles expanding and looming against the dark background.
- The Horizontal Grating consisted of 15 horizontal lines moving downward. Each line was masked in the central 20% of the screen to reduce cueing as each line passed the fixation point.
- The Vertical Grating was similar to the Horizontal Grating but rotated anti-clockwise (moving rightward).
- The Cartwheel consisted of 15 radial spokes rotating anti-clockwise around the fixation point. The innermost 10% of each line was masked for comparison to other stimuli.
- The Flashing Tunnel was similar to the Expanding Tunnel but stationary and with a sinusoidally varying luminosity.

Each trial was 45s long (see Figure 2) and repeated 18 times for each pattern:

- An instruction denoting a target presentation and for the walking speed, either 'stop', 'very slow', 'slow', 'normal', 'fast' or 'very fast' was displayed for 5s giving the subject time to reach this speed from rest before…
- A target pattern (moving at 5cm/s at the mid-hemifield position or flashing at 2Hz) was presented for 10s.
- The pattern was removed for 5s and replaced with instructions to stop walking and to adjust the optic-flow speed, using a potentiometer placed near their right hand, to the target speed perceived during walking.
- A test pattern whose velocity was controlled by the subject was presented for 10s.
- A second test pattern followed in an identical manner.

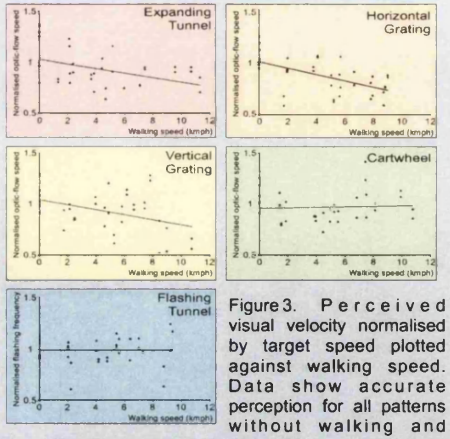

Figure 3. Perceived visual velocity normalised by target speed plotted against walking speed. Data show accurate perception for all patterns without walking and reduced perceived velocity at higher walking speeds for the Expanding Tunnel and both gratings for this subject, but not for the Cartwheel or the Flashing Tunnel. Slopes of linear best fits were 0.023 (Expanding Tunnel), -0.031 (Horizontal Grating), -0.025 (Vertical Grating), -0.0025 (Cartwheel) and 0.00039 (Flashing Tunnel).

Results

- 9 out of 15 subjects showed the previously reported effect of reduced perceived optic-flow speed during walking.
- The effects of walking speed on the perceived Expanding Tunnel and Horizontal Grating speeds were significantly different from zero ($P < 0.05$), but not from each other.
- The effect of walking speed on the perceived Vertical Grating and Cartwheel speeds and the perceived Flashing Tunnel frequency were not significantly different from zero.

Discussion

Confirming our previous findings, expanding optic-flow perception is influenced by walking. Downward linear motion was also significantly affected by walking speed. Linear sideways motion, rotation and flashing perception were not found to be significantly affected by walking speed. This trend may be explained by the similarity of the optic-flow pattern to that experienced during natural locomotion: Expansion as the 'gold standard' would be the most common optic-flow pattern generated by walking. Downward linear motion may correspond to motion of a ground surface while reducing conflict with an apparently non-moving sky. However, sideways linear motion, rotational motion and flashing do not normally result from walking. These results are therefore consistent with the hypothesis that non-visual signals of walking are used to disambiguate optic-flow perception.

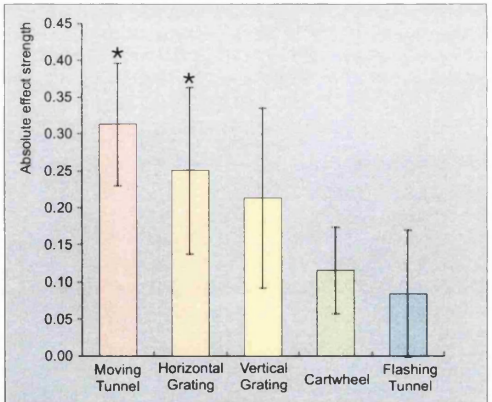

Figure 4. Intersubject mean (± s.e.m.) of absolute slopes for each optic-flow pattern showing the trend in effect magnitude from the Expanding Tunnel to the Flashing Tunnel. Asterisks denote values significantly different from zero.

References

A. Pelah, A.E.I. Thurrell and M.Berry (2001) Reduction of perceived visual speed during locomotion: Evidence for quadrupedal perceptual pathways in humans? Journal of Vision 1 (3), 307a.

A.E.I. Thurrell, A. Pelah and H.K. Distler (1998) The influence of non-visual signals of walking on the perceived speed of optic flow. Perception 27, 147.

Reduction of perceived visual speed during walking: Evidence against the involvement of attentional or vestibular mechanisms

A. Pelah [1, 2], A.E.I Thurrell [2, 3] and M. Berry [2]

ap114@cam.ac.uk, a.thurrell@ion.ucl.ac.uk and mb305@cam.ac.uk

1) Department of Electronics, University of York, Heslington, York, YO10 5DD, United Kingdom
2) Department of Physiology, University of Cambridge, Downing Street, Cambridge, CB2 3EG, United Kingdom
3) MRC Human Movement and Balance Unit, Institute of Neurology, National Hospital for Neurology and Neurosurgery, Queen Square, London, WC1N 3BG, United Kingdom

Introduction

We reported previously (Thurrell et al. 1998) that perceived expanding optic-flow speed is reduced linearly with increasing walking speed on an exercise treadmill. Any movement of the eyes, such as that resulting from locomotion, has a profound effect on the images projected on the retinae. Thus, in any visual determination of the position or movement of an object, account must be made of the movements of the eyes in space. As it is rare to walk on a moving surface, we postulated that signals of eye motion relative to the support surface, i.e. of walking speed, could preserve perceptual constancy during normal self-motion. However, two alternative mechanisms were proposed to explain the data: changes in attentional load have been shown to modulate visual motion aftereffects (Chaudhuri, 1990) suggesting that attentional changes during walking at different speeds may be responsible; and vestibular stimulation has been shown to increase visual motion detection thresholds and latencies (Probst et al. 1986) and may, therefore, extend to reductions in perceived visual motion speeds via the 'bobbing' motion of the head during walking.

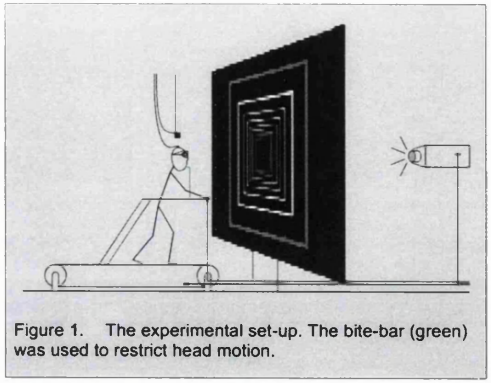

Figure 1. The experimental set-up. The bite-bar (green) was used to restrict head motion.

Methods

16 subjects between the ages of 19 and 24 were tested. Walking was performed on an exercise treadmill powered by the locomotion of the subject whilst holding the hand-rails, allowing subjects direct control of their walking velocity. Goggles were worn allowing vision only from the right eye and restricting peripheral vision. The visual stimulus consisted of a large screen (1.9m x 1.2m) directly in front of the treadmill on which was rear-projected a moveable tunnel composed of 15 bright squares on a dark background. A fixation point was also present at eye level in the center of the tunnel. The image resolution was 1024 x 768 refreshed at 35Hz, fully anti-aliased and tunnel components faded in and out of the background luminosity to reduce motion artefacts. Head position was monitored in all 6 degrees of freedom.

The order of the experiments was counterbalanced across the subjects, with 18 trials for each condition. Subjects adjusted the test tunnel velocity using a potentiometer placed near their right hand.

Each trial was 45s long (see Figure 2):

- An instruction denoting a target presentation and for the motor activity speed, either 'stop', 'very slow', 'slow', 'normal', 'fast' or 'very fast' was displayed for 5s giving the subject time to reach this speed.
- A target tunnel velocity (always expanding at 5cm/s at the mid-hemifield position) was presented for 10s.
- The tunnel was removed for 5s and replaced with instructions to stop walking and adjust the tunnel speed. The tunnel speed was to be adjusted to that perceived during walking.
- A test tunnel whose velocity was controlled by the subject was presented for 10s.
- A second test tunnel followed in an identical manner.

The three different conditions were:

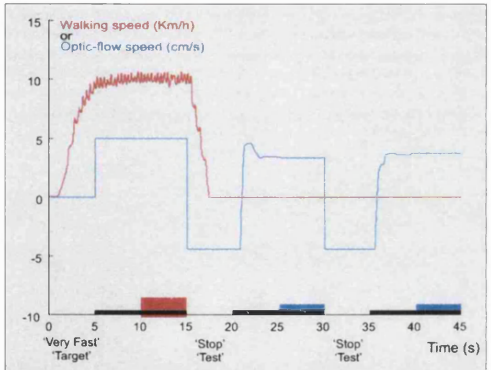

Figure 2. The time sequence of each trial. Instructions were displayed for 5s each (thin portion of time-scale) alternating with the tunnel (10s, thick portion). Mean settings during the last 5s of each test tunnel (blue bars) were plotted against the mean walking speed during the last 5s of the target tunnel (red bar), see Figure 3.

- The control condition as above.
- The attention condition, in which an auditory-verbal summing task of 5 single-digit numbers was presented concurrently with the target presentation.
- The restricted head motion condition, in which subjects' head positions were fixed using a bite-bar rigidly attached to the treadmill.

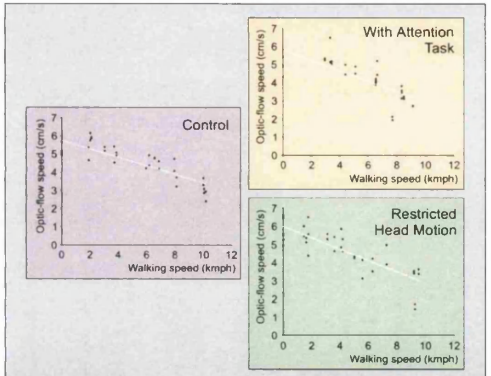

Figure 3. Perceived visual velocity plotted against walking speed for the three conditions. Data show accurate perception without walking and reduced perceived velocity at higher walking speeds for all conditions. Slopes of linear best fits for this subject were -0.23 (control), -0.29 (with concurrent attentional task), -0.27 (restricted head motion).

Results

- 12 out of 16 subjects showed the previously reported effect of reduced perceived visual velocity due to walking in the control condition. The slope of line of best fit was taken as the effect strength (see Figure 3) for each condition. Remaining subjects produced anomalous results possibly due to misinterpretation of instructions or lack of immersion in the environment and were discarded.
- In all conditions, the mean strength of the influence of walking speed on expanding optic-flow perception was significantly different from zero ($P < 0.05$).
- In the attention condition, the average effect strength was lower (slope of 0.35 vs. 0.42), though not significantly so (Paired t-test, 2 tailed, n = 10), than during the Control condition.
- In the restricted head motion condition, the average effect strength was also lower than during the control condition (slope of 0.23 vs. 0.44), though this was not significant ($P < 0.05$, paired 2 tailed t-test, n = 6). During the restricted head motion condition, linear head motion was reduced by a factor of ~15 laterally and ~5 otherwise, whilst rotational motion was reduced by a factor of ~10 for yaw and roll, though pitch motion remained unchanged.

Discussion

Confirming previous findings, visual motion perception is influenced by walking in approximately three-quarters of subjects. Neither increasing the concurrent attentional load nor reducing the vestibular stimulation due to walking, significantly alters the influence of walking speed on expanding optic-flow perception. We suggest, therefore, that these findings support the hypothesis that this reduction in perceived expanding optic-flow speed functions to maintain

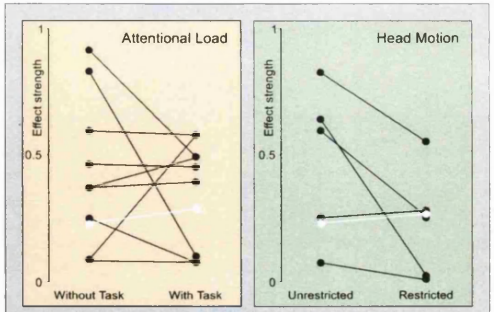

Figure 4. Comparisons of effect strength with and without the concurrent attentional task (orange) and between restricted and unrestricted head motion (green) for each subject. White values denote the data shown in Figure 3.

References

Chaudhuri A (1990) Modulation of the motion aftereffect by selective attention. Nature 344: 60-62

Probst T, Brandt T, Degner D (1986) Object-motion detection affected by concurrent self-motion perception: Psychophysics of a new phenomenon. Behav.Brain Res. 22: 1-11

Thurrell, A. E. I, Pelah, A, and Distler, H. K. The influence of non-visual signals of walking on the perceived speed of optic flow. Perception 27, 147. 1998.

Exp Brain Res (2003) 150:325–331
DOI 10.1007/s00221-003-1422-8

RESEARCH ARTICLE

A. Thurrell · K. Jáuregui-Renaud · M. A. Gresty · A. M. Bronstein

Vestibular influence on the cardiorespiratory responses to whole-body oscillation after standing

Received: 26 September 2002 / Accepted: 22 January 2003 / Published online: 11 April 2003

Abstract We assessed the influence of vestibular stimulation by whole-body oscillation in the yaw plane on the cardiorespiratory responses after a change of posture from sitting to standing. Eighteen healthy subjects (21–70 years old) and six patients with bilateral vestibular loss (46–59 years old) were tested. For comparison, a subgroup, age matched to the patients, was created from the healthy group. After a 10-min rest, subjects who were sitting, back unsupported, stood on a platform affording en bloc head and body support. The platform was either static or oscillated at 0.1 Hz and 0.5 Hz (20° amplitude) for 2 min. Presentation of the three conditions was counterbalanced. Respiration, ECG, blood pressure and head position were recorded. During oscillation at 0.5 Hz, the respiratory responses were different between groups; healthy subjects showed a significant increase of the respiratory frequency (1.75±2.1 breaths/min), which was not observed in the patients (0.16±0.7 breaths/min) ($p<0.05$, ANOVA). Absolute changes of heart rate and blood pressure were similar for the three conditions in all the subjects. However, healthy subjects showed a decrease of power spectrum density of the high-frequency ('respiratory') component of heart rate variability on standing during all three conditions. This response was variable among the patients and the age-matched group. The study shows that semicircular canal activation influences the respiratory rhythm during movements in the yaw plane in standing subjects. In addition, we observed that changes of the respiratory influence on heart rate variability during orthostatic stress are not affected by yaw oscillation or chronic vestibular loss, but may be affected by factors related to age.

Keywords Vestibular influence · Cardiorespiratory responses · Whole-body oscillation · Bilateral vestibular loss · Respiratory frequency · Power spectrum density

A. Thurrell · M. A. Gresty · A. M. Bronstein
Academic Department of Neuro-otology,
Division of Neurosciences and Psychological Medicine,
Imperial College,
London, UK

K. Jáuregui-Renaud (✉)
Unidad de Investigación Medica,
HG Centro Médico Nacional 'La Raza', IMSS,
Av Vallejo y Jacarandas, CP02990 Colonia La Raza, Mexico
e-mail: kjauren@data.net.mx
Tel.: +52-55-57821976
Fax: +52-55-57821976

Introduction

The assumption of upright posture causes a displacement of blood pressure towards the lower body and provokes a cascade of haemodynamic and autonomic adjustments (Cook et al. 1999). Animal studies and clinical observations indicate that the vestibular system participates in the autonomic responses to postural changes (Doba and Reis 1974; Yates et al. 1999; Jáuregui-Renaud et al. 2001a). Although human data also show a similar trend, studies on vestibuloautonomic control in the normal upright position are scarce (Jáuregui-Renaud et al. 2001a).

Reorientations of the body also provoke respiratory changes. When a subject stands up, the end-expiratory lung volume is set and maintained below the neutral position of the respiratory system by abdominal contraction (De Troyer 1983). Furthermore, not only do challenges to posture challenge ventilation, but, conversely, coordinated contraction of the diaphragm may contribute to control of the trunk during postural reorientation (Gandevia et al. 2002). A component of the alterations in respiratory muscle activity during movement and postural changes has been shown to result from activation of vestibular receptors (Yates et al. 2002). The properties of the vestibular signal are ideal for both triggering the onset of such respiratory changes, should they be pre-programmed, or for a continuous mode of control for continuous reorientation. Thus, a vestibulorespiratory drive may contribute to coupling respiration with movements of the whole body in the upright standing position.

Some evidence that semicircular canal activation can modulate breathing rate in humans has been recently

reported. Dynamic head movements at 15 and 30 cycles/min (pitch, roll and yaw) can modify respiratory frequency in healthy subjects (Monahan et al. 2001). Both vertical semicircular canal activation by a rotational 'stopping' stimulus (Jáuregui-Renaud et al. 2001b), and horizontal canal stimulation by caloric irrigation of the external ear canal (Jáuregui-Renaud et al. 2000), can change the respiratory pattern of healthy subjects, whereas patients with vestibular loss are unresponsive. However, studies examining a possible role of the vestibular system in respiration control in humans actively reaching the normal upright position are lacking.

In this study we investigate whether patients without vestibular function show any difference in cardiorespiratory function, with respect to healthy subjects, during rotation in the upright position. In particular, we assess the influence of whole-body oscillation in the yaw plane (0.1 Hz and 0.5 Hz) after an active change of posture, from sitting to standing. Putative differences present between patients and age-matched healthy subjects could indicate a role for the vestibular receptors in cardiovascular and respiratory control.

Materials and methods

Subjects

Eighteen healthy subjects, aged 40±17 years (mean ± SD) and body mass index 23.9±3.2 (seven females), and six patients with bilateral loss of vestibular function, aged 54±5 years and body mass index 25.6±1.75 (two females), gave their informed consent to participate in the study according to the guidelines of the local ethics committee. For comparison with the patients, an age-matched subgroup was created using six of the healthy subjects, aged 53±13 years and body mass index 24.5±4.6 (two females). An additional healthy subject was excluded from the study because we observed a sudden decrease of systolic blood pressure on standing (>30 mmHg). Neither normal subjects nor patients had a history of CNS or cardiovascular disease, nor were they receiving any medication.

In all patients the vestibular loss was idiopathic (Rinne et al. 1998) and was demonstrated by the absence of nystagmic responses to both caloric irrigation at 30°C and 44°C and horizontal rotation in the dark using velocity steps of 80°/s.

Procedures

Subjects were investigated after fasting for at least 4 h and abstaining from caffeine and alcohol for at least 12 h. They were required to stand on a platform from back-unsupported sitting, after 10 min rest. Once standing they placed their heads and arms on a framework attached to a platform, which was able to rotate about a vertical axis passing through their heads (Fig. 1) so that subject, frame and platform would rotate en bloc. The platform was either static or oscillated via a motor drive at 0.1 Hz (3.9°/s^2 peak acceleration) and 0.5 Hz (98.7°/s^2 peak acceleration), 20° peak-to-peak amplitude. These three conditions were dispensed in a counterbalanced order.

Before the first trial, all the subjects practised standing on the platform. During the study, the time required by the subjects to mount the framework was 9±4 s for the healthy group, 11±5 s for the age-matched group and 14±6 s for the patients. During all three conditions, subjects were instructed to keep their eyes open, looking at a blank white screen. The screen was earth-fixed and hemicylindrical with a radius of 50 cm originating on the axis of rotation and vertically centred at head height (Fig. 1).

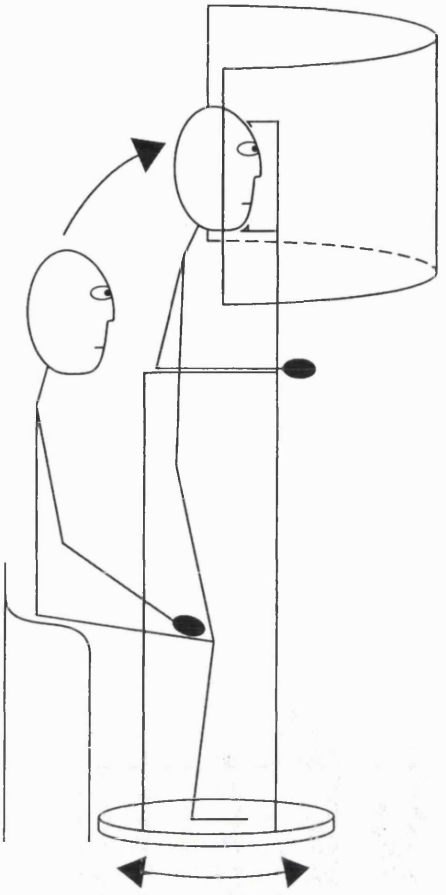

Fig. 1 Subjects were required to stand up on the rotating platform and rest their chin, forehead and arms on a frame attached to the platform. The frame was surrounded by an earth-fixed white surrounding screen. Patients kept their feet in the same predetermined position, by the rotational axis, whilst sitting and standing. As soon as subjects stood up, the platform could remain stationary or began to oscillate at 0.1 or 0.5 Hz

Recordings

Two minutes before (i.e. whilst still sitting) and 2 min after standing, recordings were taken of respiration as movements of the thorax-abdomen (Respitrace, NiMS), blood pressure in the finger with automatic, hydrostatic height-correction (Portapres, TNO), the electrocardiogram using three lead surface electrodes (Grass Instruments) and head position (Fastrack, Polhemus). Signals were acquired at a 500-Hz sampling rate. The first 20 s, during standing up, were discarded according to the presence of movement artefact.

Signal processing and data analysis

Respiration signals from abdomen and thorax were linearly added to make a composite respiration signal filtered with a zero-lag eighth-order FIR (passband 0.1–1.0 Hz). Similarly the ECG signal was zero-lag eighth-order FIR bandpass filtered (passband 1–37.5 Hz). After visual inspection of the ECG, R waves were identified as local maxima of the ECG trace, using linear interpolation to replace ectopic beats. Instantaneous heart rate, diastolic and systolic blood pressures were found for each beat.

Mean blood pressure was calculated as 1/3 systolic + 2/3 diastolic blood pressure.

All signals were resampled at 10 Hz using cubic spline interpolation. Heart rate and blood pressure signals were then zero-lag highpass filtered using a fifth-order IIR filter with a cut-off frequency of 0.05 Hz. Analysis was performed on the 2-min period preceding standing and 2 min shortly afterward, allowing time for movement transients to decay. Autoregressive spectra of heart rate and blood pressure were calculated using the modified covariance method with model order selected by the 'minimum description length' criterion (Matlab, The Mathworks). Heart rate and blood pressure power spectra were summed and divided into two bands: a 'low-frequency' band between 0.04 and 0.15 Hz and a 'high-frequency' band from 0.15 to 0.5 Hz. The power spectral density measurements were natural log transformed.

Analysis

Responses following standing were computed in terms of differences from the sitting position. Statistical analysis was performed using Friedman's ANOVA, the Kruskall-Wallis test and Spearman's correlation. Differences were considered significant when two-tailed p values were less than 0.05.

Results

Respiration rate

Sitting position

Whilst in the sitting position, respiratory rate was similar for both healthy subjects and patients, over the three conditions, and did not show significant differences between the groups (Table 1).

Standing position

During the static condition and oscillation at 0.1 Hz, to stand up induced variable changes in healthy subjects and patients (Fig. 2). However, during oscillation at 0.5 Hz, the healthy subjects showed an increase in respiratory rate (Fig. 2), which was not observed in the patients (Figs. 2, 3). This difference between groups was still evident when patients were compared with the age-matched group ($p<0.05$, Kruskall-Wallis).

Heart rate and blood pressure

In all subjects, measurements of heart rate and blood pressure while subjects were sitting were similar during the three conditions (Table 1). Comparison of responses to standing up did not show significant differences between conditions or groups.

In all subjects, frequency domain analysis of heart rate variability while sitting and standing showed no significant differences between conditions (Table 2). In the two positions, the power spectral density measurements of the low- and high-frequency components of heart rate variability were linearly related to the age of the subjects; Spearman's $r=0.6$ for the two components ($p<0.05$).

Table 1 Absolute values of respiration rate, heart rate and blood pressure, 2 min while sitting and 2 min after standing, of 18 healthy subjects and 6 patients with bilateral vestibular loss. At 0.1 Hz the blood pressure measurements are only from five patients (*SD* standard deviation, *bpm* beats per minute)

Condition	Healthy subjects (n=18)		Age-matched healthy subjects (n=6)		Patients (n=6)	
	Sitting Mean ± SD	Standing Mean ± SD	Sitting Mean ± SD	Standing Mean ± SD	Sitting Mean ± SD	Standing Mean ± SD
Respiration rate						
Static	16.7±3.8	15.6±3.4	17.7±4.9	15.9±4.4	14.1±3.5	15.6±2.6
Rotation at 0.1 Hz	16.3±3.7	15.6±3.1	16.3±5.0	16.5±4.6	15.1±2.3	16.1±1.8
Rotation at 0.5 Hz	16.1±3.7	17.8±3.6	16.4±5.1	18.8±5.1	15.8±2.5	16.0±2.8
Heart Rate (bpm)						
Static	68±8	74±12	64±5	68±9	66±10	73±11
Rotation at 0.1 Hz	70±8	75±13	63±6	69±12	70±12	73±11
Rotation at 0.5 Hz	68±9	75±13	63±4	68±9	68±9	73±9
Systolic BP (mmHg)						
Static	107±14	97±13	107±12	99±10	116±22	110±14
Rotation at 0.1 Hz	107±14	99±14	104±11	102±4	115±15	106±17
Rotation at 0.5 Hz	107±16	100±16	114±10	104±8	116±15	108±15
Diastolic BP (mmHg)						
Static	60±12	58±12	57±13	56±14	68±17	67±12
Rotation at 0.1 Hz	60±13	59±12	59±13	58±13	69±14	66±15
Rotation at 0.5 Hz	60±13	59±13	61±11	59±13	69±13	66±12
Mean BP (mmHg)						
Static	75±12	71±11	74±12	70±12	86±20	83±14
Rotation at 0.1 Hz	75±13	72±12	76±12	72±11	85±16	80±18
Rotation at 0.5 Hz	76±13	73±13	79±10	74±11	85±15	81±15

Table 2 Power spectrum density of heart rate variability (/ms^2/Hz), absolute values, while sitting and standing of 18 healthy subjects and 6 patients with bilateral vestibular loss

Condition	Healthy subjects (n=18)		Age-matched healthy subjects (n=6)		Patients (n=6)	
	Sitting Median, 25–75 percentiles	Standing Median, 25–75 percentiles	Sitting Median, 25–75 percentiles	Standing Median, 25–75 percentiles	Sitting Median, 25–75 percentiles	Standing Median, 25–75 percentiles
Static						
Low freq.	2095	3511	969	1089	2193	2082
(0.04–0.15 Hz)	1527–5929	1253–13,749	457–1485	816–3082	1396–2540	1000–4794
High freq.	1423	1382	422	451	1029	1576
(0.15–0.5 Hz)	557–4550	464–1958[a]	352–793	356–1054	464–1609	687–1699
Total	5317	5269	1583	1879	3186	3620
(0.04–0.5 Hz)	2044–9654	1827–16,597	935–1904	962–4529	1986–4808	1746–6472
Rotation at 0.1 Hz						
Low freq.	2476	2965	1059	1000	2184	1770
(0.04–0.15 Hz)	1284–8015	899–9083	624–1291	692–1995	825–3146	834–4802
High freq.	1267	696	526	419	1112	1362
(0.15–0.5 Hz)	646–3300	451–3245[a]	335–720	301–468	495–1960	589–2802
Total	5183	3685	1395	1533	3170	3576
(0.04–0.5 Hz)	1713–14,371	1397–15,076	1093–1908	1057–2552	1889–6173	2181–6343
Rotation at 0.5 Hz						
Low freq.	3552	3012	882	1639	2083	2646
(0.04–0.15 Hz)	1315–4199	1170–7500	298–3286	685–3392	863–2953	1109–3485
High freq.	886	1096	541	423	1194	980
(0.15–0.5 Hz)	561–3796	387–1668[a]	527–596	293–601	593–1650	626–1519
Total	4786	4103	1332	2140	3276	3863
(0.04–0.5 Hz)	1878–10,740	1744–10,331	799–4014	1208–3685	2407–3597	2196–4786

[a] Significant reduction from sitting, Friedman's ANOVA (p<0.05)

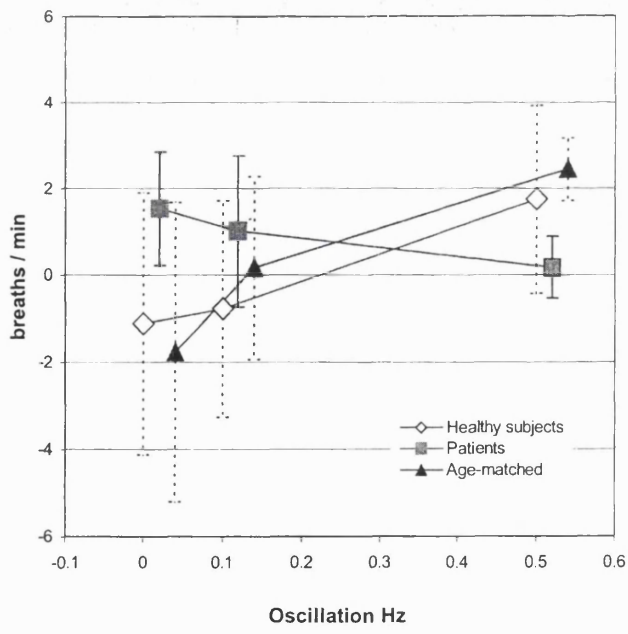

Fig. 2 Respiratory rate differences between standing and sitting of healthy subjects and patients with loss of vestibular function during the three conditions of platform oscillation: 0 Hz (static), 0.1 Hz (low frequency) and 0.5 Hz (high frequency)

In the group of 18 healthy subjects, the power spectral density of the high-frequency (respiratory) component was consistently decreased after standing during the three conditions (Fig. 4) (p<0.05, Friedman's ANOVA), but was variable in patients. Although there was no significant linear correlation between the age of the subjects and the response to standing, the difference between healthy subjects and patients was no longer apparent when patients were compared with the age-matched group (Table 2). In all three conditions, after standing up, the amplitude of the high-frequency component of heart rate variability of healthy subjects and patients was consistently depressed relative to the amplitude of the low-frequency component, but there were not consistent changes of the low-frequency component on standing (Fig. 4).

Discussion

During daily activities, sit-to-stand movements are usually combined with other movements of the body. Although the position of the head whilst moving may be variable, angular acceleration in the horizontal plane is a frequent component of motion. In this study we observed an influence of whole-body horizontal oscillation on the respiratory pattern of healthy subjects after standing. Although this effect was small, it was not present in patients with bilateral vestibular loss. The change of the respiratory rhythm could be described as

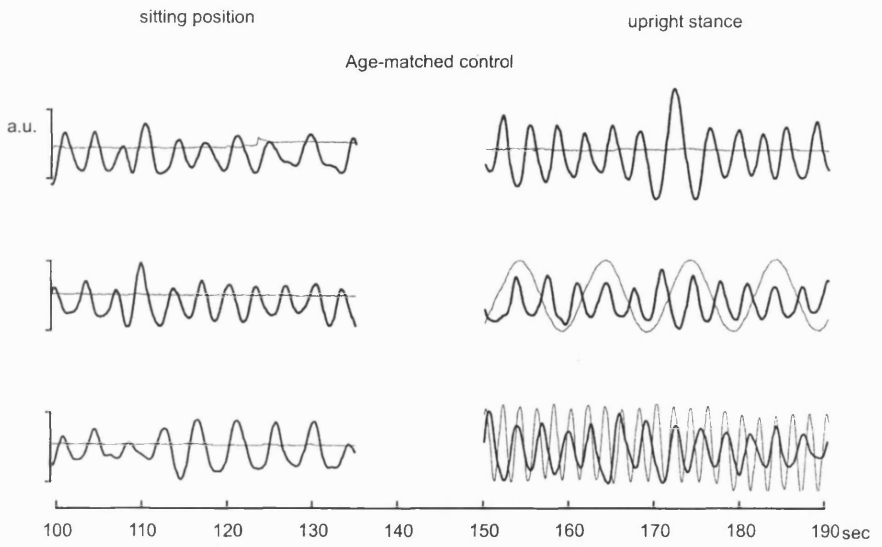

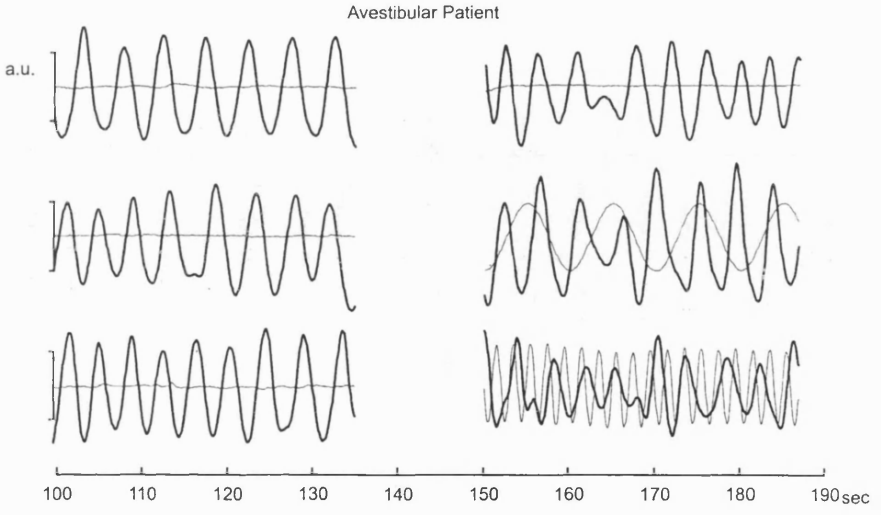

Fig. 3 Respiratory movements (*thick line*) and platform movements (*thin line*) of a patient with vestibular loss and an age-matched healthy subject, during the three platform conditions: static (0 Hz), 0.1 Hz and 0.5 Hz (*a.u.* arbitrary units)

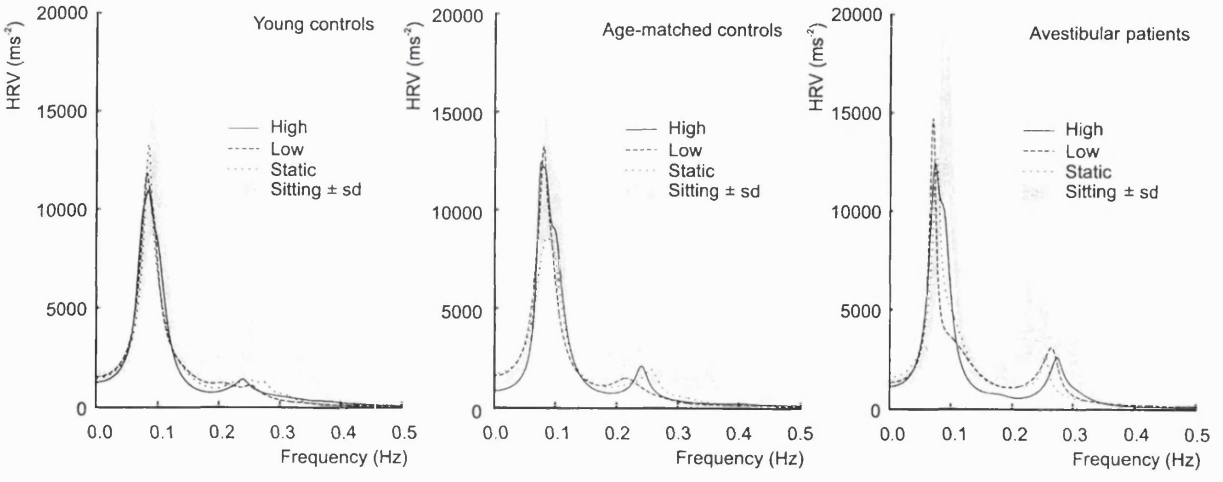

Fig. 4 Heart rate spectra of healthy subjects and patients with loss of vestibular function: while sitting during the three conditions (mean ± SD), and during static, 0.1-Hz and 0.5-Hz conditions

(appeared to be) entrainment of breathing by oscillation. The implication is that the vestibular system may be partly responsible for the entrainment of respiratory muscles with the underlying pattern of body motion.

Central neural modulation initiates the generation of the breathing rhythm whereas peripheral pulmonary stretch receptors delineate the timing of the inspiratory phase of each tidal breath. However, interactions between respiratory and motion patterns may lead to changes of the respiratory rhythm, coupling it with the ongoing movement (entrainment). Entrainment of respiration has been observed during different protocols of exercise (Persegol et al. 1991; Bonsignore et al. 1998) and when rocking a newborn baby (Sammon and Darnall 1994). Rocking a newborn provides natural vestibular stimulation which may underlie the respiratory entraining (Sammon and Darnall 1994).

Although oscillation at 0.5 Hz induced an increase of the respiratory rate, the response to oscillation at 0.1 Hz was variable among subjects. The variable response to low-frequency oscillation could be attributed to several factors: entrainment of respiration by the frequency of the movement evolves and is not present at all frequencies imposed (Persegol et al. 1991). Oscillation at 0.5 Hz is a stronger stimulus to the semicircular canals than oscillation at 0.1 Hz; in this study, the respiratory rate of the subjects while sitting was >0.2 Hz, so entrainment of a lower respiratory rate was not likely to improve the efficiency of ventilation.

Oscillation after standing up induced respiratory changes that were not related to changes of the heart rate and blood pressure responses. The independence of the respiratory findings from any cardiovascular parameter could relate to the dynamic changes in cardiac control, which are necessary to adapt to an orthostatic position. On standing, the high-frequency component of the heart rate spectra decreased significantly and was always depressed relative to the low-frequency component. This result agrees with previous whole-body-tilt studies showing that the respiratory rate influence on heart rate variability decreases at high head-up angles (Cook et al. 1999) and on standing (Sarno et al. 2000). Our results support the view that, during orthostatic stress, the increase in sympathetic stimulation may overwhelm respiratory influences and vagal stimulation decreases (Cook et al. 1999).

The magnitude by which the high-frequency component of heart rate variability decreased on standing was consistently observed in younger subjects but was more variable among older subjects. This suggests that age-related factors may influence the respiratory modulation of the vascular response to orthostatic stress but further studies are needed to test this hypothesis.

Respiration also affects the cardiovascular and autonomic systems via changes in lung volume (Saul 1998; Seals et al. 1990) and CO_2 (Van de Borne et al. 2001). An increase in CO_2 during standing, due to metabolic demands, may influence respiratory patterns via chemoreflexes (Van den Aardweg 2002) and sympathetic activation (Somers et al. 1989). Unfortunately, during this study we did not measure or control tidal volume or gas exchange and we cannot exclude the possibility that these factors could have influenced the response. However, such mechanisms would affect respiratory responses in all conditions similarly and therefore would not account for the differences we observed between normal subjects and patients.

In conclusion, this study shows that semicircular canal activation influences respiratory rhythm during movements in the yaw plane in standing human subjects, particularly at higher frequencies/accelerations of motion. The results also show that changes of the respiratory influence on heart rate variability during orthostatic stress are not affected by yaw oscillation or chronic vestibular loss, but may be affected by factors related to age.

Acknowledgements K.J.R. was supported by grants from the Instituto Mexicano del Seguro Social and Fundación Aventis.

References

Bonsignore MR, Morici G, Abate P, Romano S, Bonsignore G (1998) Ventilation and entrainment of breathing during cycling and running in triathletes. Med Sci Sports Exerc 30:239–245

Cook WH, Hoag JB, Crossman AA, Kuusela TA, Tahvanainen KUO, Eckberg DL (1999) Human responses to upright tilt: a window on central autonomic integration. J Physiol 517:617–628

De Troyer A (1983) Mechanical role of abdominal muscles in relation to posture. Resp Physiol 53:341–353

Doba N, Reis DJ (1974) Role of the cerebellum and vestibular apparatus in regulation of orthostatic reflexes in the cat. Circ Res 34:9–18

Gandevia SC, Butler JE, Hodges PW, Taylor JL (2002) Balancing acts: respiratory sensations, motor control and human posture. Clin Exp Pharmacol Physiol 29:118–121

Jáuregui-Renaud K, Yarrow K, Oliver R, Gresty M, Bronstein A (2000) Effects of caloric stimulation on heart rate and blood pressure variability and respiratory frequency. Brain Res Bull 53:17–23

Jáuregui-Renaud K, Hermosillo GA, Gómez A, Marquez M, Bronstein AM (2001a) Autonomic function during vertigo due to acute unilateral vestibular failure. J Neurol Sci 187 Suppl 1:S133

Jáuregui-Renaud K, Gresty M, Reynolds R, Bronstein A (2001b) Respiratory responses of human beings to rotation in the yaw and pitch planes. Neurosci Lett 298:17–20

Monahan KD, Sharpe MK, Drury D, Ertl AC, Ray CA (2002) Influence of vestibular activation on respiration in humans. Am J Physiol Regul Integr Comp Physiol 282:R689–R694

Persegol L, Jordan M, Viala D (1991) Evidence for the entrainment of breathing by locomotor pattern in human. J Physiol (Paris) 85:38–43

Rinne T, Bronstein AM, Rudge P, Gresty MA, Luxon LM (1998) Bilateral loss of vestibular function: clinical findings in 53 patients. J Neurol 245:314–321

Sammon MP, Darnall RA (1994) Entrainment of respiration to rocking in premature infants: coherence analysis. J Appl Physiol 77:1548–1554

Sarno AJ, Pearson MA, Nabors-Oberg R, Sollers JJ 3rd, Thayer JF (2000) Autonomic changes during orthostatis: a time-frequency analysis. Biomed Sci Instrum 36:251–256

Saul JP (1998) Respiration and blood pressure variability, mechanical and autonomic influences. Fundam Clin Pharmacol 12 (Suppl 1):17s–22s

Appendix B: Computer Programs

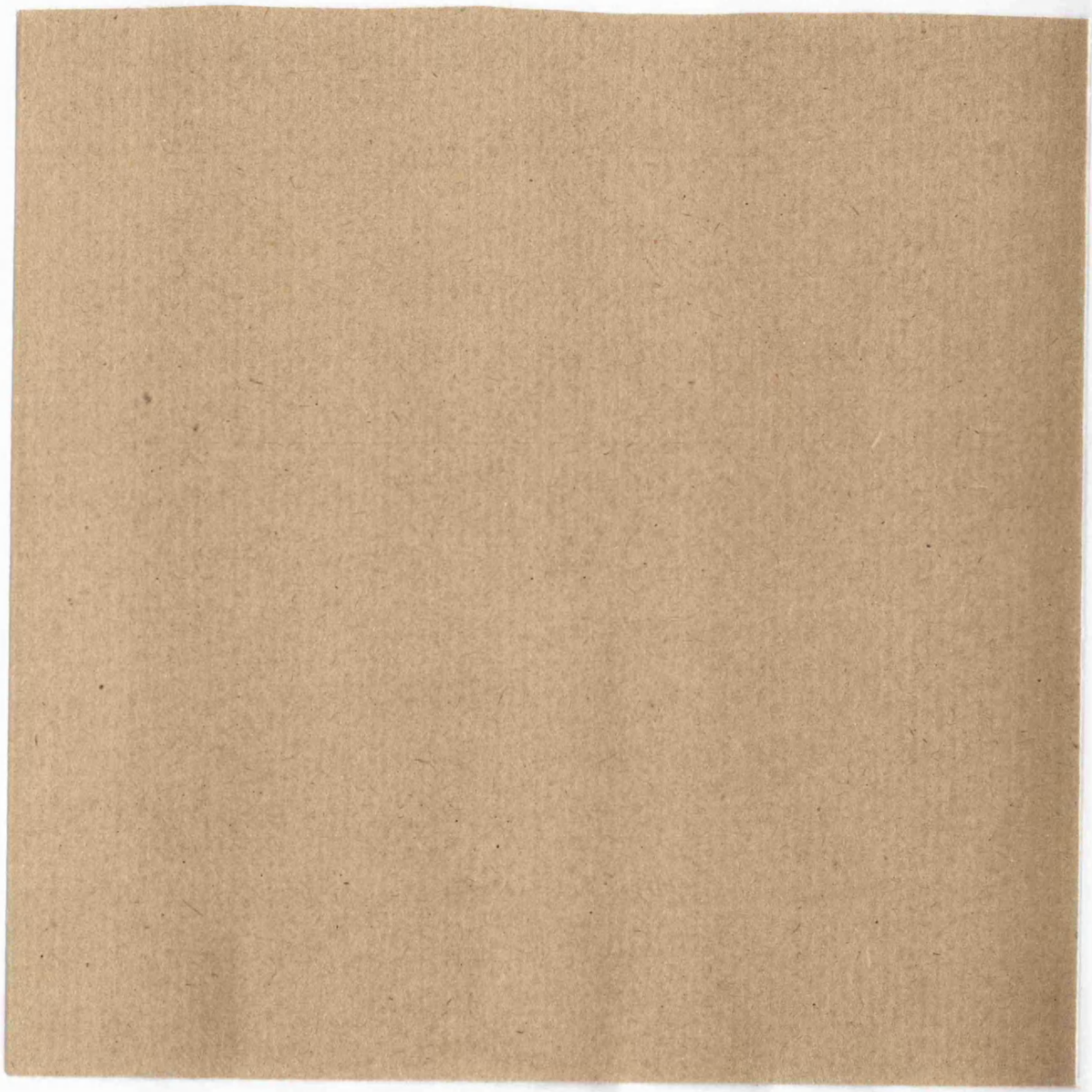

Appendix C: Raw Data

Reorientation of Visually Induced Sway During Whole Body Passive Rotation

For explanation of plots see Figure 11. Only COP data are produced here. The slope of the line of best-fit was significantly non-zero for all individual plots (both onset and offset).

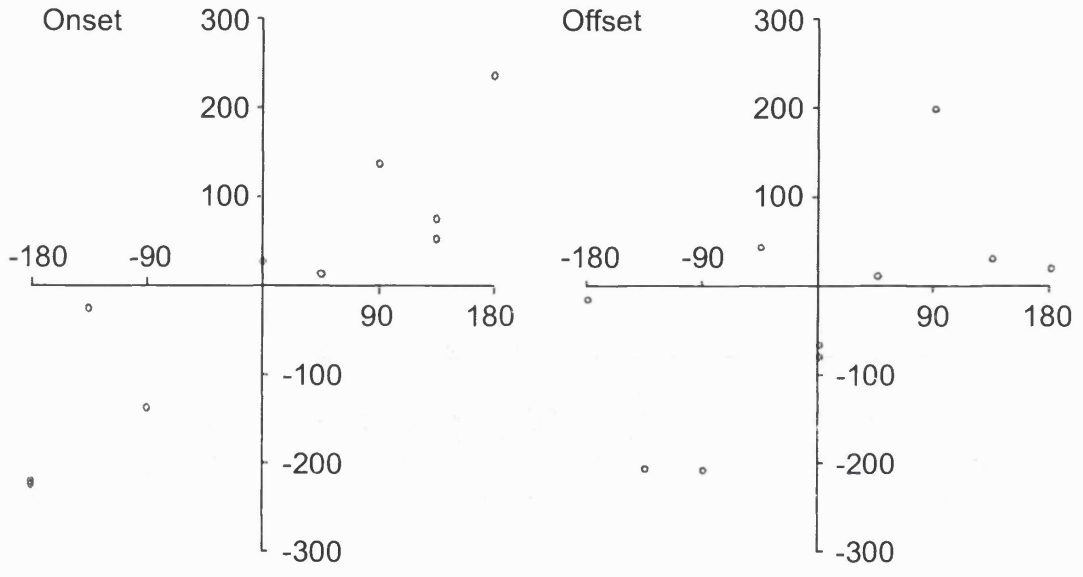

Subject AT, onset gain 0.89, offset gain 0.47

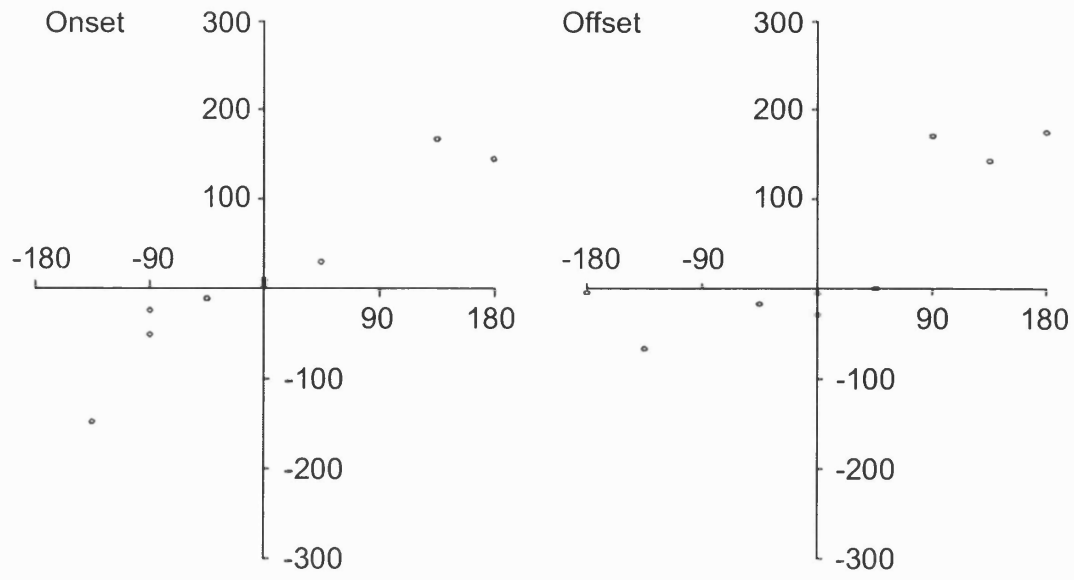

Subject AM, onset gain 0.87, offset gain 0.65

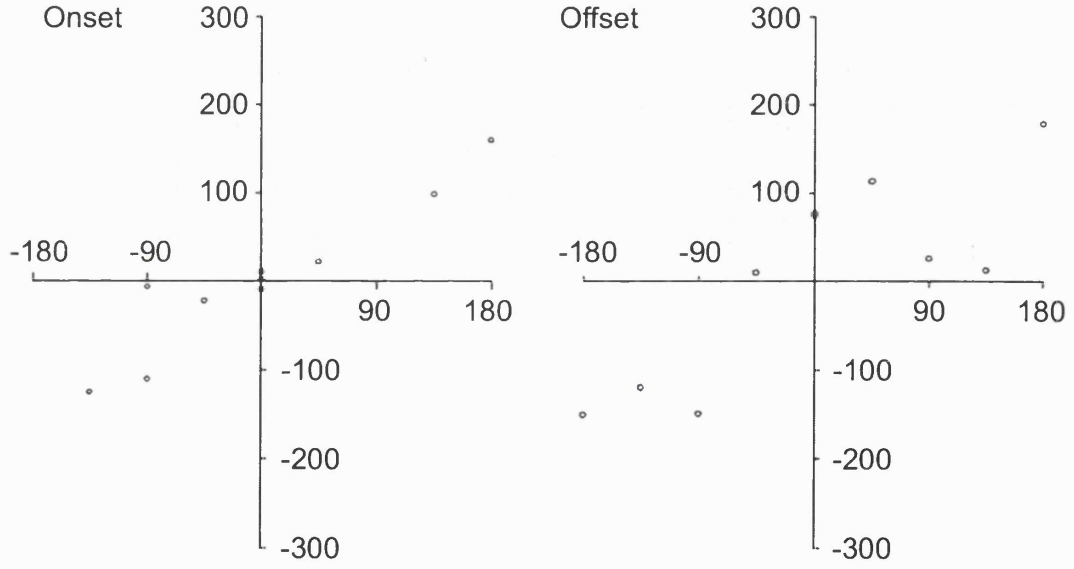

Subject HB, onset gain 0.80, offset gain 0.81

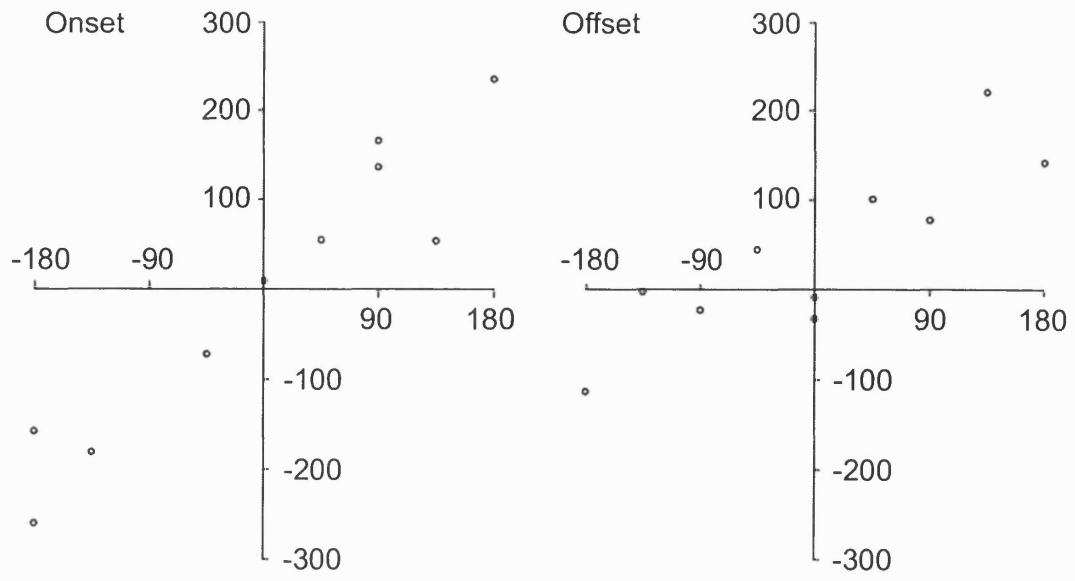

Subject JB, onset gain 1.18, offset gain 0.72

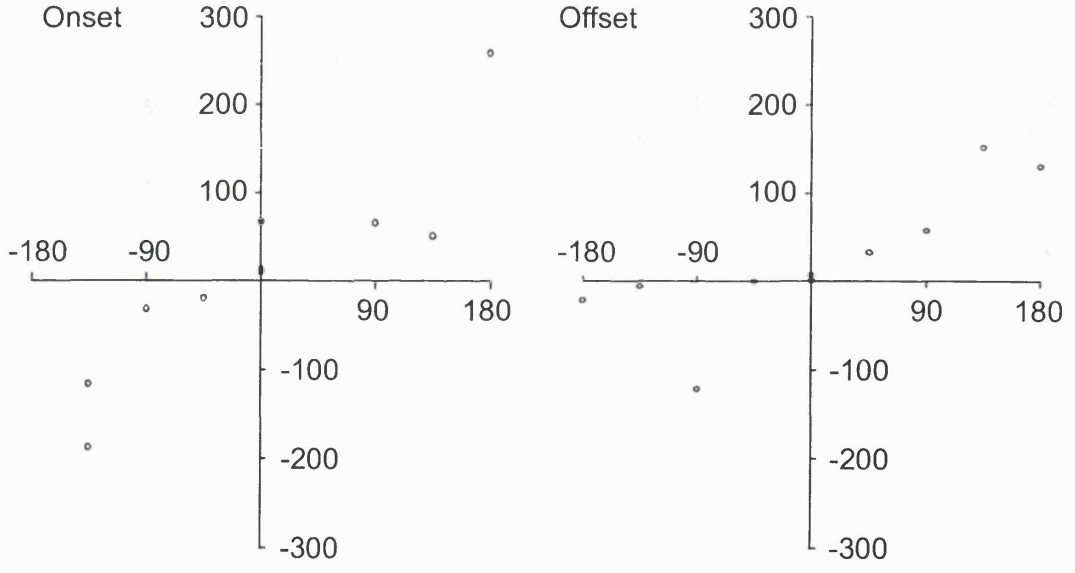

Subject JR, onset gain 0.99, offset gain 0.54

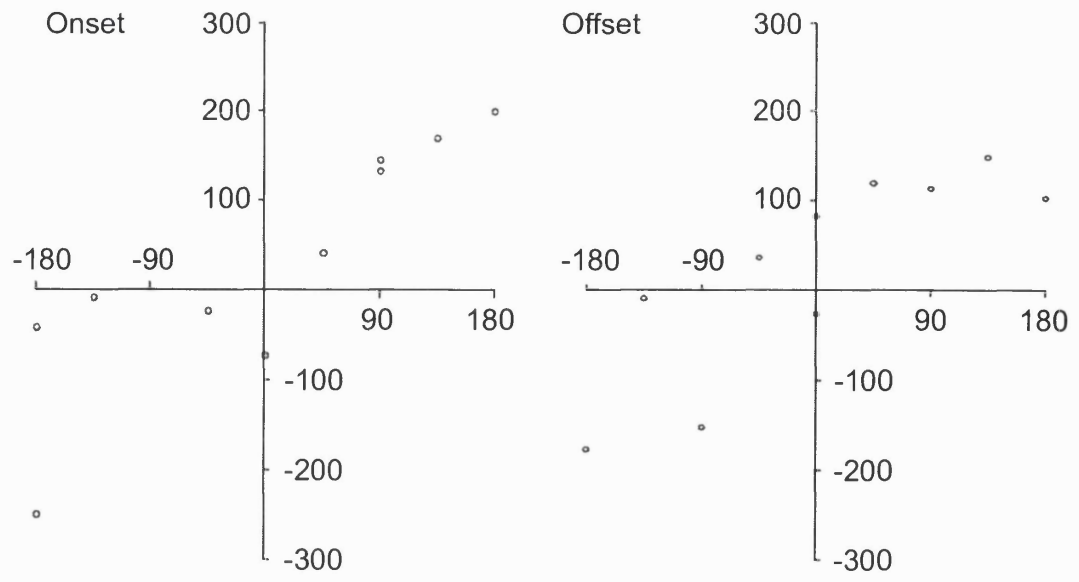

Subject KT, onset gain 0.91, offset gain 0.82

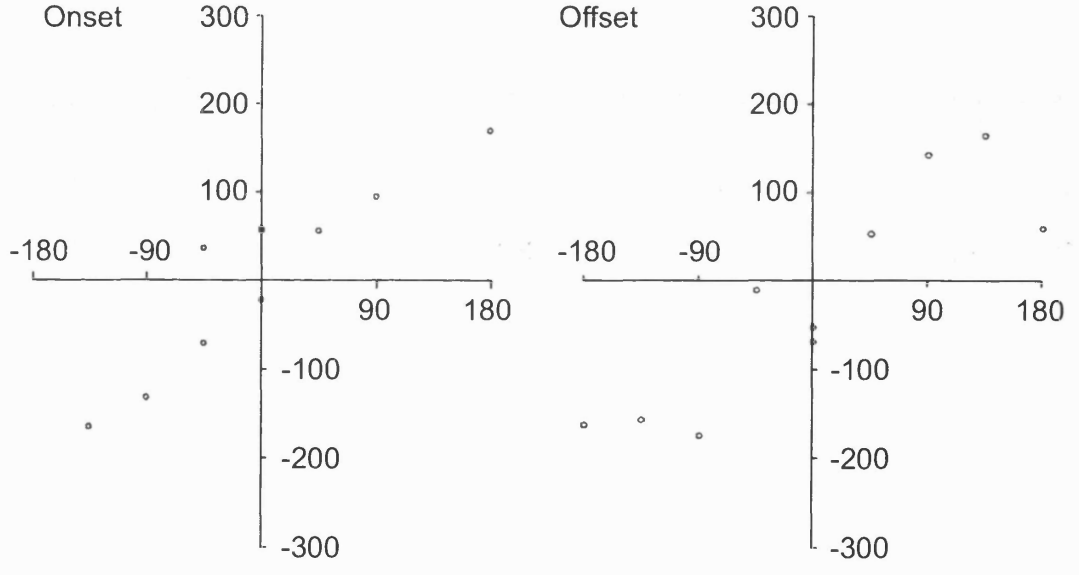

Subject MG, onset gain 1.06, offset gain 0.95

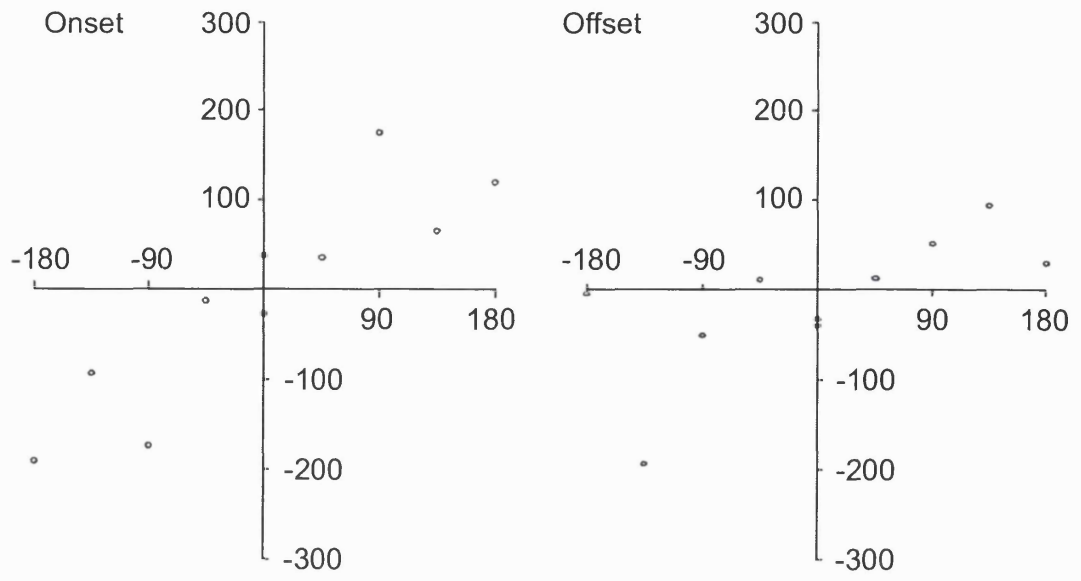

Subject PB, onset gain 0.91, offset gain 0.45

For explanation of histograms see Figure 16.

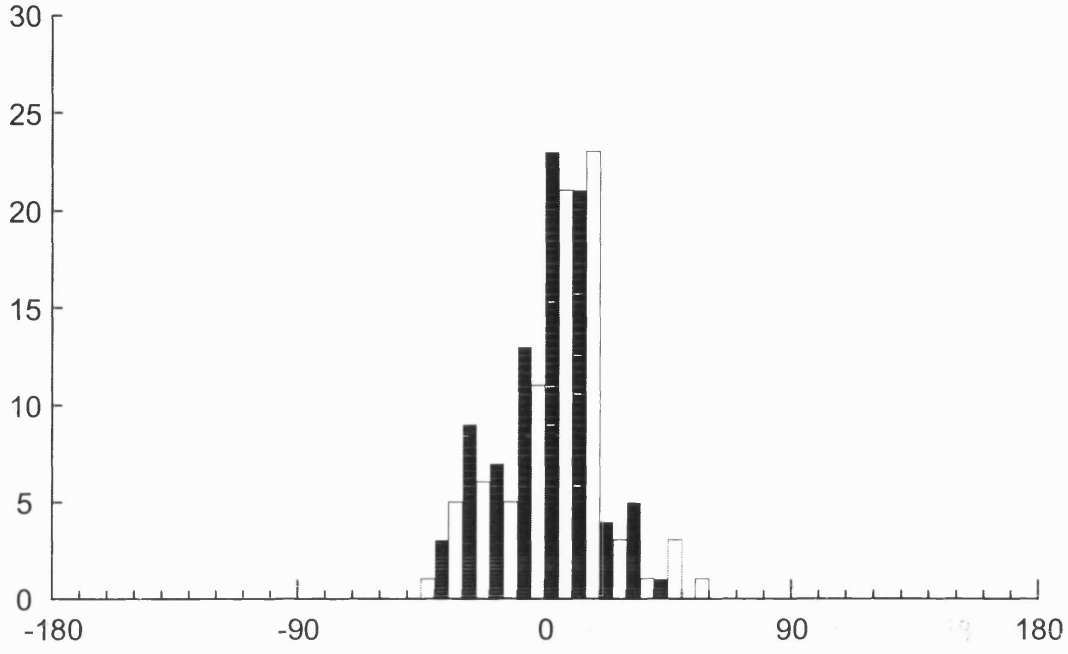

Subject DK R_V (black) = 2.9 ± 16.7 and R_{OMP} (white) = 3.4 ± 19.2

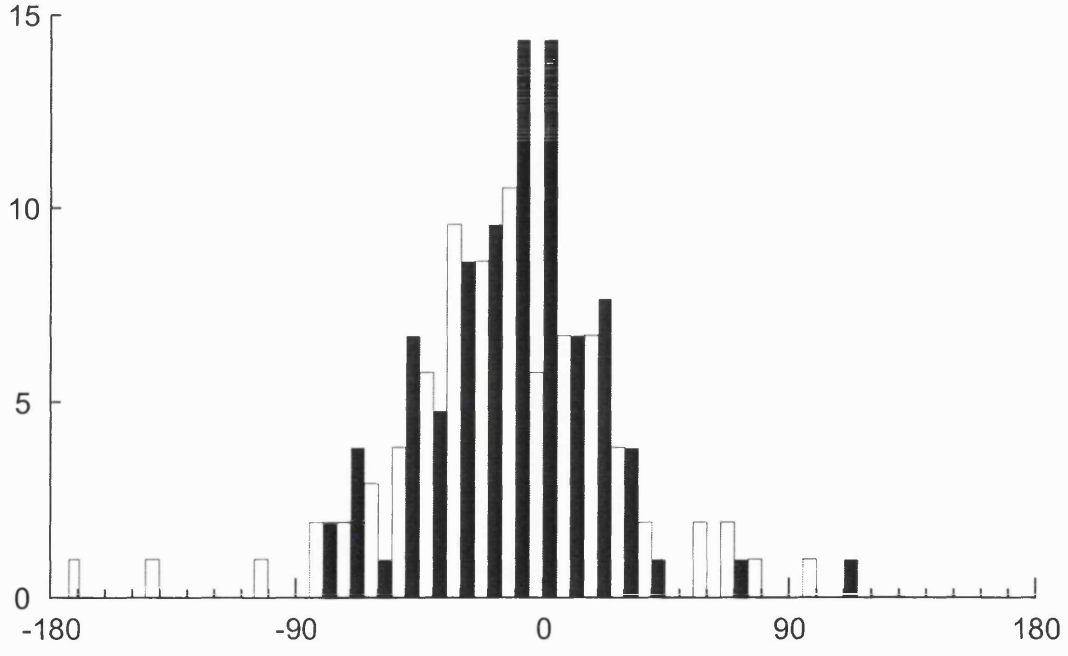

Subject KT R_V (black) = -7.1 ± 31.8 and R_{OMP} (white) = -18.0 ± 43.6

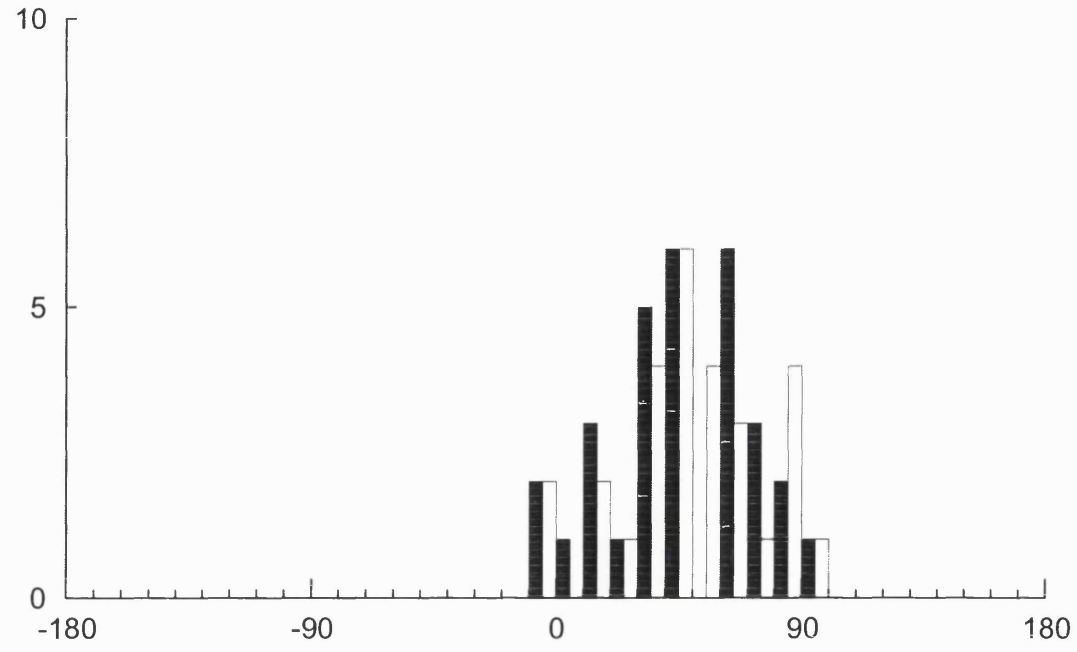

Subject RR R_V (black) = 47.7 ± 25.9 and R_{OMP} (white) = 48.7 ± 24.8

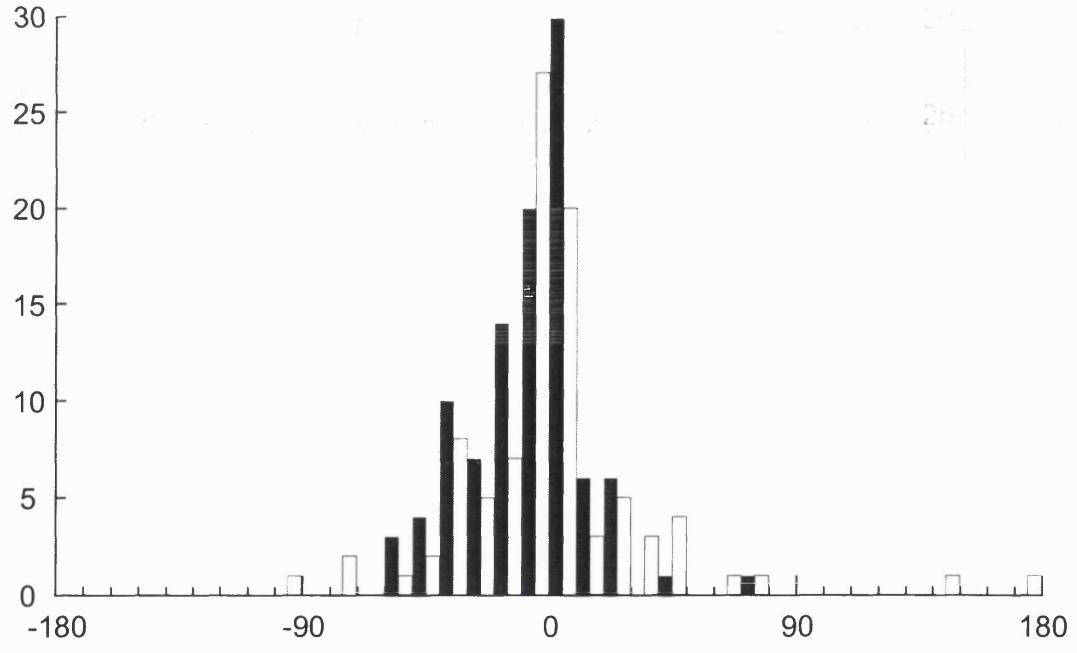

Subject SP (this graph appears as Figure 16) R_V (black) = -6.3 ± 21.8 and R_{OMP} (white) = -1.4 ± 32.0 (mean ± s.d.).

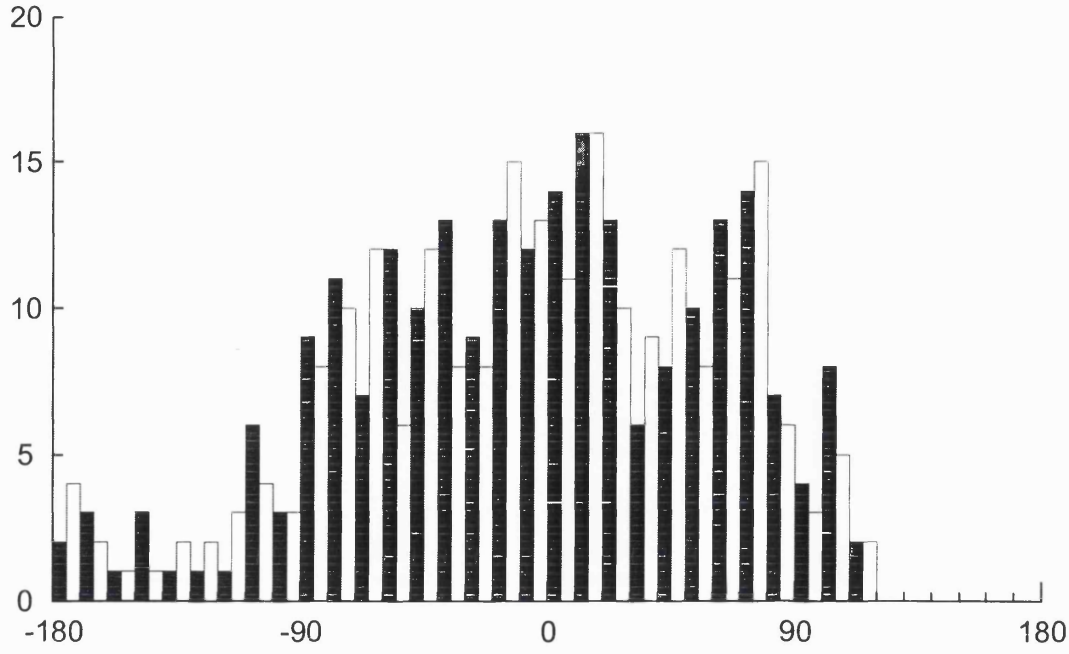

Subject WG R_V (black) = -4.7 ± 65.9 and R_{OMP} (white) = -7.1 ± 66.2

Reversal of the Order of Walking and Standing

Normalised optic flow speed (NOFS) plotted against normalised walking velocity (NWV), so details see Figure 32.

Type 1

Type 2

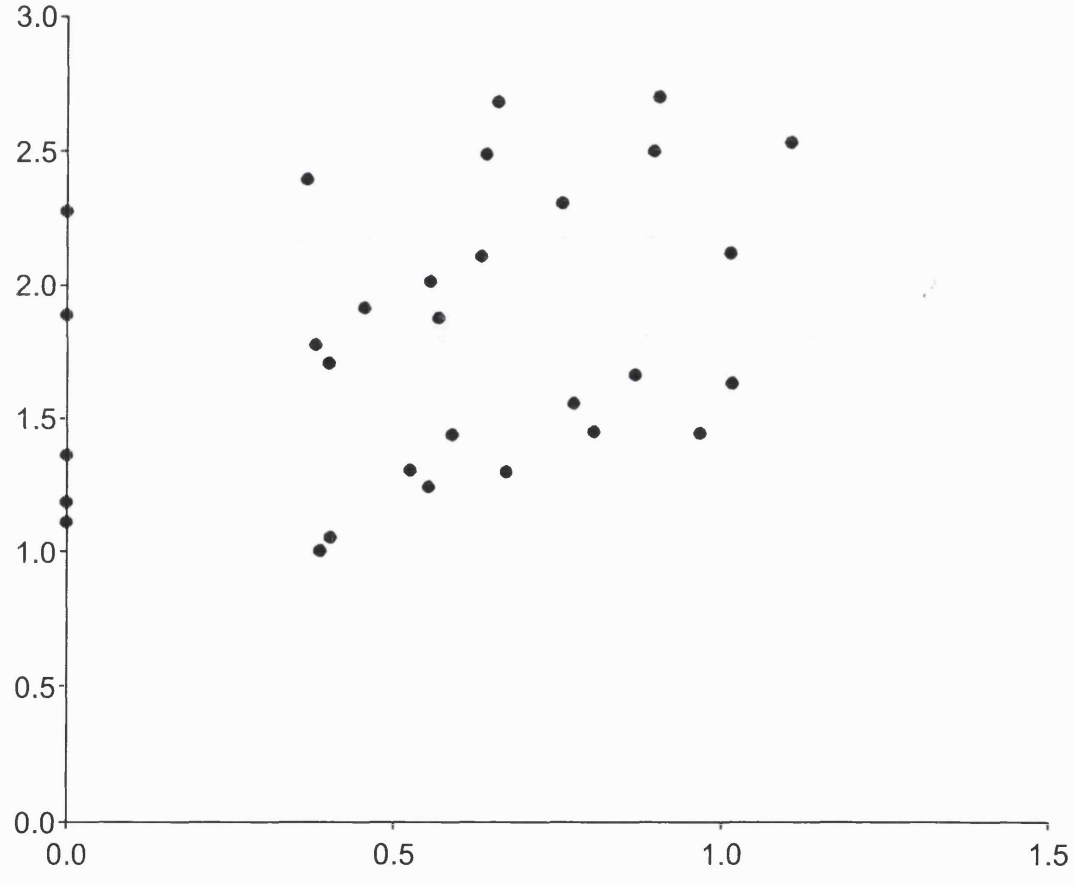

Subject AP Line of best fit: NOFS = 1.49 + 0.55 × NWV, R^2 = 0.12 and P > 0.05

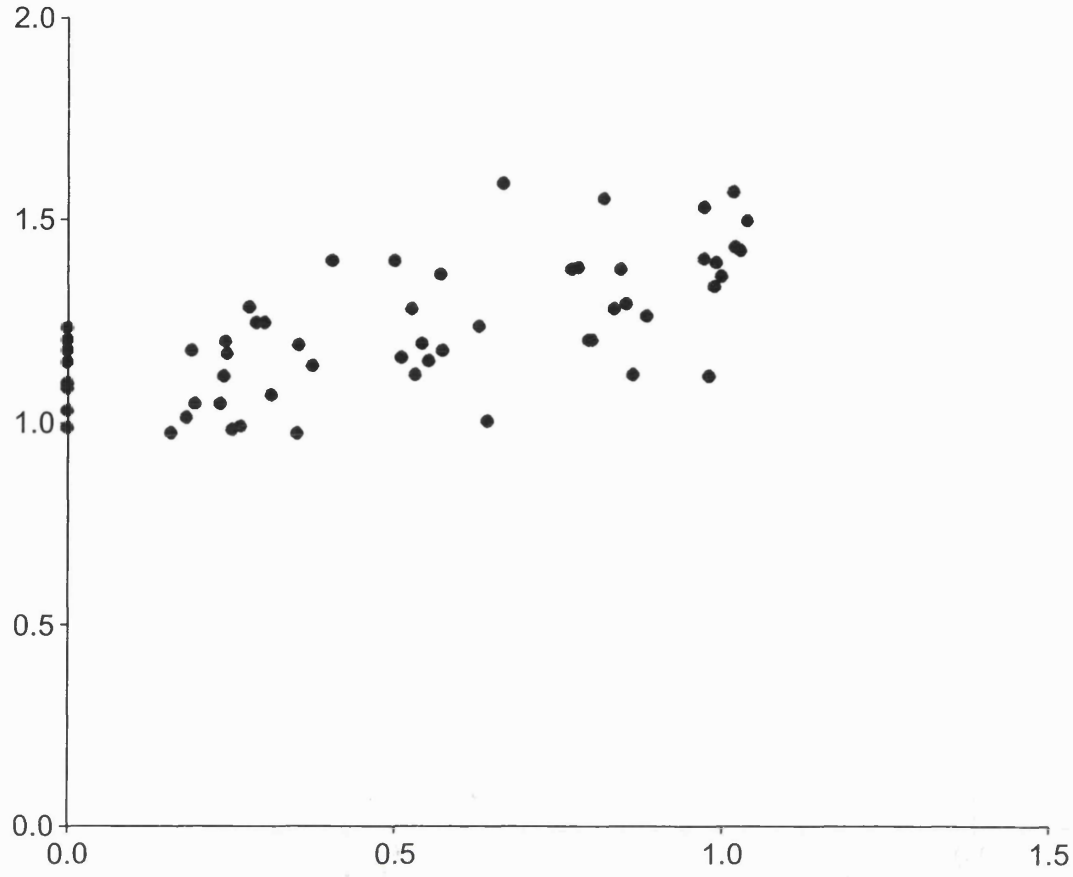

Subject AT Line of best fit: NOFS = 1.06 + 0.32 × NWV, R^2 = 0.46 and P < 0.05

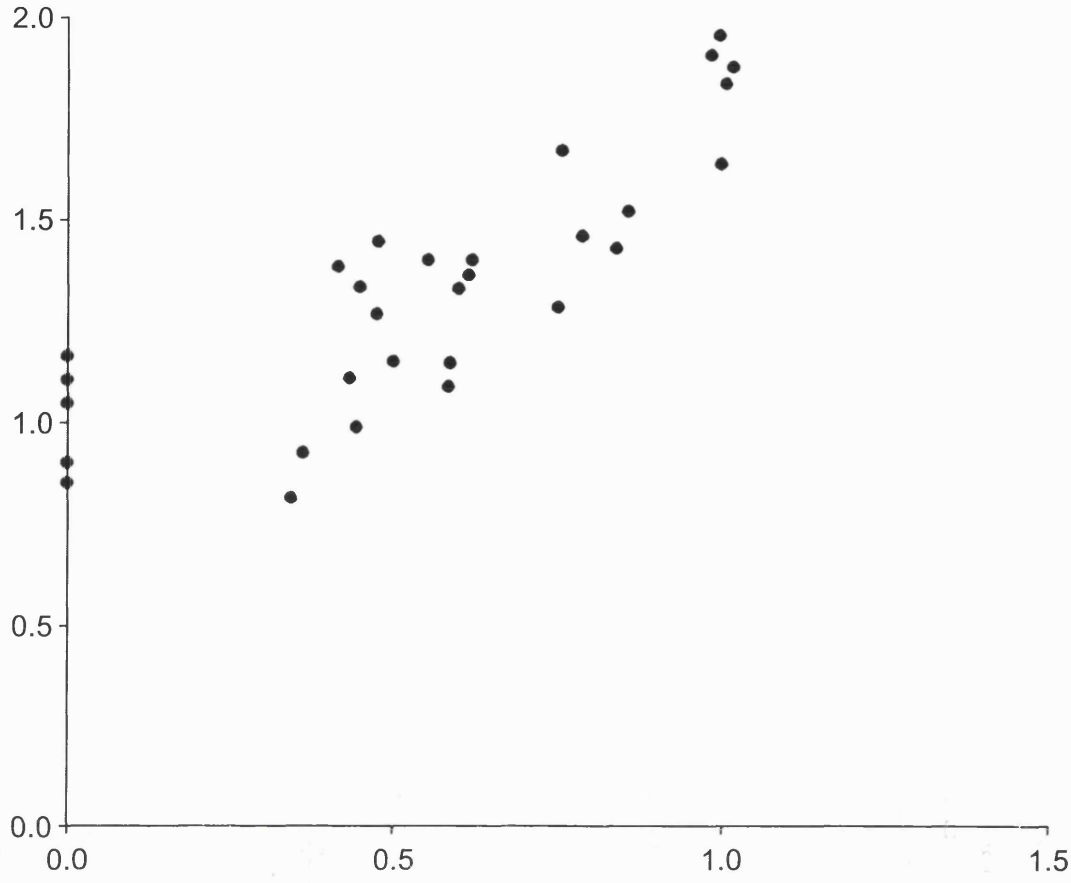

Subject FP Line of best fit: NOFS = 0.88 + 0.81 × NWV, R^2 = 0.69 and P < 0.05

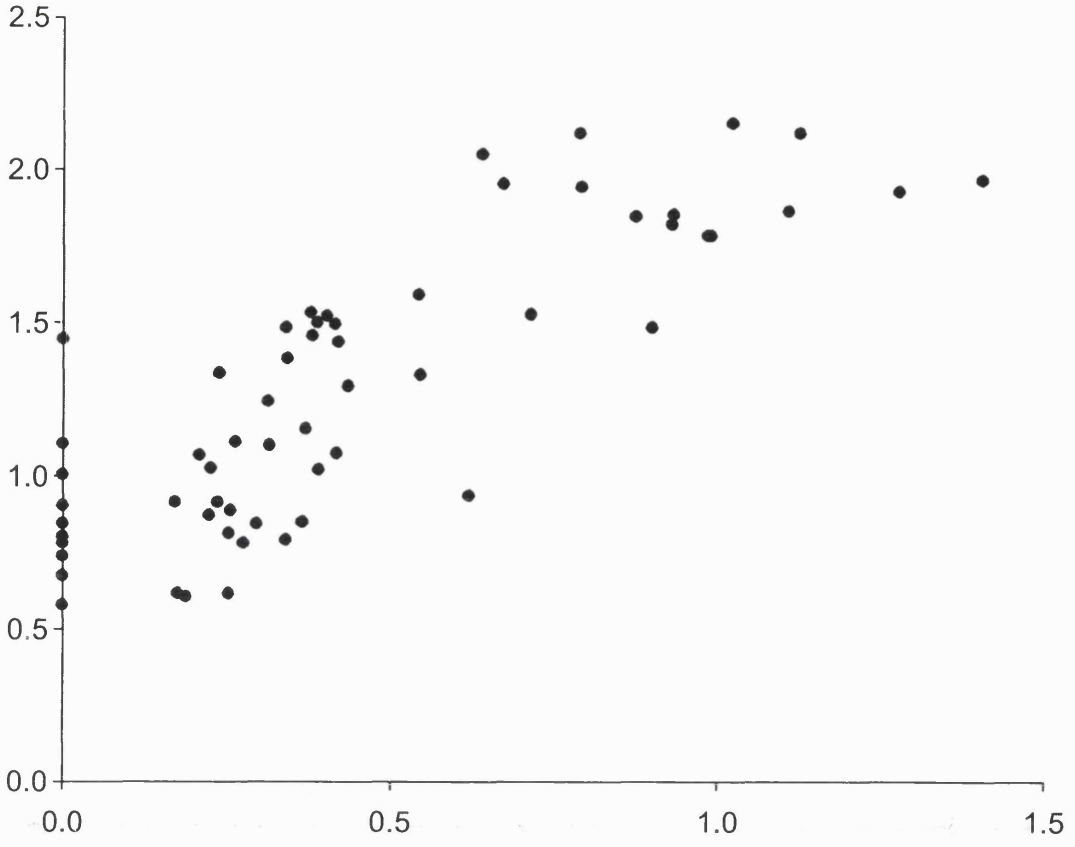

Subject RH Line of best fit: NOFS = 0.81 + 1.06 × NWV, R^2 = 0.68 and P < 0.05

Attentional Control

Normalised optic flow speed (NOFS) plotted against normalised walking velocity (NWV).

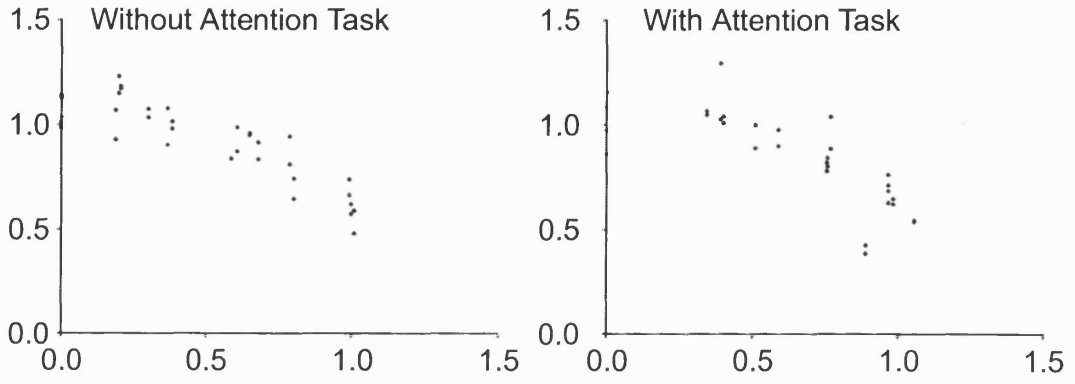

Subject AT Line of best fit without attentional task: NOFS = 1.15 - 0.47 × NWV, R^2 = 0.72 and P < 0.05 Line of best fit with attentional task: NOFS = 1.16 - 0.50 × NWV, R^2 = 0.58 and P < 0.05

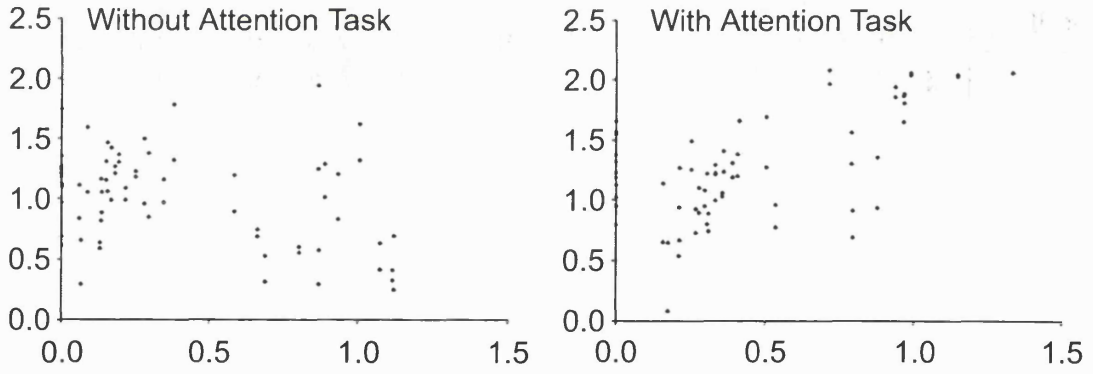

Subject BJ Line of best fit without attentional task: NOFS = 1.17 - 0.37 × NWV, R^2 = 0.13 and P < 0.05 Line of best fit with attentional task: NOFS = 0.93 + 0.77 × NWV, R^2 = 0.38 and P < 0.05

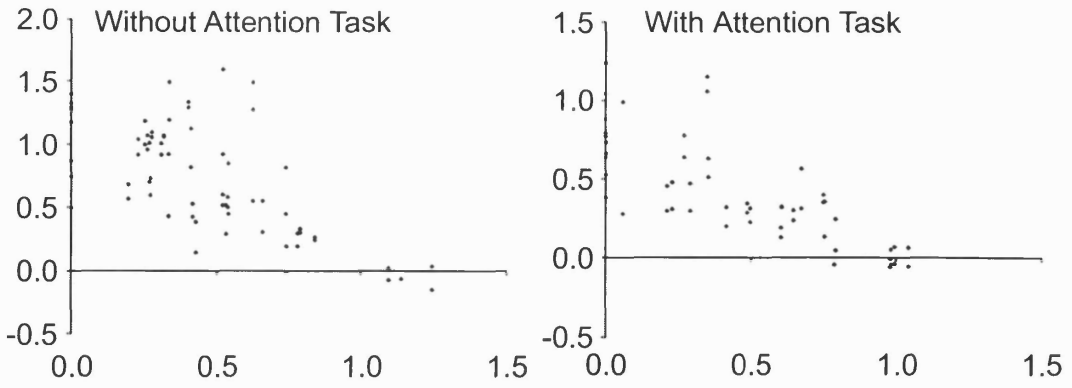

Subject BW Line of best fit without attentional task: NOFS = 1.18 - 1.00 × NWV, R^2 = 0.49 and P < 0.05 Line of best fit with attentional task: NOFS = 0.75 - 0.73 × NWV, R^2 = 0.59 and P < 0.05

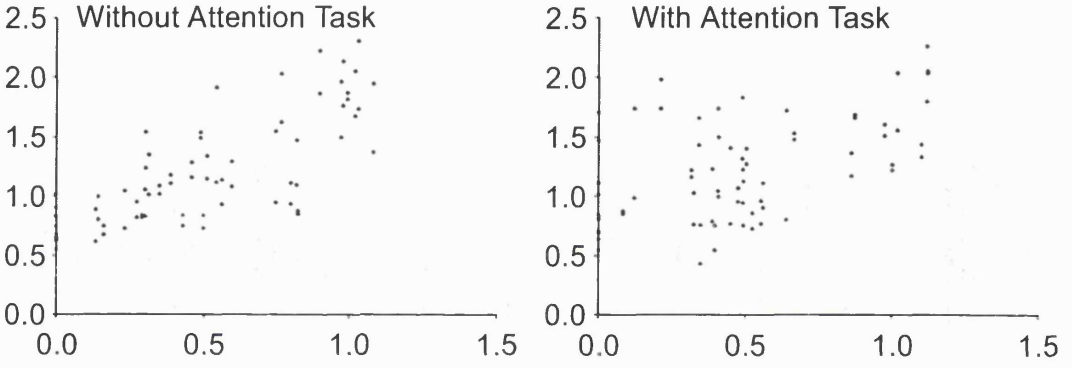

Subject BS Line of best fit without attentional task: NOFS = 0.68 + 1.02 × NWV, R^2 = 0.59 and P < 0.05 Line of best fit with attentional task: NOFS = 0.91 + 0.63 × NWV, R^2 = 0.26 and P < 0.05

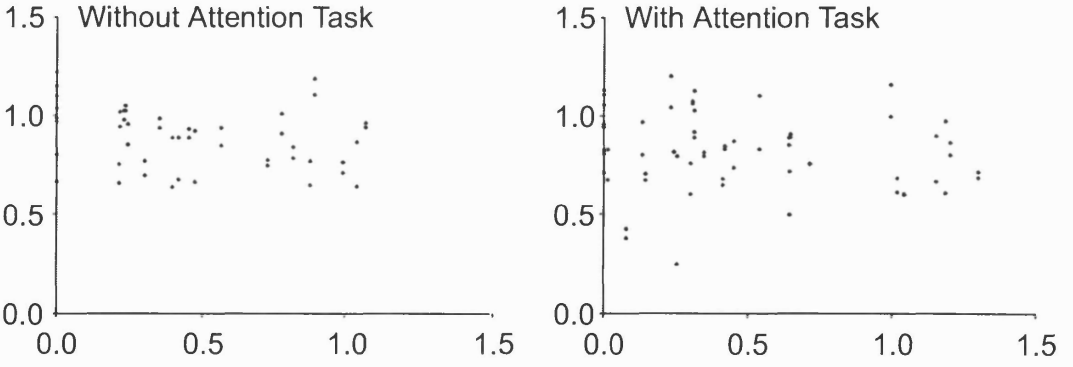

Subject CD Line of best fit without attentional task: NOFS = 0.94 - 0.11 × NWV, R^2 = 0.07 and P > 0.05 Line of best fit with attentional task: NOFS = 0.85 - 0.06 × NWV, R^2 = 0.02 and P > 0.05

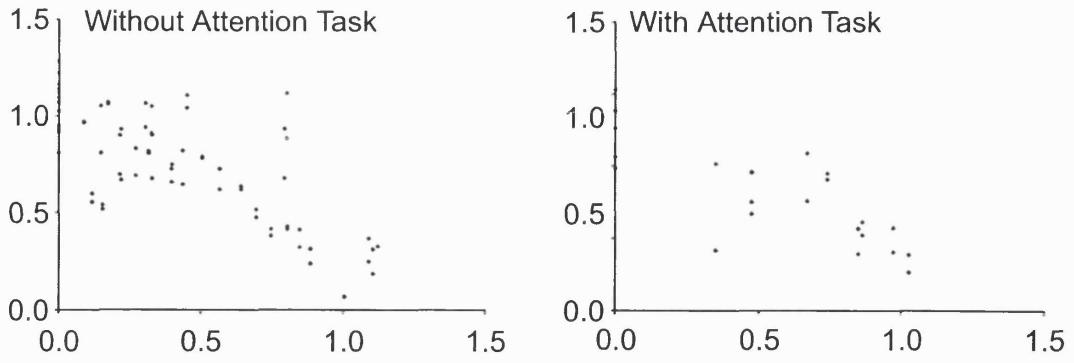

Subject CJB Line of best fit without attentional task: NOFS = 1.02 - 0.65 × NWV, R^2 = 0.59 and P < 0.05 Line of best fit with attentional task: NOFS = 1.24 - 0.78 × NWV, R^2 = 0.67 and P < 0.05

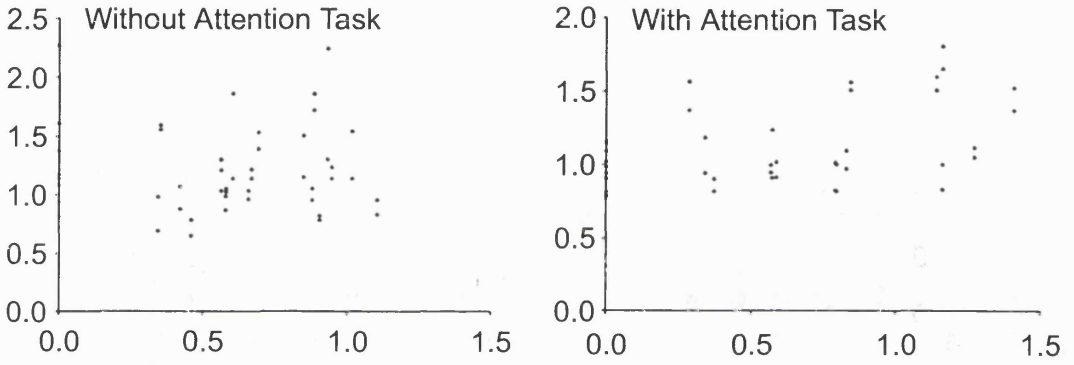

Subject CLB Line of best fit without attentional task: NOFS = 1.21 + 0.00 × NWV, R^2 = 0.00 and P > 0.05 Line of best fit with attentional task: NOFS = 0.95 + 0.28 × NWV, R^2 = 0.29 and P < 0.05

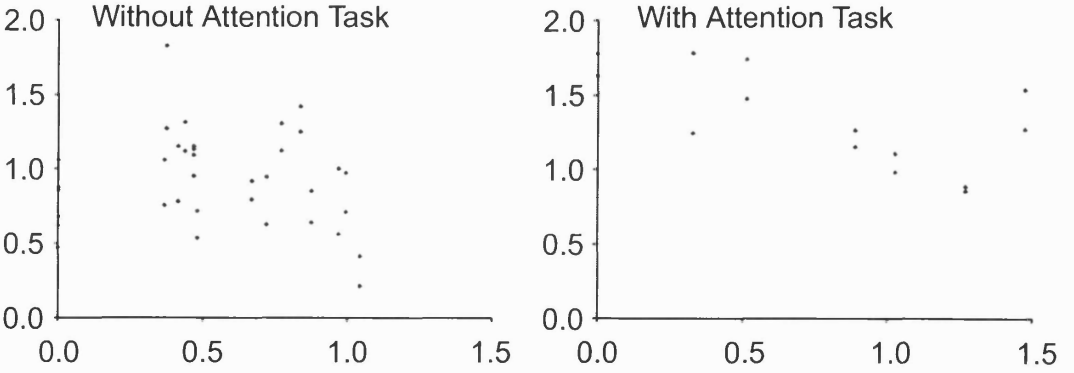

Subject DC Line of best fit without attentional task: NOFS = 0.97 - 0.10 × NWV, R^2 = 0.01 and P > 0.05 Line of best fit with attentional task: NOFS = 1.54 - 0.23 × NWV, R^2 = 0.27 and P < 0.05

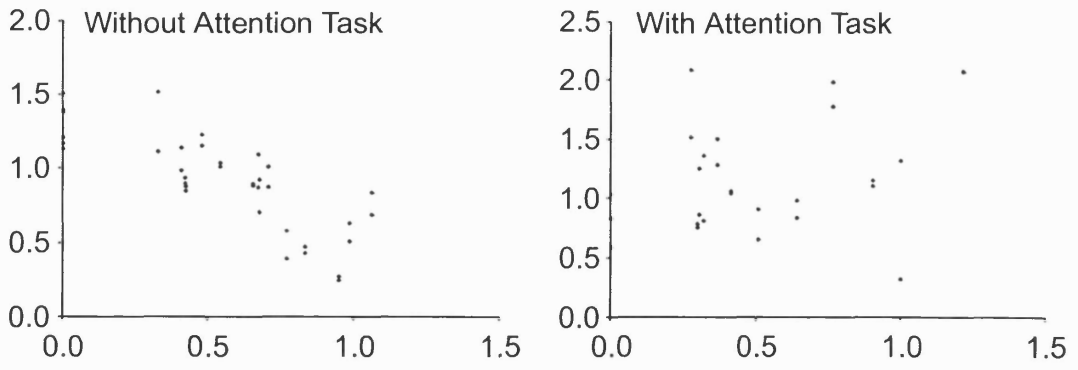

Subject HG Line of best fit without attentional task: NOFS = 1.36 - 0.81 × NWV, R^2 = 0.64 and P < 0.05 Line of best fit with attentional task: NOFS = 0.91 + 0.52 × NWV, R^2 = 0.14 and P < 0.05

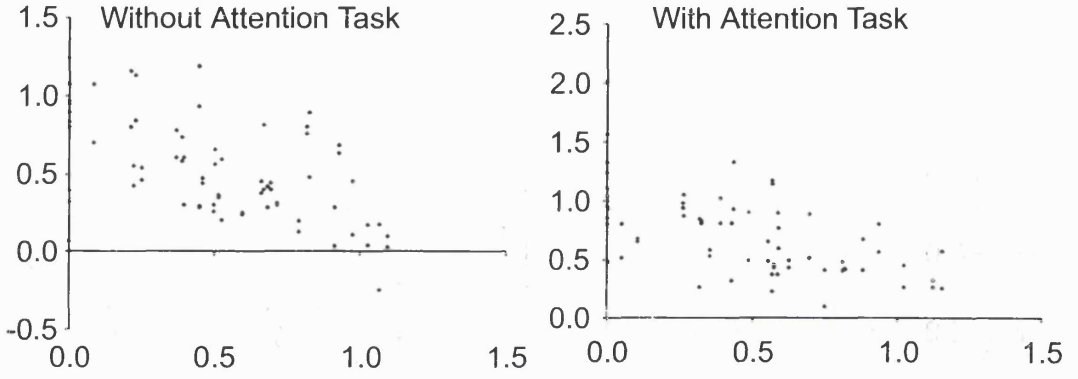

Subject JP Line of best fit without attentional task: NOFS = 0.82 - 0.59 × NWV, R^2 = 0.36 and P < 0.05 Line of best fit with attentional task: NOFS = 1.01 - 0.62 × NWV, R^2 = 0.36 and P < 0.05

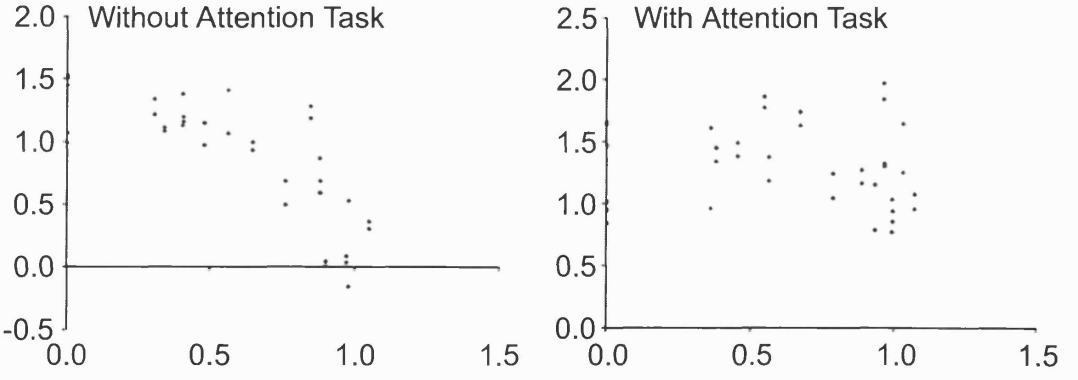

Subject MB Line of best fit without attentional task: NOFS = 1.46 - 1.03 × NWV, R^2 = 0.57 and P < 0.05 Line of best fit with attentional task: NOFS = 1.38 - 0.12 × NWV, R^2 = 0.02 and P > 0.05

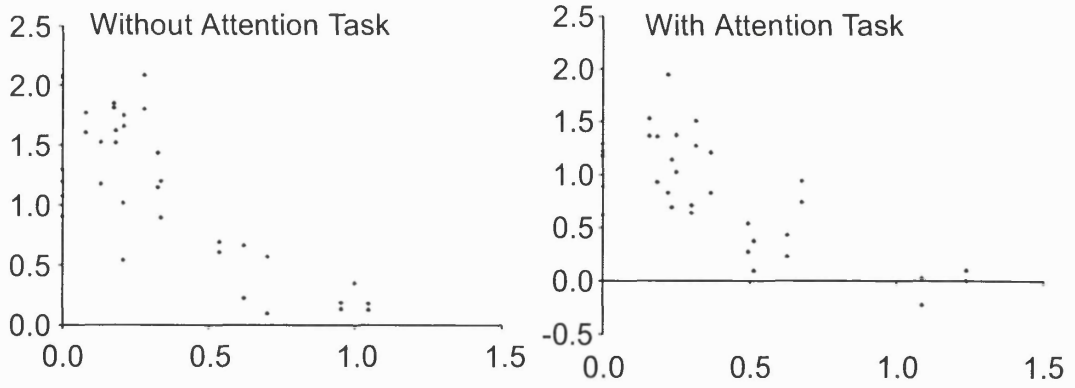

Subject MC Line of best fit without attentional task: NOFS = 1.65 - 1.49 × NWV, R^2 = 0.65 and P < 0.05 Line of best fit with attentional task: NOFS = 1.26 - 1.10 × NWV, R^2 = 0.55 and P < 0.05

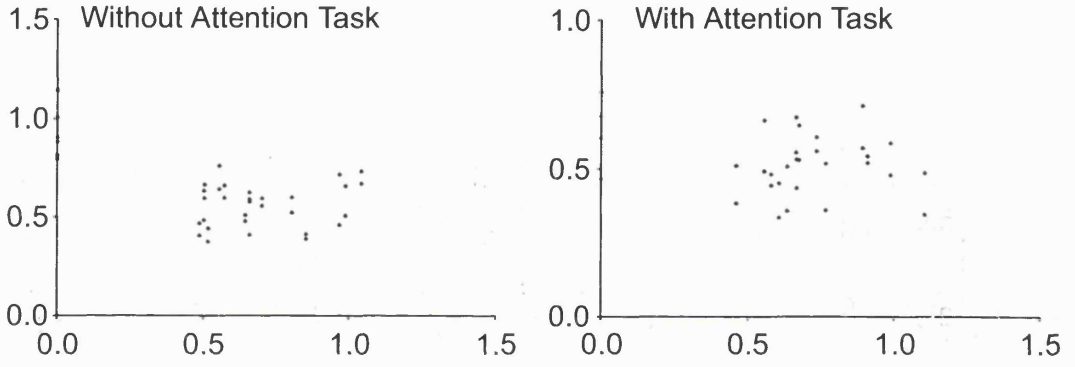

Subject NW Line of best fit without attentional task: NOFS = 0.82 - 0.34 × NWV, R^2 = 0.36 and P < 0.05 Line of best fit with attentional task: NOFS = 0.59 - 0.10 × NWV, R^2 = 0.07 and P > 0.05

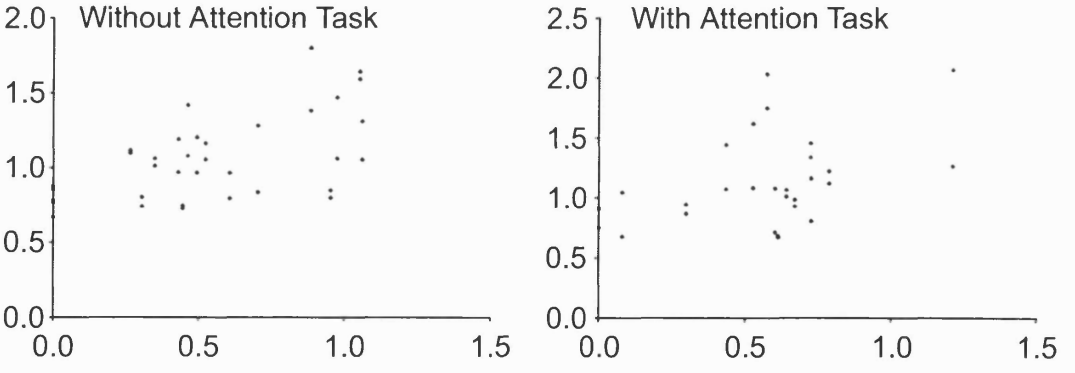

Subject PE Line of best fit without attentional task: NOFS = 0.80 + 0.47 × NWV, R^2 = 0.34 and P < 0.05 Line of best fit with attentional task: NOFS = 0.82 + 0.56 × NWV, R^2 = 0.19 and P < 0.05

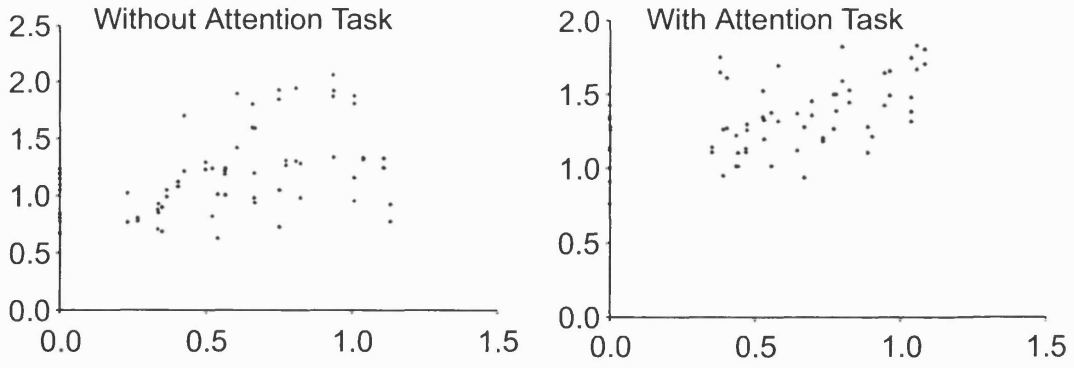

Subject RS Line of best fit without attentional task: NOFS = 0.90 + 0.51 × NWV, R^2 = 0.22 and P < 0.05 Line of best fit with attentional task: NOFS = 1.11 + 0.39 × NWV, R^2 = 0.28 and P < 0.05

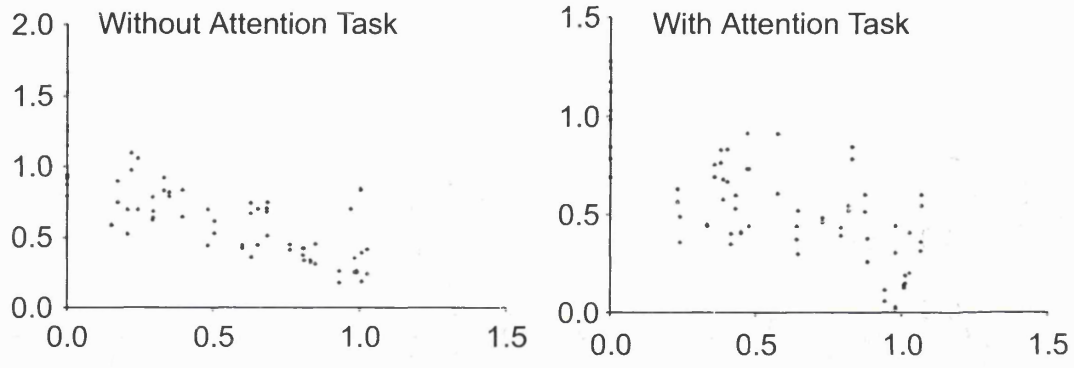

Subject SP Line of best fit without attentional task: NOFS = 1.03 - 0.71 × NWV, R^2 = 0.60 and P < 0.05 Line of best fit with attentional task: NOFS = 0.88 - 0.58 × NWV, R^2 = 0.51 and P < 0.05

Head Motion Control

Normalised optic flow speed (NOFS) plotted against normalised walking velocity (NWV).

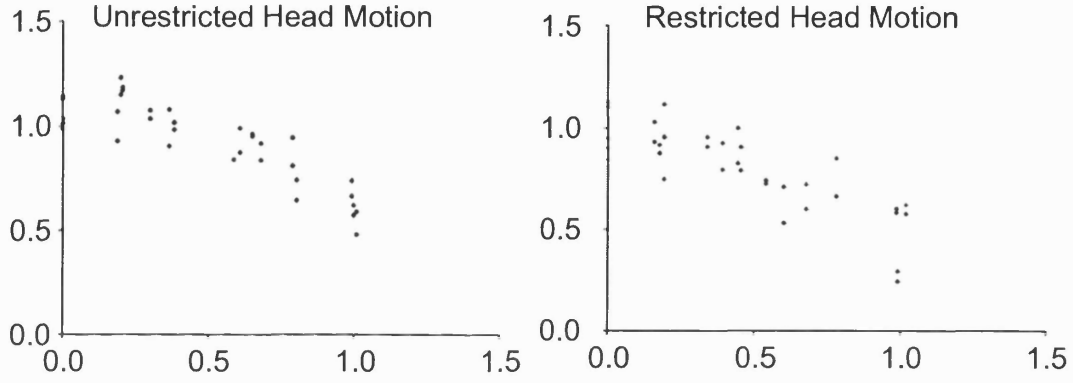

Subject AT Line of best fit with unrestricted head motion: NOFS = 1.15 - 0.47 × NWV, R^2 = 0.72 and P < 0.05 Line of best fit with restricted head motion: NOFS = 1.02 - 0.50 × NWV, R^2 = 0.67 and P < 0.05

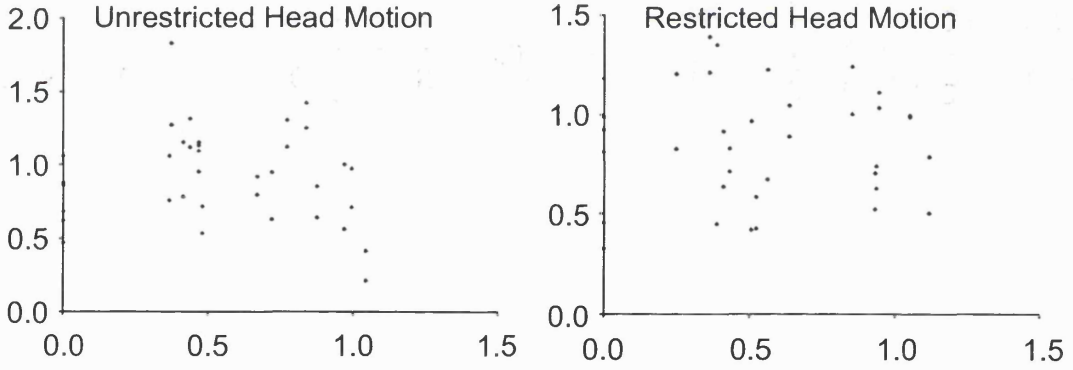

Subject DC Line of best fit with unrestricted head motion: NOFS = 0.97 - 0.10 × NWV, R^2 = 0.01 and P > 0.05 Line of best fit with restricted head motion: NOFS = 0.85 - 0.01 × NWV, R^2 = 0.00 and P > 0.05

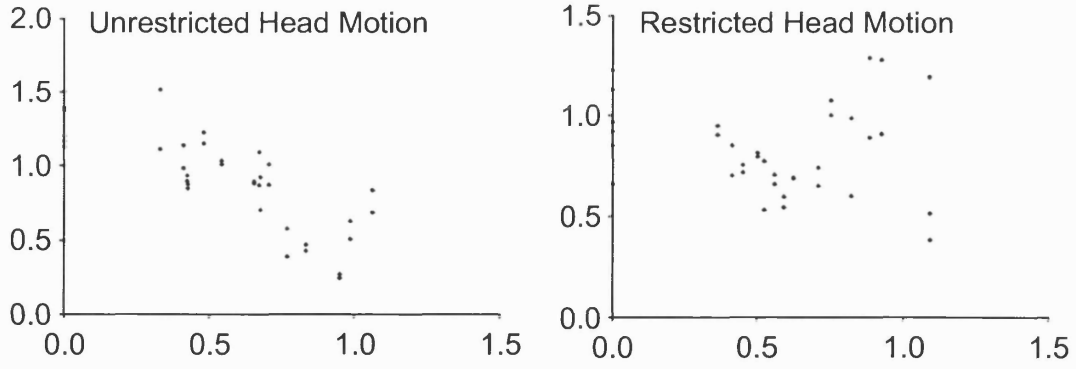

Subject HG Line of best fit with unrestricted head motion: NOFS = 1.36 - 0.81 × NWV, R^2 = 0.64 and P < 0.05 Line of best fit with restricted head motion: NOFS = 0.85 + 0.02 × NWV, R^2 = 0.00 and P > 0.05

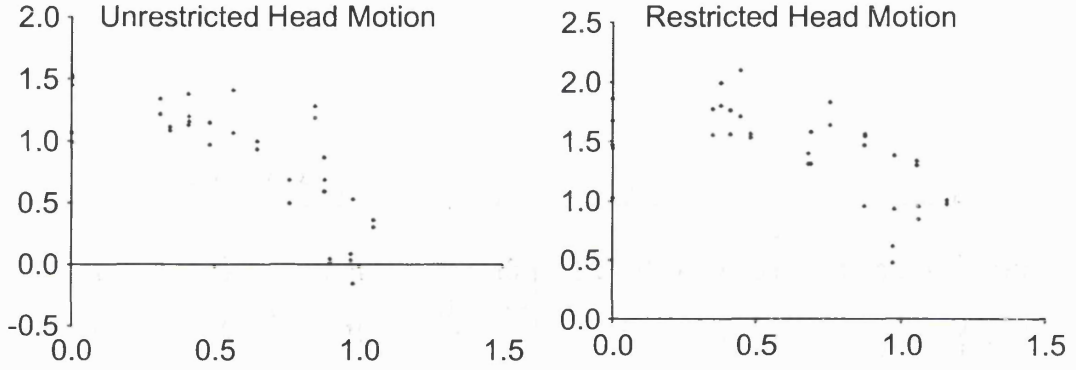

Subject MB Line of best fit with unrestricted head motion: NOFS = 1.46 - 1.03 × NWV, R^2 = 0.57 and P < 0.05 Line of best fit with restricted head motion: NOFS = 1.79 - 0.60 × NWV, R^2 = 0.34 and P < 0.05

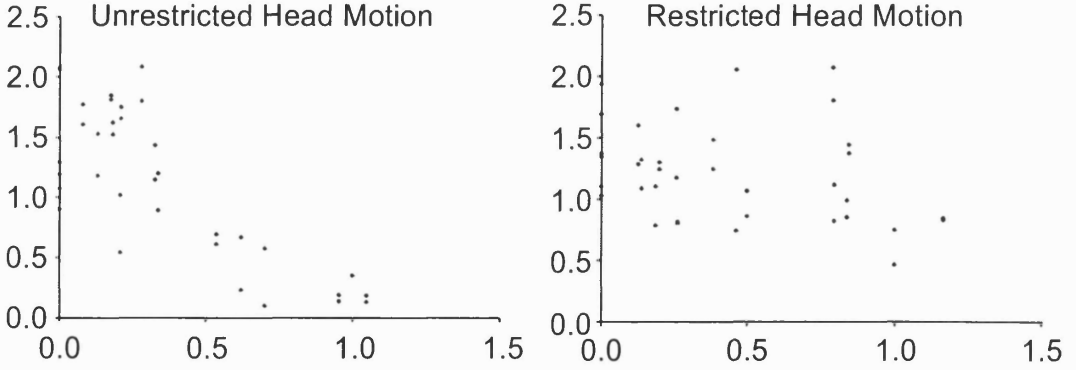

Subject MC Line of best fit with unrestricted head motion: NOFS = 1.65 - 1.49 × NWV, R^2 = 0.65 and P < 0.05 Line of best fit with restricted head motion: NOFS = 1.35 - 0.32 × NWV, R^2 = 0.09 and P > 0.05

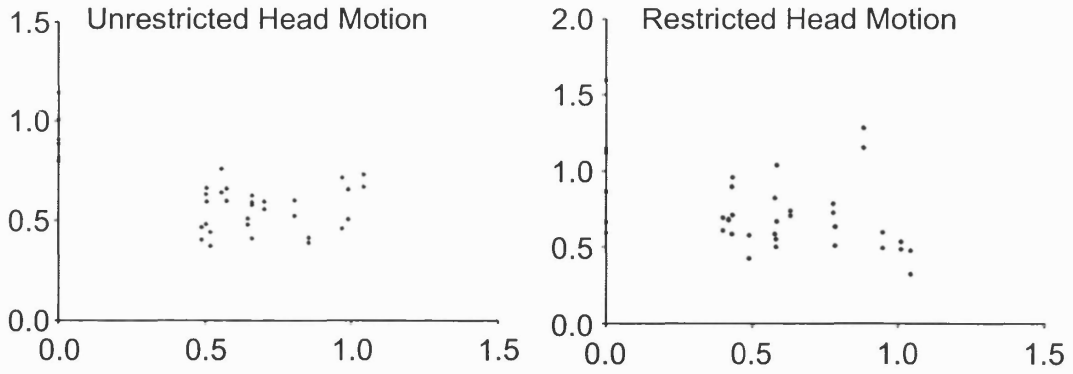

Subject NW Line of best fit with unrestricted head motion: NOFS = 0.82 - 0.34 × NWV, R^2 = 0.36 and P < 0.05 Line of best fit with restricted head motion: NOFS = 0.92 - 0.35 × NWV, R^2 = 0.18 and P < 0.05

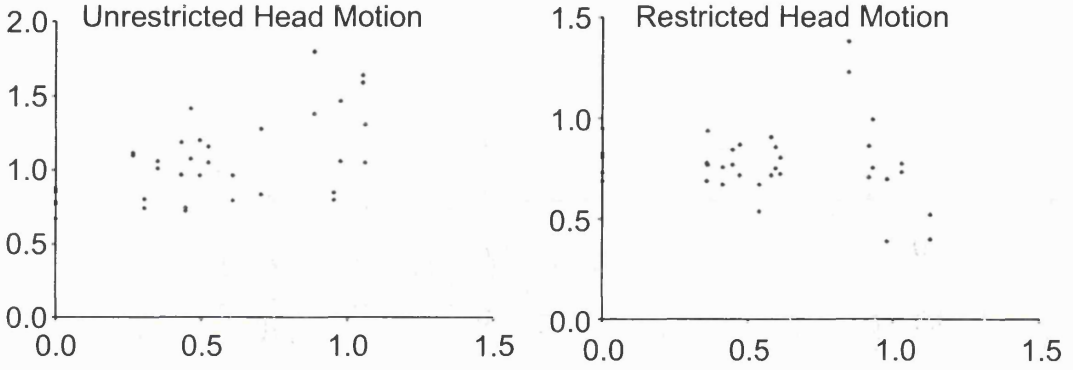

Subject PE Line of best fit with unrestricted head motion: NOFS = 0.80 + 0.47 × NWV, R^2 = 0.34 and P < 0.05 Line of best fit with restricted head motion: NOFS = 0.82 - 0.07 × NWV, R^2 = 0.02 and P > 0.05

Timing Perception Investigation

Normalised optic flow speed (NOFS) plotted against normalised walking velocity (NWV).

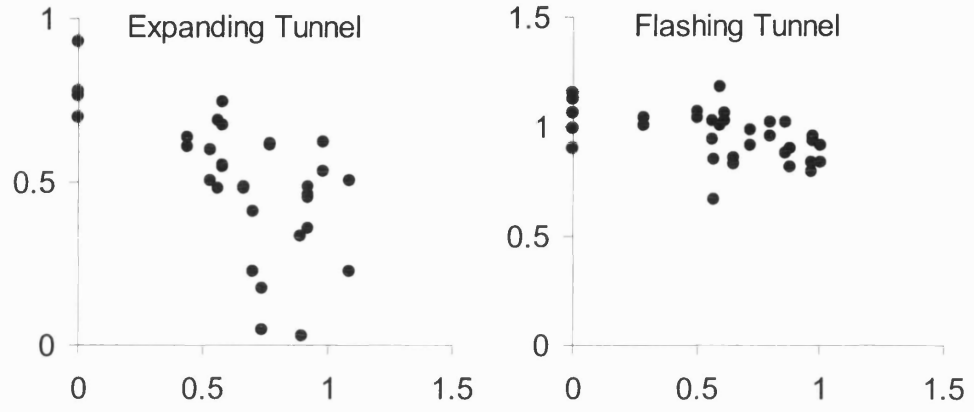

Subject DB Line of best fit for the Expanding Tunnel: NOFS = 0.80 - 0.46 × NWV, R^2 = 0.45 and P < 0.05 Line of best fit for the Flashing Tunnel: NOFS = 1.04 - 0.14 × NWV, R^2 = 0.19 and P < 0.05

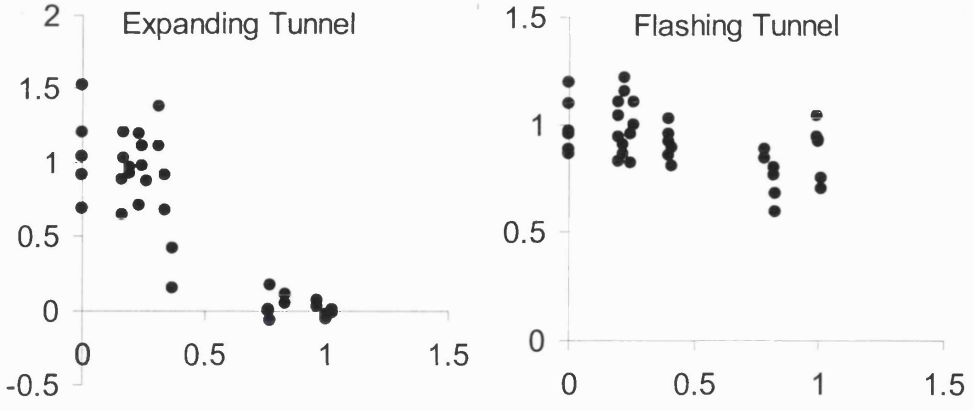

Subject KH Line of best fit for the Expanding Tunnel: NOFS = 1.13 - 1.19 × NWV, R^2 = 0.75 and P < 0.05 Line of best fit for the Flashing Tunnel: NOFS = 1.01 - 0.20 × NWV, R^2 = 0.25 and P < 0.05

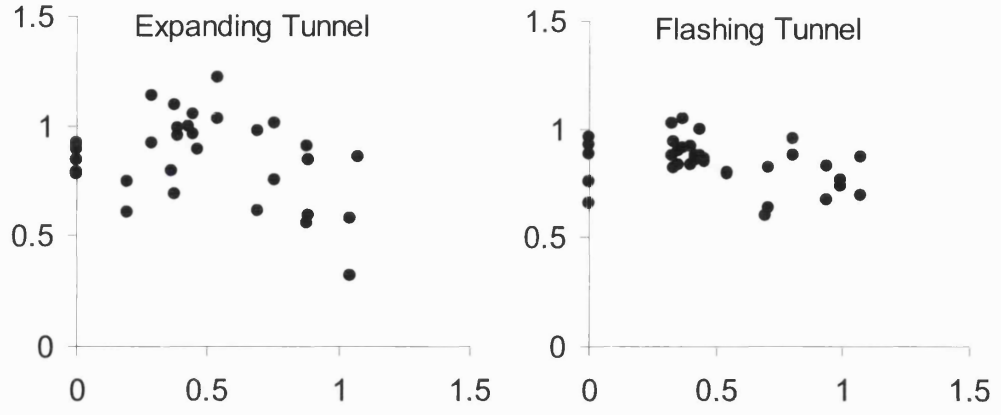

Subject PW Line of best fit for the Expanding Tunnel: NOFS = 0.94 - 0.19 × NWV, R^2 = 0.10 and P > 0.05 Line of best fit for the Flashing Tunnel: NOFS = 0.91 - 0.12 × NWV, R^2 = 0.14 and P < 0.05

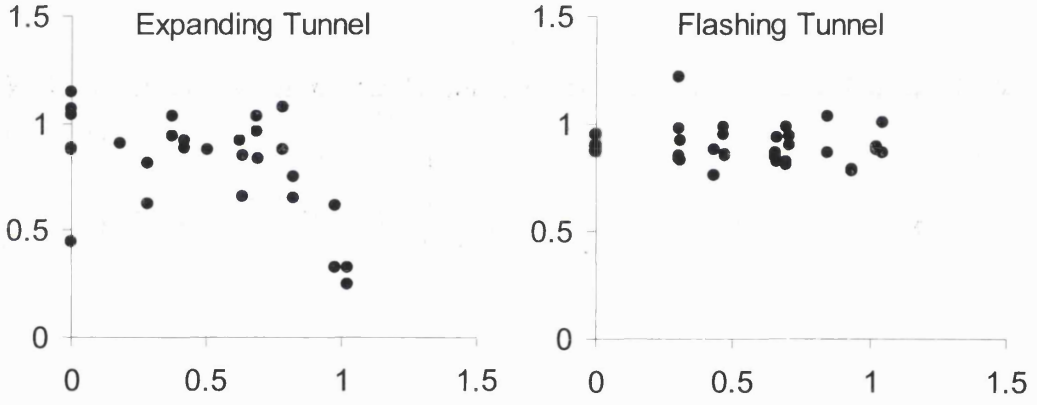

Subject RS Line of best fit for the Expanding Tunnel: NOFS = 0.98 - 0.34 × NWV, R^2 = 0.25 and P < 0.05 Line of best fit for the Flashing Tunnel: NOFS = 0.91 - 0.02 × NWV, R^2 = 0.01 and P > 0.05

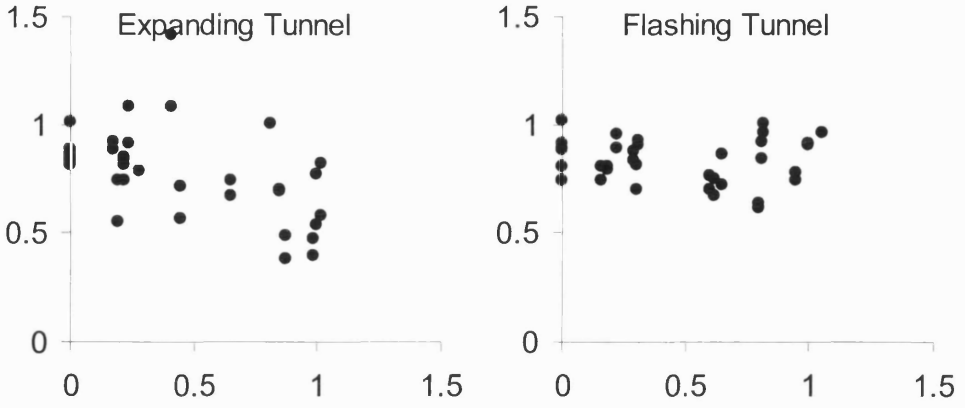

Subject SD Line of best fit for the Expanding Tunnel: NOFS = 0.91 - 0.29 × NWV, R^2 = 0.26 and P < 0.05 Line of best fit for the Flashing Tunnel: NOFS = 0.84 - 0.01 × NWV, R^2 = 0.00 and P > 0.05

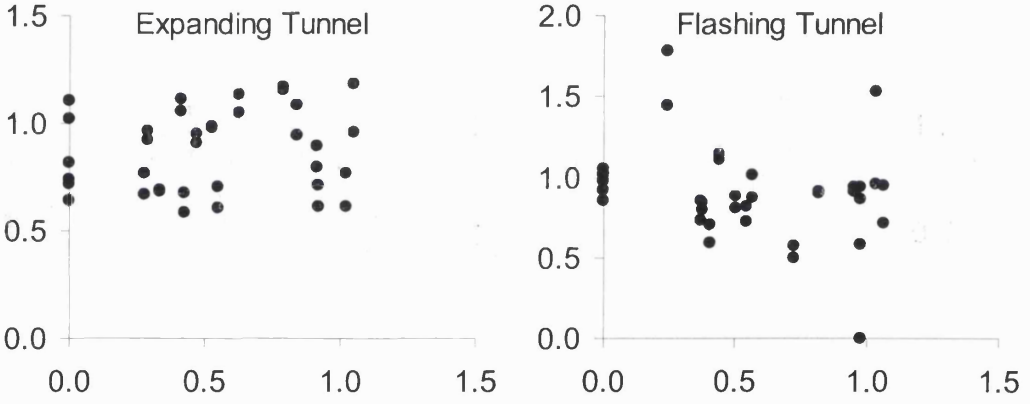

Subject DT Line of best fit for the Expanding Tunnel: NOFS = 0.83 + 0.08 × NWV, R^2 = 0.02 and P > 0.05 Line of best fit for the Flashing Tunnel: NOFS = 1.01 - 0.21 × NWV, R^2 0.06 and P > 0.05

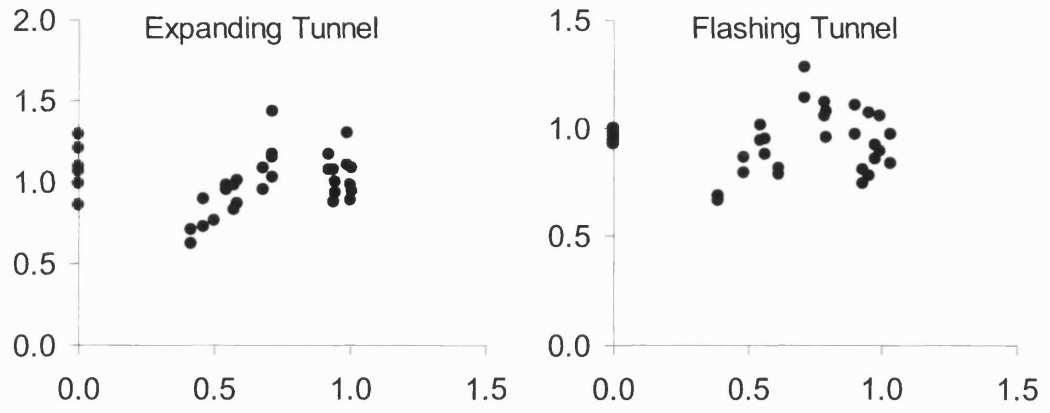

Subject EB Line of best fit for the Expanding Tunnel: NOFS = 0.98 + 0.04 × NWV, R^2 = 0.01 and P > 0.05 Line of best fit for the Flashing Tunnel: NOFS = 0.91 + 0.03 × NWV, R^2 0.01 and P > 0.05

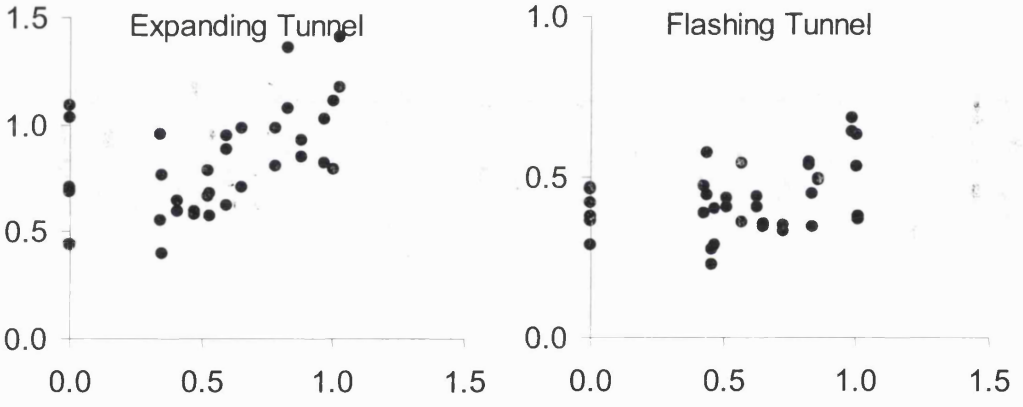

Subject GT Line of best fit for the Expanding Tunnel: NOFS = 0.63 + 0.36 × NWV, R^2 = 0.24 and P < 0.05 Line of best fit for the Flashing Tunnel: NOFS = 0.36 + 0.13 × NWV, R^2 0.15 and P < 0.05

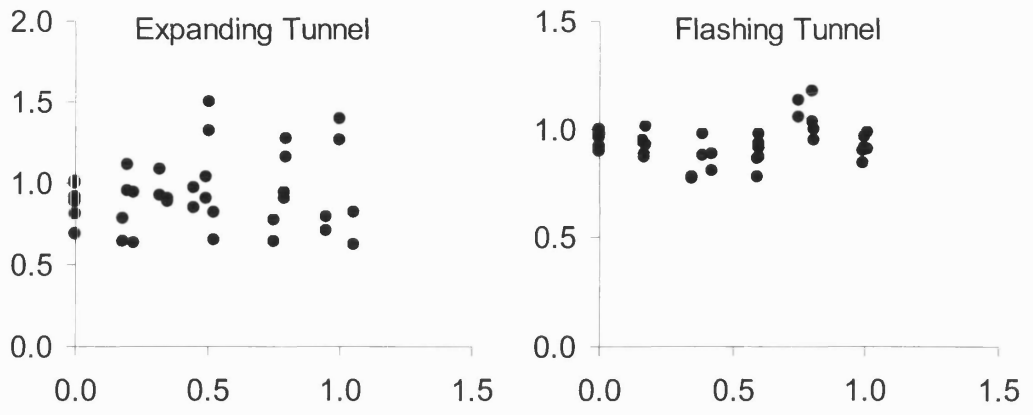

Subject JT Line of best fit for the Expanding Tunnel: NOFS = 0.89 + 0.08 × NWV, R^2 = 0.02 and P > 0.05 Line of best fit for the Flashing Tunnel: NOFS = 0.92 + 0.03 × NWV, R^2 0.02 and P > 0.05

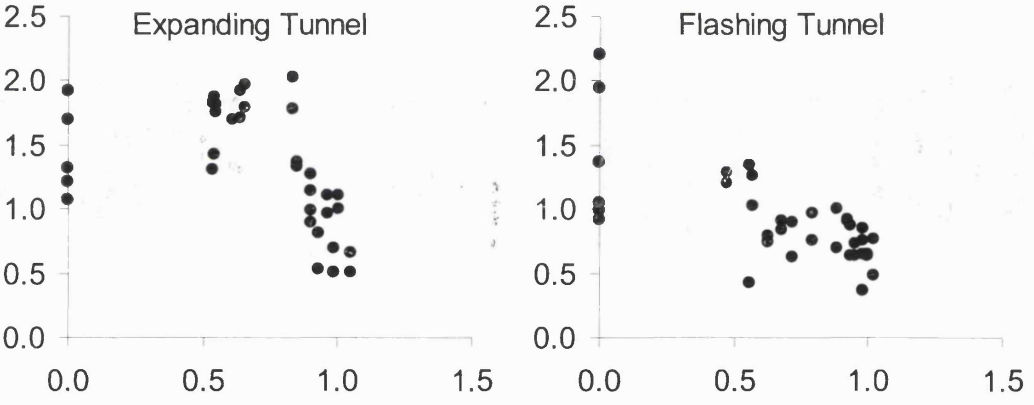

Subject MB Line of best fit for the Expanding Tunnel: NOFS = 1.78 - 0.66 × NWV, R^2 = 0.24 and P < 0.05 Line of best fit for the Flashing Tunnel: NOFS = 1.42 - 0.74 × NWV, R^2 0.48 and P < 0.05

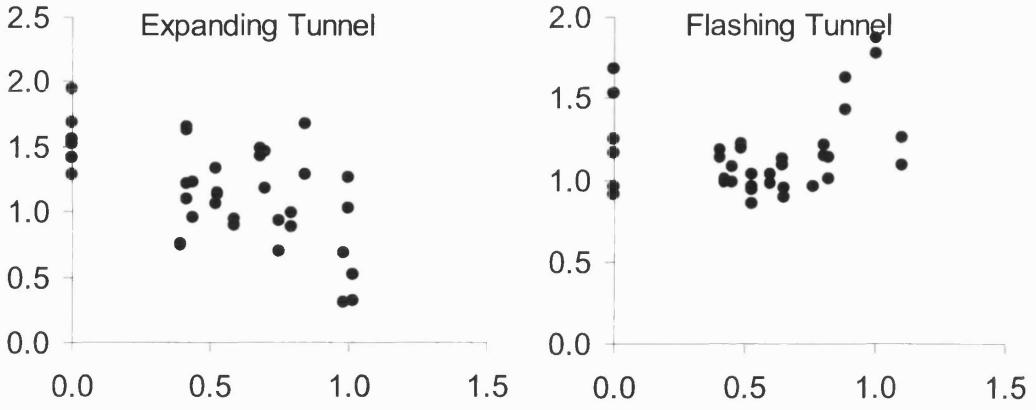

Subject MO Line of best fit for the Expanding Tunnel: NOFS = 1.54 - 0.71 × NWV, R^2 = 0.34 and P < 0.05 Line of best fit for the Flashing Tunnel: NOFS = 1.08 + 0.13 × NWV, R^2 0.02 and P > 0.05

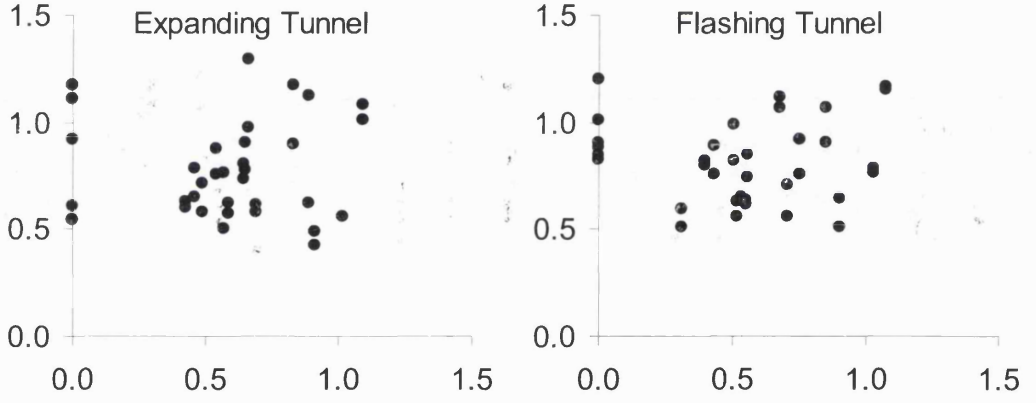

Subject MP Line of best fit for the Expanding Tunnel: NOFS = 0.84 - 0.09 × NWV, R^2 = 0.02 and P > 0.05 Line of best fit for the Flashing Tunnel: NOFS = 0.82 + 0.00 × NWV, R^2 0.00 and P > 0.05

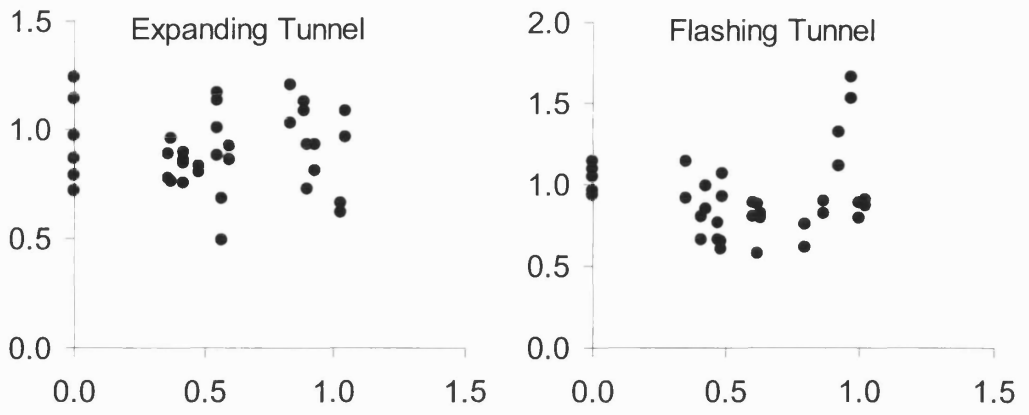

Subject RT Line of best fit for the Expanding Tunnel: NOFS = 0.91 - 0.01 × NWV, R^2 = 0.00 and P > 0.05 Line of best fit for the Flashing Tunnel: NOFS = 0.89 + 0.06 × NWV, R^2 0.01 and P > 0.05

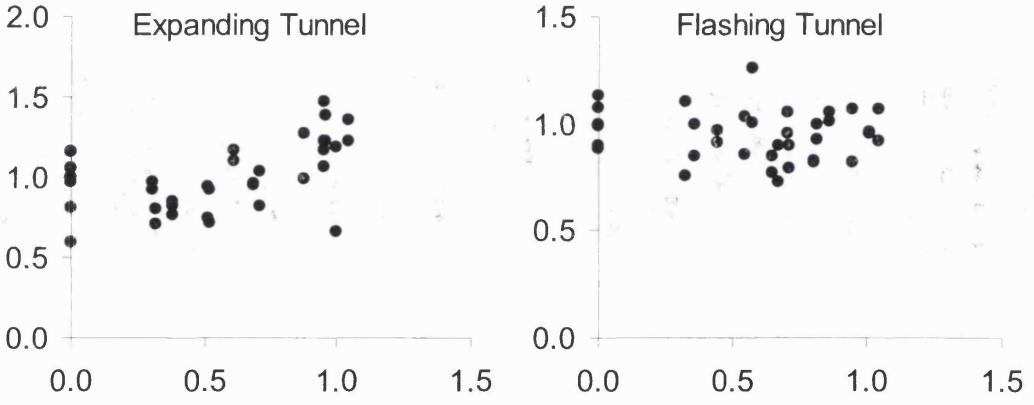

Subject TO Line of best fit for the Expanding Tunnel: NOFS = 0.82 + 0.32 × NWV, R^2 = 0.28 and P < 0.05 Line of best fit for the Flashing Tunnel: NOFS = 0.97 - 0.04 × NWV, R^2 0.01 and P > 0.05

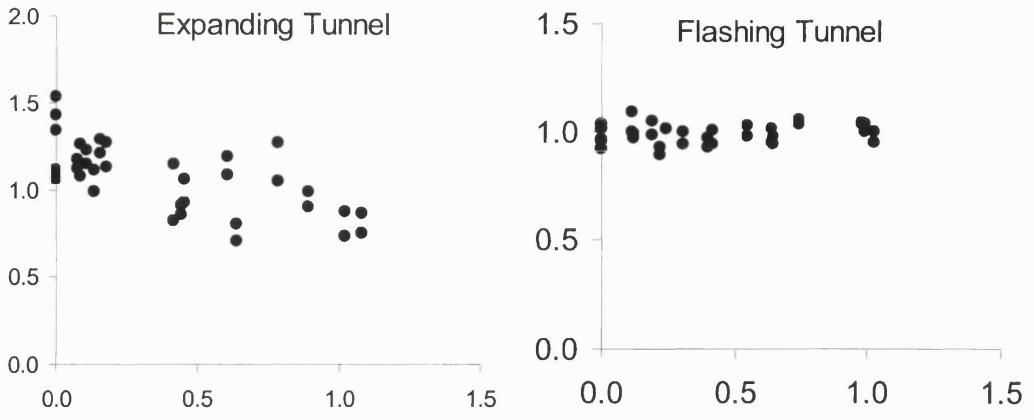

Subject AP Line of best fit for the Expanding Tunnel: NOFS = 1.21 - 0.36 × NWV, R^2 = 0.44 and P < 0.05 Line of best fit for the Flashing Tunnel: NOFS = 0.97 + 0.03 × NWV, R^2 0.06 and P > 0.05

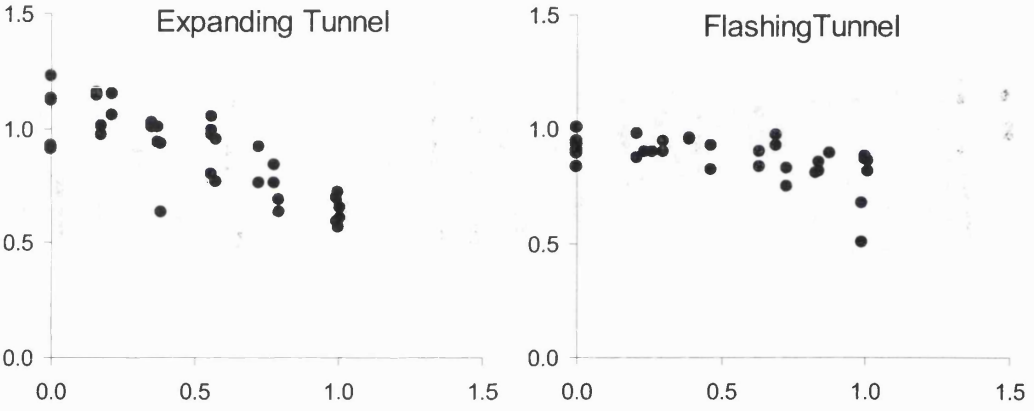

Subject AT Line of best fit for the Expanding Tunnel: NOFS = 1.10 - 0.43 × NWV, R^2 = 0.64 and P < 0.05 Line of best fit for the Flashing Tunnel: NOFS = 0.95 - 0.14 × NWV, R^2 0.29 and P < 0.05

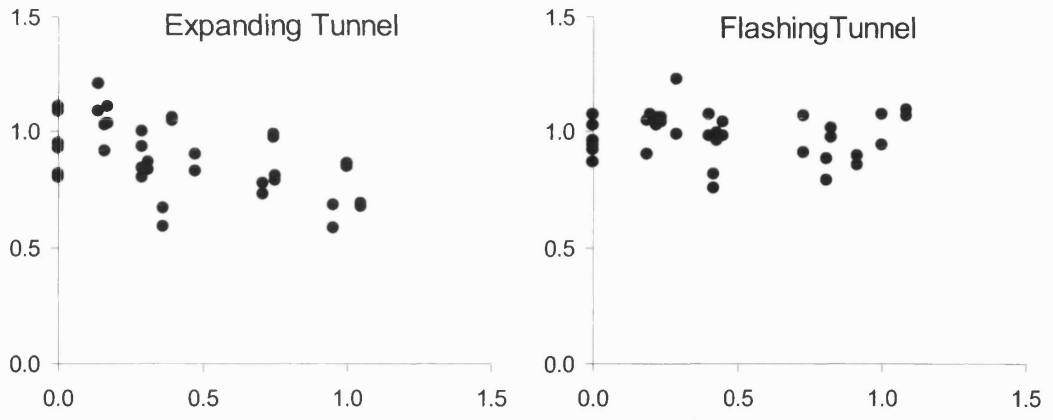

Subject BW Line of best fit for the Expanding Tunnel: NOFS = 0.99 - 0.25 × NWV, R^2 = 0.30 and P < 0.05 Line of best fit for the Flashing Tunnel: NOFS = 1.00 - 0.03 × NWV, R^2 0.01 and P > 0.05

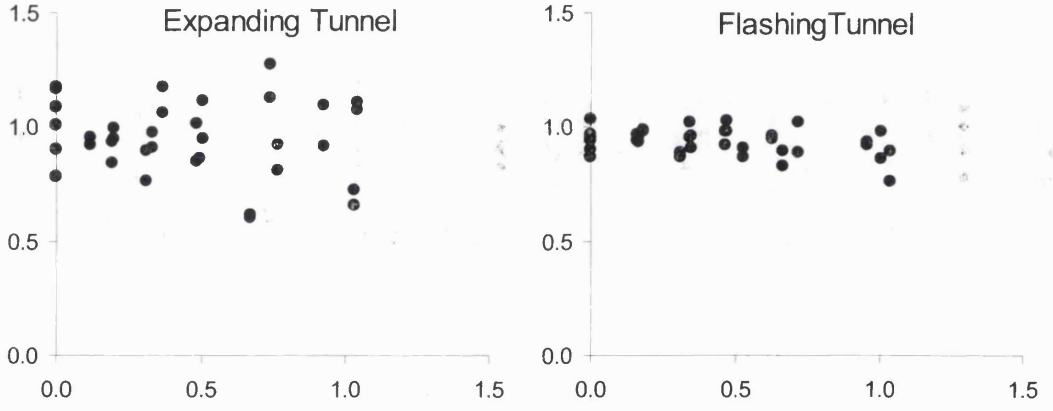

Subject CJ Line of best fit for the Expanding Tunnel: NOFS = 0.98 - 0.07 × NWV, R^2 = 0.02 and P > 0.05 Line of best fit for the Flashing Tunnel: NOFS = 0.96 - 0.06 × NWV, R^2 0.11 and P < 0.05

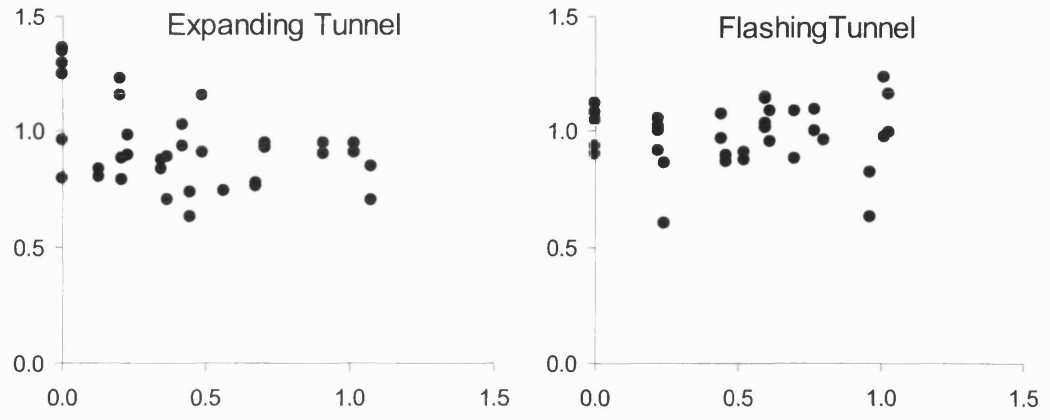

Subject JN Line of best fit for the Expanding Tunnel: NOFS = 1.03 - 0.24 × NWV, R^2 = 0.18 and P < 0.05 Line of best fit for the Flashing Tunnel: NOFS = 0.98 + 0.00 × NWV, R^2 0.00 and P > 0.05

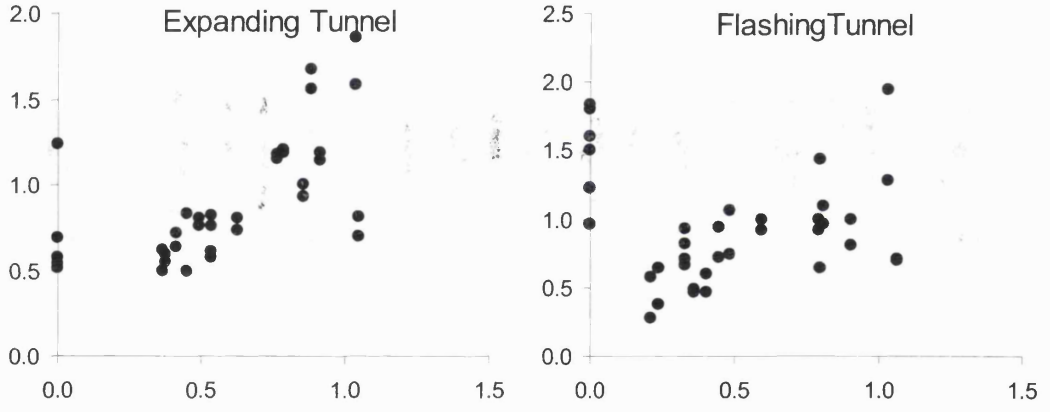

Subject LH Line of best fit for the Expanding Tunnel: NOFS = 0.58 + 0.60 × NWV, R^2 = 0.30 and P < 0.05 Line of best fit for the Flashing Tunnel: NOFS = 0.97 - 0.06 × NWV, R^2 0.00 and P > 0.05

Extension to other Motor Activities

Normalised optic flow speed (NOFS) plotted against normalised walking velocity (NWV), for details see Figure 36.

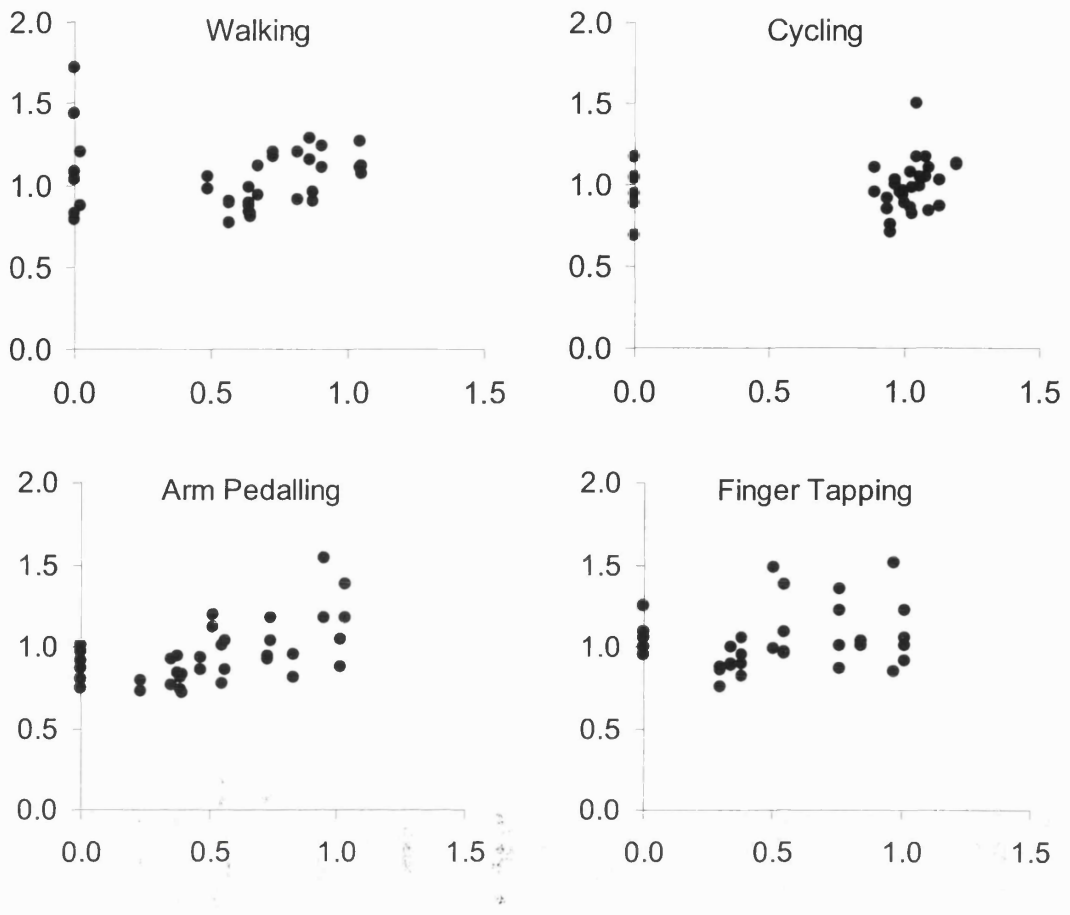

Subject AB Line of best fit during Walking: NOFS = 1.05 - 0.02 × NWV, R^2 = 0.00 and P > 0.05 Line of best fit during Cycling: NOFS = 0.94 + 0.05 × NWV, R^2 = 0.02 and P > 0.05 Line of best fit during Arm Pedalling: NOFS = 0.79 + 0.31 × NWV, R^2 = 0.31 and P < 0.05 Line of best fit during Finger Tapping: NOFS = 0.96 + 0.13 × NWV, R^2 0.05 and P > 0.05

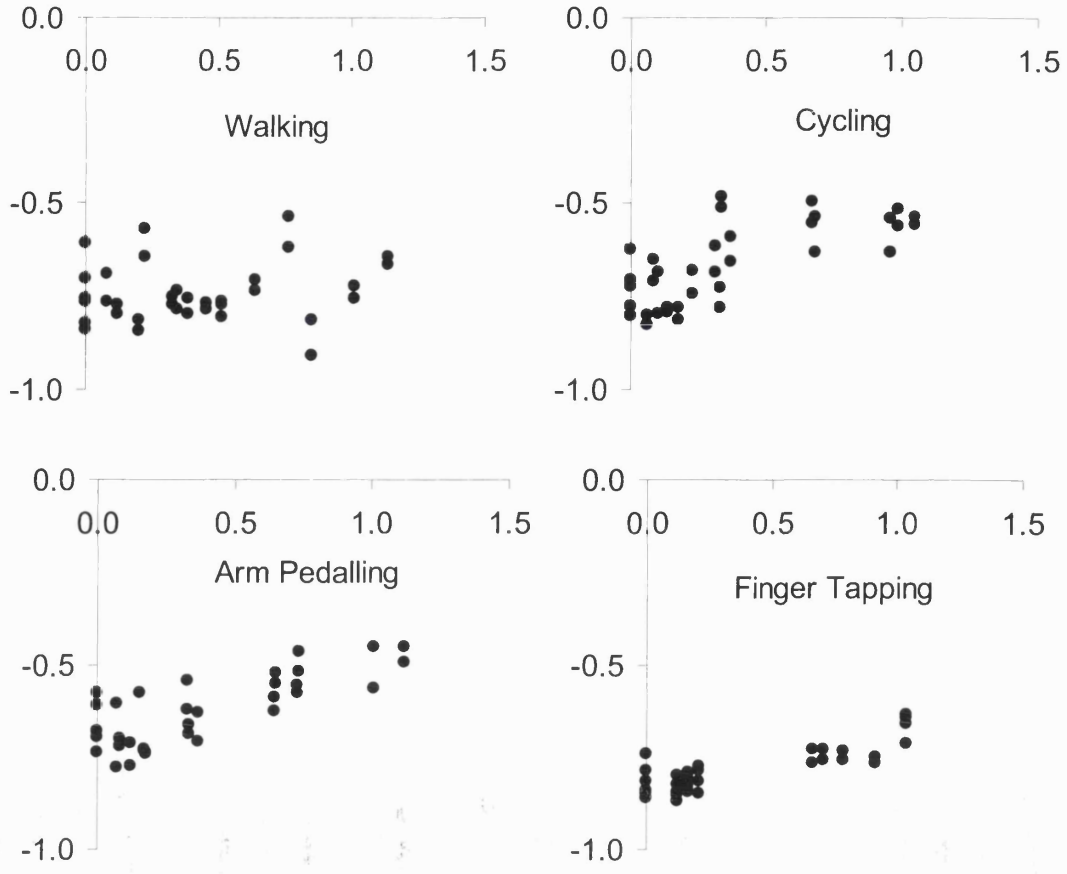

Subject AC Line of best fit during Walking: NOFS = -0.76 + 0.04 × NWV, R^2 = 0.03 and P > 0.05 Line of best fit during Cycling: NOFS = -0.75 + 0.22 × NWV, R^2 = 0.52 and P < 0.05 Line of best fit during Arm Pedalling: NOFS = -0.71 + 0.21 × NWV, R^2 = 0.60 and P < 0.05 Line of best fit during Finger Tapping: NOFS = -0.84 + 0.14 × NWV, R^2 0.71 and P < 0.05

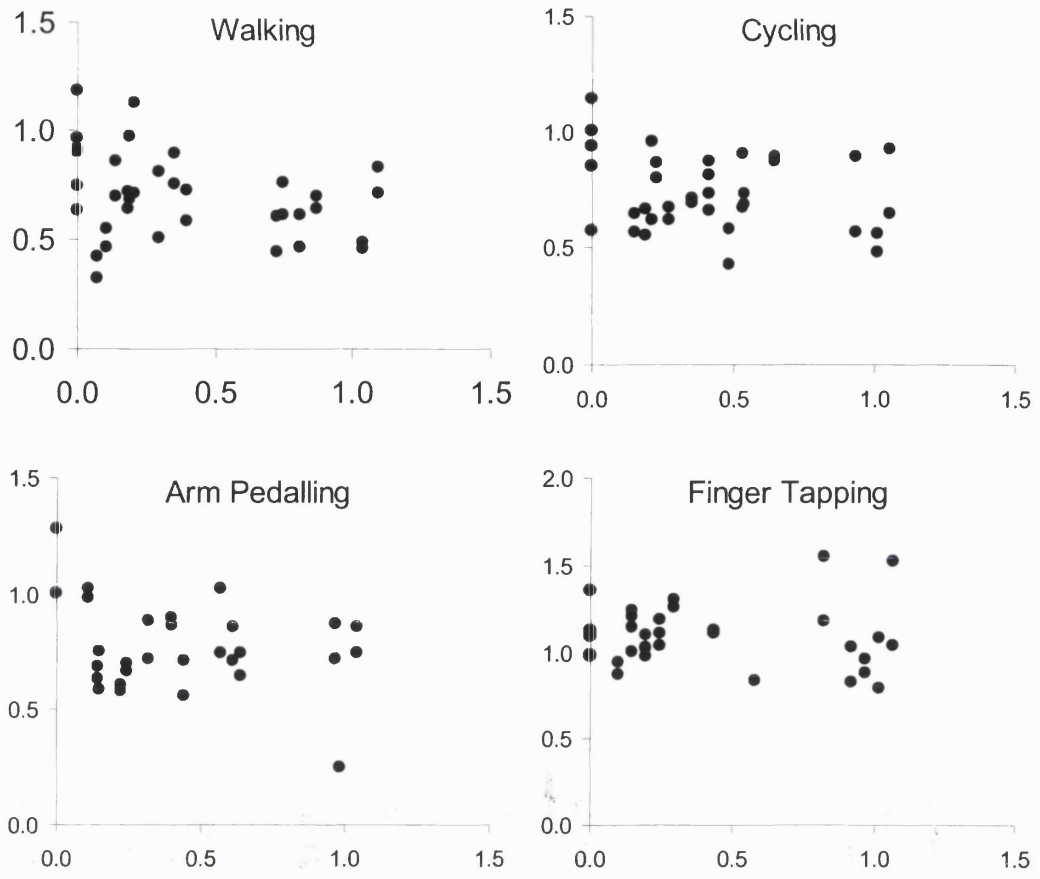

Subject BD Line of best fit during Walking: NOFS = 0.76 - 0.16 × NWV, R^2 = 0.09 and P > 0.05 Line of best fit during Cycling: NOFS = 0.77 - 0.09 × NWV, R^2 = 0.03 and P > 0.05 Line of best fit during Arm Pedalling: NOFS = 0.84 - 0.17 × NWV, R^2 = 0.08 and P > 0.05 Line of best fit during Finger Tapping: NOFS = 1.10 - 0.02 × NWV, R^2 0.00 and P > 0.05

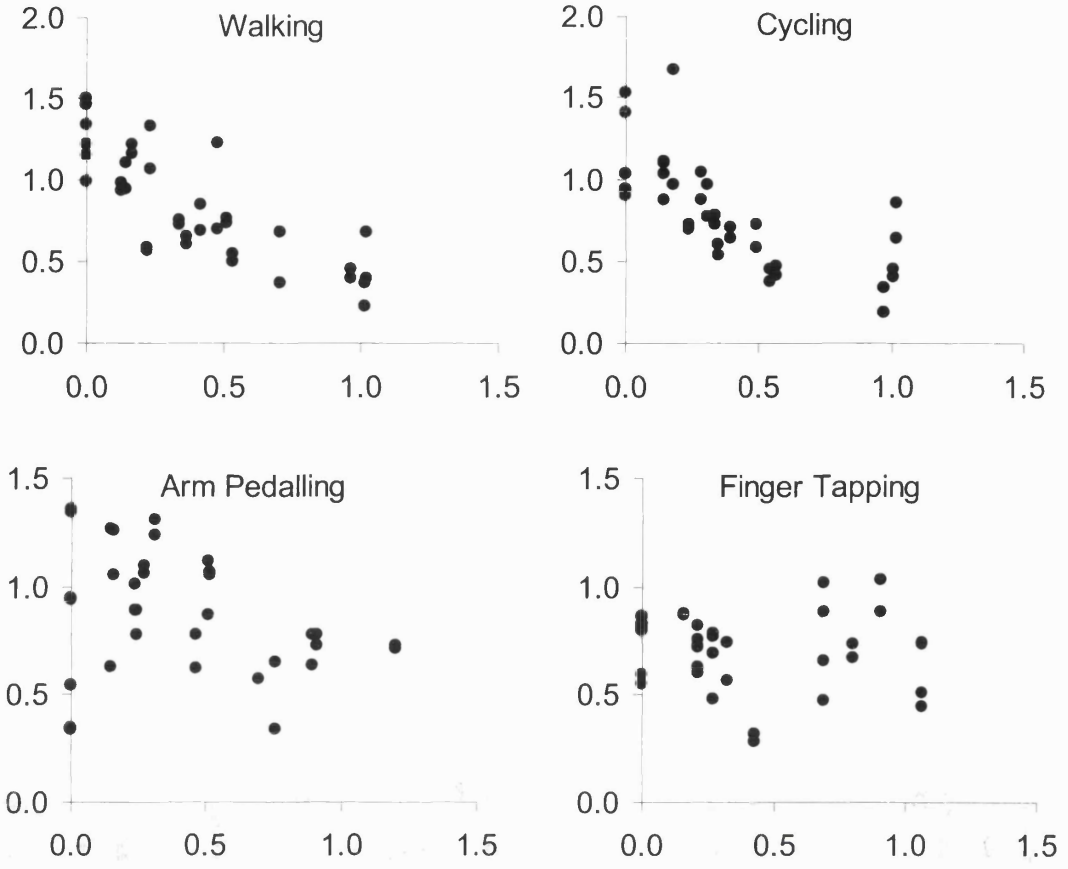

Subject BKW Line of best fit during Walking: NOFS = 1.16 - 0.81 × NWV, R^2 = 0.63 and P < 0.05 Line of best fit during Cycling: NOFS = 1.07 - 0.71 × NWV, R^2 = 0.49 and P < 0.05 Line of best fit during Arm Pedalling: NOFS = 0.94 - 0.20 × NWV, R^2 = 0.06 and P > 0.05 Line of best fit during Finger Tapping: NOFS = 0.72 - 0.03 × NWV, R^2 0.00 and P > 0.05

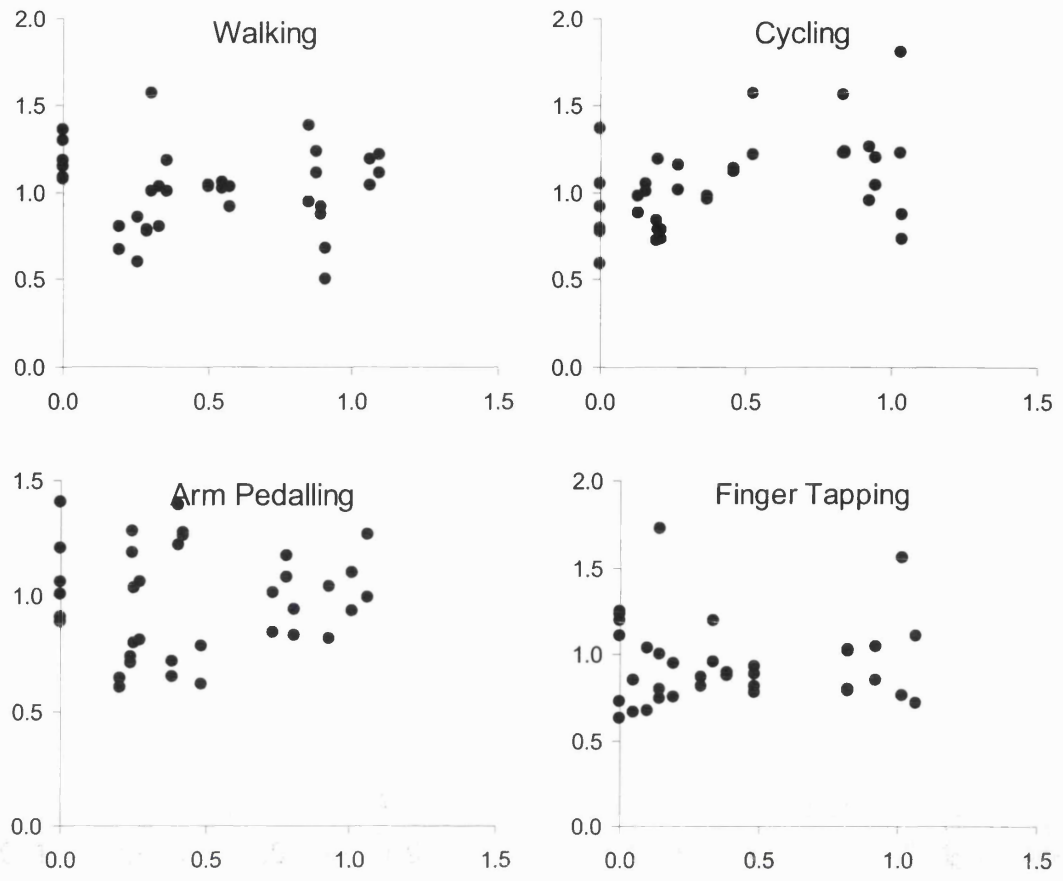

Subject CH Line of best fit during Walking: NOFS = 1.03 - 0.03 × NWV, R^2 = 0.00 and P > 0.05 Line of best fit during Cycling: NOFS = 0.91 + 0.32 × NWV, R^2 = 0.21 and P < 0.05 Line of best fit during Arm Pedalling: NOFS = 0.97 + 0.02 × NWV, R^2 = 0.00 and P > 0.05 Line of best fit during Finger Tapping: NOFS = 0.94 + 0.01 × NWV, R^2 0.00 and P > 0.05

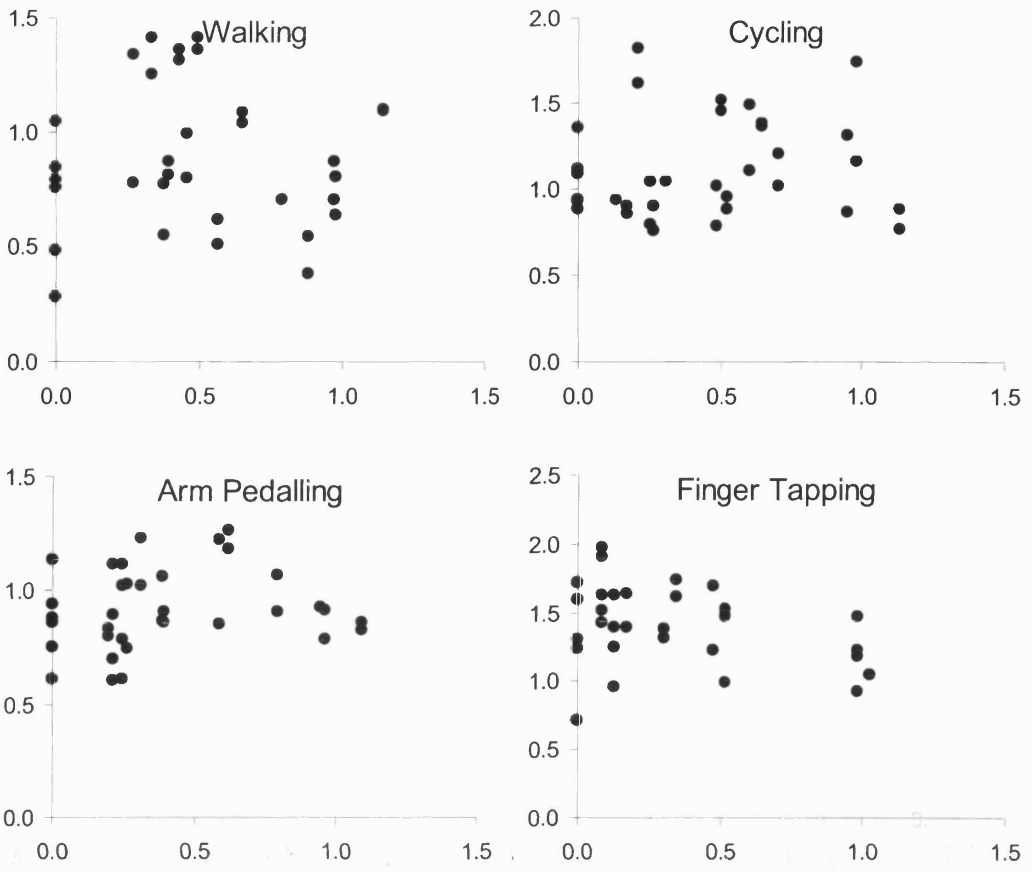

Subject DS Line of best fit during Walking: NOFS = 0.89 - 0.02 × NWV, R^2 = 0.00 and P > 0.05 Line of best fit during Cycling: NOFS = 1.07 + 0.09 × NWV, R^2 = 0.01 and P > 0.05 Line of best fit during Arm Pedalling: NOFS = 0.89 + 0.07 × NWV, R^2 = 0.02 and P > 0.05 Line of best fit during Finger Tapping: NOFS = 1.50 - 0.29 × NWV, R^2 0.12 and P < 0.05

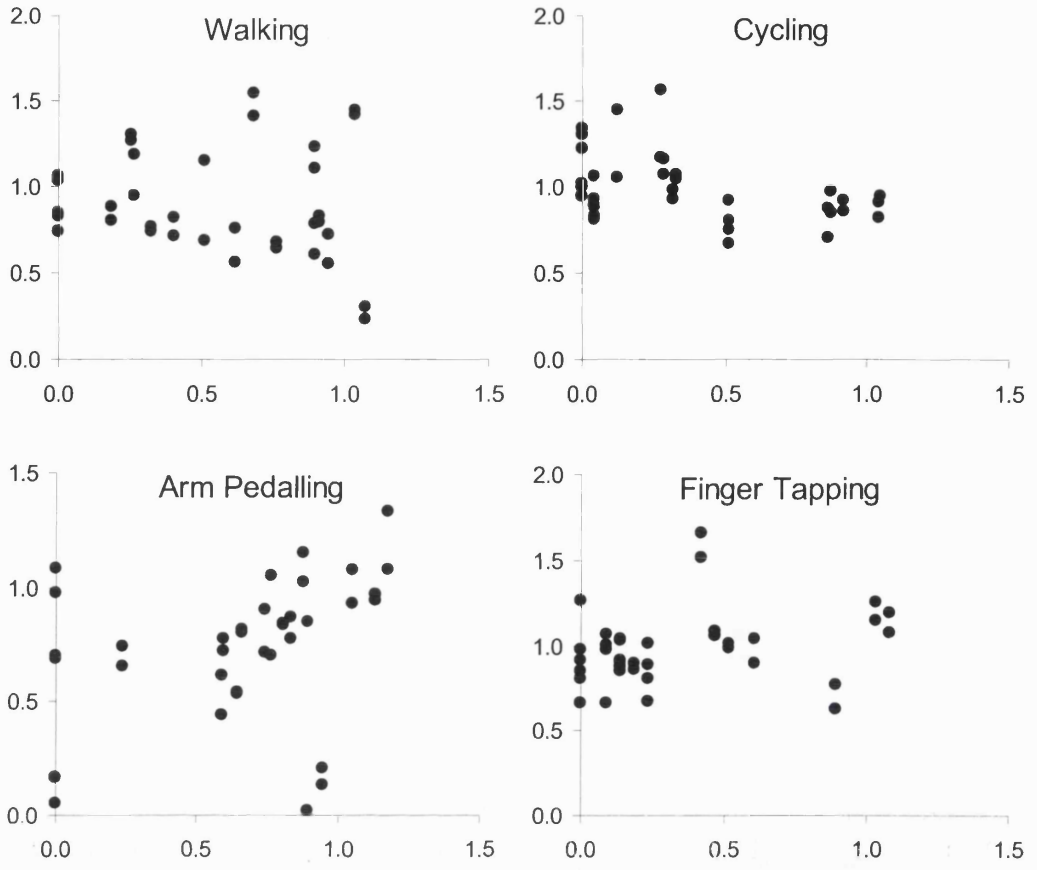

Subject EB Line of best fit during Walking: NOFS = 0.95 - 0.11 × NWV, R^2 = 0.02 and P > 0.05 Line of best fit during Cycling: NOFS = 1.08 - 0.22 × NWV, R^2 = 0.18 and P < 0.05 Line of best fit during Arm Pedalling: NOFS = 0.57 + 0.26 × NWV, R^2 = 0.09 and P > 0.05 Line of best fit during Finger Tapping: NOFS = 0.92 + 0.16 × NWV, R^2 0.07 and P > 0.05

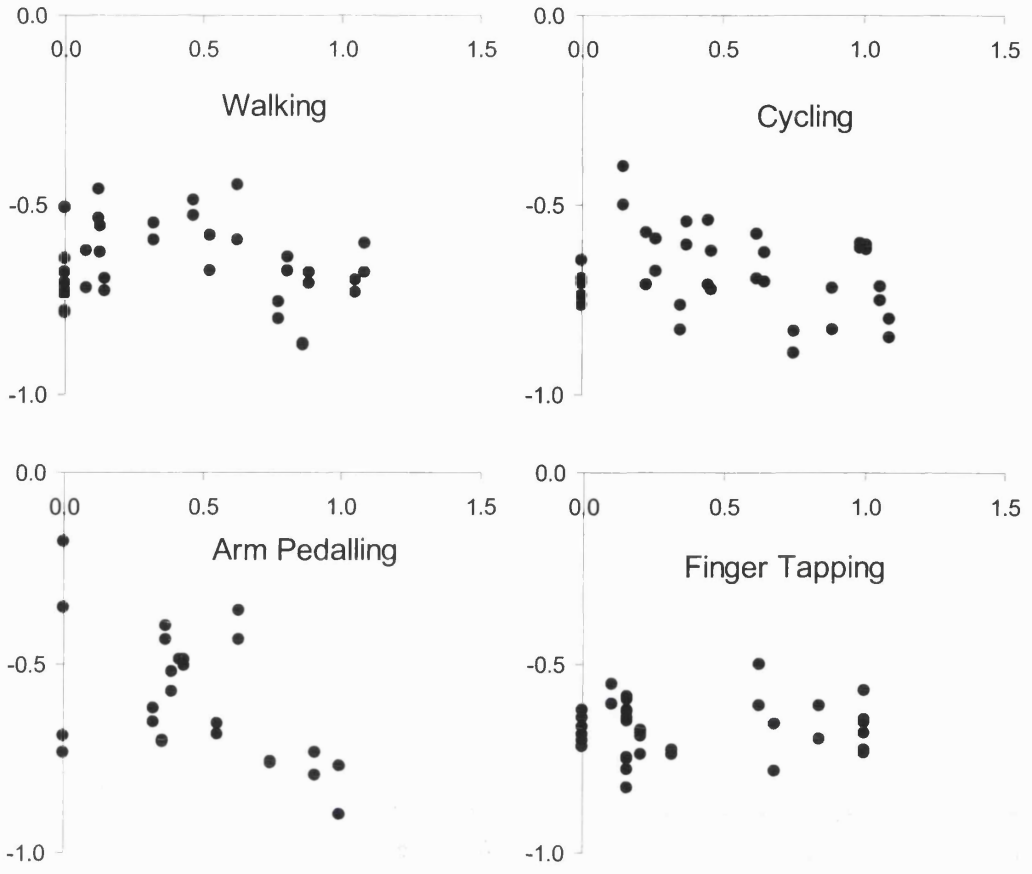

Subject EJ Line of best fit during Walking: NOFS = -0.64 - 0.05 × NWV, R^2 = 0.03 and P > 0.05 Line of best fit during Cycling: NOFS = -0.64 - 0.07 × NWV, R^2 = 0.06 and P > 0.05 Line of best fit during Arm Pedalling: NOFS = -0.45 - 0.31 × NWV, R^2 = 0.28 and P < 0.05 Line of best fit during Finger Tapping: NOFS = -0.68 + 0.01 × NWV, R^2 0.00 and P > 0.05

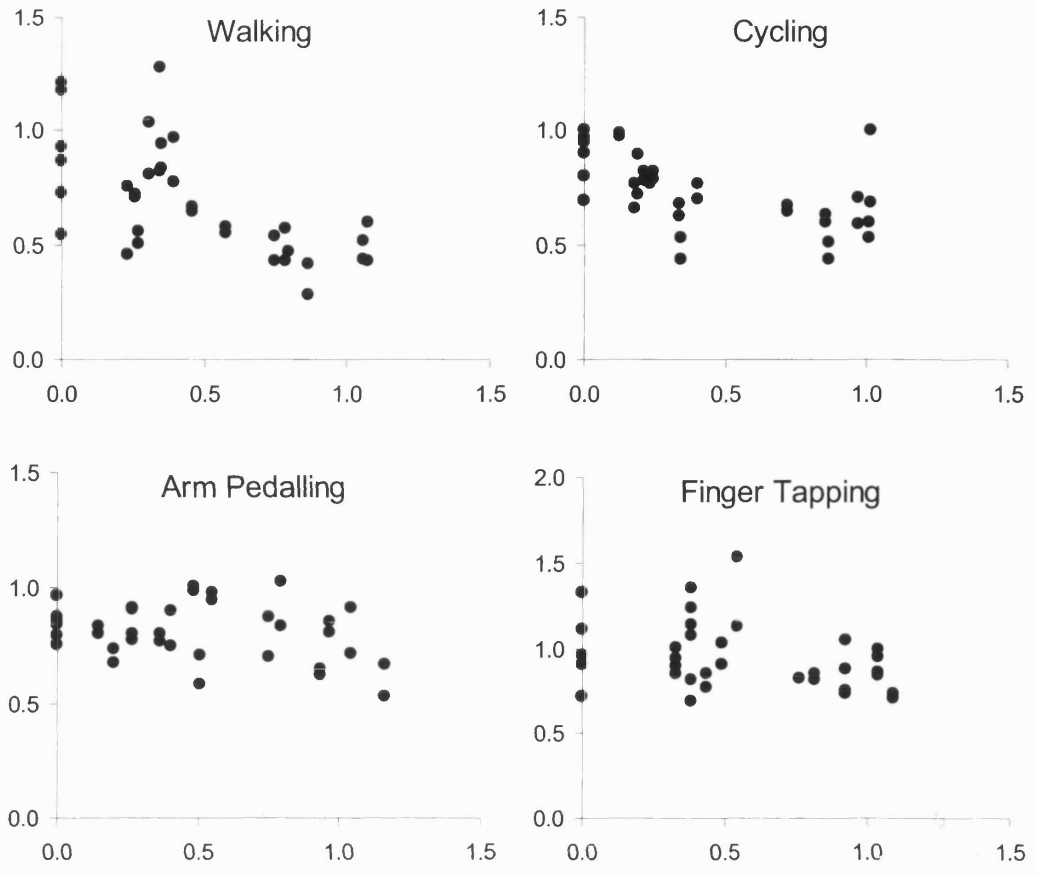

Subject EM Line of best fit during Walking: NOFS = 0.91 - 0.47 × NWV, R^2 = 0.42 and P < 0.05 Line of best fit during Cycling: NOFS = 0.84 - 0.24 × NWV, R^2 = 0.30 and P < 0.05 Line of best fit during Arm Pedalling: NOFS = 0.86 - 0.09 × NWV, R^2 = 0.07 and P > 0.05 Line of best fit during Finger Tapping: NOFS = 1.02 - 0.14 × NWV, R^2 0.07 and P > 0.05

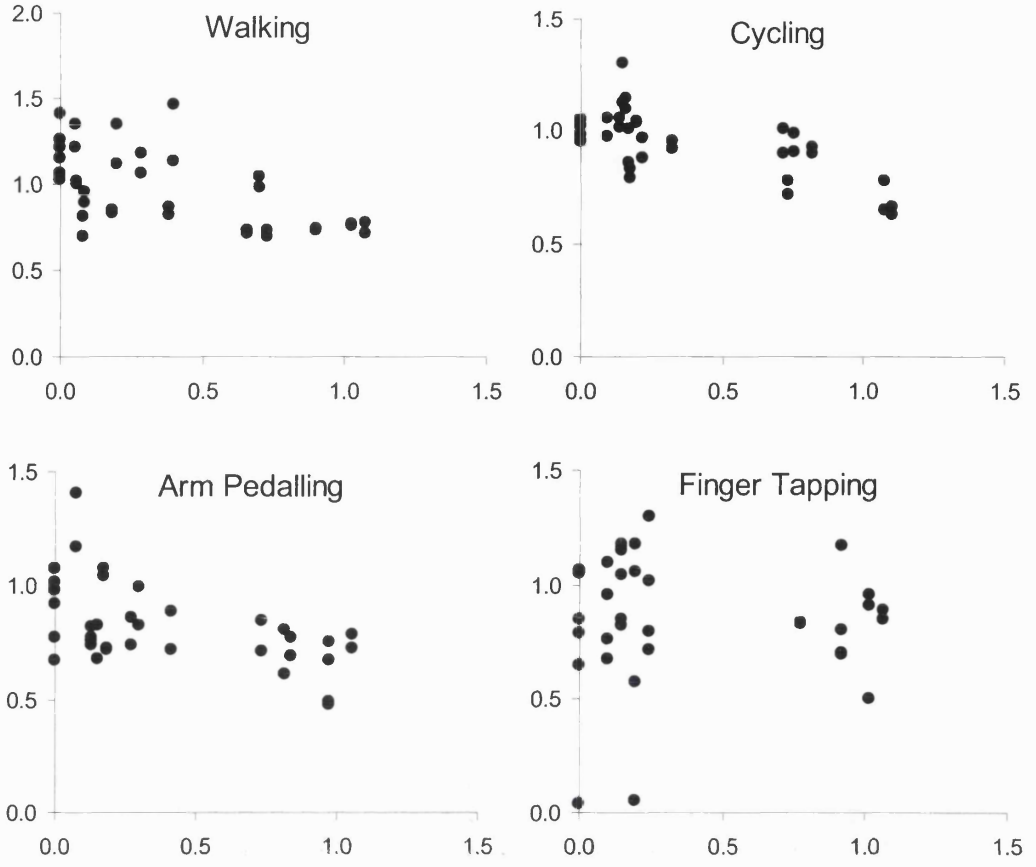

Subject EW Line of best fit during Walking: NOFS = 1.11 - 0.37 × NWV, R^2 = 0.35 and P < 0.05 Line of best fit during Cycling: NOFS = 1.04 - 0.27 × NWV, R^2 = 0.47 and P < 0.05 Line of best fit during Arm Pedalling: NOFS = 0.93 - 0.26 × NWV, R^2 = 0.28 and P < 0.05 Line of best fit during Finger Tapping: NOFS = 0.87 - 0.01 × NWV, R^2 0.00 and P > 0.05

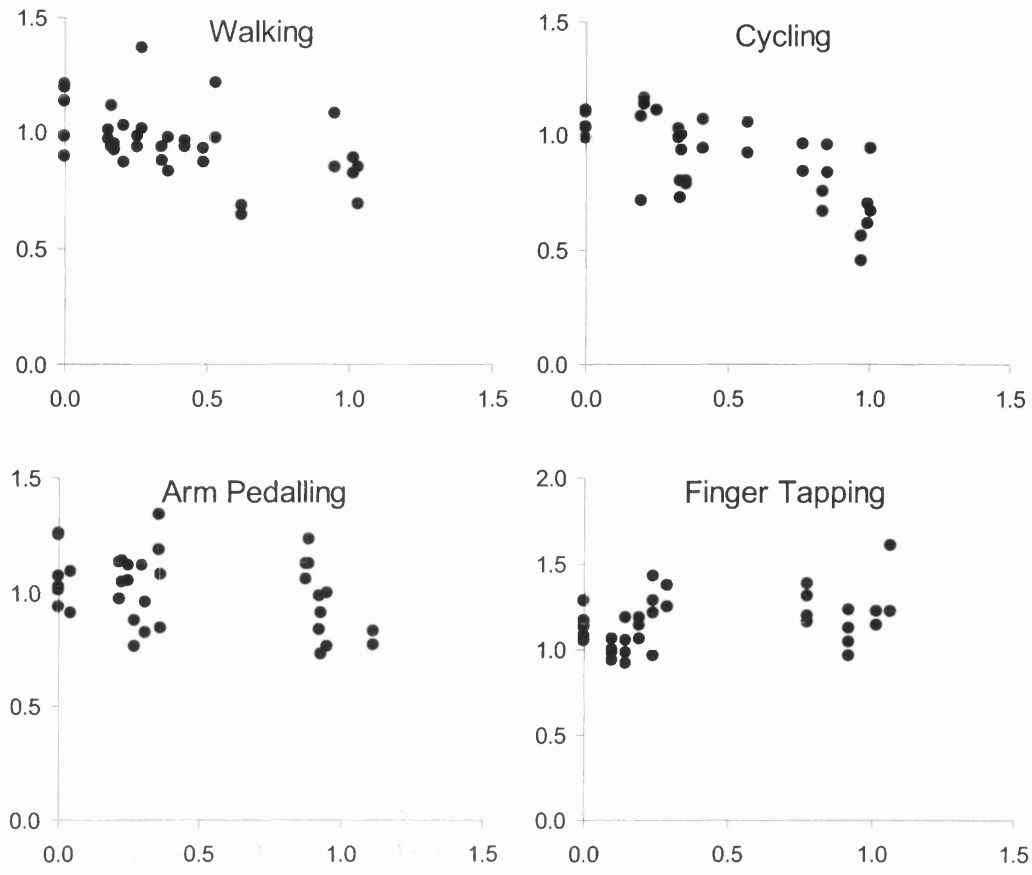

Subject HP Line of best fit during Walking: NOFS = 1.05 - 0.23 × NWV, R^2 = 0.25 and P < 0.05 Line of best fit during Cycling: NOFS = 1.08 - 0.37 × NWV, R^2 = 0.46 and P < 0.05 Line of best fit during Arm Pedalling: NOFS = 1.08 - 0.15 × NWV, R^2 = 0.13 and P < 0.05 Line of best fit during Finger Tapping: NOFS = 1.11 + 0.13 × NWV, R^2 0.12 and P < 0.05

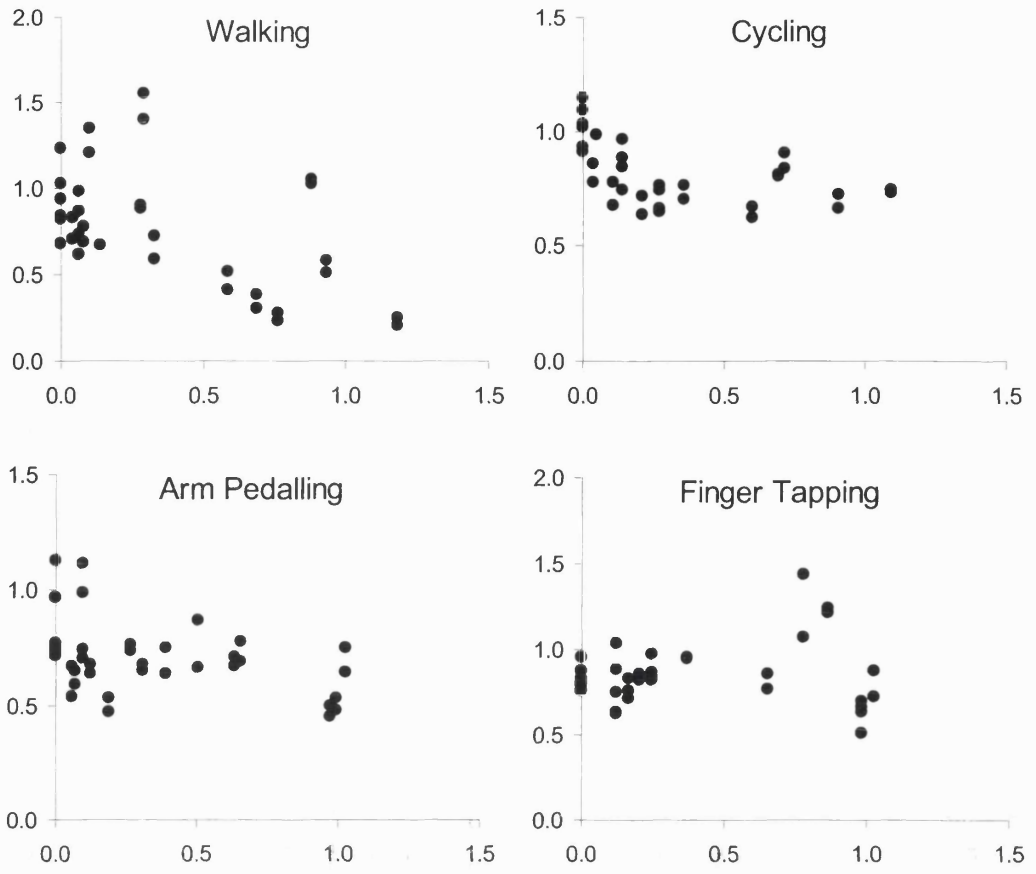

Subject JG Line of best fit during Walking: NOFS = 0.93 - 0.48 × NWV, R^2 = 0.29 and P < 0.05 Line of best fit during Cycling: NOFS = 0.88 - 0.20 × NWV, R^2 = 0.24 and P < 0.05 Line of best fit during Arm Pedalling: NOFS = 0.77 - 0.19 × NWV, R^2 = 0.17 and P < 0.05 Line of best fit during Finger Tapping: NOFS = 0.82 + 0.06 × NWV, R^2 0.02 and P > 0.05

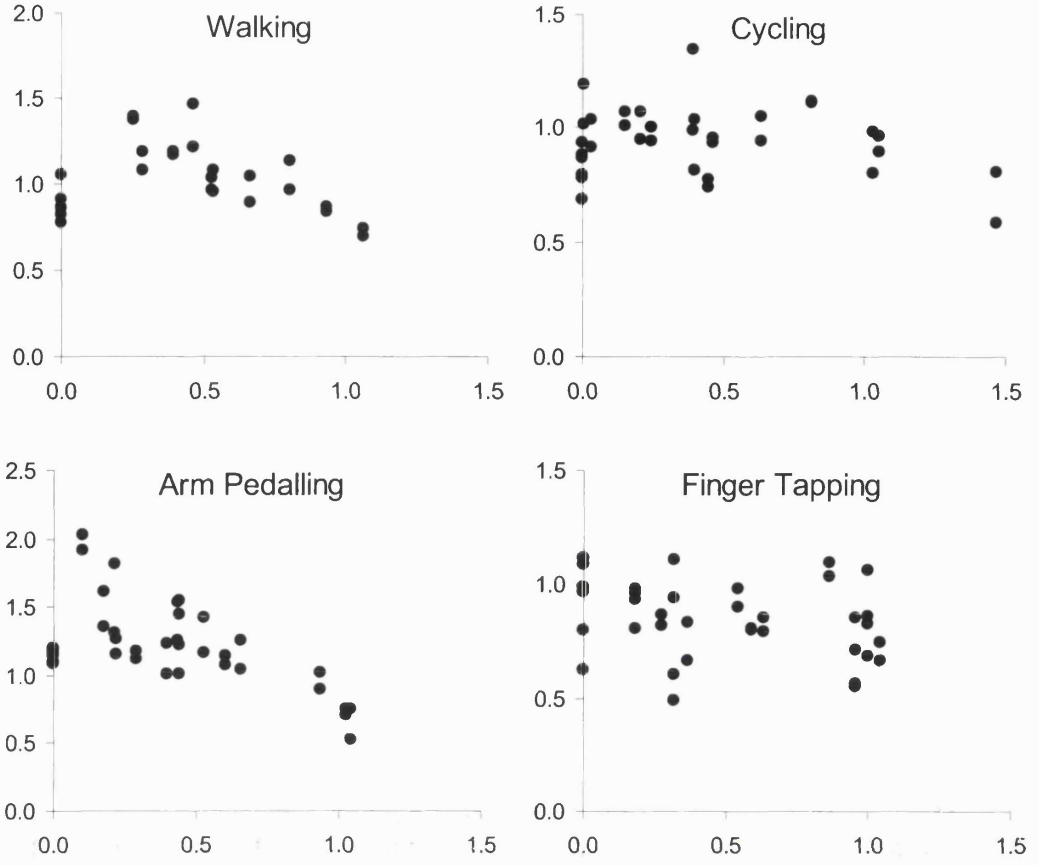

Subject KL Line of best fit during Walking: NOFS = 1.08 - 0.12 × NWV, R^2 = 0.04 and P > 0.05 Line of best fit during Cycling: NOFS = 0.98 - 0.12 × NWV, R^2 = 0.13 and P < 0.05 Line of best fit during Arm Pedalling: NOFS = 1.45 - 0.57 × NWV, R^2 = 0.35 and P < 0.05 Line of best fit during Finger Tapping: NOFS = 0.90 - 0.12 × NWV, R^2 0.07 and P > 0.05

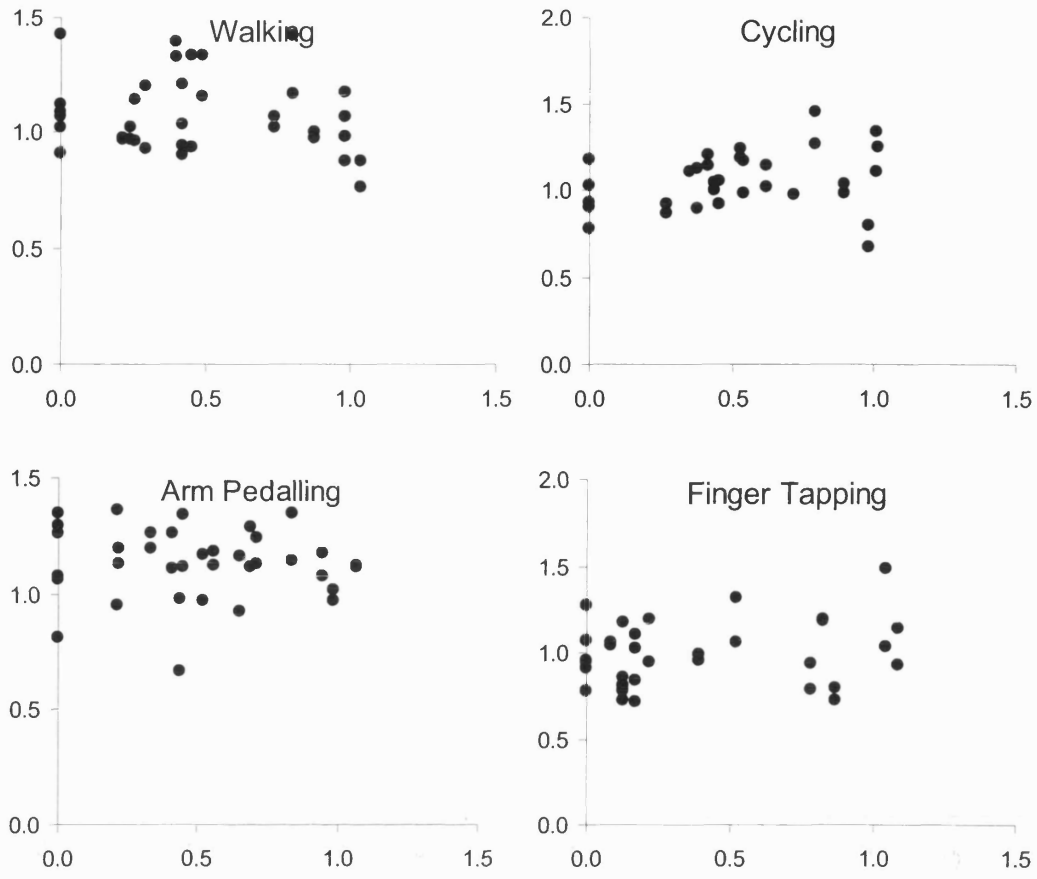

Subject KR Line of best fit during Walking: NOFS = 1.12 - 0.08 × NWV, R^2 = 0.03 and P > 0.05 Line of best fit during Cycling: NOFS = 0.97 + 0.16 × NWV, R^2 = 0.10 and P > 0.05 Line of best fit during Arm Pedalling: NOFS = 1.15 - 0.03 × NWV, R^2 = 0.01 and P > 0.05 Line of best fit during Finger Tapping: NOFS = 0.95 + 0.11 × NWV, R^2 0.05 and P > 0.05

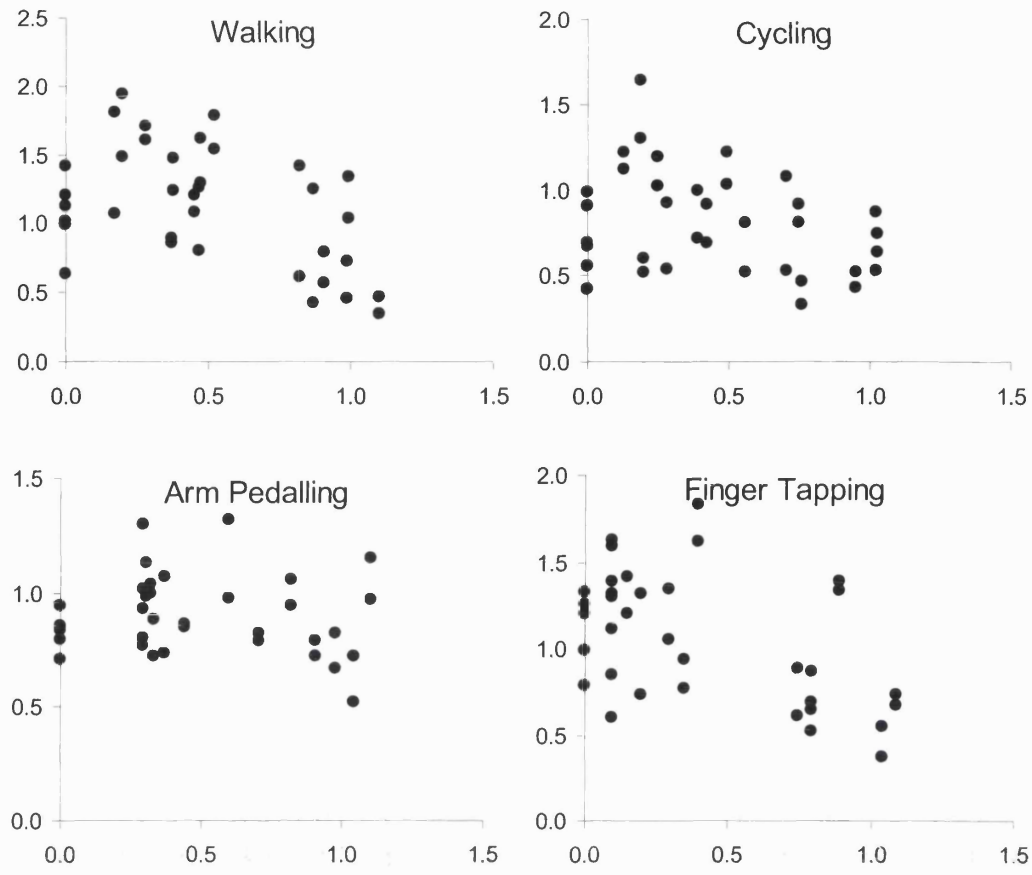

Subject LO Line of best fit during Walking: NOFS = 1.41 - 0.56 × NWV, R^2 = 0.22 and P < 0.05 Line of best fit during Cycling: NOFS = 0.93 - 0.26 × NWV, R^2 = 0.09 and P > 0.05 Line of best fit during Arm Pedalling: NOFS = 0.92 - 0.05 × NWV, R^2 = 0.01 and P > 0.05 Line of best fit during Finger Tapping: NOFS = 1.25 - 0.49 × NWV, R^2 0.25 and P < 0.05

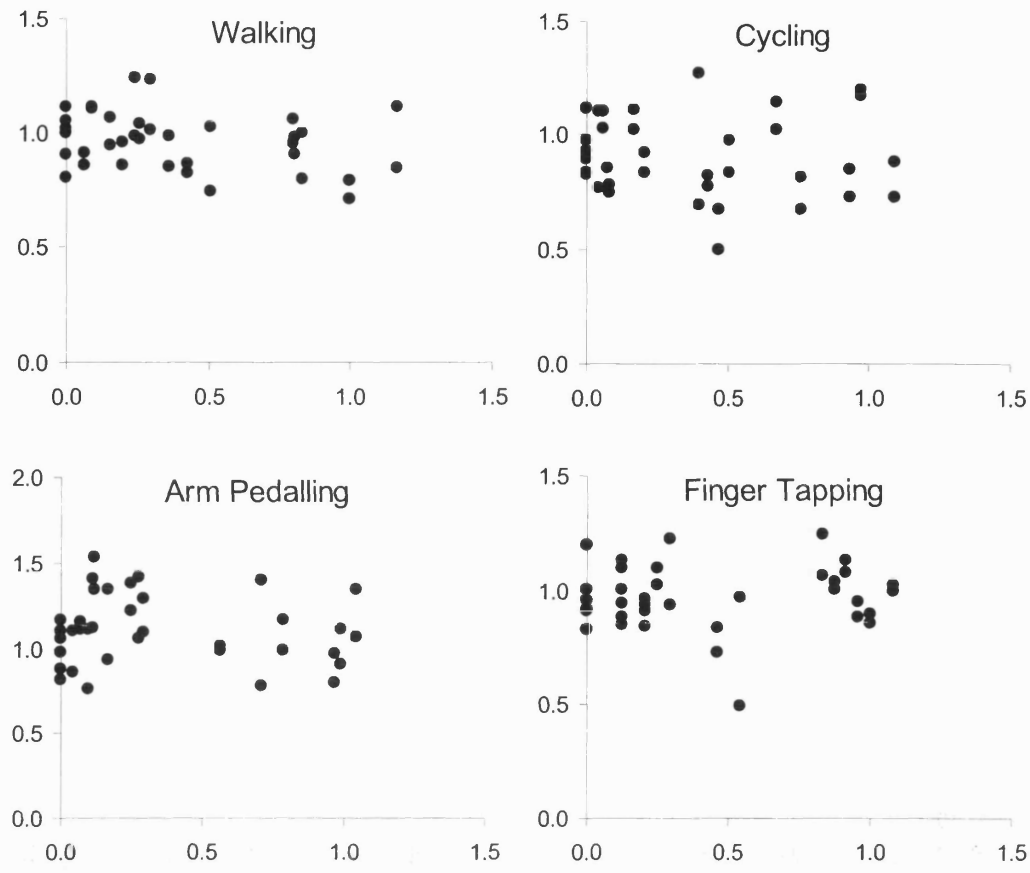

Subject MDB Line of best fit during Walking: NOFS = 1.00 - 0.10 × NWV, R^2 = 0.08 and P > 0.05 Line of best fit during Cycling: NOFS = 0.91 - 0.02 × NWV, R^2 = 0.00 and P > 0.05 Line of best fit during Arm Pedalling: NOFS = 1.13 - 0.06 × NWV, R^2 = 0.01 and P > 0.05 Line of best fit during Finger Tapping: NOFS = 0.96 + 0.02 × NWV, R^2 0.00 and P > 0.05

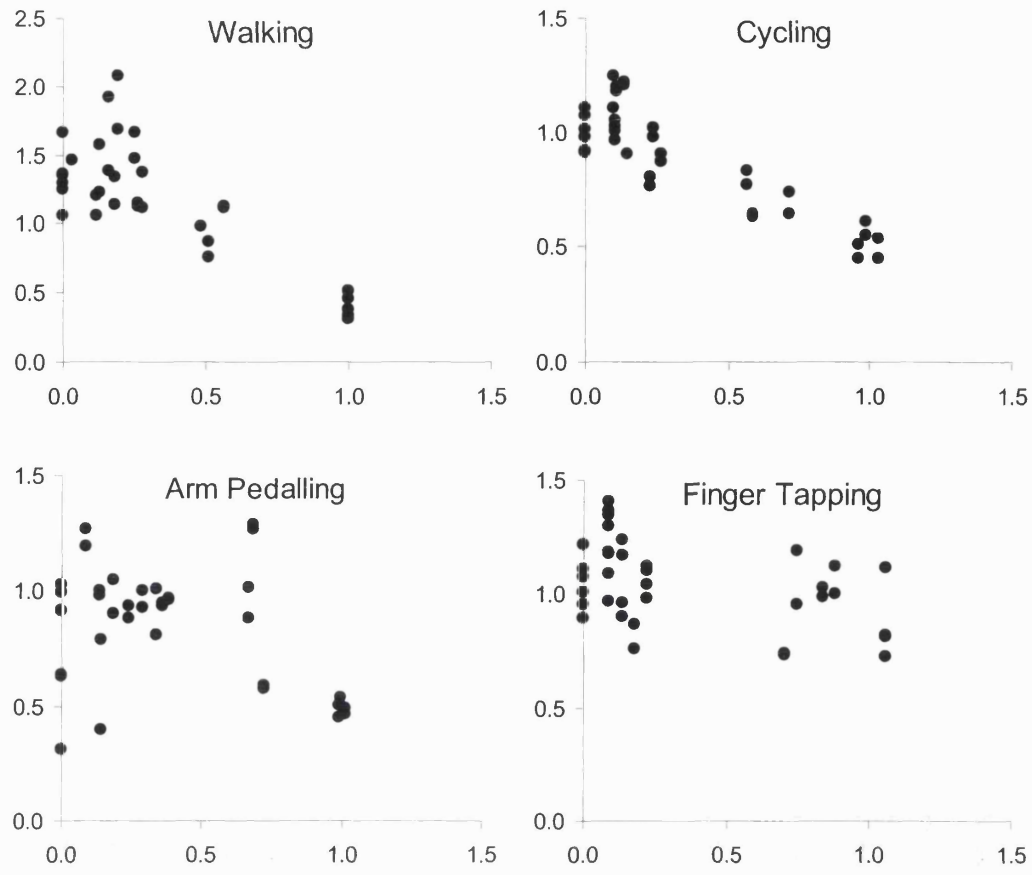

Subject MH Line of best fit during Walking: NOFS = 1.52 - 1.04 × NWV, R^2 = 0.67 and P < 0.05 Line of best fit during Cycling: NOFS = 1.08 - 0.57 × NWV, R^2 = 0.78 and P < 0.05 Line of best fit during Arm Pedalling: NOFS = 0.95 - 0.29 × NWV, R^2 = 0.14 and P < 0.05 Line of best fit during Finger Tapping: NOFS = 1.11 - 0.20 × NWV, R^2 0.18 and P < 0.05

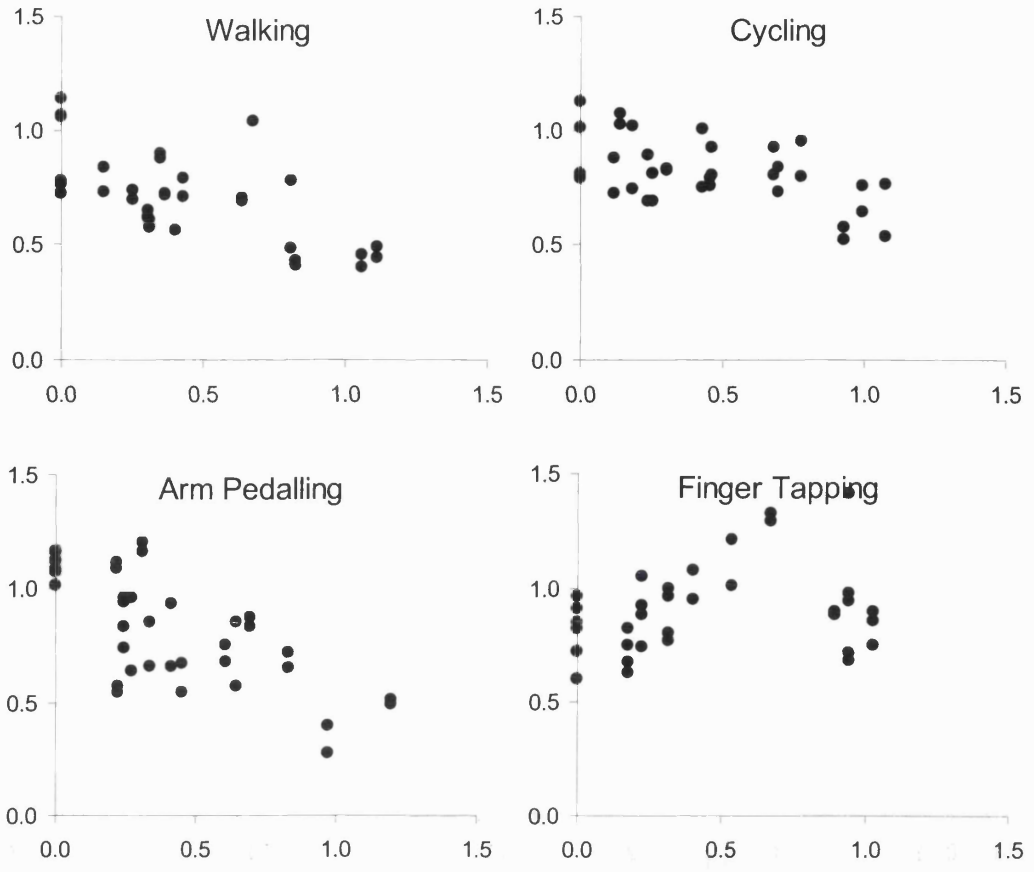

Subject MN Line of best fit during Walking: NOFS = 0.86 - 0.34 × NWV, R^2 = 0.35 and P < 0.05 Line of best fit during Cycling: NOFS = 0.91 - 0.21 × NWV, R^2 = 0.27 and P < 0.05 Line of best fit during Arm Pedalling: NOFS = 1.03 - 0.51 × NWV, R^2 = 0.49 and P < 0.05 Line of best fit during Finger Tapping: NOFS = 0.85 + 0.11 × NWV, R^2 0.05 and P > 0.05

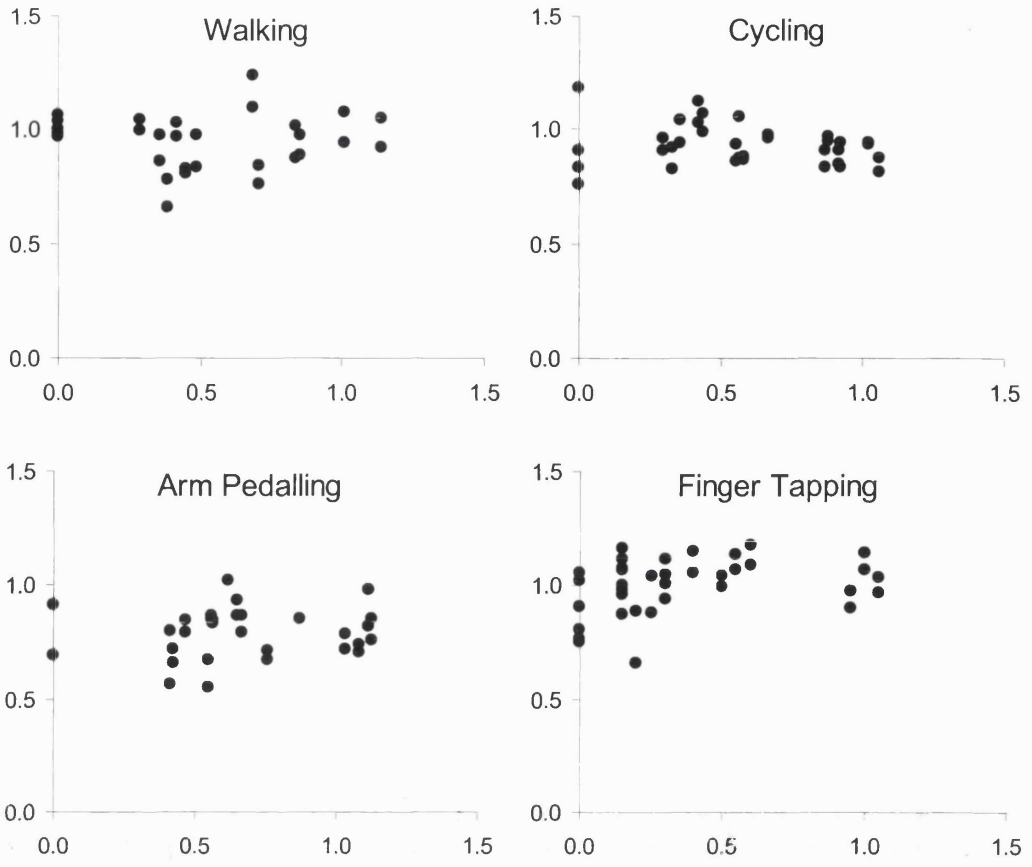

Subject PL Line of best fit during Walking: NOFS = 0.95 - 0.01 × NWV, R^2 = 0.00 and P > 0.05 Line of best fit during Cycling: NOFS = 0.95 - 0.03 × NWV, R^2 = 0.02 and P > 0.05 Line of best fit during Arm Pedalling: NOFS = 0.78 + 0.03 × NWV, R^2 = 0.01 and P > 0.05 Line of best fit during Finger Tapping: NOFS = 0.96 + 0.12 × NWV, R^2 0.10 and P > 0.05

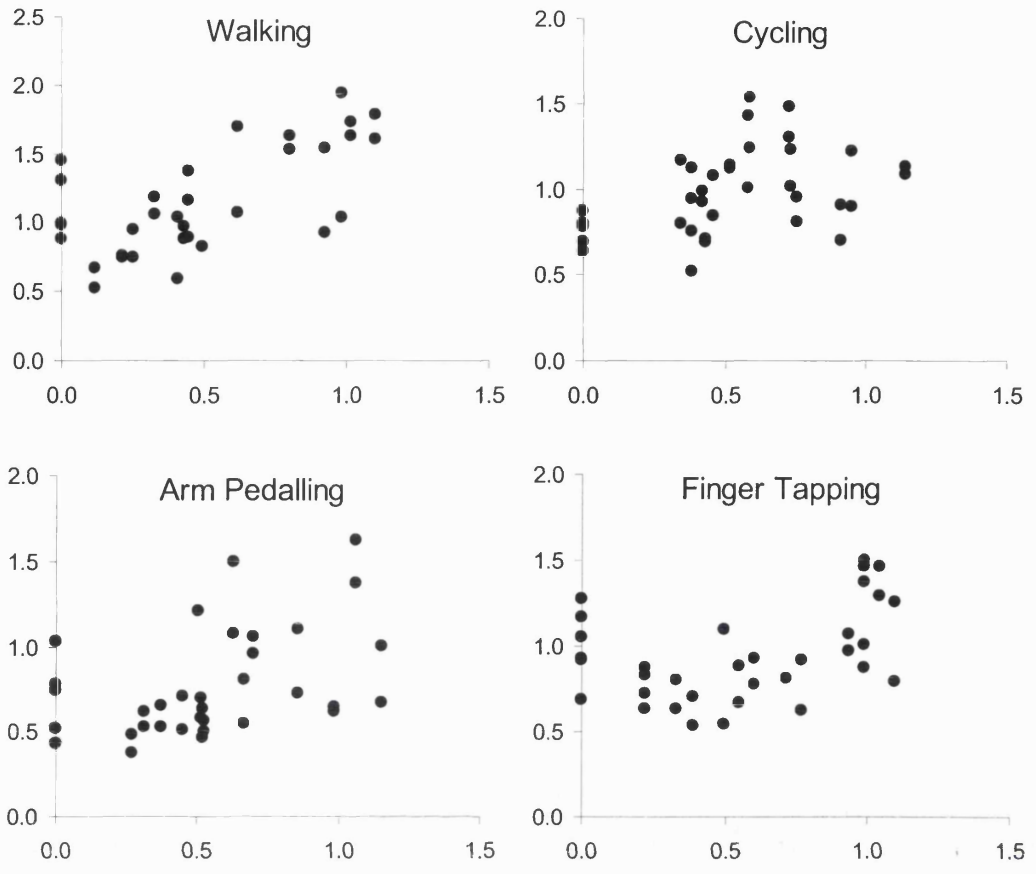

Subject PM Line of best fit during Walking: NOFS = 0.82 + 0.69 × NWV, R^2 = 0.41 and P < 0.05 Line of best fit during Cycling: NOFS = 0.80 + 0.34 × NWV, R^2 = 0.20 and P < 0.05 Line of best fit during Arm Pedalling: NOFS = 0.57 + 0.39 × NWV, R^2 = 0.17 and P < 0.05 Line of best fit during Finger Tapping: NOFS = 0.79 + 0.27 × NWV, R^2 0.15 and P < 0.05

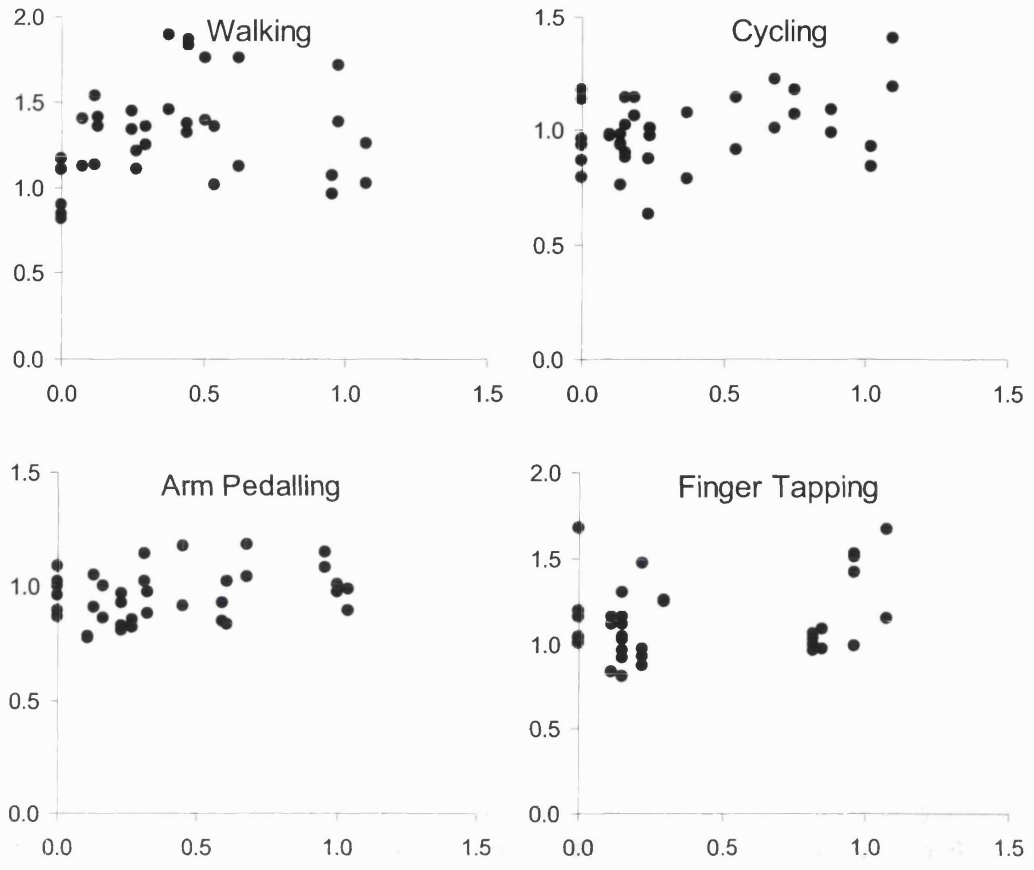

Subject RB Line of best fit during Walking: NOFS = 1.25 + 0.15 × NWV, R^2 = 0.03 and P > 0.05 Line of best fit during Cycling: NOFS = 0.94 + 0.15 × NWV, R^2 = 0.13 and P < 0.05 Line of best fit during Arm Pedalling: NOFS = 0.92 + 0.10 × NWV, R^2 = 0.09 and P > 0.05 Line of best fit during Finger Tapping: NOFS = 1.06 + 0.16 × NWV, R^2 0.07 and P > 0.05

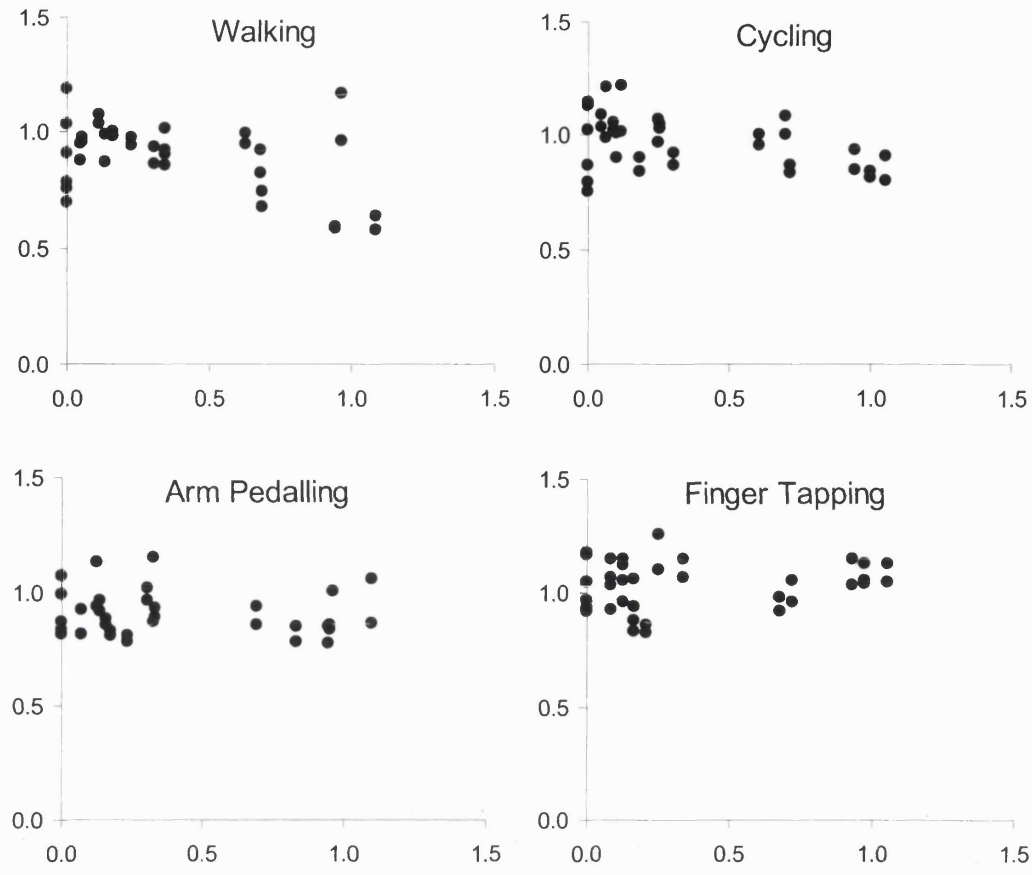

Subject SM Line of best fit during Walking: NOFS = 0.96 - 0.19 × NWV, R^2 = 0.20 and P < 0.05 Line of best fit during Cycling: NOFS = 1.02 - 0.14 × NWV, R^2 = 0.18 and P < 0.05 Line of best fit during Arm Pedalling: NOFS = 0.91 - 0.01 × NWV, R^2 = 0.00 and P > 0.05 Line of best fit during Finger Tapping: NOFS = 1.02 + 0.04 × NWV, R^2 0.02 and P > 0.05

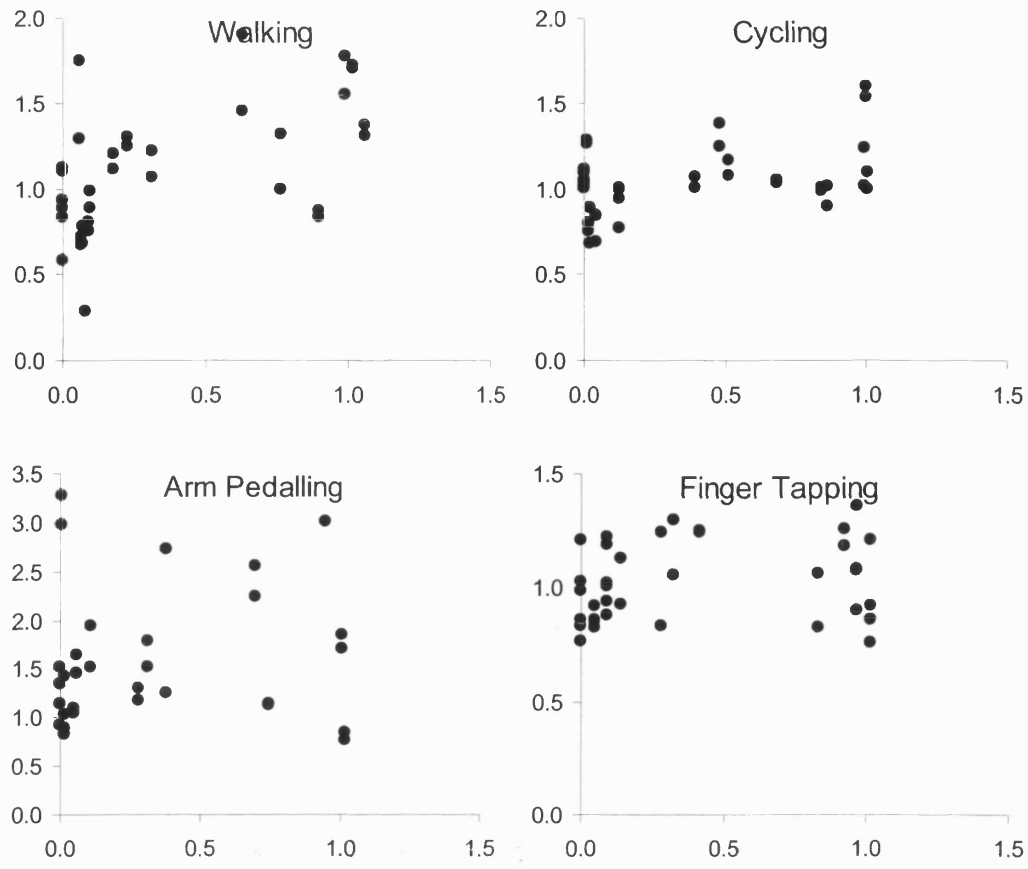

Subject SS Line of best fit during Walking: NOFS = 0.91 + 0.54 × NWV, R^2 = 0.32 and P > 0.05 Line of best fit during Cycling: NOFS = 0.96 + 0.21 × NWV, R^2 = 0.17 and P < 0.05 Line of best fit during Arm Pedalling: NOFS = 1.53 + 0.17 × NWV, R^2 = 0.01 and P > 0.05 Line of best fit during Finger Tapping: NOFS = 0.99 + 0.08 × NWV, R^2 0.03 and P > 0.05

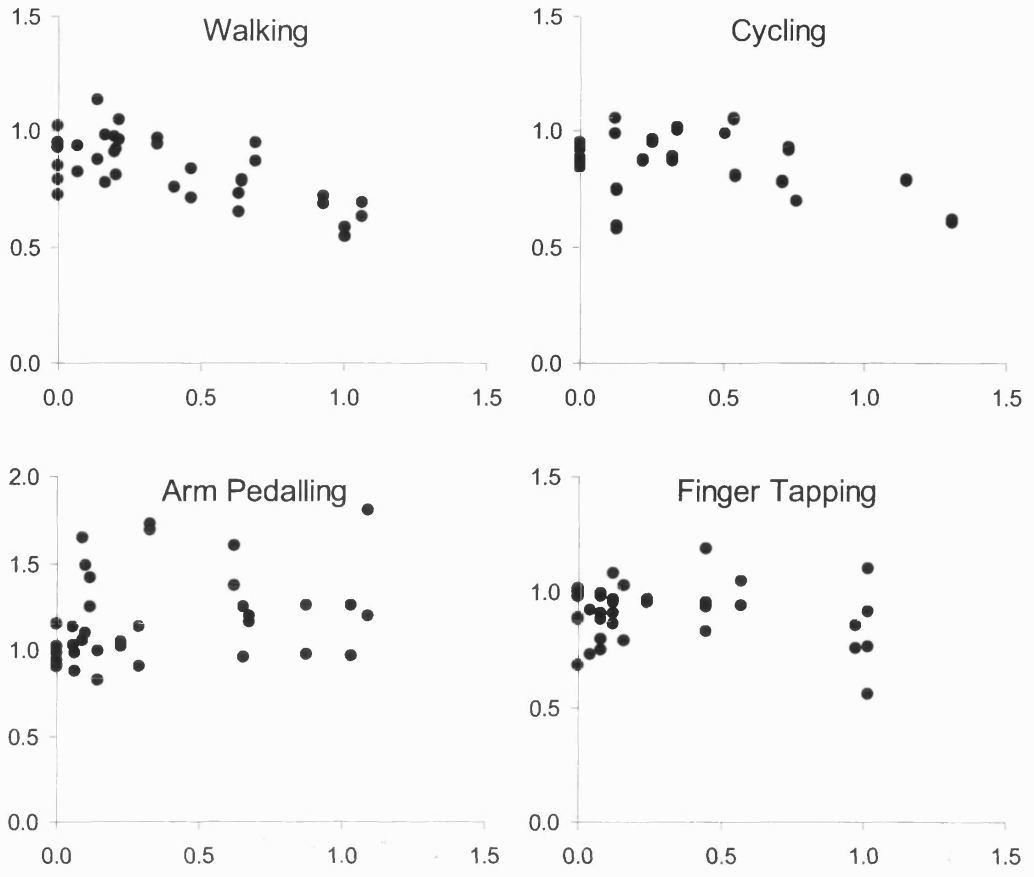

Subject TR Line of best fit during Walking: NOFS = 0.94 - 0.27 × NWV, R^2 = 0.45 and P < 0.05 Line of best fit during Cycling: NOFS = 0.91 - 0.12 × NWV, R^2 = 0.12 and P < 0.05 Line of best fit during Arm Pedalling: NOFS = 1.10 + 0.21 × NWV, R^2 = 0.08 and P > 0.05 Line of best fit during Finger Tapping: NOFS = 0.92 - 0.05 × NWV, R^2 0.02 and P > 0.05

Walking Direction

Normalised optic flow speed (NOFS) plotted against normalised walking velocity (NWV), for details see Figure 38.

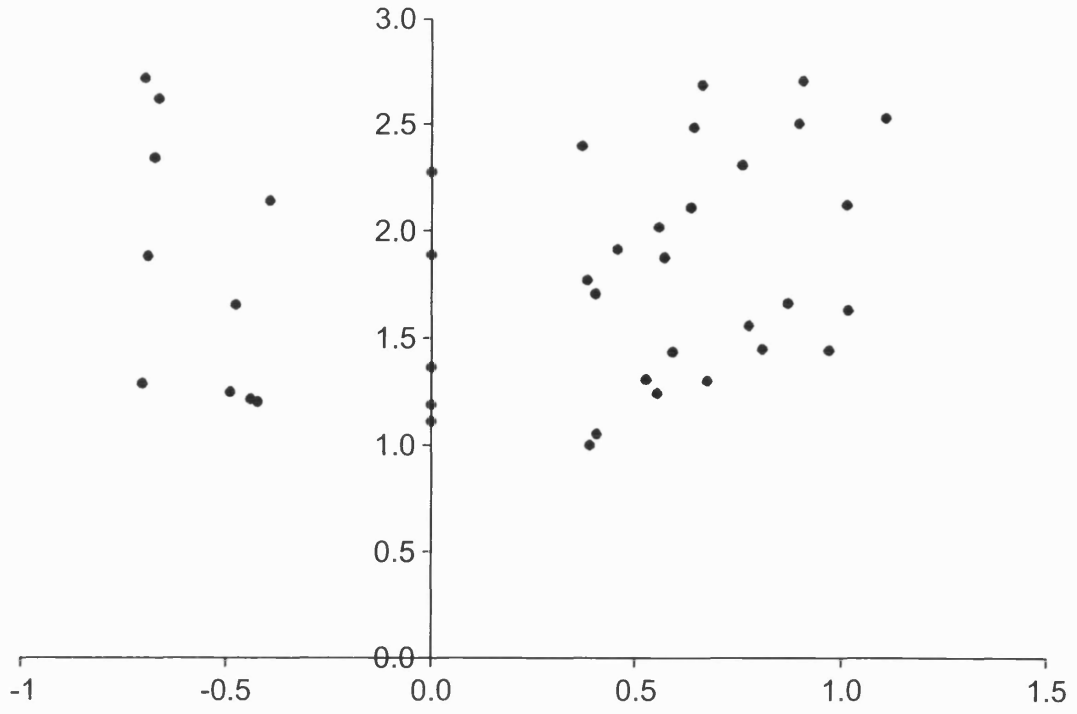

Subject AP Line of best fit during backwards walking: NOFS = 1.47 - 0.70 × NWV, R^2 = 0.13 and P > 0.05 Line of best fit during forwards walking: NOFS = 1.49 + 0.55 × NWV, R^2 = 0.12 and P > 0.05

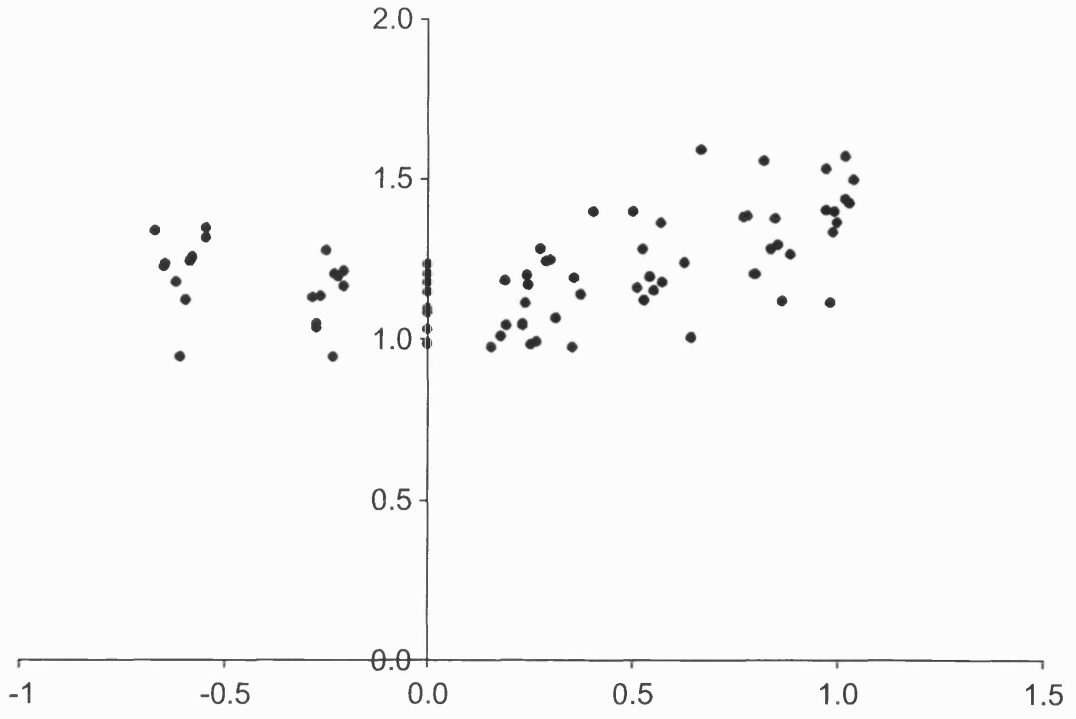

Subject AT Line of best fit during backwards walking: NOFS = 1.10 - 0.18 × NWV, R^2 = 0.18 and P < 0.05 Line of best fit during forwards walking: NOFS = 1.06 + 0.32 × NWV, R^2 = 0.46 and P < 0.05

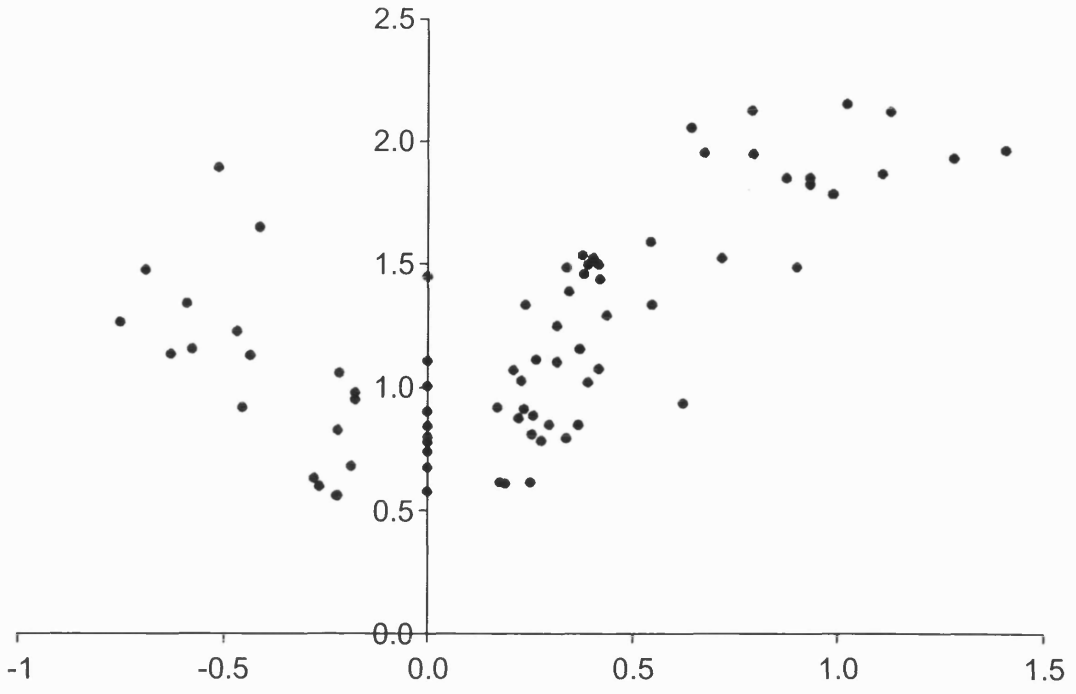

Subject RH (this graph appears as Figure 38) Line of best fit during backwards walking: NOFS = 0.80 - 0.76 × NWV, R^2 = 0.30 and P < 0.05 Line of best fit during forwards walking: NOFS = 0.81 + 1.06 × NWV, R^2 = 0.68 and P < 0.05

Extension to Other Optic flow Patterns

Normalised optic flow speed (NOFS) plotted against normalised walking velocity (NWV).

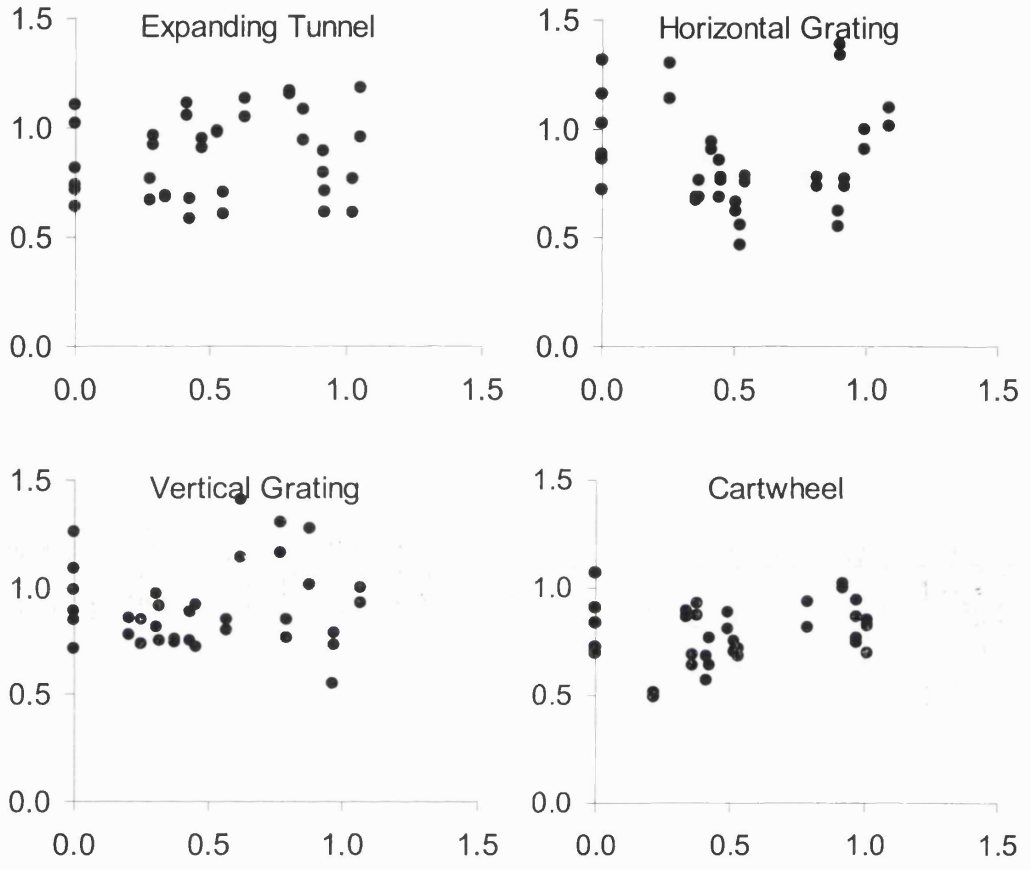

Subject DT Line of best fit for the Expanding Tunnel: NOFS = 0.83 + 0.08 × NWV, R^2 = 0.02 and P > 0.05 Line of best fit for the Horizontal Grating: NOFS = 0.88 - 0.04 × NWV, R^2 = 0.00 and P > 0.05 Line of best fit for the Vertical Grating: NOFS = 0.90 + 0.00 × NWV, R^2 = 0.00 and P > 0.05 Line of best fit for the Cartwheel: NOFS = 0.76 + 0.07 × NWV, R^2 0.03 and P > 0.05

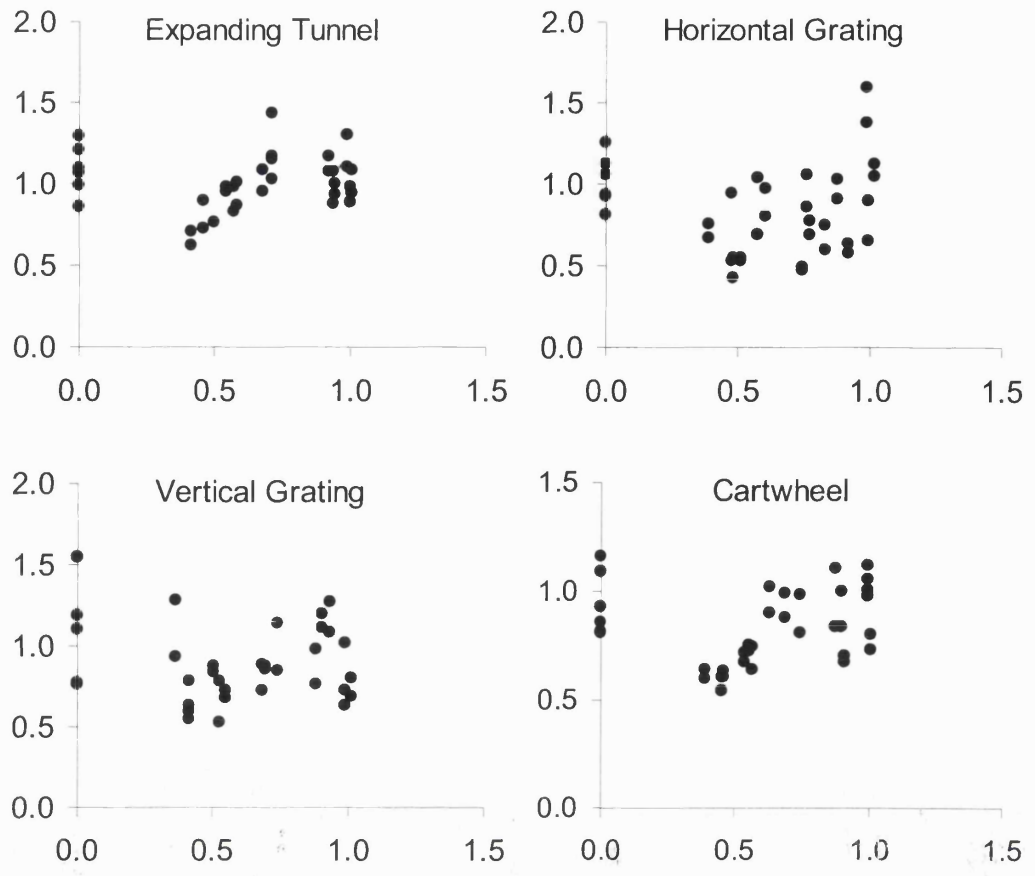

Subject EB Line of best fit for the Expanding Tunnel: NOFS = 0.98 + 0.04 × NWV, R^2 = 0.01 and P > 0.05 Line of best fit for the Horizontal Grating: NOFS = 0.84 - 0.01 × NWV, R^2 = 0.00 and P > 0.05 Line of best fit for the Vertical Grating: NOFS = 0.95 - 0.09 × NWV, R^2 = 0.02 and P > 0.05 Line of best fit for the Cartwheel: NOFS = 0.80 + 0.06 × NWV, R^2 0.01 and P > 0.05

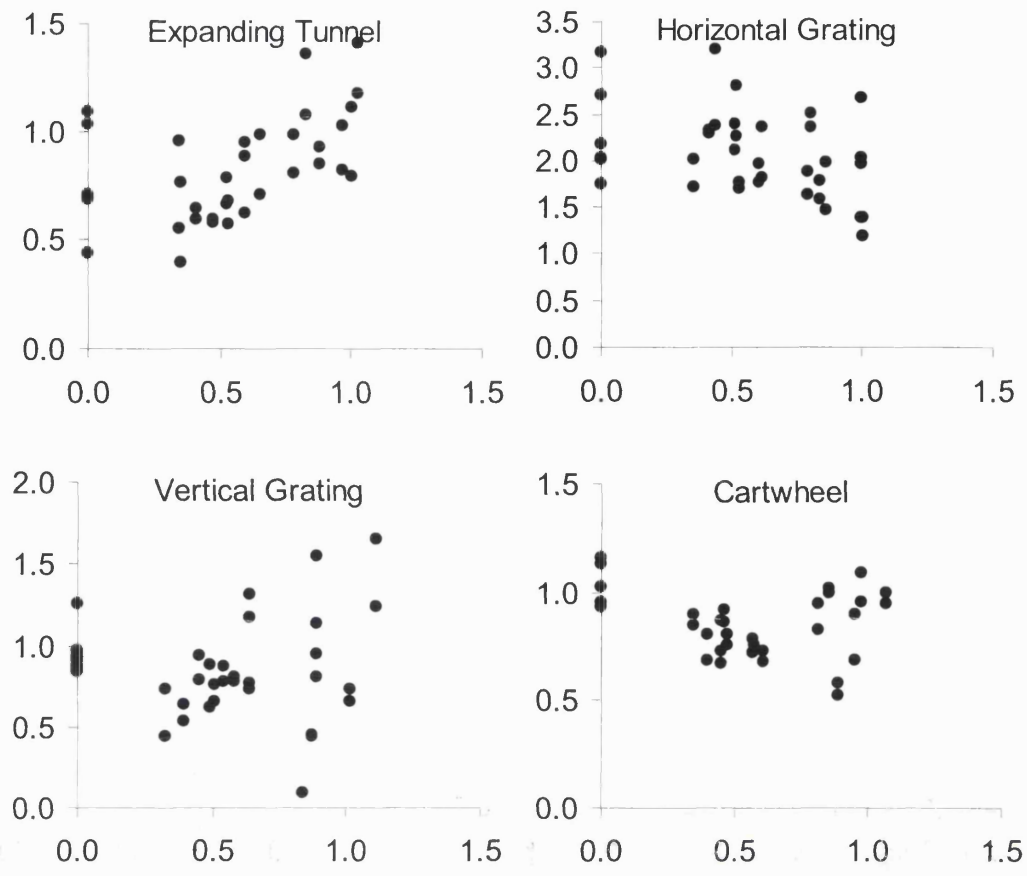

Subject GT Line of best fit for the Expanding Tunnel: NOFS = 0.63 + 0.36 × NWV, R^2 = 0.24 and P < 0.05 Line of best fit for the Horizontal Grating: NOFS = 2.40 - 0.58 × NWV, R^2 = 0.16 and P < 0.05 Line of best fit for the Vertical Grating: NOFS = 0.81 + 0.08 × NWV, R^2 = 0.01 and P > 0.05 Line of best fit for the Cartwheel: NOFS = 0.91 - 0.11 × NWV, R^2 0.06 and P > 0.05

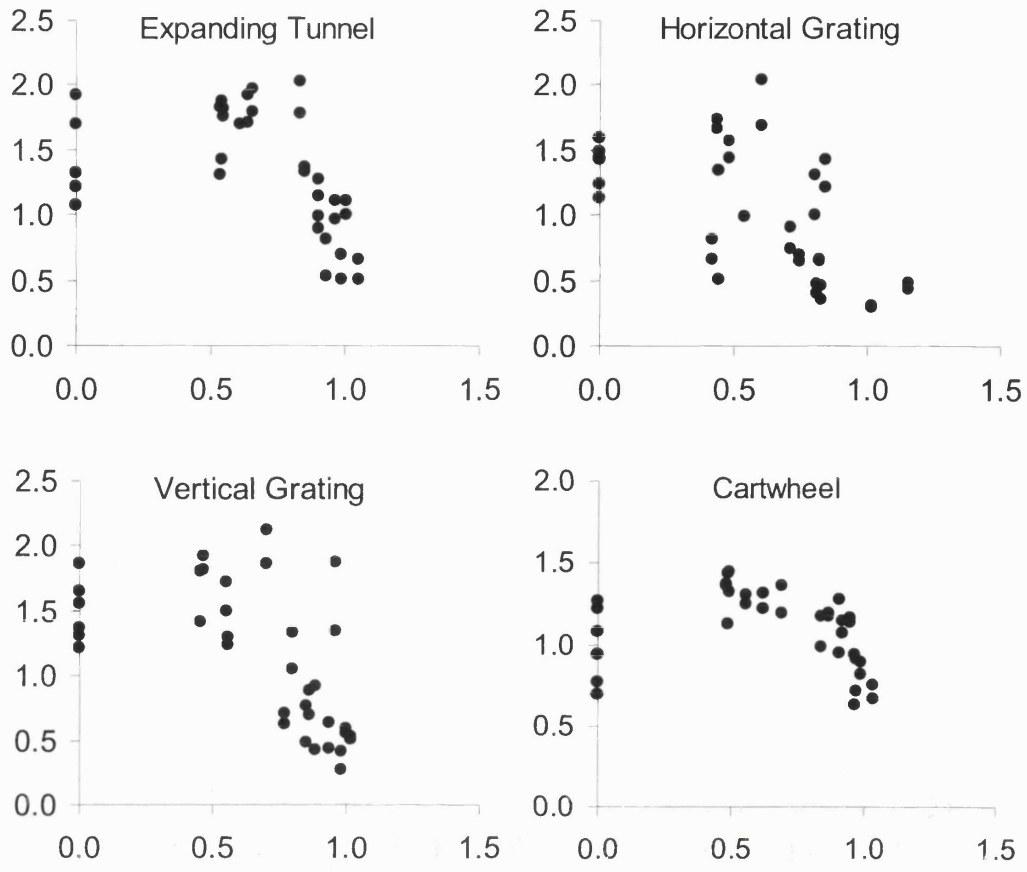

Subject MB Line of best fit for the Expanding Tunnel: NOFS = 1.78 - 0.66 × NWV, R^2 = 0.24 and P < 0.05 Line of best fit for the Horizontal Grating: NOFS = 1.52 - 0.87 × NWV, R^2 = 0.35 and P < 0.05 Line of best fit for the Vertical Grating: NOFS = 1.76 - 0.96 × NWV, R^2 = 0.36 and P < 0.05 Line of best fit for the Cartwheel: NOFS = 1.19 - 0.15 × NWV, R^2 0.05 and P > 0.05

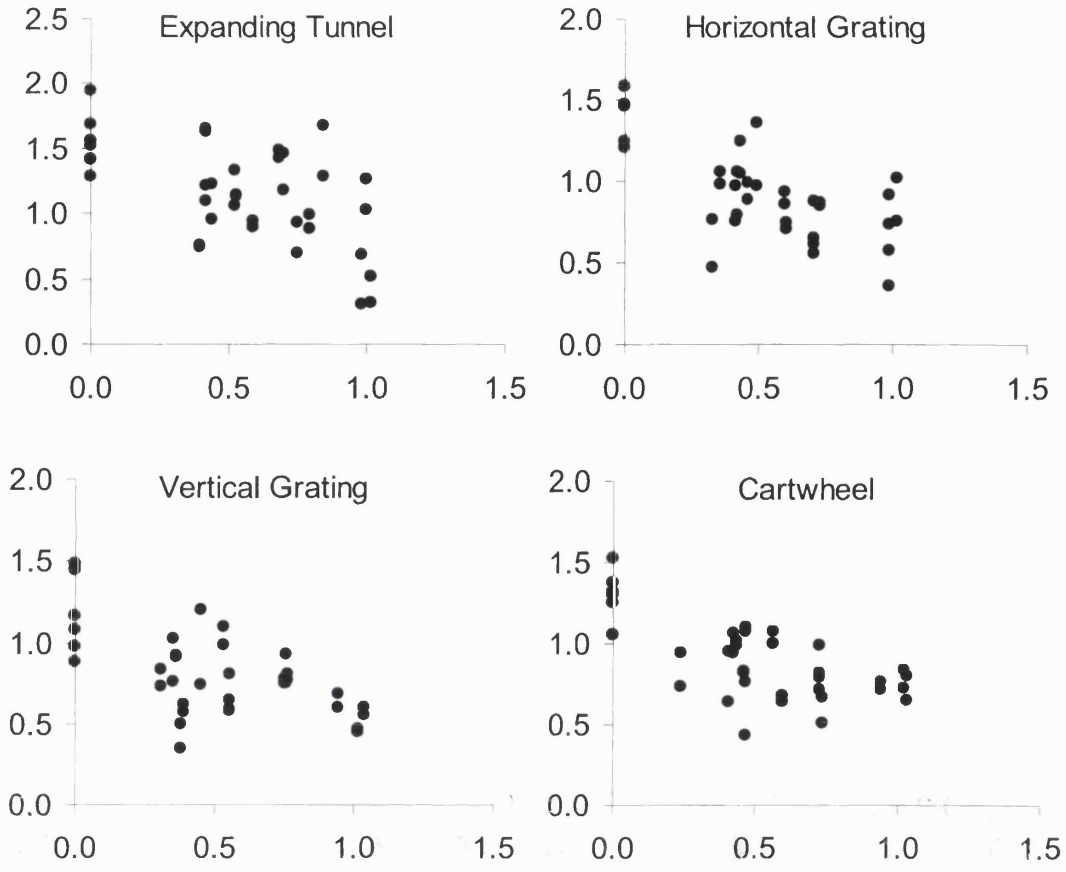

Subject MO Line of best fit for the Expanding Tunnel: NOFS = 1.54 - 0.71 × NWV, R^2 = 0.34 and P < 0.05 Line of best fit for the Horizontal Grating: NOFS = 1.28 - 0.66 × NWV, R^2 = 0.49 and P < 0.05 Line of best fit for the Vertical Grating: NOFS = 1.06 - 0.56 × NWV, R^2 = 0.37 and P < 0.05 Line of best fit for the Cartwheel: NOFS = 1.18 - 0.53 × NWV, R^2 0.46 and P < 0.05

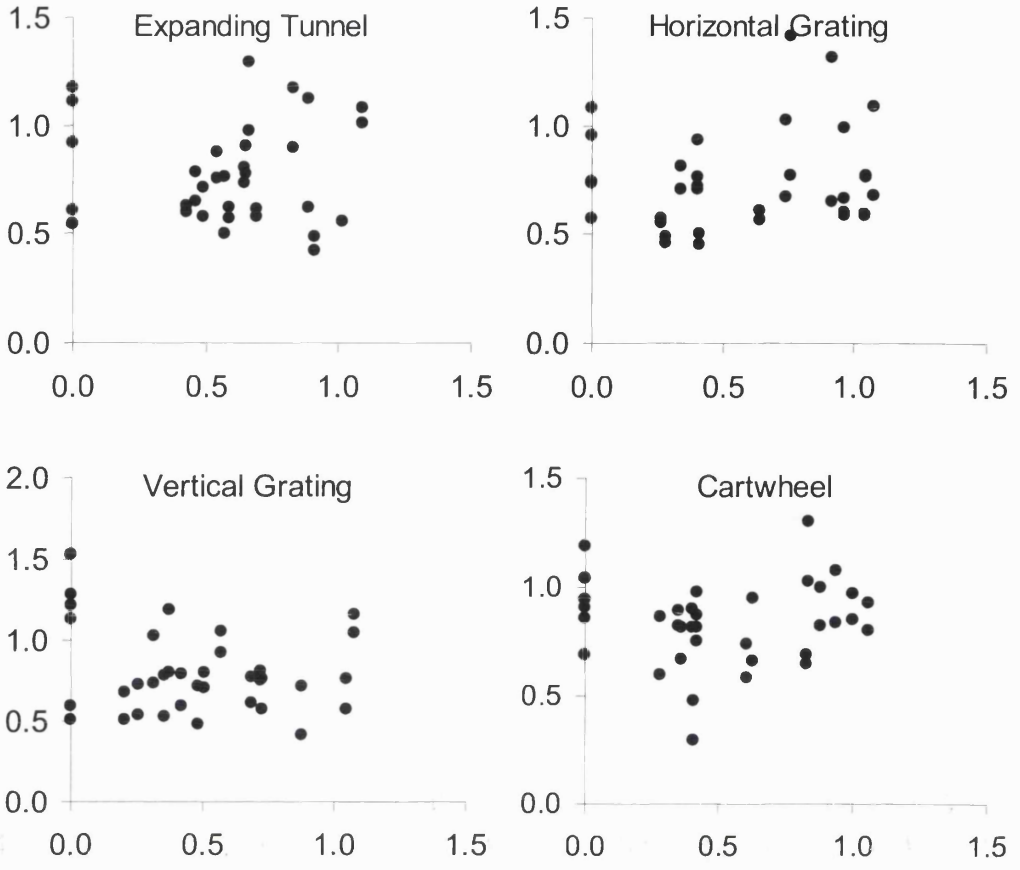

Subject MP Line of best fit for the Expanding Tunnel: NOFS = 0.84 - 0.09 × NWV, R^2 = 0.02 and P > 0.05 Line of best fit for the Horizontal Grating: NOFS = 0.69 + 0.10 × NWV, R^2 = 0.03 and P > 0.05 Line of best fit for the Vertical Grating: NOFS = 0.87 - 0.15 × NWV, R^2 = 0.04 and P > 0.05 Line of best fit for the Cartwheel: NOFS = 0.82 + 0.04 × NWV, R^2 0.01 and P > 0.05

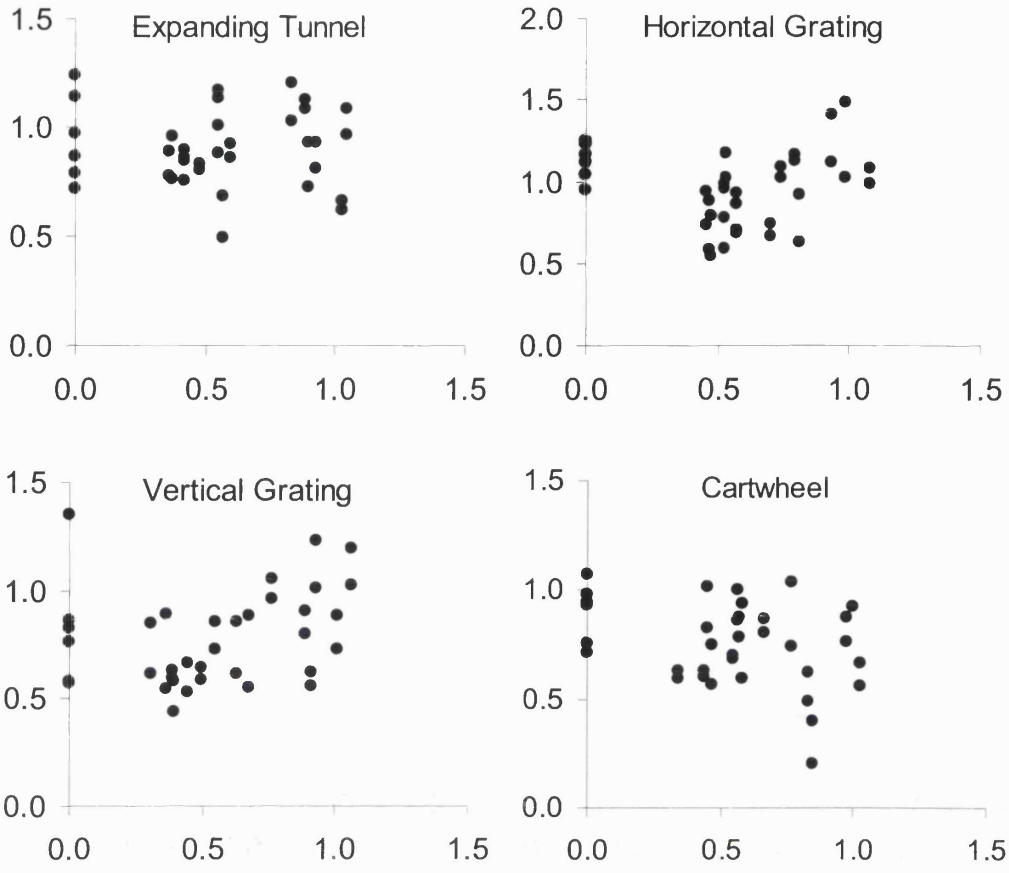

Subject RT Line of best fit for the Expanding Tunnel: NOFS = 0.91 - 0.01 × NWV, R^2 = 0.00 and P > 0.05 Line of best fit for the Horizontal Grating: NOFS = 0.94 + 0.02 × NWV, R^2 = 0.00 and P > 0.05 Line of best fit for the Vertical Grating: NOFS = 0.68 + 0.17 × NWV, R^2 = 0.07 and P > 0.05 Line of best fit for the Cartwheel: NOFS = 0.86 - 0.17 × NWV, R^2 0.08 and P > 0.05

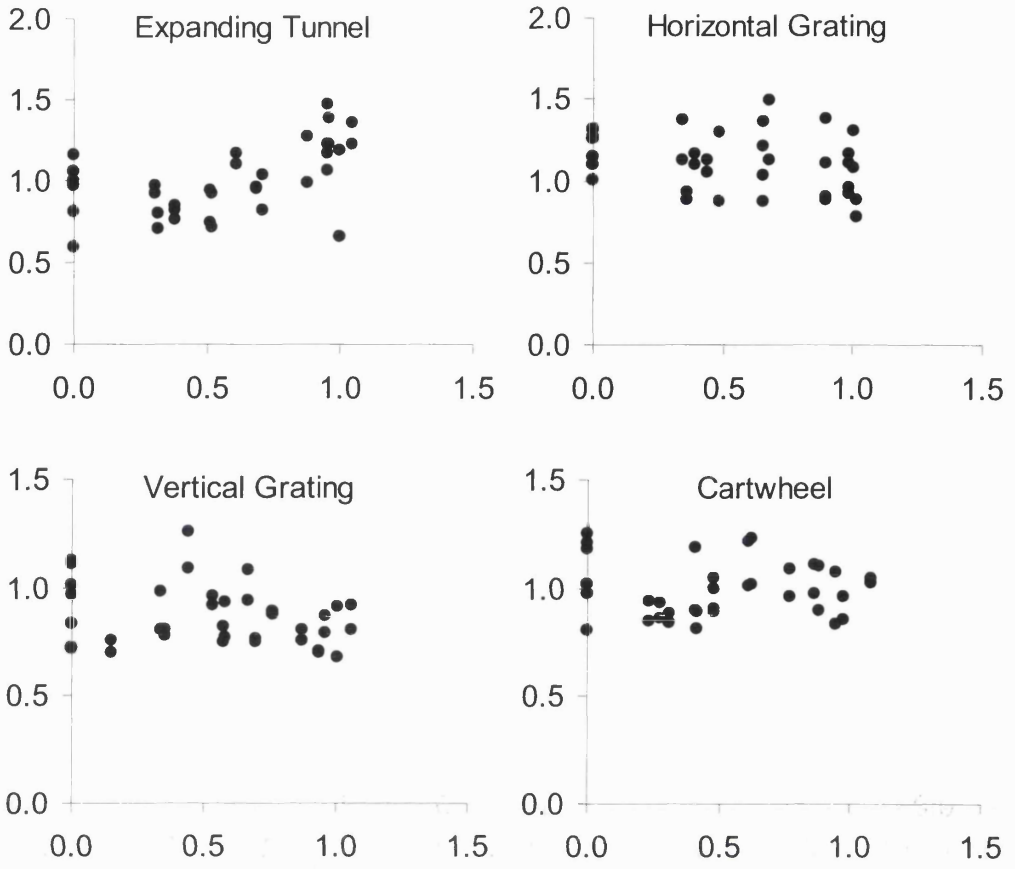

Subject TO Line of best fit for the Expanding Tunnel: NOFS = 0.82 + 0.32 × NWV, R^2 = 0.28 and P < 0.05 Line of best fit for the Horizontal Grating: NOFS = 1.17 - 0.12 × NWV, R^2 = 0.06 and P > 0.05 Line of best fit for the Vertical Grating: NOFS = 0.94 - 0.12 × NWV, R^2 = 0.10 and P > 0.05 Line of best fit for the Cartwheel: NOFS = 1.00 - 0.01 × NWV, R^2 0.00 and P > 0.05

Investigation of Reorientation of the Arthrovisual Effect

Normalised optic flow speed (NOFS) plotted against normalised walking velocity (NWV).

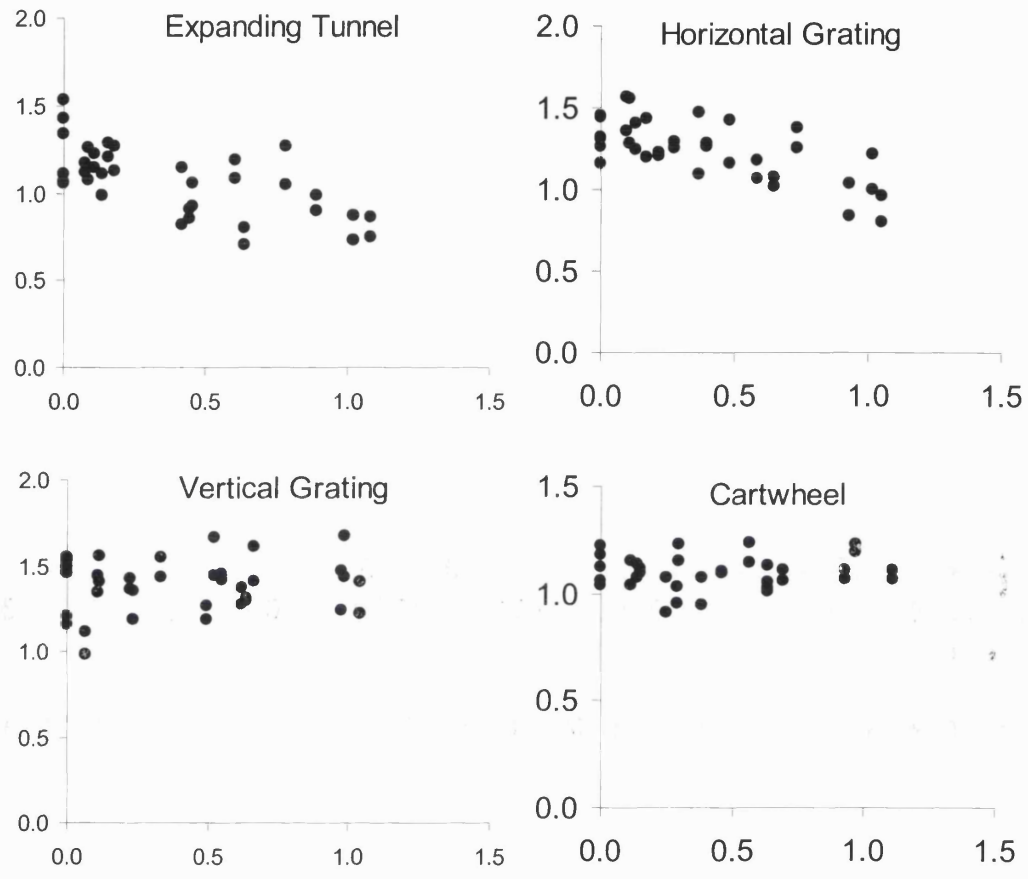

Subject AP mid-line

Line of best fit for the Expanding Tunnel: NOFS = 1.21 - 0.36 × NWV, R^2 = 0.44 and P < 0.05 Line of best fit for the Horizontal Grating: NOFS = 1.38 - 0.37 × NWV, R^2 = 0.49 and P < 0.05 Line of best fit for the Vertical Grating: NOFS = 1.36 + 0.06 × NWV, R^2 = 0.02 and P > 0.05 Line of best fit for the Cartwheel: NOFS = 1.09 + 0.02 × NWV, R^2 0.01 and P > 0.05

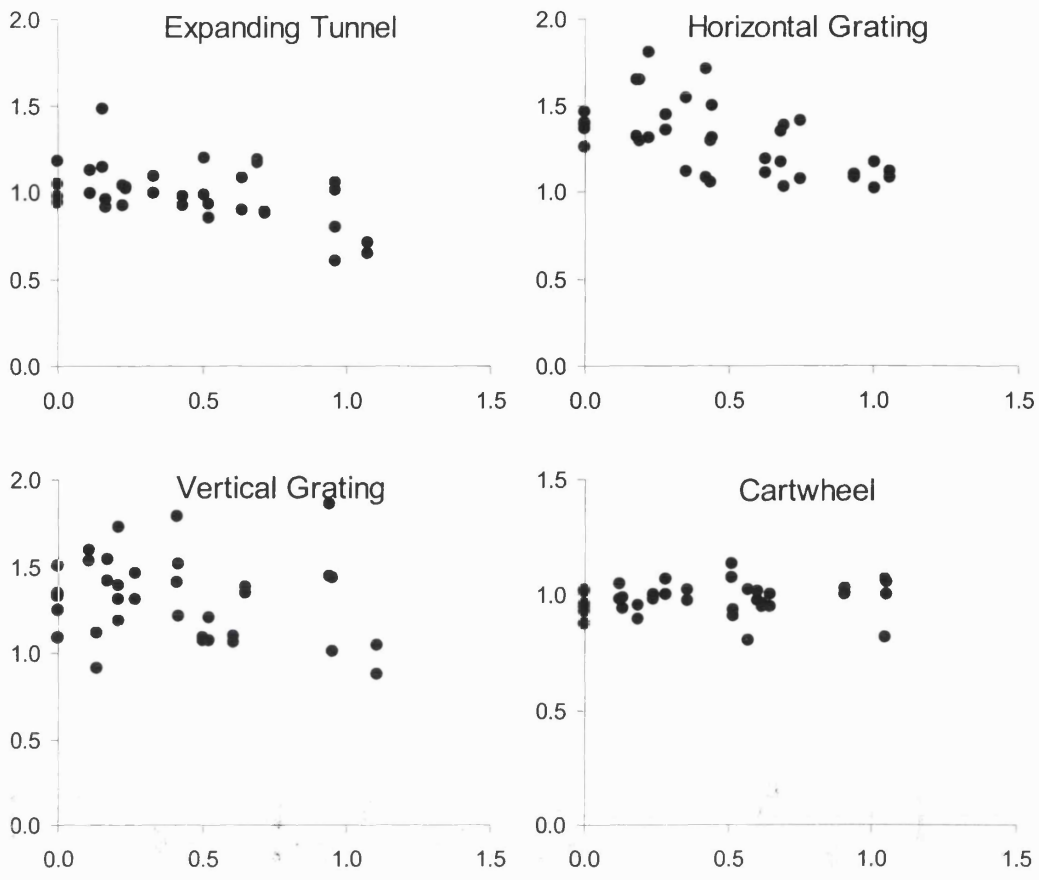

Subject AP mid-right

Line of best fit for the Expanding Tunnel: NOFS = 1.09 - 0.23 × NWV, R^2 = 0.22 and P < 0.05 Line of best fit for the Horizontal Grating: NOFS = 1.45 - 0.33 × NWV, R^2 = 0.31 and P < 0.05 Line of best fit for the Vertical Grating: NOFS = 1.36 - 0.13 × NWV, R^2 = 0.04 and P > 0.05 Line of best fit for the Cartwheel: NOFS = 0.97 + 0.02 × NWV, R^2 0.01 and P > 0.05

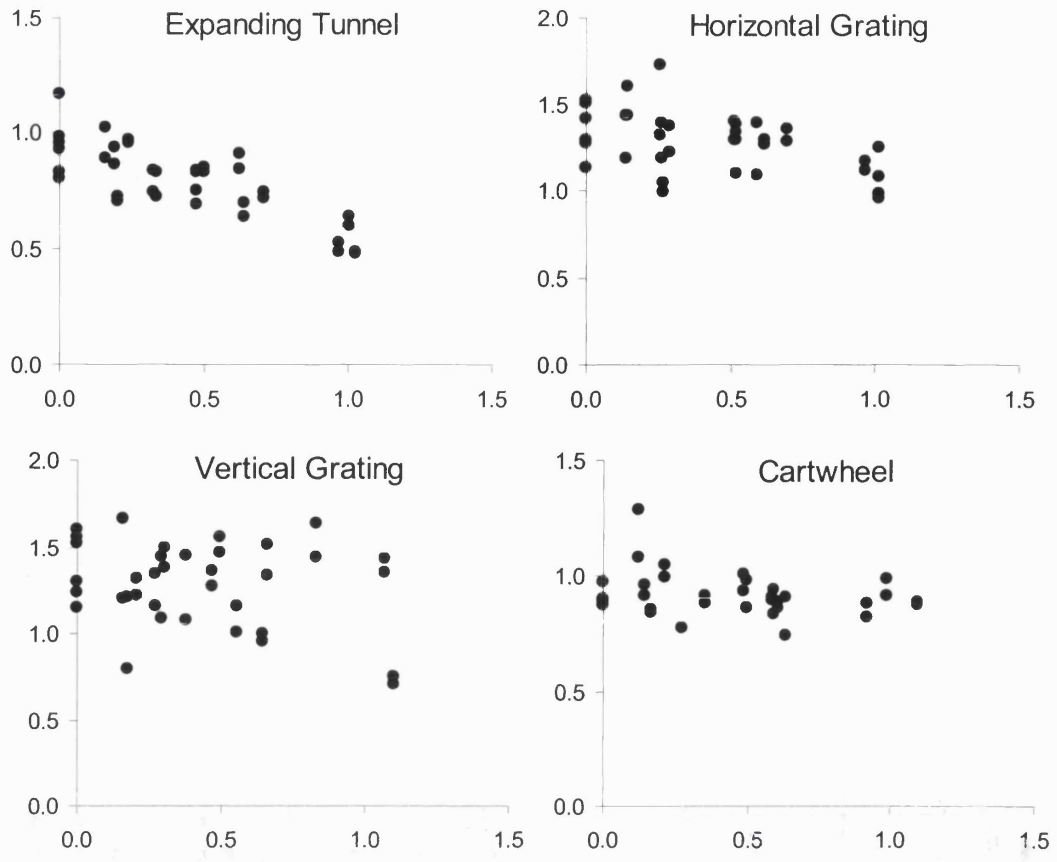

Subject AP full-right

Line of best fit for the Expanding Tunnel: NOFS = 0.96 - 0.38 × NWV, R^2 = 0.64 and P < 0.05 Line of best fit for the Horizontal Grating: NOFS = 1.39 - 0.25 × NWV, R^2 = 0.24 and P < 0.05 Line of best fit for the Vertical Grating: NOFS = 1.36 - 0.19 × NWV, R^2 = 0.06 and P > 0.05 Line of best fit for the Cartwheel: NOFS = 0.95 - 0.07 × NWV, R^2 0.06 and P > 0.05

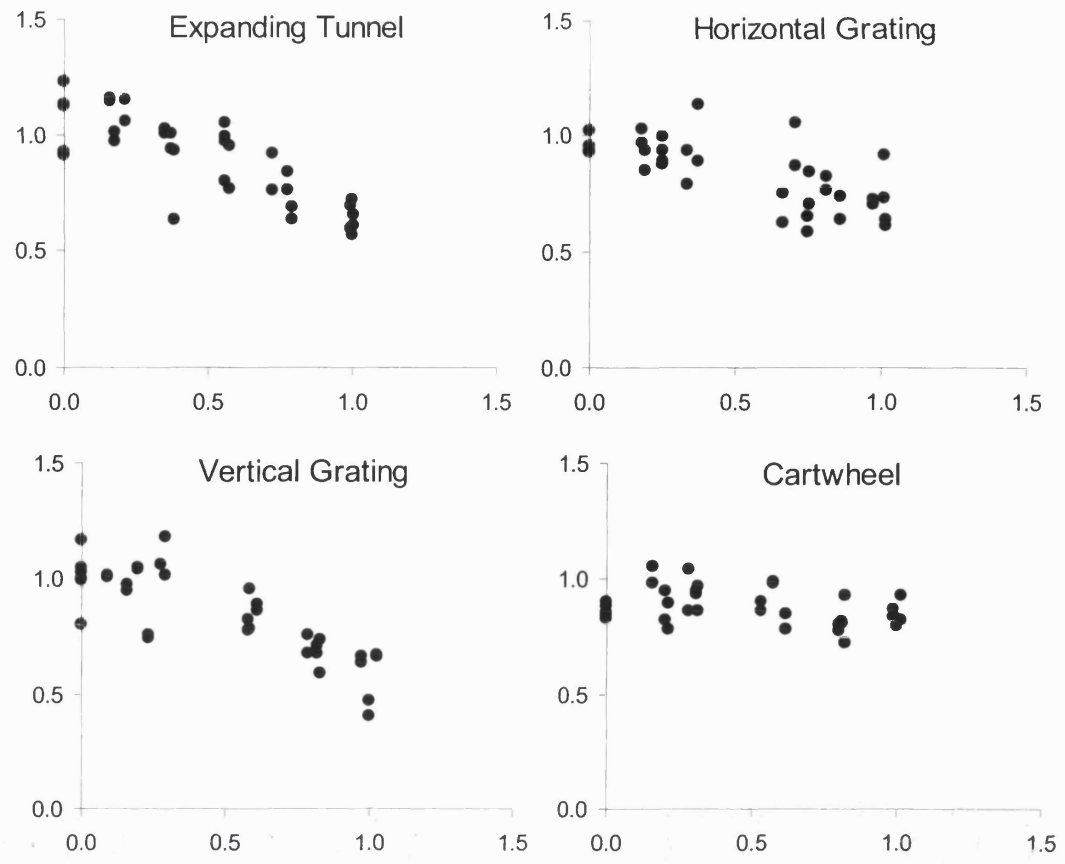

Subject AT mid-line

Line of best fit for the Expanding Tunnel: NOFS = 1.10 - 0.43 × NWV, R^2 = 0.64 and P < 0.05 Line of best fit for the Horizontal Grating: NOFS = 0.99 - 0.28 × NWV, R^2 = 0.50 and P < 0.05 Line of best fit for the Vertical Grating: NOFS = 1.06 - 0.43 × NWV, R^2 = 0.68 and P < 0.05 Line of best fit for the Cartwheel: NOFS = 0.91 - 0.07 × NWV, R^2 0.11 and P < 0.05

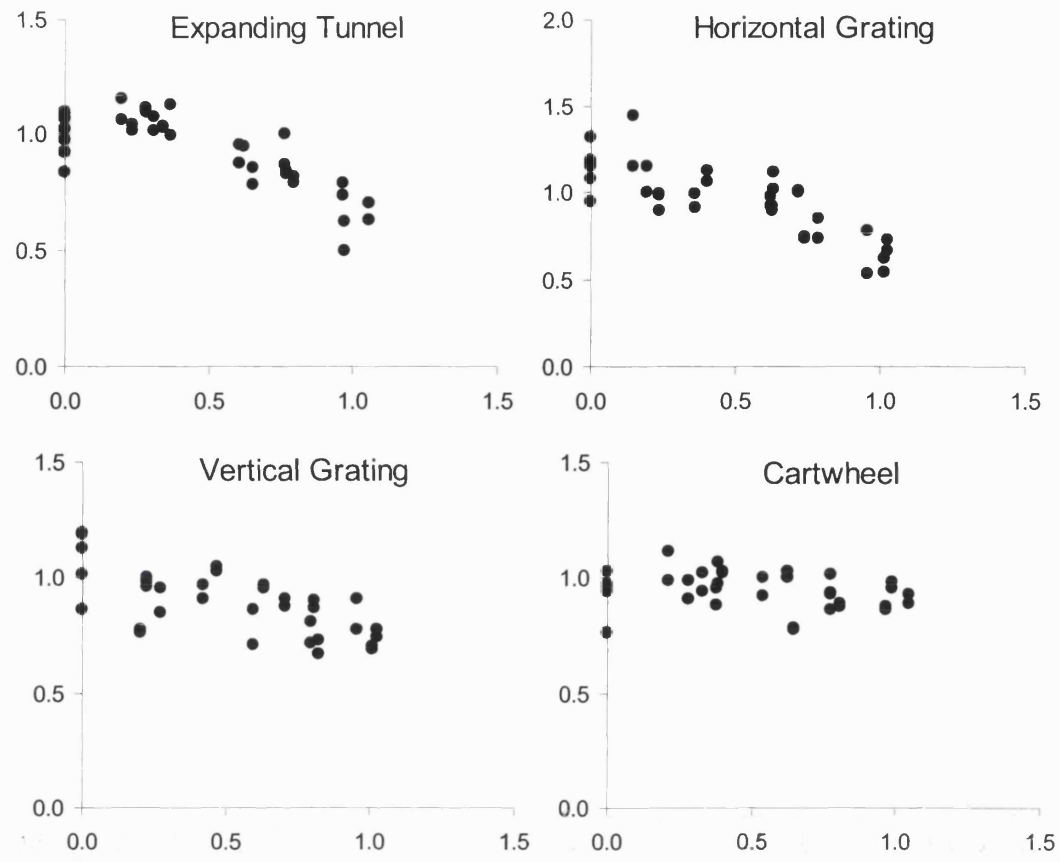

Subject AT mid-right

Line of best fit for the Expanding Tunnel: NOFS = 1.10 - 0.36 × NWV, R^2 = 0.60 and P < 0.05 Line of best fit for the Horizontal Grating: NOFS = 1.18 - 0.47 × NWV, R^2 = 0.63 and P < 0.05 Line of best fit for the Vertical Grating: NOFS = 1.02 - 0.25 × NWV, R^2 = 0.42 and P < 0.05 Line of best fit for the Cartwheel: NOFS = 0.98 - 0.07 × NWV, R^2 0.08 and P > 0.05

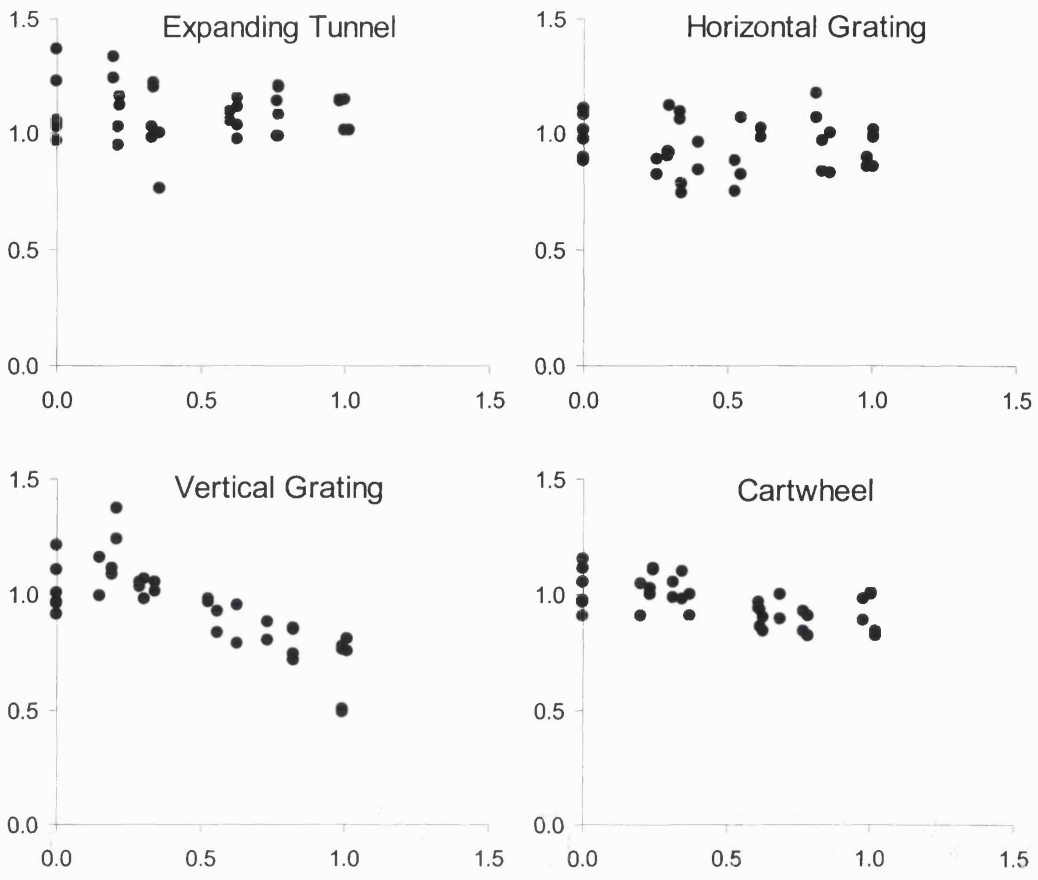

Subject AT full-right

Line of best fit for the Expanding Tunnel: NOFS = 1.11 - 0.03 × NWV, R^2 = 0.01 and P > 0.05 Line of best fit for the Horizontal Grating: NOFS = 0.95 - 0.02 × NWV, R^2 = 0.00 and P > 0.05 Line of best fit for the Vertical Grating: NOFS = 1.14 - 0.42 × NWV, R^2 = 0.62 and P < 0.05 Line of best fit for the Cartwheel: NOFS = 1.04 - 0.15 × NWV, R^2 0.33 and P < 0.05

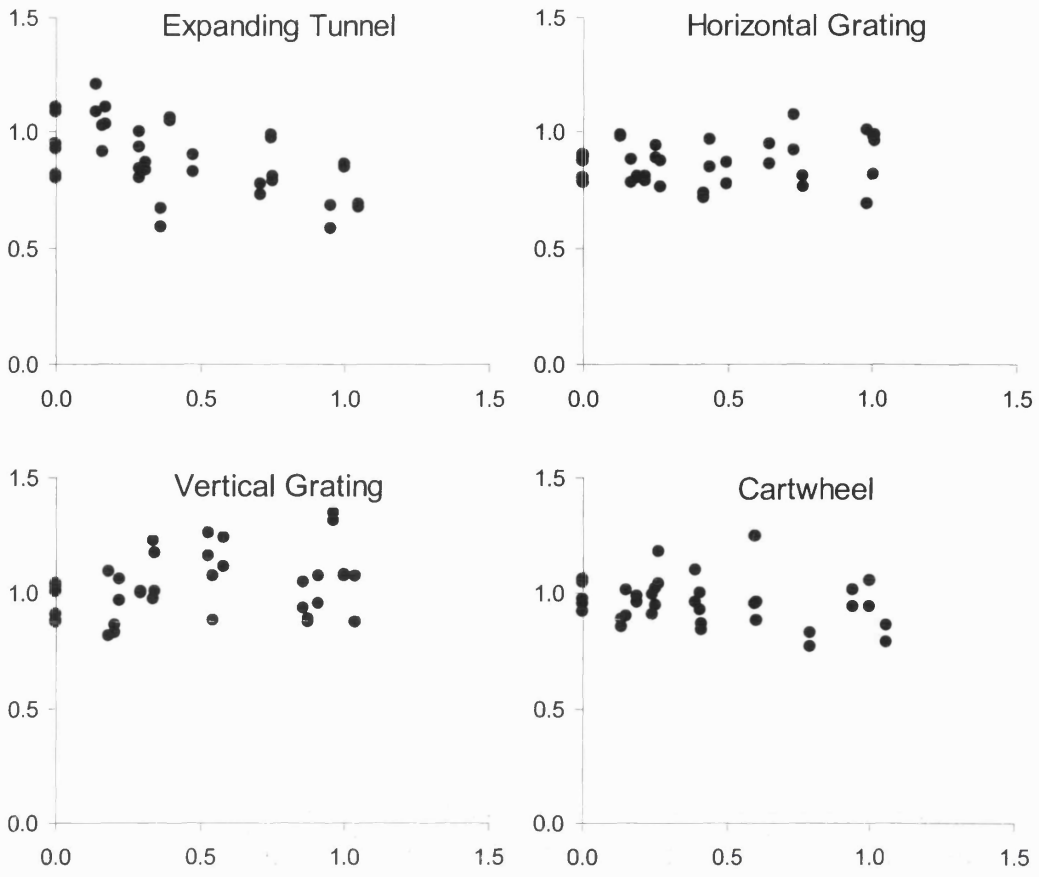

Subject BW mid-line

Line of best fit for the Expanding Tunnel: NOFS = 0.99 - 0.25 × NWV, R^2 = 0.30 and P < 0.05 Line of best fit for the Horizontal Grating: NOFS = 0.85 + 0.05 × NWV, R^2 = 0.04 and P > 0.05 Line of best fit for the Vertical Grating: NOFS = 0.98 + 0.11 × NWV, R^2 = 0.08 and P > 0.05 Line of best fit for the Cartwheel: NOFS = 0.99 - 0.06 × NWV, R^2 0.05 and P > 0.05

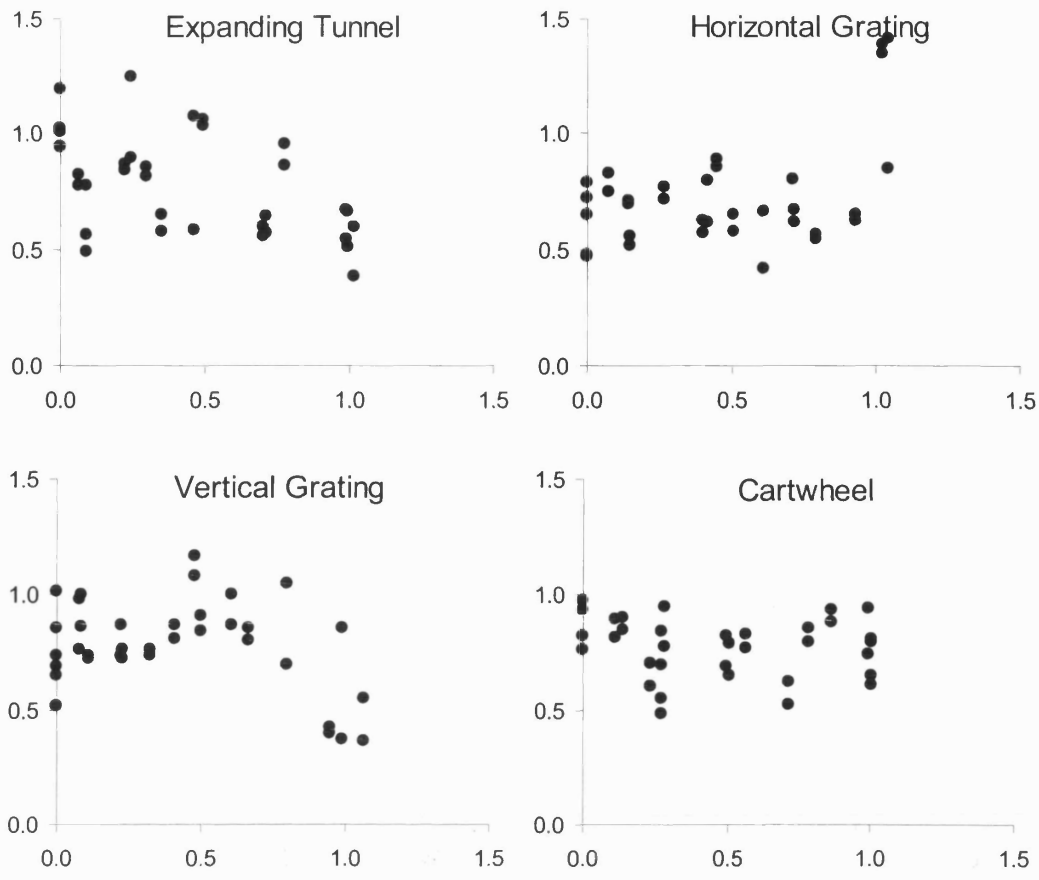

Subject BW mid-right

Line of best fit for the Expanding Tunnel: NOFS = 0.94 - 0.33 × NWV, R^2 = 0.29 and P < 0.05 Line of best fit for the Horizontal Grating: NOFS = 0.59 + 0.30 × NWV, R^2 = 0.21 and P < 0.05 Line of best fit for the Vertical Grating: NOFS = 0.86 - 0.19 × NWV, R^2 = 0.11 and P < 0.05 Line of best fit for the Cartwheel: NOFS = 0.80 - 0.05 × NWV, R^2 0.02 and P > 0.05

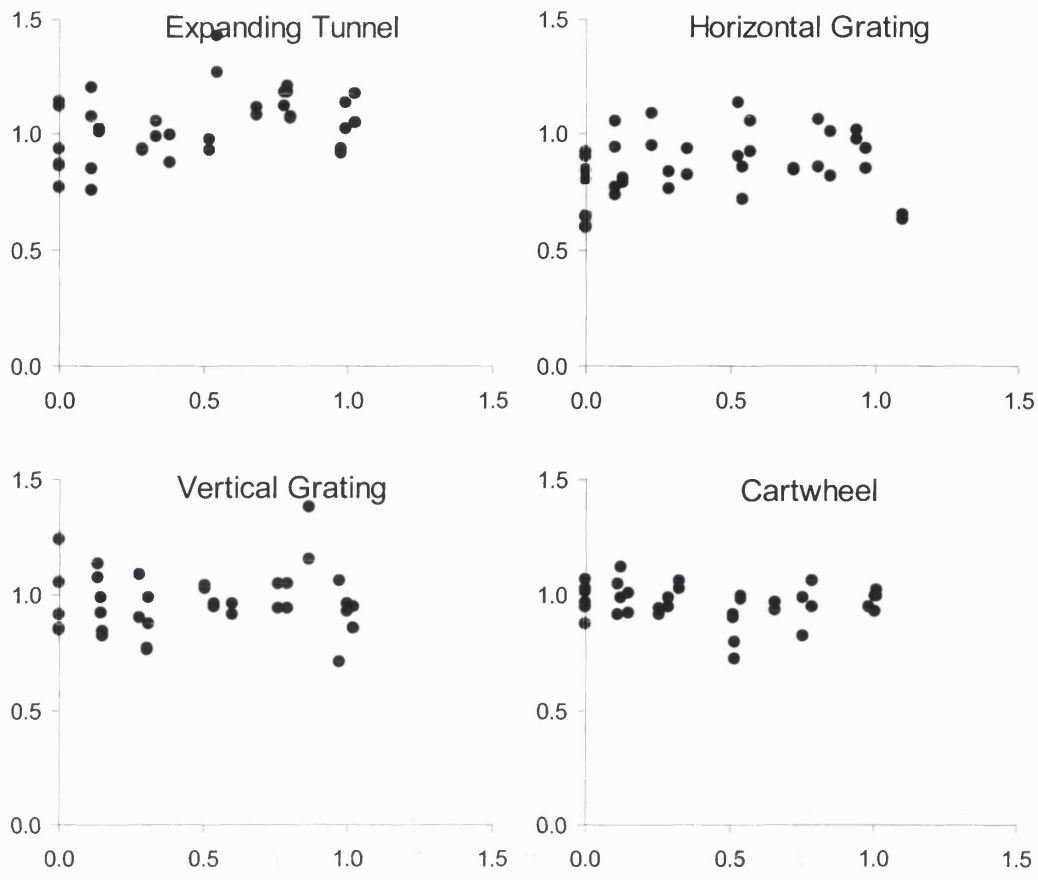

Subject BW full-right

Line of best fit for the Expanding Tunnel: NOFS = 0.97 + 0.15 × NWV, R^2 = 0.14 and P < 0.05 Line of best fit for the Horizontal Grating: NOFS = 0.85 + 0.04 × NWV, R^2 = 0.01 and P > 0.05 Line of best fit for the Vertical Grating: NOFS = 0.95 + 0.04 × NWV, R^2 = 0.01 and P > 0.05 Line of best fit for the Cartwheel: NOFS = 0.98 - 0.03 × NWV, R^2 0.02 and P > 0.05

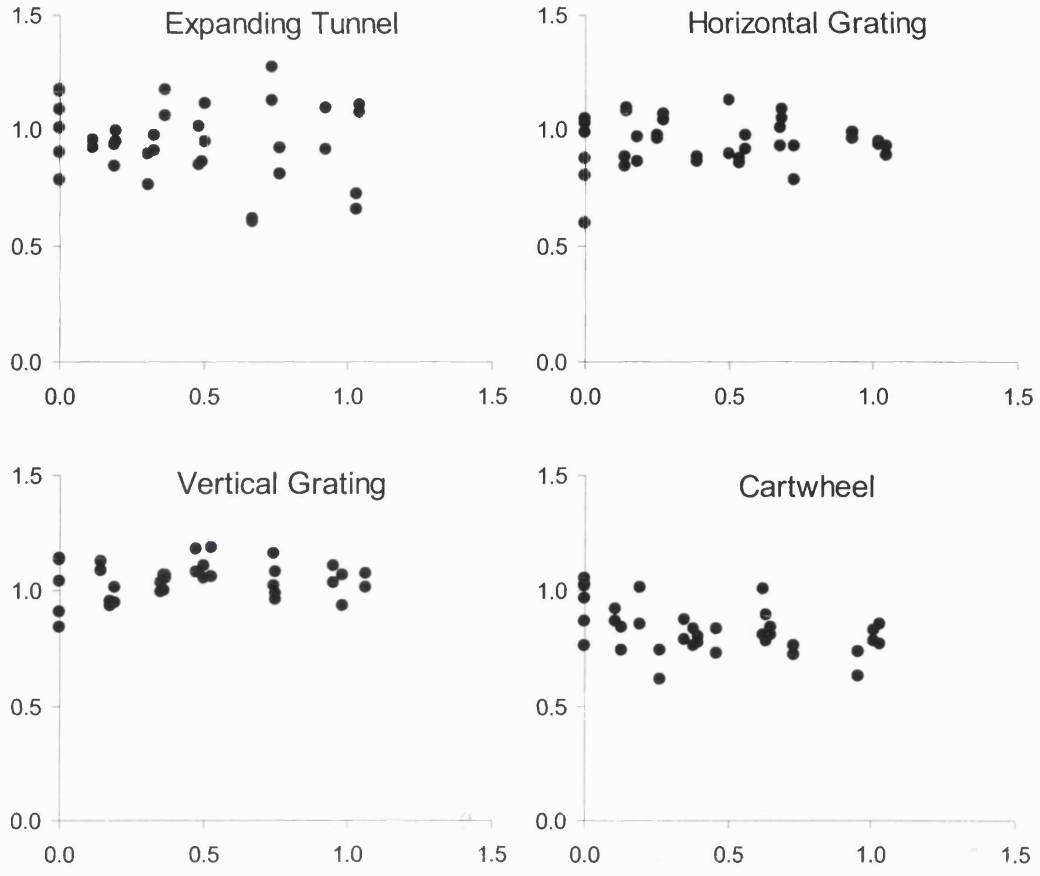

Subject CJ mid-line

Line of best fit for the Expanding Tunnel: NOFS = 0.98 - 0.07 × NWV, R^2 = 0.02 and P > 0.05 Line of best fit for the Horizontal Grating: NOFS = 0.93 + 0.02 × NWV, R^2 = 0.00 and P > 0.05 Line of best fit for the Vertical Grating: NOFS = 1.04 + 0.01 × NWV, R^2 = 0.00 and P > 0.05 Line of best fit for the Cartwheel: NOFS = 0.89 - 0.14 × NWV, R^2 0.19 and P < 0.05

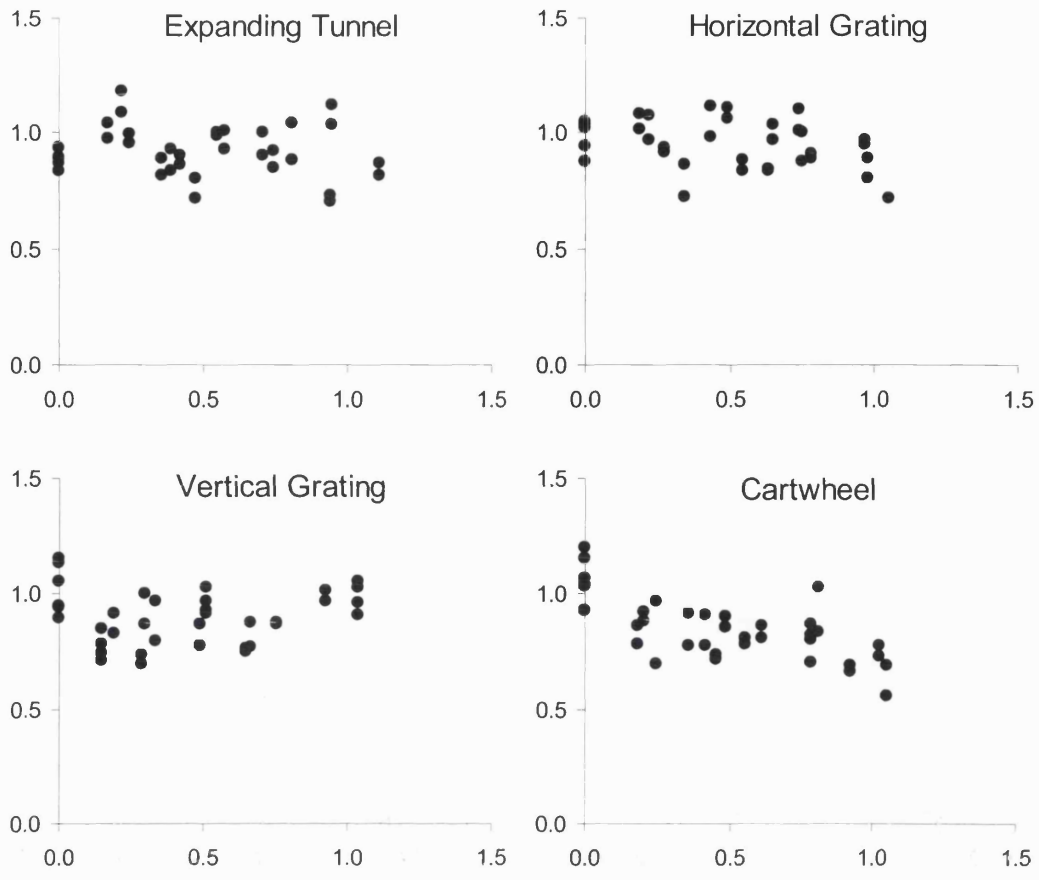

Subject CJ mid-right

Line of best fit for the Expanding Tunnel: NOFS = 0.94 - 0.04 × NWV, R^2 = 0.01 and P > 0.05 Line of best fit for the Horizontal Grating: NOFS = 1.01 - 0.13 × NWV, R^2 = 0.17 and P < 0.05 Line of best fit for the Vertical Grating: NOFS = 0.89 + 0.02 × NWV, R^2 = 0.00 and P > 0.05 Line of best fit for the Cartwheel: NOFS = 0.99 - 0.28 × NWV, R^2 0.47 and P < 0.05

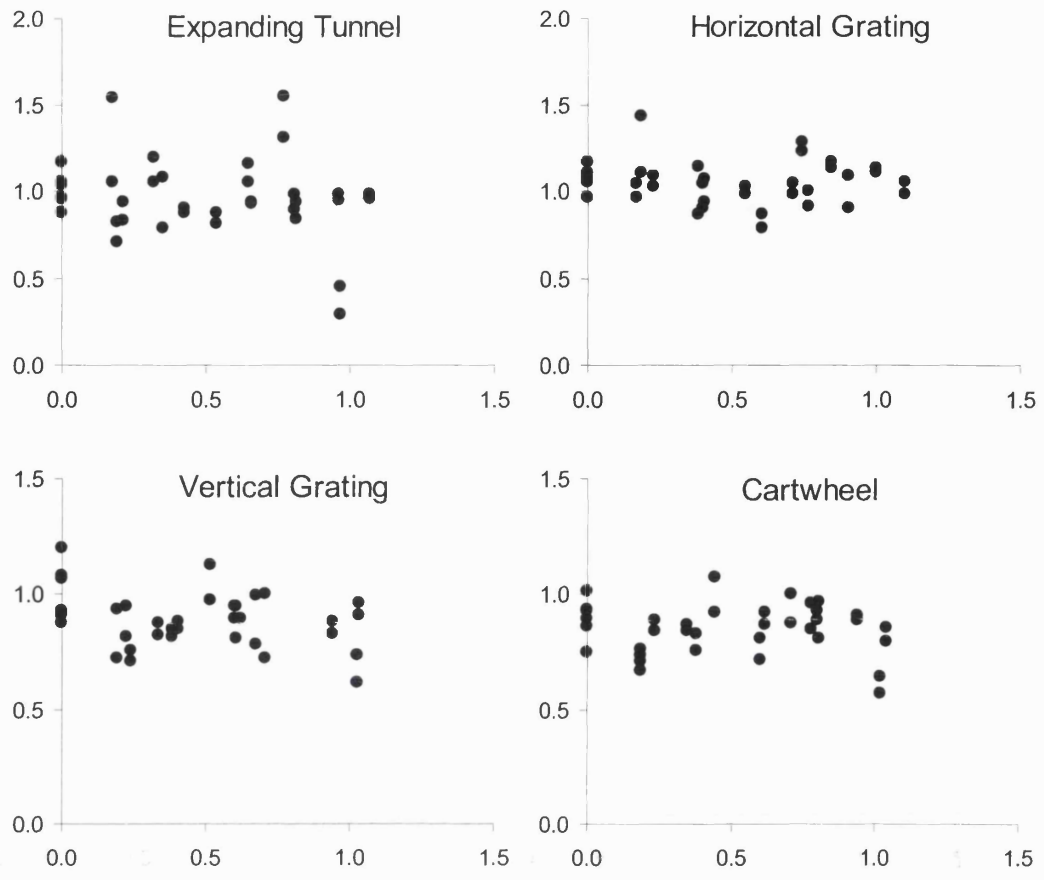

Subject CJ full-right

Line of best fit for the Expanding Tunnel: NOFS = 1.03 - 0.13 × NWV, R^2 = 0.04 and P < 0.05 Line of best fit for the Horizontal Grating: NOFS = 1.05 - 0.01 × NWV, R^2 = 0.00 and P > 0.05 Line of best fit for the Vertical Grating: NOFS = 0.94 - 0.11 × NWV, R^2 = 0.09 and P > 0.05 Line of best fit for the Cartwheel: NOFS = 0.86 - 0.03 × NWV, R^2 = 0.01 and P > 0.05

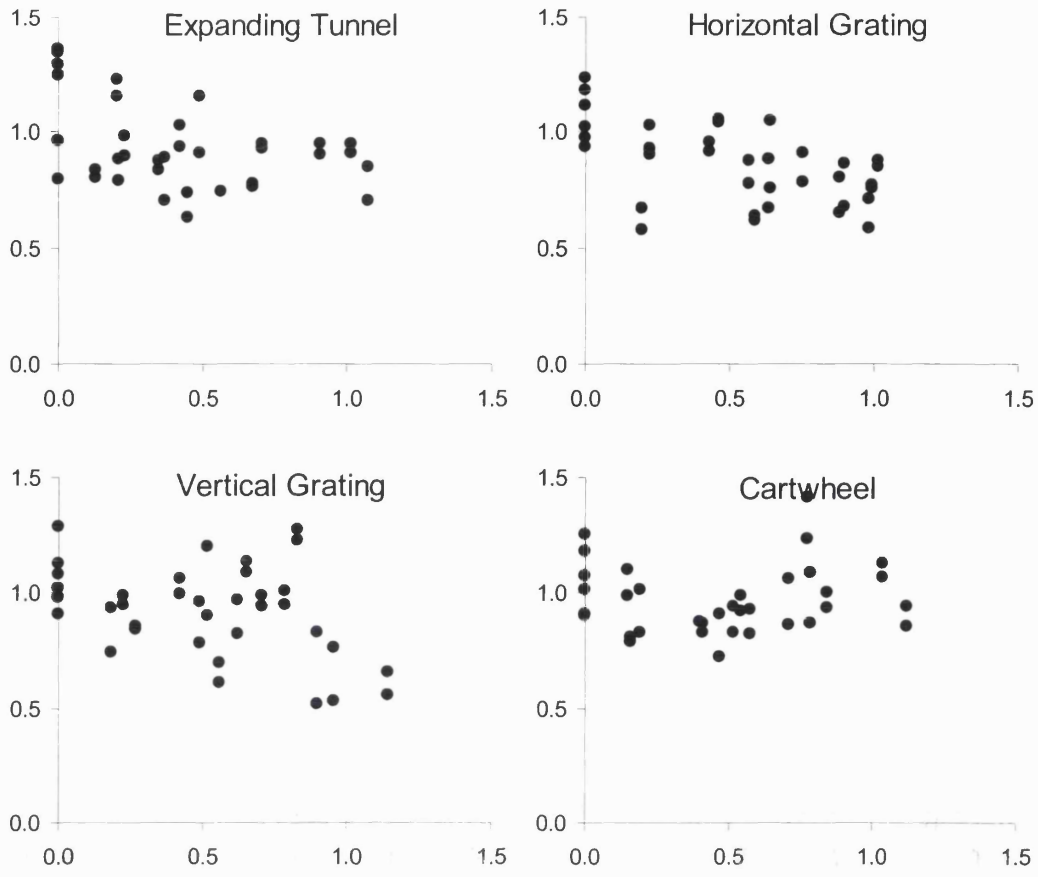

Subject JN mid-line

Line of best fit for the Expanding Tunnel: NOFS = 1.03 - 0.24 × NWV, R^2 = 0.18 and P < 0.05 Line of best fit for the Horizontal Grating: NOFS = 1.00 - 0.27 × NWV, R^2 = 0.32 and P < 0.05 Line of best fit for the Vertical Grating: NOFS = 1.04 - 0.23 × NWV, R^2 = 0.16 and P < 0.05 Line of best fit for the Cartwheel: NOFS = 0.96 - 0.02 × NWV, R^2 0.00 and P > 0.05

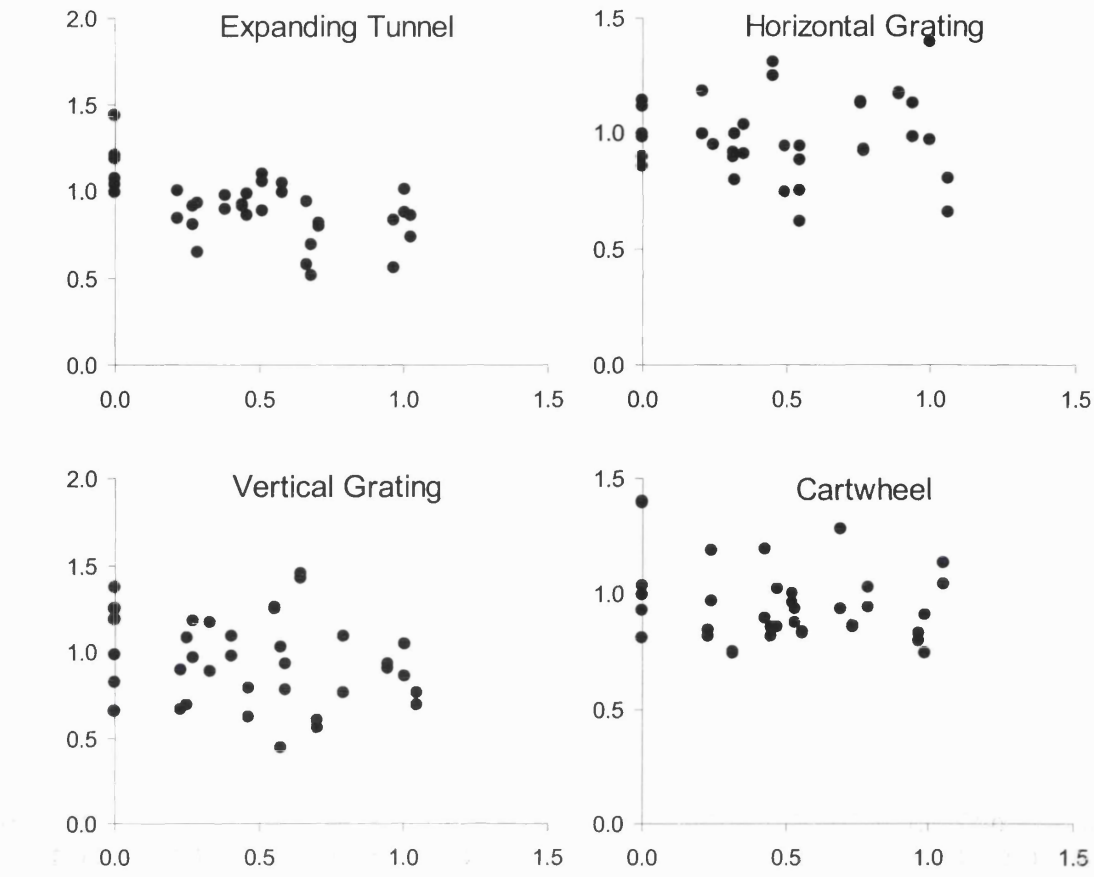

Subject JN mid-right

Line of best fit for the Expanding Tunnel: NOFS = 1.062 - 0.36 × NWV, R^2 = 0.31 and P < 0.05 Line of best fit for the Horizontal Grating: NOFS = 0.97 + 0.02 × NWV, R^2 = 0.00 and P > 0.05 Line of best fit for the Vertical Grating: NOFS = 1.01 - 0.14 × NWV, R^2 = 0.03 and P > 0.05 Line of best fit for the Cartwheel: NOFS = 1.01 - 0.11 × NWV, R^2 = 0.05 and P > 0.05

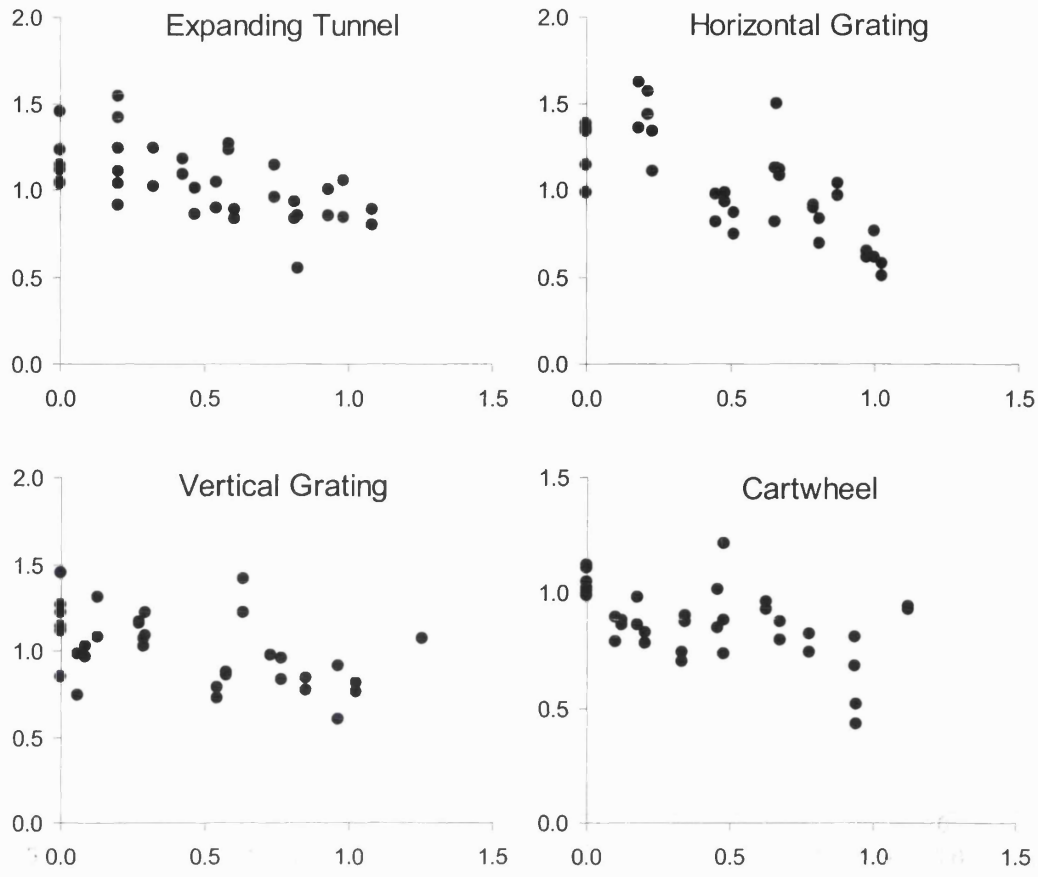

Subject JN full-right

Line of best fit for the Expanding Tunnel: NOFS = 1.22 - 0.35 × NWV, R^2 = 0.36 and P < 0.05 Line of best fit for the Horizontal Grating: NOFS = 1.37 - 0.64 × NWV, R^2 = 0.56 and P < 0.05 Line of best fit for the Vertical Grating: NOFS = 1.12 - 0.26 × NWV, R^2 = 0.23 and P < 0.05 Line of best fit for the Cartwheel: NOFS = 0.97 - 0.21 × NWV, R^2 = 0.23 and P < 0.05

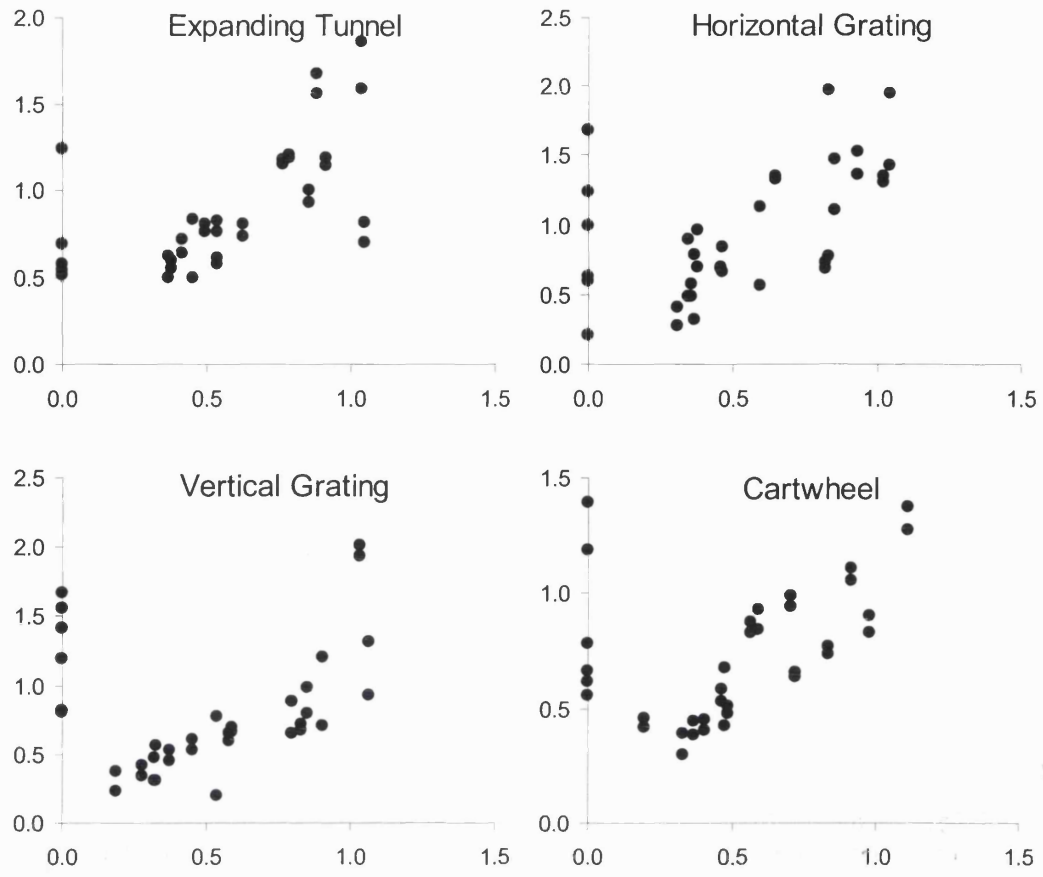

Subject LH mid-line

Line of best fit for the Expanding Tunnel: NOFS = 0.58 + 0.60 × NWV, R^2 = 0.30 and P < 0.05 Line of best fit for the Horizontal Grating: NOFS = 0.57 + 0.72 × NWV, R^2 = 0.28 and P < 0.05 Line of best fit for the Vertical Grating: NOFS = 0.66 + 0.28 × NWV, R^2 = 0.04 and P > 0.05 Line of best fit for the Cartwheel: NOFS = 0.55 + 0.35 × NWV, R^2 0.15 and P < 0.05

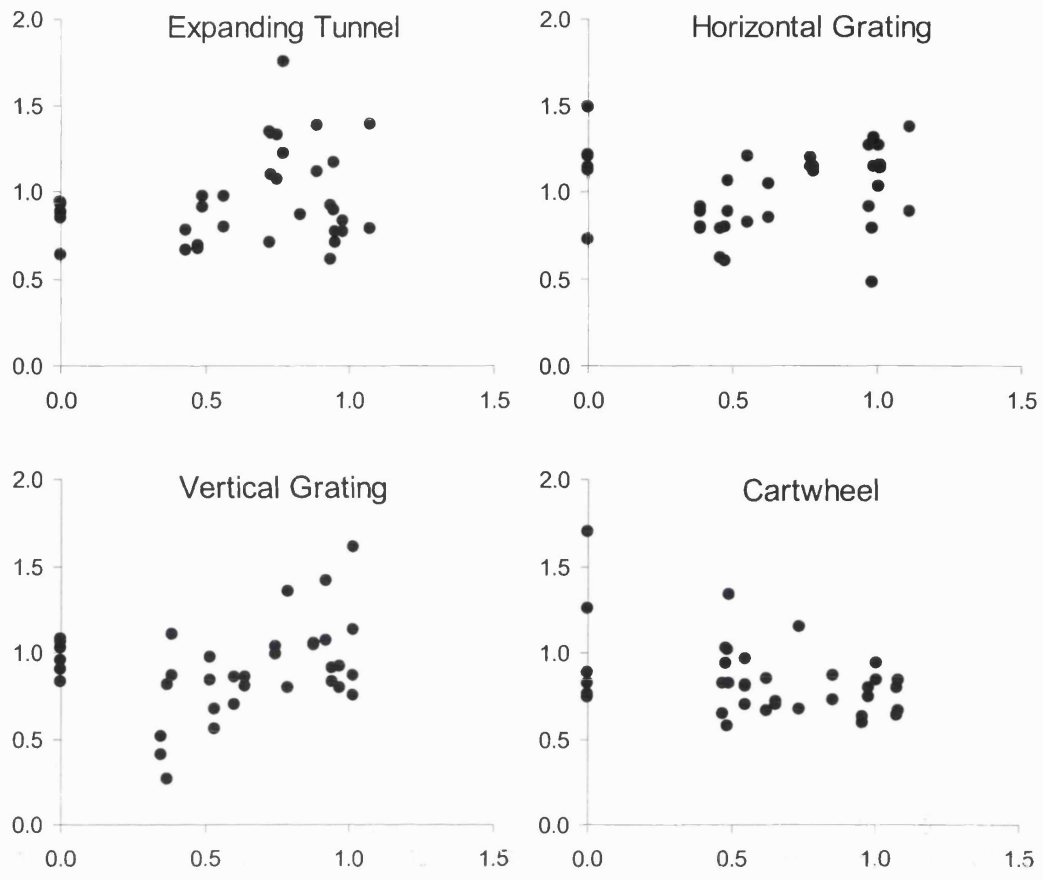

Subject LH mid-right

Line of best fit for the Expanding Tunnel: NOFS = 0.84 + 0.19 × NWV, R^2 = 0.06 and P > 0.05 Line of best fit for the Horizontal Grating: NOFS = 0.98 + 0.04 × NWV, R^2 = 0.00 and P > 0.05 Line of best fit for the Vertical Grating: NOFS = 0.80 + 0.19 × NWV, R^2 = 0.06 and P > 0.05 Line of best fit for the Cartwheel: NOFS = 1.01 - 0.27 × NWV, R^2 0.17 and P < 0.05

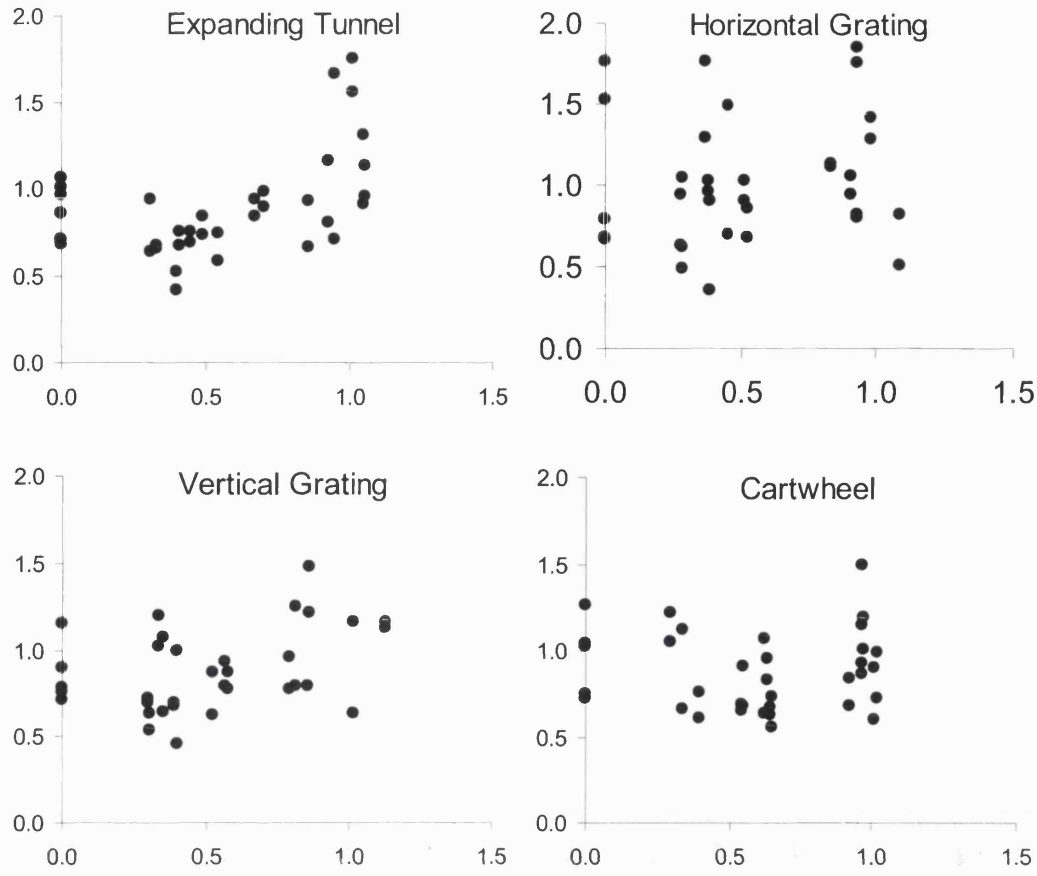

Subject LH full-right

Line of best fit for the Expanding Tunnel: NOFS = 0.67 + 0.40 × NWV, R^2 = 0.22 and P < 0.05 Line of best fit for the Horizontal Grating: NOFS = 1.00 + 0.06 × NWV, R^2 = 0.00 and P > 0.05 Line of best fit for the Vertical Grating: NOFS = 0.75 + 0.25 × NWV, R^2 = 0.13 and P > 0.05 Line of best fit for the Cartwheel: NOFS = 0.90 - 0.03 × NWV, R^2 0.00 and P > 0.05

Specification of Spatial Scale

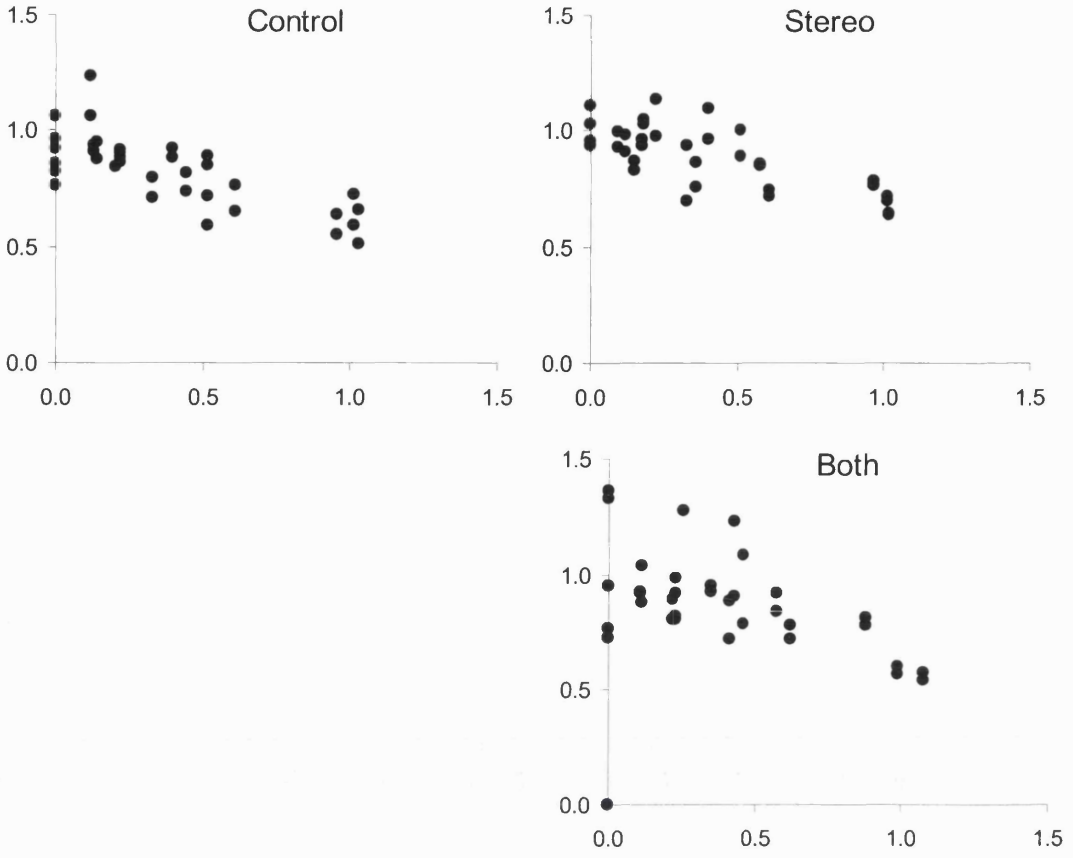

Subject AP Line of best fit without stereo or parallax: NOFS = 0.95 - 0.34 × NWV, R^2 = 0.57 and P < 0.05 Line of best fit with stereo only: NOFS = 1.01 - 0.30 × NWV, R^2 = 0.57 and P < 0.05 Line of best with stereo and parallax: NOFS = 0.96 - 0.26 × NWV, R^2 = 0.13 and P < 0.05

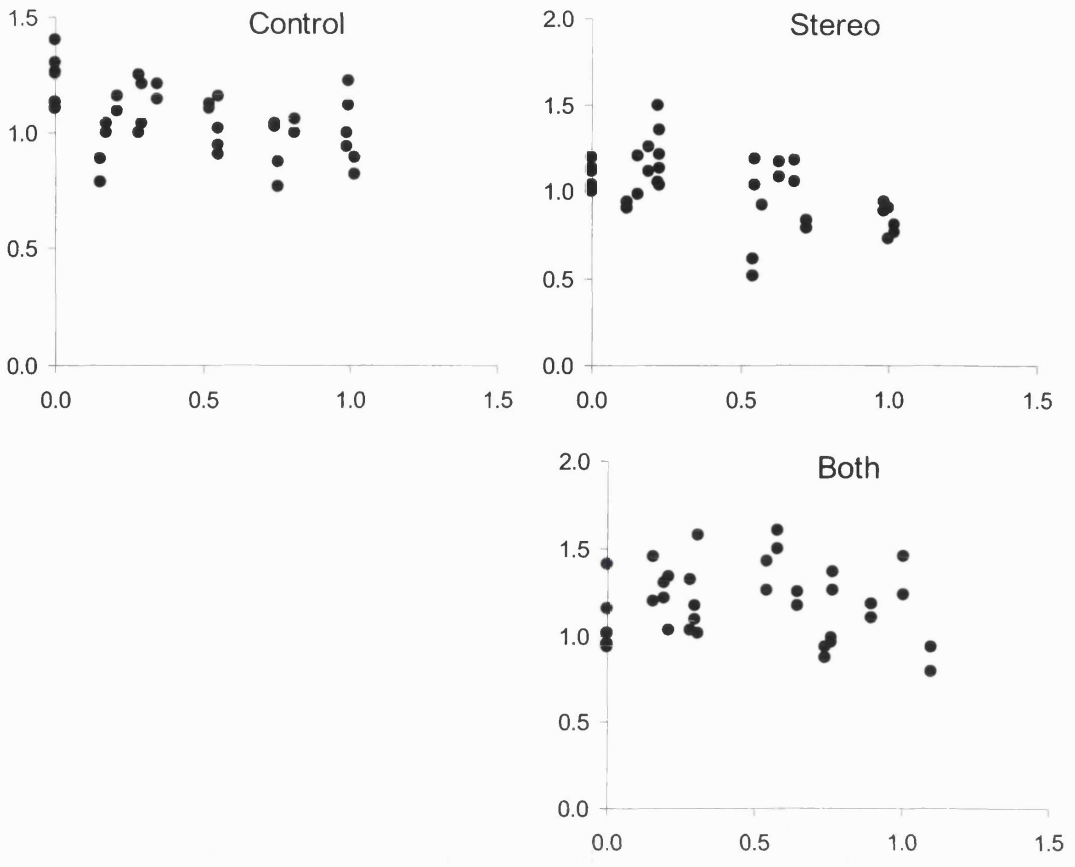

Subject AT Line of best fit without stereo or parallax: NOFS = 1.15 - 0.20 × NWV, R^2 = 0.21 and P < 0.05 Line of best fit with stereo only: NOFS = 1.14 - 0.29 × NWV, R^2 = 0.25 and P < 0.05 Line of best with stereo and parallax: NOFS = 1.21 - 0.06 × NWV, R^2 = 0.01 and P > 0.05

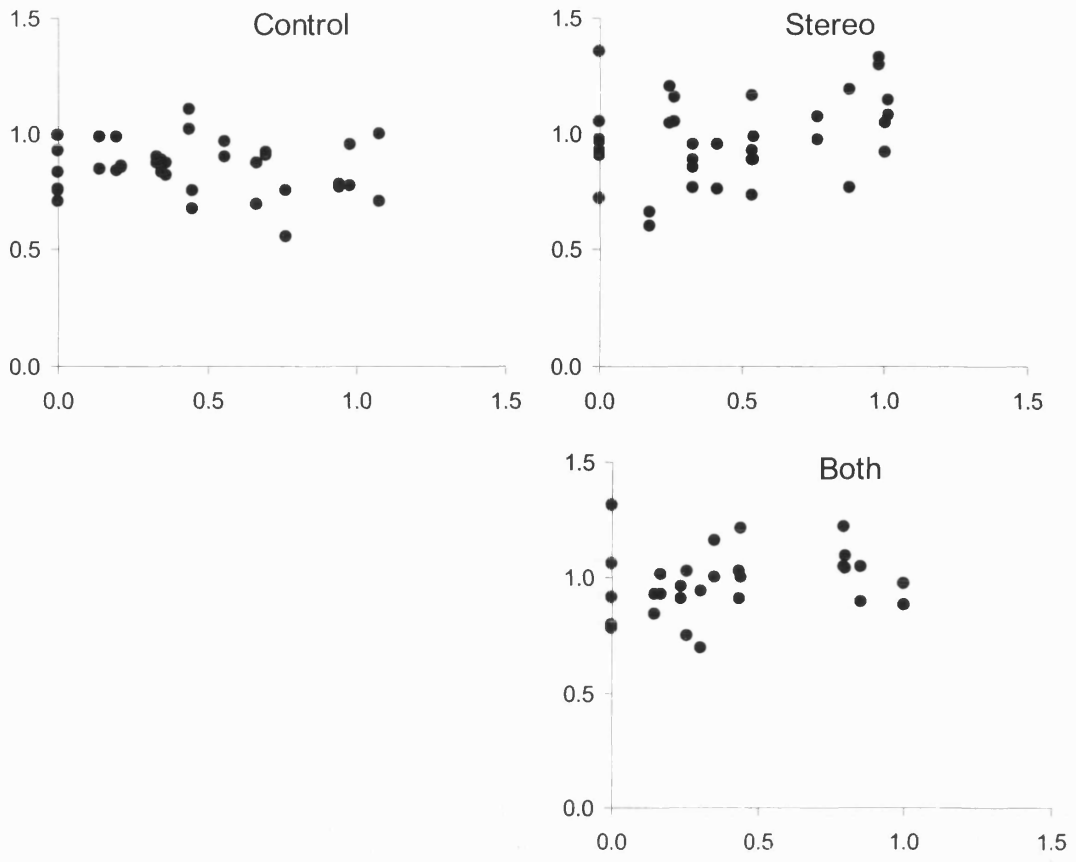

Subject BW Line of best fit without stereo or parallax: NOFS = 0.87 - 0.05 × NWV, R^2 = 0.02 and P > 0.05 Line of best fit with stereo only: NOFS = 0.91 + 0.14 × NWV, R^2 = 0.08 and P > 0.05 Line of best with stereo and parallax: NOFS = 0.93 + 0.11 × NWV, R^2 = 0.06 and P > 0.05

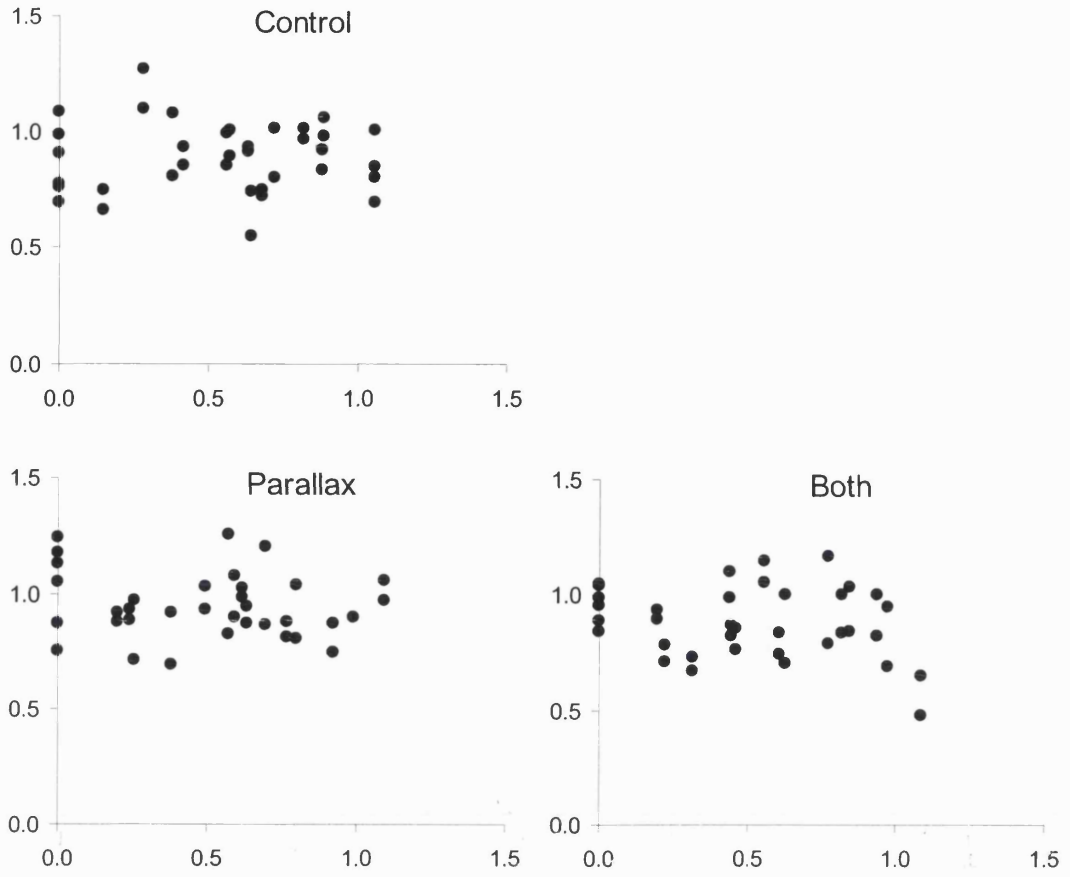

Subject CJ Line of best fit without stereo or parallax: NOFS = 0.89 + 0.00 × NWV, R^2 = 0.00 and P > 0.05 Line of best fit with parallax only: NOFS = 0.98 - 0.06 × NWV, R^2 = 0.02 and P > 0.05 Line of best with stereo and parallax: NOFS = 0.93 - 0.10 × NWV, R^2 = 0.05 and P > 0.05

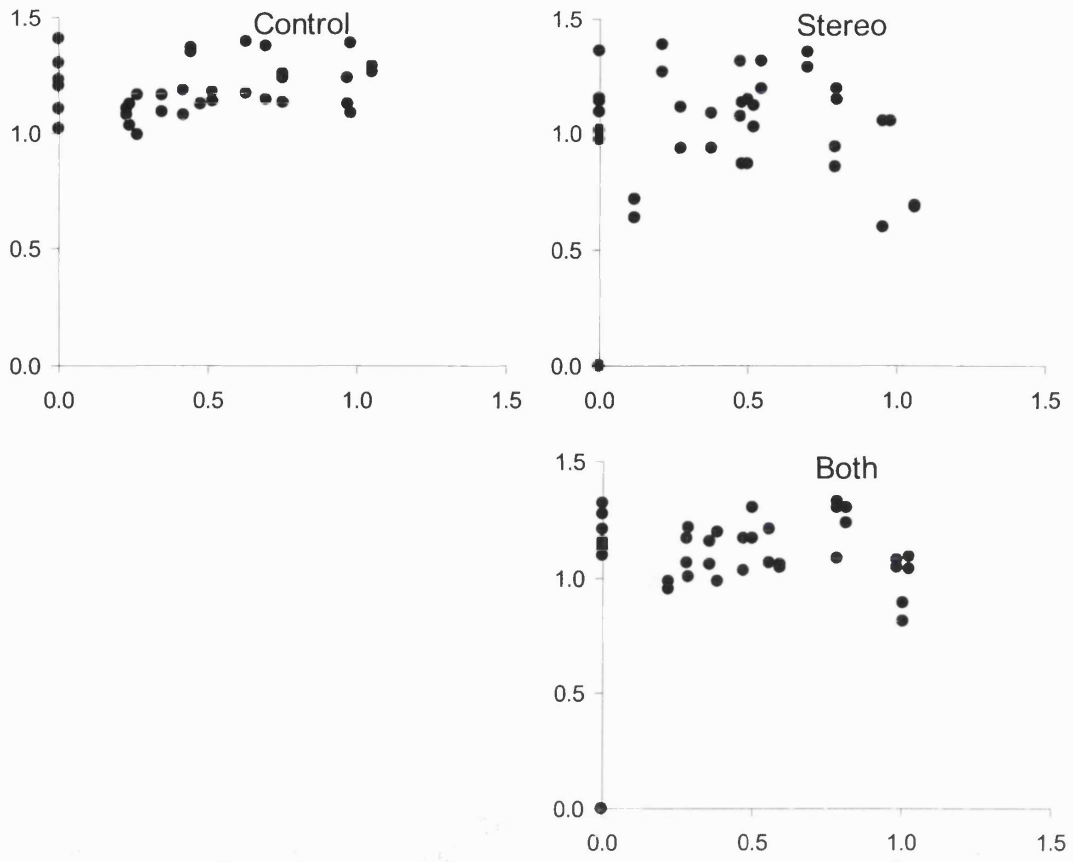

Subject JN Line of best fit without stereo or parallax: NOFS = 1.15 + 0.08 × NWV, R^2 = 0.06 and P > 0.05 Line of best fit with stereo only: NOFS = 1.03 - 0.02 × NWV, R^2 = 0.00 and P > 0.05 Line of best with stereo and parallax: NOFS = 1.07 + 0.05 × NWV, R^2 = 0.01 and P > 0.05